Titre: Title:	Nonlinear vibration and Supersonic Flutter of Conical Shells
Auteur: Author:	Mehrdad Bakhtiari
Date:	2020
Type:	Mémoire ou thèse / Dissertation or Thesis
Référence: Citation:	Bakhtiari, M. (2020). Nonlinear vibration and Supersonic Flutter of Conical Shells [Thèse de doctorat, Polytechnique Montréal]. PolyPublie. https://publications.polymtl.ca/5267/

POLYTECHNIQUE MONTRÉAL
affiliée à l'Université de Montréal

Nonlinear Vibration and Supersonic Flutter of Conical Shells

MEHRDAD BAKHTIARI
Département de Génie mécanique

Thèse présentée en vue de l'obtention du diplôme de *Philosophiæ Doctor*
Génie mécanique

Avril 2020

POLYTECHNIQUE MONTRÉAL

affiliée à l'Université de Montréal

Cette thèse intitulée :

Nonlinear Vibration and Supersonic Flutter of Conical Shells

présentée par **Mehrdad BAKHTIARI**

en vue de l'obtention du diplôme de *Philosophiæ Doctor*

a été dûment acceptée par le jury d'examen constitué de :

Marek BALAZINSKI, président

Aouni A. LAKIS, membre et directeur de recherche

Njuki MUREITHI, membre

Manouchehr NEJAD ENSAN, membre externe

DEDICATION

To my family

ACKNOWLEDGEMENTS

First and foremost, I would like to express my gratitude to my PhD advisor, Professor Aouni A. Lakis, for his support, guidance and encouragement throughout the course of my study. I would also like to thank Dr. Youcef Kerboua for his scientific advice, patience and fruitful discussions that have saved me from losing my focus on more than one occasion. The indirect support and understanding I received from my colleagues at Salford Systems, especially Dr. Dan Steinberg and Mr. Phil Colla, made an otherwise difficult journey possible, and I am grateful for that. The author is also sincerely grateful for the partial financial support received from NSERC (Canada).

RÉSUMÉ

Les coques coniques sont utilisées dans la conception d'une variété de composants de véhicules aérospatiaux, allant des réservoirs de carburant externes des avions de chasse aux lanceurs de satellites. Par conséquent, l'analyse de leurs comportements dynamique et aéroélastique est de grande importance pour la conception de ces structures. Depuis que des études expérimentales ont rapporté que le flottement supersonique se produit à des amplitudes ayant le même ordre de grandeur que l'épaisseur de la coque, les théories géométriques non-linéaires des coques sont de plus en plus utilisées. Ces dernières permettent une meilleure compréhension du phénomène et des résultats plus précis. Plusieurs théories des coques basées sur différentes hypothèses simplificatrices de la cinématique non linéaire ont été développées au cours des dernières décennies, y compris les théories des coques de Donnell, de Sanders et de Novozhilov. Ces théories se distinguent principalement par leurs différentes hypothèses dans le développement des relations de déplacements à la surface moyenne de la coque. La théorie de Donnell a introduit l'effet non linéaire du second ordre du déplacement normal à la surface moyenne lors du développement de la déformation dans le plan. La théorie de Sanders utilise la forme exacte des équations de « petites déformations » pour les déformations membranaires et un ensemble d'équations linéarisées pour les changements des courbures et des torsions de la surface de référence. Plus récemment, Nemeth a développé une théorie qui utilise les relations exactes non linéaires de déformation-déplacement avec des hypothèses de rotations modérées et de petites déformations. Cette théorie peut reproduire la théorie de Donnell et celle de Sanders en tant que cas particuliers, tout en offrant la possibilité de mener une étude comparative entre les prédictions de ces deux théories. Les relations déformation-déplacement peuvent être utilisées pour obtenir les équations d'équilibre et du mouvement des coques. La discrétisation de ces équations est faite en utilisant la méthode des éléments finis (MEF). Un avantage attrayant de cette méthode est sa flexibilité supérieure dans la gestion de différentes conditions aux limites. L'objectif de cette thèse est d'étudier les vibrations non linéaires et le flottement supersonique des coques

coniques tronquées. Une formulation par la MEF hybride est d'abord développée sur la base de la solution exacte de la théorie améliorée de la première approximation de Sanders pour les coquilles minces. Par la suite, les équations non linéaires du mouvement des coques ont été obtenues en utilisant la méthode des coordonnées généralisées et des théories de coques non linéaires. Les coordonnées généralisées ont été choisies en fonction du déplacement nodaux de la coque. L'interaction fluide-structure induite par l'écoulement supersonique a été modélisée en utilisant la théorie de piston. Les effets de raidissement dus aux charges axiales et à la pression interne ont également été modélisés en les exprimant en termes des déplacements nodaux. Pour obtenir la réponse non linéaire de la vibration de la coque sans fluide, un algorithme a été développé basé sur la méthode de réponse harmonique modifiée et sur l'approche de Galerkin dans le domaine temporel. Cet algorithme peut fournir la fréquence de vibration non linéaire en fonction de la variation de l'amplitude de vibration. Une version améliorée du ce même algorithme a également été utilisée pour obtenir la réponse de flottement supersonique. Le modèle développé et l'outil numérique ont la capacité d'effectuer les analyses suivantes:

i) Prédiction des vibrations naturelles linéaires des coques coniques tronquées sous pression et/ou sous charges axiales. Différents schémas de conditions aux limites ont pu être étudiés et les prédictions obtenues sont en bon accord avec les résultats expérimentaux rapportés dans la littérature. ii) Prédiction du début de divergence et du flottement linéaire des coques coniques tronquées sous pression et/ou sous charges axiales pour différentes conditions aux limites. Les prédictions de cette méthode ont été validées positivement par des expériences sélectionnées dans la littérature. Les réservoirs sous pression se sont révélés déstabilisés à des pressions dynamiques plus élevées. iii) Prédiction des vibrations non linéaires des coques coniques tronquées à vide prédite par les théories de Donnell, Sanders et Nemeth. La réponse axisymétrique des coques coniques tronquées étudiées a démontré un comportement de durcissement selon des courbes de l'épine dorsale. Dans les cas étudiés, bien que de légères différences entre la force des prédictions de la cinématique non linéaire de Donnell et deux autres théories aient pu être identifiées, il a été constaté que les différences entre les prédictions des théories de Sanders et de Nemeth sont négligeables. Par conséquent, en raison de son coût de calcul moins cher, la

théorie de Sanders peut être utilisée pour les classes de coques étudiées dans les travaux en cours. iv) Prédiction du comportement de flottement supersonique non linéaire de cônes tronqués sous pression et/ou sous charges axiales pour les trois théories non linéaires susmentionnées. Pour les cas étudiés, la cinématique non linéaire a diminué la stabilité de la coque lorsqu'elle est exposée au champ d'écoulement supersonique. Les vibrations non linéaires et le flottement ont été validés par les cas rapportés de coques cylindriques, qui ont été simulées via un cône tronqué avec un angle de cône très petit. L'application de la MEF permet la modélisation de différentes conditions aux limites et géométries des coques coniques tronquées. Ce programme, en comparaison avec les logiciels commerciaux, est moins coûteux en termes de calcul et il capable de modéliser comportement non linéaire qui reste une tâche difficile pour beaucoup de logiciel.

ABSTRACT

Conical shells have important applications in the design of a variety of aerospace vehicles, ranging from external fuel tanks of fighter jets to satellite launch vehicles. Hence, vibrational and aeroelastic analyses are important criteria in the design of these structures. Since experimental studies have reported that supersonic flutter occurs at amplitudes with the same order of magnitude as the thickness of the shell, geometrically nonlinear shell theories can provide a better and more accurate understanding of these problems.
Different shell theories with different levels of approximation and simplifying assumptions for nonlinear kinematics have been developed in past decades, including Donnell's, Sanders' and Novozhilov's shell theories. The differences between these theories mostly can be attributed to their different assumptions in the development of the strain-displacement relationship on the middle surface of the shell. Donnell's theory introduced the second-order nonlinear effect of normal-to-surface displacement in developing the in-plane strain. Sanders' theory employed the exact form of the "small-strain" equations for the membrane strains and a set of linearized equations for the changes in the reference-surface curvature and torsions. More recently, Nemeth developed a theory that employed the exact nonlinear strain-displacement relations with presumptions of moderate rotations and small strains. This theory can reproduce Donnell's and Sanders' theories as an explicit subset while providing an opportunity to conduct a comparative study between the predictions of those theories. The strain-displacement relationships can be employed to obtain the equilibrium and equations of motion for shells.One important family of discretization of these equations is the finite elements method (FEM). One attractive advantage of the FEM is its superior flexibility in handling different boundary conditions. The objective of this thesis is to investigate the nonlinear vibration and supersonic flutter of truncated conical shells.
In this thesis, a hybrid FEM formulation is first developed based on the exact solution of Sanders' improved first-approximation theory for thin shells. Then, utilizing the generalized coordinates method and nonlinear shell theories, the nonlinear equations of motion

for shells were obtained. The generalized coordinates were chosen in terms of the nodal displacement of the shell. Fluid structure interaction as a result of exposure to the supersonic flow was modeled using the piston theory. The effects of axial loads and internal pressure were also modeled in terms of nodal displacements. To obtain the nonlinear response of the shell's vibration in vacuo, an algorithm was developed based on the modified harmonic response method that employed Galerkin's approach in the time domain. This algorithm can provide the nonlinear vibration frequency as a result of the variation in vibration amplitude. An improved version of the same algorithm was also used to obtain the supersonic flutter response. The developed model and numerical tool have the capability to perform the following analyses:

i) Prediction of linear natural vibration of pressurized truncated conical shells under axial loads. Different schemes for boundary conditions could be studied and the predictions found to be in good accordance with the experimental results reported in literature.

ii) Prediction of linear flutter onset and divergence of pressurized truncated conical shells under axial loads under different boundary conditions. The predictions of this method were validated against selected experiments in the literature with good agreement. The pressurized shells were found to be destabilized at higher dynamic pressures.

iii) Prediction of nonlinear vibration of truncated conical shells in vacuo predicted by Donnell's, Sanders' and Nemeth's theories. The axisymmetric response of the studied truncated conical shells demonstrated a hardening behavior in the backbone curves. In the studied cases, while slight differences between the strength of predictions of Donnell's nonlinear kinematics and two other theories could be identified, it was found that the differences between the predictions of Sanders' and Nemeth's theories were negligible. Hence, due to its less expensive computational cost, Sanders' theory can be used for the classes of shells investigated in the current work.

iv) Prediction of nonlinear supersonic flutter behavior of pressurized truncated conical shells under axial loads for three selected nonlinear theories. For the studied cases, the nonlinear kinematics decreased the shell's stability when it was exposed to the supersonic flow field. Both nonlinear vibration and flutter were validated against reported cases of

cylindrical shells, which were simulated via a truncated cone with a very small cone angle. The developed FEM application can be used to model different boundary conditions and geometries of truncated conical shells.

Both nonlinear vibration and flutter were validated against reported cases of cylindrical shells which were simulated via a truncated cone with a very small cone angle. The developed FEM application can be used to model different boundary conditions and geometries of truncated conical shells. This program in comparison to general application commercial applications is computationally less expensive and can model nonlinear behaviors that are difficult to model with them.

TABLE OF CONTENTS

LIST OF TABLES

LIST OF FIGURES

CHAPTER 1 INTRODUCTION

1.1 Overview

The primary objective of any structural design analysis is to predict and avoid catastrophic failure of the structure and subsequently achieve a reliable structure at the lowest possible weight. Shells, particularly, shells of revolution, are inseparable structural components of aerospace vehicles, and they can be found in various places from the external fuel tanks of fighter jets to the propellant tanks of monstrous satellite launch vehicles [1] [2].

In the past decades, problems such as the linear behavior and response of conical shell structures in relation to small amplitude vibration, linear buckling and linear flutter have been relatively well-studied[3]. But other phenomena, including large amplitude vibration, post-buckling behavior and flutter have been studied less often since they require more elaborate mathematical models that take into account the geometrical nonlinearity. This is due to the fact that the amplitude of deflections in those cases, especially in flutter, is closer or exceeds the shell thickness that in itself breaches the simplifying assumptions that were used in developing the linear models[4].

As will be shown in the literature review, in most of the analytical and semi-analytical models that have been developed for nonlinear analysis of truncated conical shells, several aspects of the nonlinear problem, including developing a method that can explicitly handle different boundary conditions, have been left unaddressed. This can be associated with the fact that the majority of previous works utilized the Galerkin method in conjunction with Airy stress function to obtain the dynamic model of the system. The finite element method (FEM) could alleviate some of those issues, but conventional, commercially available FEM applications require heavy computational efforts and are unable to accurately model some aspects of these problems, including the fluid-structure interactions. The hybrid finite element method proposed in the current study attempts to provide a fast and precise approach to analyze the nonlinear vibration and flutter of conical shells.

1.2 Nonlinear Kinematics

A shell is a solid body or medium bounded by two curved surfaces, where the distance between the surfaces is small in comparison with other body dimensions. The locus of points that are placed at equal distances from these two surfaces is known as the middle surface or base surface of the shell. It is common to treat the elastic body as a two-dimensional medium with a base surface and relate the strain and stress fields of a point at a certain distance from the base surface to the values of the corresponding points on the base surface. The kinematics defines the relationships between the displacements and strains on the middle surface and, in the case of nonlinear expressions, it is called geometrical nonlinearities. The following theories were investigated and compared at different stages of the current study:

- Kirchhoff-Love theory: This theory assumes that the normal lines of materials to the middle surface remain normal and straight after deformation and that strains follow linear relationships with the displacements. The specific derivation of Sanders from Love's assumption that is known as "best first approximation"[5]" was employed in the current study.
- Donnell's nonlinear theory: In this theory, the in-plane displacements are infinitesimal and the transverse deformations are assumed to be in the same order as the shell's thickness. Moreover, in-plane inertia was assumed to be negligible, and nonlinear terms were kept only in the transverse direction [6].
- Sanders-Koiter nonlinear theory: This theory was developed based on the assumption of small strains and moderately small rotations, therefore, the nonlinearities for both the in-plane displacements and transverse displacements were introduced, but the changes in curvature and torsion on the middle surface were assumed to be linear. The Sanders-Koiter theory gives accurate results for vibration amplitudes significantly larger than the shell thickness[7].
- Nemeth's nonlinear theory: This theory provides Donnell's and Sanders' theories as subsets. Nemeth's derivation does not contain any shell-thinness approximations involving the ratio of the maximum thickness to the minimum radius of curvature.

Therefore, the strain-displacement relations are exact within the presumptions of "small" strains and "moderate" rotations[8].

1.3 Dynamic Model

The dynamic model of shell structures subjected to supersonic flows needs to take into account the mass, linear and nonlinear elasticity, supersonic flow pressure field and the initial stiffening due to axial loads and internal pressurization. The common practice that is widely used in literature is to employ the virtual works method to obtain the governing equilibrium equations of the shell. This yields a set of partial differential equations that presents the variation of displacement of any point on the shell based on geometric and elastic properties. These equations need to be discretized for the solution. The common practices for discretization include the Ritz method, the semi-analytical Airy stress function-Galerkin method and the finite element method. Then Hamilton's principle can be used to obtain the Lagrangian equations of motion in terms of generalized coordinates. These generalized coordinates represent Galerkin's or FEM's degrees of freedom. The pressure field of supersonic flow is modeled using the linear piston theory, taking into account the correction terms for curvature. Then, using the common conventions of FEM, this pressure field is expressed in terms of FEM nodal displacements. The same approach is taken to express the initial stiffening effect as a result of internal pressurization and axial loads. The obtained equations of motion describe the dynamic behavior of the shell in the form of a system of nonlinear, ordinary differential equations in the time domain. These equations take the form of multivariate polynomials up to the third degree of the generalized coordinates.

While the semi-analytical Airy stress function-Galerkin method seems to be the most widely used method of discretization, it offers limited choices for the boundary conditions. On the other hand, the FEM can provide more flexible options for the constraints. This leads to the capability to handle a wider range of problems.

1.4 Free Vibration

One important aspect of the shell's dynamic behavior is linear and nonlinear free vibration. The effect of geometrical nonlinearities becomes significant for large amplitude vibrations, usually those at the same order or larger than the shell thickness. Given the general dynamic model that was described in the previous section, the associated mathematical model for free vibrations can be obtained by nullifying terms that are related to flowing fluids, such as supersonic pressure field. If, from the multivariate polynomial equations of the dynamic model, all the monomials with powers greater than one are further omitted, the linear model of the system can be obtained. Having this model and assuming a periodic response, the linear free vibration frequencies can be calculated by solving the associated eigenvalue problem[9].

The nonlinear vibration is more focused on the nature of change of behavior due to the presence of geometrical nonlinearities—in other words, whether the structure demonstrates softening or hardening behavior. Different methods are employed to resolve and analyze nonlinear behavior, including numerical continuation such as pseudo arc length, variations of harmonic response and point collocation. Results are usually provided in the form of backbone curves that show the deviation of nonlinear vibration frequency from the linear one at different amplitudes of vibration[3].

1.5 Flutter

Flutter or self-incitement vibration due to fluid-structure interactions is one of the most important failure modes of high-speed aerospace structures, and the earliest observations of flutter in supersonic speeds goes back to the V-2 rocket[4]. Though flutter in cylindrical shells and flat panels that are exposed to supersonic axial flows has been the subject of numerous studies in past decades, as will be shown in the literature review, there is a limited number of studies on flutter in conical shells. Moreover, even in the existing studies on flutter in panels and cylindrical shells, very few studies have used nonlinear theories in their kinematics models[4].

Different aerodynamic models can be found in scientific literature for different flow regimes

in terms of Mach number and flow-wall angle of interaction. While Newton's impact theory and improved impact theory are methods of choice for hypersonic flows at moderate and high angles of attack, the piston theory has been used successfully for supersonic aeroelastic studies. The piston theory, which was introduced in the late 1950s by Ashley [10] , uses the analogy of a moving piston inside a tube to predict the aerodynamic forces on a surface in supersonic flows. The underlying assumption is that a deflection on a surface that is subjected to supersonic flows makes the free stream form a small angle at the corner of the deflection. Depending on the size of this angle, the presence of that deflection creates either an oblique shock (high pressure) or an expansion wave (low pressure). But it should be noted that, the changes of the speed in the direction of the free stream are negligible compared with its gradient in the normal direction to the free stream (and the surface). Therefore, the gradients of flow parameters in the free stream direction follow the same pattern in the normal direction. From these two facts, it can be stated that in unsteady supersonic flows, a flow column normal to the free stream moves along the direction of the free stream while it keeps its unsteady motion normal to the surface. Considering this analogy, the surface pressure ratio to the free stream static pressure can be estimated using the concept of one-dimensional wave propagation in a tube. To improve the accuracy of the original piston theory that was developed for flat panels, [11] an improved theory was developed that takes into account the effect of curvature in cylindrical shells that can also be applied to the case of conical shells.

References

[1] F. Sabri, "Aeroelastic analysis of circular cylindrical and truncated conical shells subjected to a supersonic flow," Ph.D., Ecole Polytechnique, Montreal (Canada), Canada, 2009. [Online]. Available: http://search.proquest.com/dissertations/docview/305137997/abstract/840D004A76F74731PQ/1?accountid=40695

[2] F. Sabri, A. Lakis, and M. Toorani, "Hybrid finite element method in supersonic flutter analysis of circular cylindrical shells," in *31st International Conference on Boundary Elements and Other Mesh Reduction Methods, BEM/MRM 31*, ser. WIT Transactions

on Modelling and Simulation, vol. 49. WITPress, 2009, pp. 233–244.

[3] M. Amabili and M. P. Paıdoussis, "Review of studies on geometrically nonlinear vibrations and dynamics of circular cylindrical shells and panels, with and without fluid-structure interaction," *Applied Mechanics Reviews*, vol. 56, no. 4, pp. 349–381, 2003. [Online]. Available: http://materialstechnology.asmedigitalcollection.asme.org/article.aspx?articleid=1397681

[4] M. Amabili, *Nonlinear vibrations and stability of shells and plates*. Cambridge University Press, 2008. [Online]. Available: https://books.google.ca/books?hl=en&lr=&id=0Ymw-pi7-x4C&oi=fnd&pg=PA52&dq=Nonlinear+Vibrations+and+Stability+of+Shells+and+Plates&ots=uZtdkX_GUL&sig=hStbpt8yVKKY4Eeh6L0QEzyT2NY

[5] J. L. Sanders Jr, "An improved first-approximation theory for thin shells," NASA, Tech. Rep. TR R-24, 1959.

[6] L. H. Donnell, "A new theory for the buckling of thin cylinders under axial compression and bending," *Trans. ASME*, vol. 56, no. 11, pp. 795–806, 1934. [Online]. Available: http://cybra.lodz.pl/Content/6356/AER_56_12.pdf

[7] J. L. Sanders Jr., "Nonlinear theories for thin shells," DTIC Document, Tech. Rep. AD0253822, 1961. [Online]. Available: http://oai.dtic.mil/oai/oai?verb=getRecord&metadataPrefix=html&identifier=AD0253822

[8] M. P. Nemeth, "An Exposition on the Nonlinear Kinematics of Shells, Including Transverse Shearing Deformations," NASA, Tech. Rep. NASA/TM–2013-217964, 2013. [Online]. Available: http://ntrs.nasa.gov/search.jsp?R=20130011025

[9] A. A. Lakis and M. P. Paidoussis, "Free vibration of cylindrical shells partially filled with liquid," *Journal of Sound and Vibration*, vol. 19, no. 1, pp. 1–15, 1971.

[10] H. Ashley, "Piston Theory -A New Aerodynamic Tool for the Aeroelastician," *Journal of the Aeronautical Sciences*, vol. 23, no. 12, pp. 1109–1118, 1956. [Online]. Available: http://arc.aiaa.org/doi/abs/10.2514/8.3740

[11] H. Krumhaar, "The accuracy of linear piston theory when applied to cylindrical shells," *AIAA Journal*, vol. 1, no. 6, pp. 1448–1449, 1963.

CHAPTER 2 LITERATURE REVIEW

The aeroelastic stability of shells and plates in flow regimes with Mach numbers greater than one has been the subject of several studies in past decades. While several studies can be found in the literature on the flutter characteristics of cylindrical shells, the number of articles on the supersonic flutter of conical shells is limited. Moreover, even in the existing studies on the flutter of cylindrical shells, very few have employed geometrically nonlinear or transversal shear deformation theories in their models. Employing nonlinear shell theories is important since experimental studies have shown that the oscillation amplitude of flutter has the same order of magnitude as the shell thickness [1].

Dixon and Hudson [2] studied the flutter, vibration and buckling of truncated orthotropic thin conical shells with general boundary conditions at the edges. They employed the Donnell type of nonlinear kinematics in conjunction with the modified first-order piston theory to model the structure behavior. An approximate solution using the Galerkin method was employed to solve the governing equations [2] [3]. In a later study, they compared different modes of structural instabilities of conical shells and argued that, for shells subjected to static external pressure loads, divergence governed the design conditions for small semi-cone angle values, flutter for moderate semi-cone angle values, and buckling is the dominant phenomena in large semi-cone angles [4].

Miserentino and Dixon [5] expanded the works of Dixon and Hudson [2] and [4]) by performing experimental studies on the vibration and flutter of thin-walled truncated orthotropic conical shells. The experimental results provided the variations of resonant frequency with internal pressure and circumferential wave number at constant Mach numbers. The results were found to verify the theoretical works of Dixon and Hudson [2] for thin shells with good accuracy [5].

The work of Ueda et al. [6] explored the theoretical and experimental aspects of supersonic flutter in conical shells. Donnell's shell theory was used in conjunction with FEM for modeling the problem. They stated that FEM was a powerful tool for panel flutter analysis. Moreover, it was demonstrated during the experiment that, contrary to the the-

oretical work, the flutter preceded the buckling of the shell.

Bismarck-Nasr and Costa Savio [7] developed a finite element method for supersonic flutter of truncated conical shells. In that work, Novozhilov's shell theory for thin shells was employed to model elastic behavior. In the shell model, the in-plane inertia was preserved within kinetic energy formulations while the rotary inertia was neglected. The aerodynamic loads were modeled using the first-order high Mach number piston theory. A finite element formulation was derived and a solution using separation of variables was presented. Results for minimum critical pressure and the associated circumferential wave number were calculated and compared to the existing results in the literature. Based on the results, it was argued that the curvature effect in modeling the aerodynamic loads had little effect on the stability conditions [7]. Moreover, it was argued that neglecting in-plane inertia in Donnell's theory explained the small differences between their results and those of Ueda et al. [6].

Fallon and Thornton [8] developed a numerical model for predicting the aerodynamic instability with thermal pre-stress in general shells of revolution. They employed a classic finite element using the Fourier series in circumferential direction and polynomials in the meridian direction as displacement function. The aerodynamic loads were modeled using the first-order piston theory along with a variation of Novozhilov's nonlinear shell theory as governing equations of the elastic shell [8].

Mason and Blotter [9] applied the finite element method to study the aeroelasticity of truncated thin conical shells subjected to internal supersonic flows. The study employed linear shell theory and used eigenvalues for stability analysis. An analytical finite element formulation was developed and the variation in critical pressure versus chamber pressure was presented. It has been stated that for the analyzed case studies, the engine chamber pressure was always beneath the flutter critical pressure [9].

Pidaparti [10] developed a quadrilateral thin-shell finite element method for analyzing the supersonic flutter of doubly curved composite shells. The presented quadrilateral element had eight nodes and 48 degrees of freedom. The displacement functions were chosen in the form of bi-cubic Hermitian polynomials and the classical lamination theory (Love-Kirchhoff linear thin-shell theory) was employed for modeling the elastic behav-

ior. First-order high Mach number piston theory was employed for modeling the aerodynamic loads. Aeroelastic equations were derived using Hamilton's principle for the non-conservative elastic system. Eigenvalue analysis was performed to determine the critical parameters using normal mode approach. Results for cylindrical and conical shells and flat plates were compared to various existing analyses in the literature and showed good agreement. The effects of various parameters, including orthotropy, fiber angle, flow angle, circumferential wave number and semi-cone angle for conical shells on critical pressure, were presented and discussed. Based on the results, it was argued that the fiber angle and orthotropy impose significant effects on flutter boundaries for cylindrical and conical shells and flat plates [10].

Kiiko and Nadzhafov [11] studied the flutter behavior of conical shells with small semi-cone angles subjected to internal supersonic flow. Instead of the classic piston theory, a new asymptotic approach was used to model the interactive effects of aerodynamic forces. Shell elastic behavior was modeled through the Love-Kirchhoff linear theory. The author argued that the newly developed aerodynamic model is more accurate at lower supersonic Mach numbers [11].

Sabri and Lakis [12] studied the flutter behavior of partially filled truncated conical shells in supersonic flows using a hybrid finite element method. Sanders' linear thin-shell theory was used for modeling the elastic behavior of the shell. The aerodynamic loads were assumed to follow the first-order potential piston theory with correction terms for curvature. The effects of stiffening due to pressurization was also considered in this study. The potential flow theory was used to derive the governing equation of the internal hydrodynamic pressure field. The shell was assumed to be made of isotropic materials. An exact solution was developed for shell equilibrium equations and that solution was used for developing a hybrid finite element method. Effects of boundary conditions, internal pressure, semi-cone angle, length-to-radius ratio and filling ratio were investigated to determine the shell's stability. It was concluded in this work that conical shells are susceptible to coupled mode flutter in the first and second axial modes. Moreover, it was stated that a lower semi-cone angle decreases the critical dynamic pressure [13][12].

Mahmoudkhani et al. [14]studied the aero-thermoelastic stability of FGM-truncated con-

ical shells in supersonic flows. The Donnell type of nonlinearities was introduced in the shell strain-displacement relationships. Hamilton's principle was used to derive the shell equation of motion. The shell's temperature-dependent elastic properties were assumed to follow the rule of mixture based on the power-law function of compositional profile of the functionally graded material. The aerodynamic pressure field was assumed to follow the linear piston theory. A solution based on power series in conjunction with the Galerkin method was developed to solve the linearized equilibrium equations, taking into account the aerodynamic and thermal loadings. The initial stresses and displacements due to the thermal and aerodynamic loading of the aforementioned solution was incorporated into the aeroelastic equations. The eigenvalue analysis was used to obtain the critical parameters. Effects of the material's compositional profile, temperature gradient, semi-cone angle were investigated to check the shell's stability. Among the conclusions, it was stated that the compositional profile of FGM material has a significant effect on the stability of the shell. In addition, a higher temperature gradient between the outer and inner surface of the shell was found to affect the shell's stability greatly [14].

Davar and Shokrollahi [15] provided an analysis on the supersonic flutter of FGM conical shells with clamped and simply supported boundary conditions. First-order shear deformation theory was employed in conjunction with the classical Love-Kirchhoff linear in-plane kinematics. Aerodynamic modeling in this study was based on the linear first-order piston theory. The composition profile of the material was chosen to have a power law distribution for volumetric fractions and the elastic properties were calculated from that distribution. The displacements and rotations were assumed to have a form of trigonometric series and the Galerkin method was used to solve the governing equations. Critical flutter parameters were determined using eigenvalue analysis. The verification of the solution was performed by comparing it to the existing results in scientific literature. The effects of material compositional profile, semi-cone angle, thickness and radius-to-length ratio on the critical aerodynamic pressure were studied. Based on the obtained results, it was concluded that changing the boundary conditions from simply supported to clamped increases all the frequencies, but there is no general trend in the critical aerodynamic pressure. Moreover, it was argued that the effect of thickness on the critical

aerodynamic pressure is several times greater than the similar effect on the frequencies [15].

Zhang et al. [16] employed the Love-Kirchhoff linear thin-shell theory to study the flutter behavior of conical shells subjected to internal supersonic flow. The quasi-steady linear piston theory with correction terms for curvature was used for modeling the aerodynamic loads. The truncated conical shell was assumed to be clamped at the smaller end and free at the larger diameter. The differential quadrature method was employed to solve the governing equations, and an eigenvalue analysis was utilized to identify the effects of various parameters, including wave number, cone angle, radius-to-thickness ratio and length-to-radius ratio, on the critical internal pressure. Based on the results, it was argued that, in the studied case, increasing the semi-cone angle increases the flutter resistance to $\alpha = 30°$. Beyond that value, an opposite behavior was observed. On the other hand, increasing the length-to-radius ratio generally increases the flutter resistance [16].

Vasilev [17] presented a new formulation for flutter analysis of truncated conical shells exposed to supersonic flows. The shell was assumed to be made of isotropic materials and a linear type of kinematics (Love-Kirchhoff theory) was employed to define the shell's elastic behavior. Instead of using the piston theory, a quasi-static pressure formulation was developed, taking into account the added mass, the rotary inertia and the forces in the mid-plane. The equations were defined using a spherical coordinate system, and an asymptotic approach was used to solve the dimensionless governing equations. An eigenvalue analysis over the roots of the dynamic system was utilized to identify the flutter conditions. Results provided the critical Mach number for a range of height-to-radius ratios, cone angles and shell thicknesses. Based on the results, the authors argued that the linear piston theory significantly overestimates the critical dynamic pressure at low Mach numbers [17].

Yang et al. [18] investigated the supersonic flutter in FGM truncated conical shells. They employed first-order shear deformation theory with Love-Kirchhoff assumptions for the elastic model of the shell. A power-law equation was used for defining the FGM material's compositional profile and elastic properties. The aerodynamic loads were modeled by first-order quasi-static linear piston theory. The shell was assumed to be simply

supported at both ends and the Fourier series was used to obtain the solution. A direct Runge-Kutta integration was used to investigate the periodic and chaotic motion of the shell, considering the presence of a steady-state, constant temperature distribution. It was shown that it is possible to control the periodic and chaotic instabilities through variation of the material's compositional profile [18].

Mehri et al. [19] studied the flutter characteristics of a functionally graded carbon nanotube reinforced composite (FGCNTRC) truncated conical shell under simultaneous actions of a hydrostatic pressure and yawed supersonic airflow. They employed Novozhilov's nonlinear shell theory for the elastic model and corrected the piston theory for the effect of curvature as the aerodynamics mode. The effects of boundary conditions, semi-vertex angle, distribution and volume fraction of CNT, Mach number and airflow yaw angle on the stability of the shell were investigated. The differential quadrature method was used to obtain a numerical solution. Among the conclusions, it was stated that increasing the Mach number significantly decreases the critical free stream static pressure due to increased aerodynamic load. In a follow-up study, Mehri et al. [20] employed the harmonic differential quadrature method (HDQM) to solve the nonlinear equations of motion of truncated conical curved panels. It was demonstrated that the FGM composition plays a pivotal role in the flutter critical pressure and buckling critical load, while the critical circumferential mode number is not affected by it.

Hao et al. [21] studied the supersonic flutter of FGM shallow conical panels under steady thermal stress. They employed the linear piston theory and Donnell's type of kinematic nonlinearities in combination with first-order shear deformation theory in their model. Using the Galerkin method and the Hamilton principle, the nonlinear flutter problem was solved using a combination of numerical continuation and the Newton-Raphson algorithm. They concluded that aerodynamic dampening can stabilize the system by consuming some energy. In another study,Hao et al. [22] employed the same Donnell-type nonlinear kinematics in time-domain simulation to identify the three stages of FGM conical shells subjected to supersonic flows: vibration, limit cycle oscillation, and chaotic motion.

References

[1] M. Amabili and F. Pellicano, "Nonlinear Supersonic Flutter of Circular Cylindrical Shells," *AIAA Journal*, vol. 39, no. 4, pp. 564–573, 2001. [Online]. Available: http://dx.doi.org/10.2514/2.1365

[2] S. C. Dixon and M. L. Hudson, "Flutter, vibration, and buckling of truncated orthotropic conical shells with generalized elastic edge restraint," Tech. Rep. NASA-TN-D-5759, L-6663, Jul. 1970. [Online]. Available: http://ntrs.nasa.gov/search.jsp?R=19700024015

[3] ——, "Flutter, vibration, and buckling of truncated orthotropic conical shells with generalized elastic edge restraint, supplement," Tech. Rep. NASA-TN-D-5759-SUPPL, Jul. 1970. [Online]. Available: http://ntrs.nasa.gov/search.jsp?R=19700024016

[4] ——, "Supersonic asymmetric flutter and divergence of truncated conical shells with ring supported edges," Tech. Rep. NASA-TN-D-6223, L-7527, May 1971. [Online]. Available: http://ntrs.nasa.gov/search.jsp?R=19710016314

[5] R. Miserentino and S. C. Dixon, "Vibration and flutter tests of a pressurized thin-walled truncated conical shell," Tech. Rep. NASA-TN-D-6106, L-7345, 1971. [Online]. Available: http://ntrs.nasa.gov/archive/nasa/casi.ntrs.nasa.gov/19710007880.pdf

[6] T. Ueda, S. Kobayashi, and M. Kihira, "Supersonic Flutter of Truncated Conical Shells." *Transactions of the Japan Society for Aeronautical and Space Sciences*, vol. 20, no. 47, pp. 13–30, 1977.

[7] M. N. Bismarck-Nasr and H. R. Costa Savio, "Finite-element solution of the supersonic flutter of conical shells," *AIAA Journal*, vol. 17, no. 10, pp. 1148–1150, 1979. [Online]. Available: http://arc.aiaa.org/doi/pdf/10.2514/3.61291

[8] D. J. Fallon and E. A. Thornton, "Flutter: A finite element program for aerodynamic instability analysis of general shells of revolution with thermal prestress," Tech. Rep., Mar. 1983. [Online]. Available: http://ntrs.nasa.gov/search.jsp?R=19830011485

[9] D. Mason and P. Blotter, "FINITE-ELEMENT APPLICATION TO ROCKET NOZZLE AEROELASTICITY." *Journal of Propulsion and Power*, vol. 2, no. 6, pp. 499–507, 1986.

[10] R. Pidaparti, "Flutter analysis of cantilevered curved composite panels," *Proceedings of the 7th International Conference on Composite Structures, August 1, 1993 - August 1, 1993*, vol. 25, no. 1-4, pp. 89–93, 1993.

[11] I. Kiiko and M. Nadzhafov, "To a formulation of the flutter problem for a conical shell with a small apex angle," *Moscow University Mechanics Bulletin*, vol. 64, no. 4, pp. 89–92, 2009.

[12] F. Sabri and A. A. Lakis, "Hybrid finite element method applied to supersonic flutter of an empty or partially liquid-filled truncated conical shell," *Journal of Sound and Vibration*, vol. 329, no. 3, pp. 302–316, 2010. [Online]. Available: http://www.sciencedirect.com/science/article/pii/S0022460X09007470

[13] F. Sabri, "Aeroelastic analysis of circular cylindrical and truncated conical shells subjected to a supersonic flow," Ph.D., Ecole Polytechnique, Montreal (Canada), Canada, 2009. [Online]. Available: http://search.proquest.com/dissertations/docview/305137997/abstract/840D004A76F74731PQ/1?accountid=40695

[14] S. Mahmoudkhani, H. Haddadpour, and H. Navazi, "Supersonic flutter prediction of functionally graded conical shells," *Composite Structures*, vol. 92, no. 2, pp. 377–386, 2010.

[15] A. Davar and H. Shokrollahi, "Flutter of functionally graded open conical shell panels subjected to supersonic air flow," *Proceedings of the Institution of Mechanical Engineers, Part G: Journal of Aerospace Engineering*, pp. 1036–1052, 2012. [Online]. Available: http://pig.sagepub.com/content/early/2012/06/06/0954410012448340.abstract

[16] R. Zhang, Z. Yang, and Y. Gao, "The flutter of truncated conical shell subjected to internal supersonic air flow," *Multidiscipline Modeling in Materials and Structures*, vol. 10, no. 1, pp. 18–35, 2014. [Online]. Available: http://search.proquest.com/docview/1536488408/abstract

[17] A. Vasilev, "Flutter of conical shells under external flow of a supersonic gas," *Moscow University Mechanics Bulletin*, vol. 70, no. 2, pp. 23–27, 2015.

[18] S. W. Yang, Y. X. Hao, W. Zhang, and S. B. Li, "Nonlinear Dynamic Behavior of Functionally Graded Truncated Conical Shell Under Complex Loads," *International Journal of Bifurcation and Chaos*, vol. 25, no. 2, p. 1550025(33 pp.), Feb. 2015, wOS:000350485800011.

[19] M. Mehri, H. Asadi, and Q. Wang, "On dynamic instability of a pressurized functionally graded carbon nanotube reinforced truncated conical shell subjected to yawed supersonic airflow," *Composite Structures*, vol. 153, pp. 938–951, Oct. 2016. [Online]. Available: http://www.sciencedirect.com/science/article/pii/S0263822316310972

[20] M. Mehri, H. Asadi, and M. A. Kouchakzadeh, "Computationally efficient model for flow-induced instability of CNT reinforced functionally graded truncated conical curved panels subjected to axial compression," *Computer Methods in Applied Mechanics and Engineering*, vol. 318, pp. 957–980, May 2017. [Online]. Available: http://www.sciencedirect.com/science/article/pii/S0045782516316061

[21] Y. X. Hao, Y. Niu, W. Zhang, S. B. Li, M. H. Yao, and A. W. Wang, "Supersonic flutter analysis of FGM shallow conical panel accounting for thermal effects," *Meccanica*, vol. 53, no. 1-2, pp. 95–109, 2018.

[22] Y. X. Hao, S. W. Yang, W. Zhang, M. H. Yao, and A. W. Wang, "Flutter of high-dimension nonlinear system for a FGM truncated conical shell," *Mechanics of Advanced Materials and Structures*, vol. 25, no. 1, pp. 47–61, 2018.

CHAPTER 3 PROJECT DESCRIPTION

3.1 Motivations and Objective

As it is shown in the literature review, few studies have addressed the problem of nonlinear vibration and supersonic flutter of truncated conical shells. This is an important problem in the design of high speed aerospace vehicles. Moreover, the differences between the vibration predictions of different nonlinear shell theories have not received sufficient attention. This is important, since theories with simplifying assumptions are usually less expensive in terms of development and computations, but the question of their relative accuracy compared to more precise theories has not been sufficiently explored. In addition, the common approach in the development of equations of motion usually takes the expanded non-matrix form that dramatically increases the efforts required for developing and programming the model. Hence, the objectives of this thesis are as follows:

- To develop a concise and methodical mathematical framework to express third-order nonlinear elastic systems such as thin shells in matrix form.
- To develop the Lagrangian nonlinear equation for the vibration of shells based on Donnell's, Sanders' and Nemeth's theories using the hybrid finite element method.
- To investigate the linear and nonlinear vibrations of truncated conical shells and the effects of geometrical and boundary conditions using the developed tool.
- To provide a comparative study on the predictions of nonlinear vibration using different nonlinear theories for selected cases.
- To develop a hybrid FEM solution for linear and nonlinear flutter of truncated conical shells, taking into account the effects of pressurization and axial loads.
- To provide characteristics of linear and nonlinear flutter of truncated conical shells in supersonic flows.

3.2 Structure of thesis

This dissertation composed of six chapters:

- Chapter 1 presents the introduction and explores the general aspect and the importance of the problem.
- Chapter 2 provides the literature review and summarizes the work that has been done on the subject.
- Chapter 3 defines the objectives and the structure of this thesis.
- Chapter 4 contains the first article that provides a generic mathematical framework for formulating third-order nonlinear kinematics of elastic systems in a concise matrix form.
- Chapter 5 contains the second article on the nonlinear vibration of truncated conical shells using three different theories, Donnell's, Sanders' and Nemeth's.
- Chapter 6 contains the third article on the nonlinear flutter of truncated conical shells.
- Chapter 7 provides a brief discussion on the findings and results.
- Chapter 8 provides the summary of the current work and possible areas for future research.

This work includes the presented introduction, literature review, project description, and three articles, followed by the conclusion and references.

3.3 Contributions

During the course of this Ph.D. study, a technical report that contains the elaborate details of the developed nonlinear mathematical model for truncated conical shells was first published:

M. Bakhtiari, A. A. LAKIS, and Y. Kerboua, "Nonlinear vibration of truncated conical shells: Donnell, Sanders and Nemeth theories," EPM-RT-2018-01, 2018.

This was necessary because the limited length of typical journal articles could not capture all the required details. The above technical report is open source and available online.

Some of the essential parts of the current work, such as stress resultants, linear equilibrium equations, through-the-thickness elasticity coefficients and solution basic functions are presented only in that report. Since that report was published independently and there are overlapping contents with this thesis, it was not reproduced here.

The main component of the contribution of this work, includes the following articles that were published or submitted during the course of this Ph.D study:

M. Bakhtiari, A. A. Lakis, and Y. Kerboua, "Derivatives of fourth order Kronecker power systems with applications in nonlinear elasticity," Applied Mathematics and Computation, vol. 362, p. 124501, Dec. 2019.

M. Bakhtiari, A. A. Lakis, and Y. Kerboua, "Nonlinear vibration of truncated conical shells: Donnell, Sanders and Nemeth theories," International Journal of Nonlinear Sciences and Numerical Simulation, 21.1 (2020): 83-97.

M. Bakhtiari, A. A. Lakis, and Y. Kerboua, "Nonlinear supersonic flutter of truncated conical shells," Journal of Mechanical Science and Technology 34 (2020): 1375-1388.

CHAPTER 4 ARTICLE 1- DERIVATIVES OF FOURTH ORDER KRONECKER POWER SYSTEMS WITH APPLICATIONS IN NONLINEAR ELASTICITY

Mehrdad Bakhtiari, Aouni A. Lakis, Youcef Kerboua

Applied Mathematics and Computation, vol. 362, p. 124501, Dec. 2019.

Abstract

A natural way to describe systems with polynomial nonlinearities is using the Kronecker product. Particularly, third-order Kronecker power systems can express a wide range of systems from electronic engineering to nonlinear elasticity. But such development (e.g. equations of motions of elastic structures from nonlinear strain energy) requires standard formulation for the derivative of the Kronecker power of vectors with respect to the same vector. Such standard way cannot be found in literature. This paper presents a method to obtain the derivatives of Kronecker powers of vectors with respect to itself up to a power of four and also third-order Kronecker Power systems containing those terms in a concise matrix form. The matrix expression of these systems provides new approach for efficient numerical implementation, organized analysis and linearization. To demonstrate the strength of this method, an example of application for a finite element nonlinear Euler beam is also presented.

4.1 Introduction

Matrix calculus is a strong tool to develop concise mathematical models of complex systems. The general aspects and notations of various applicable problems such as "differentiation conventions", "differentiation of matrix multiplication and Kronecker, Khatri-Rao and Hadamard products", "unitary matrices and vectorization operators" are provided in many works such as [1, 2, 3, 4, 5, 6, 7]. These mathematical derivations have been vastly used in various fields of applied science and engineering ranging from econometrics to mechanical engineering and system theory(e.g. [8, 9, 10]).

One problem of particular interest is the derivatives of a Kronecker power of vectors (and

combinations of these with matrix multiplication). It has a wide range of applications including developing equations of motion in nonlinear mechanics, elasticity, kinematics, the Galerkin method and the finite element method. One natural way to express systems with polynomial nonlinearities (such as those described above) is to employ the Kronecker product:

$$\left[\mathbf{M}\right]\left\{\ddot{\boldsymbol{\delta}}\right\}+\left[\mathbf{K_1}\right]\left\{\boldsymbol{\delta}\right\}+\left[\mathbf{K_2}\right]\left(\left\{\boldsymbol{\delta}\right\}\otimes\left\{\boldsymbol{\delta}\right\}\right)+\left[\mathbf{K_2}\right]\left(\left\{\boldsymbol{\delta}\right\}\otimes\left\{\boldsymbol{\delta}\right\}\otimes\left\{\boldsymbol{\delta}\right\}\right)+\cdots=0 \tag{4.1}$$

where $\otimes$ is the Kronecker product symbol and $\left[\mathbf{M}\right]$ and $\left[\mathbf{K_i}\right]$ are accordingly mass and stiffness matrices of the system. $\left\{\boldsymbol{\delta}\right\}=\left\{\delta_1 \quad \delta_2 \quad \cdots\right\}^{\mathsf{T}}$ denote the degrees of freedom of the system. This ensures organized handling of the interactions between degrees of freedom. For example in a two degrees of freedom system $\left\{\boldsymbol{\delta}\right\}\otimes\left\{\boldsymbol{\delta}\right\}=\left\{\delta_1^2 \quad \delta_1\delta_2 \quad \delta_2\delta_1 \quad \delta_2^2\right\}^{\mathsf{T}}$ contains all the interactions in a mathematically well-organized form that are needed for numerical implementation. But as will be shown, such development requires obtaining derivatives of Kronecker powers with respect to a vector and derivatives of combined matrix multiplication and Kronecker powers that to the best knowledge of the authors has not been addressed in scientific literature. Such terms appear in the energy equations that are commonly used to derive equations of motion. The powerful method described in this article, provides an easy way to obtain the aforementioned derivatives by just multiplication of some certain integer-valued matrices by transformed versions (by column rearrangement) of the original mass and stiffness matrices that appear in the internal strain energy equation or their equivalents in similar problems. In this study, after stating the problem with the help of some examples from nonlinear elasticity:

1. The derivatives of second, third and fourth order Kronecker powers of a vector with respect to itself are developed in form of a classic matrix multiplication.
2. Using these derivations, the combined derivatives of third-order Kronecker power systems will be provided in the form of matrix multiplication.
3. An example of the application of this method is shown for a finite element model of a Euler-Bernoulli beam.

4.2 Problem Statement in the Case of Nonlinear Kinematics

Notion of the internal strain energy (U) takes the following form:

$$U = \frac{1}{2}\int_{\Omega} \sigma^{\intercal} \epsilon d\Omega \tag{4.2}$$

where σ, ϵ are accordingly the stress and strain fields in the continuum domain (Ω) that could be a beam, shell or similar structural member. It is common to express the strain field as a function of m carefully chosen arbitrary independent parameters such as $q_i \quad (i = 1 \cdots m)$. One example of these parameters is the degrees of freedom in the finite element method. In the presence of second order nonlinearities in the strain stress displacement relationships (e.g. Sanders' shell theory), the strain displacement relationship can be presented in a form of Kronecker products:

$$\epsilon(\xi) = \left[S_1(\xi)\right]\left\{q\right\} + \left[S_2(\xi)\right]\left(\left\{q\right\} \otimes \left\{q\right\}\right) \tag{4.3}$$

where $f(\xi)$ denote being a function of one, two or three dimensional spatial coordinates ξ. $\left\{q\right\}$ is the vector of arbitrary parameters and $S_1(\xi)$ and $S_2(\xi)$ are two matrices obtained from the kinematic relationships. Using the constitutive equation, the stress field can be obtained from the following equation:

$$\sigma(\xi) = \left[C\right]\epsilon(\xi) \tag{4.4}$$

where $\left[C\right]$ is the constitutive matrix. The Kronecker power operator is defined as follows (for example $q^{\otimes 3} = q \otimes q \otimes q$):

$$\begin{aligned} q^{\otimes 1} &= q \\ q^{\otimes p} &= q \otimes q^{\otimes (p-1)} \end{aligned} \tag{4.5}$$

Substituting (4.3) and (4.4) in (4.2) yields the following equation for the strain energy:

$$\begin{aligned} U = &\left\{q\right\}^{\mathrm{T}}\left(\frac{1}{2}\int_{\Omega}\left[S_1\right]^{\mathrm{T}}\left[C\right]\left[S_1\right]\mathrm{d}\Omega\right)\left\{q\right\} + \left\{q\right\}^{\mathrm{T}}\left(\frac{1}{2}\int_{\Omega}\left[S_1\right]^{\mathrm{T}}\left[C\right]\left[S_2\right]\mathrm{d}\Omega\right)\left\{q^{\otimes 2}\right\} \\ &+ \left\{q^{\otimes 2}\right\}^{\mathrm{T}}\left(\frac{1}{2}\int_{\Omega}\left[S_2\right]^{\mathrm{T}}\left[C\right]\left[S_1\right]\mathrm{d}\Omega\right)\left\{q\right\} + \left\{q^{\otimes 2}\right\}^{\mathrm{T}}\left(\frac{1}{2}\int_{\Omega}\left[S_2\right]^{\mathrm{T}}\left[C\right]\left[S_2\right]\mathrm{d}\Omega\right)\left\{q^{\otimes 2}\right\} \end{aligned} \tag{4.6}$$

By performing the integrations of Equation (4.6), the well-known linear and nonlinear stiffness matrices can be obtained. Therefore Equation (4.6) can be rewritten in the following short form:

$$U = \left\{q\right\}^{\mathrm{T}}\left[K_{11}\right]\left\{q\right\} + \left\{q\right\}^{\mathrm{T}}\left[K_{12}\right]\left\{q^{\otimes 2}\right\} + \left\{q^{\otimes 2}\right\}^{\mathrm{T}}\left[K_{21}\right]\left\{q\right\} + \left\{q^{\otimes 2}\right\}^{\mathrm{T}}\left[K_{22}\right]\left\{q^{\otimes 2}\right\} \tag{4.7}$$

. One particular and widely used example of such problems is the nonlinear internal strain energy of a thin shell or a Euler beam ([11, 12, 13, 14] and etc.) modeled with second-order nonlinear kinematics. As will be shown, developing the equations of motion of the elastic structure in their Lagrangian form, requires obtaining the derivatives of the internal strain energy with respect to the chosen arbitrary parameters (e.g. degrees of freedom in FEM). Using general notation of scalar Φ (e.g. internal strain energy in elasticity problems), x_i as independent variables (e.g. degrees of freedom in FEM), in the classic approach, due to lack of a concise mathematical matrix form for derivatives of the second, third and fourth terms, the formulation is usually expressed using an expanded system with a (very large) set of summations:

$$\Phi = \sum_{i=1}^{m}\sum_{j=1}^{m} y_{1,i,j}x_i x_j + \sum_{i=1}^{m}\sum_{j=1}^{m}\sum_{k=1}^{m} y_{2,i,j,k}x_i x_j x_k + \sum_{i=1}^{m}\sum_{j=1}^{m}\sum_{k=1}^{m}\sum_{l=1}^{m} y_{3,i,j,k,l}x_i x_j x_k x_l \tag{4.8}$$

Then, taking the derivatives of the individual terms:

$$\frac{\partial \Phi}{\partial x_q} = \sum_{i=1}^{m} z_{1,i}x_i + \sum_{i=1}^{m}\sum_{j=1}^{m} z_{2,i,j}x_i x_j + \sum_{i=1}^{m}\sum_{j=1}^{m}\sum_{k=1}^{m} z_{3,i,j,k}x_i x_j x_k \quad (q = 1 \cdots m) \tag{4.9}$$

where $y_{s,,,}$ and $z_{s,,}$ are obtained from the system properties (e.g. elements of different stiffness matrices in elasticity problems). Examples of this form of expression for equations of motion include Equations: (23-25) in [15], (24) in [16], (36) in [17], (40) in [18], (42) in

[19], (53) in [11], (41) in [20], (28) in [21], (26) in [22] and (26) in [23].

This paper presents a method to express such systems in their natural matrix form using Kronecker products:

$$\Phi = \Phi_{11} + \Phi_{12} + \Phi_{21} + \Phi_{22} \tag{4.10}$$

Where;

$$\Phi_{11} = \boldsymbol{x}^{\intercal} \boldsymbol{Y_{11}} \boldsymbol{x} \tag{4.11a}$$

$$\Phi_{12} = \boldsymbol{x}^{\intercal} \boldsymbol{Y_{12}} (\boldsymbol{x} \otimes \boldsymbol{x}) \tag{4.11b}$$

$$\Phi_{21} = (\boldsymbol{x} \otimes \boldsymbol{x})^{\intercal} \boldsymbol{Y_{21}} \boldsymbol{x} \tag{4.11c}$$

$$\varphi_{22} = (\boldsymbol{x} \otimes \boldsymbol{x})^{\intercal} \boldsymbol{Y_{22}} (\boldsymbol{x} \otimes \boldsymbol{x}) \tag{4.11d}$$

and Φ is a scalar (e.g. the strain energy), $\boldsymbol{x}$ is the vector of degrees of freedom of the system and $\boldsymbol{Y_{ij}}$ is a constant property matrix (e.g. mass or stiffness matrices in finite element formulation). There are certain advantages in formulating these systems in the form of a Kronecker product, such as development of equations of motions in Lagrangian form by employing generalized coordinates method (similar to [24]) in matrix form. The objective of this article is to develop a concise mathematical formulation that provides the derivative of this type of system in an easily implementable matrix formulation:

$$\frac{\partial \Phi}{\partial \boldsymbol{x}} = \tilde{\boldsymbol{K}}_{11} \boldsymbol{x} + \tilde{\boldsymbol{K}}_{12} \boldsymbol{x}^{\otimes 2} + \tilde{\boldsymbol{K}}_{21} \boldsymbol{x}^{\otimes 2} + \tilde{\boldsymbol{K}}_{22} \boldsymbol{x}^{\otimes 3} \tag{4.12}$$

Where the Kronecker power operator is defined as $\boldsymbol{x}^{\otimes(p+1)} = \boldsymbol{x}^{\otimes p} \otimes \boldsymbol{x}$ $(\boldsymbol{x}^{\otimes 1} = \boldsymbol{x}$ and $p = 1, 2, \cdots)$.

4.2.1 Vector Kronecker Power Derivatives

In this subsection the derivatives of Kronecker powers of a vector with respect to itself are presented. These are necessary components to obtain derivatives of combined matrix-vector Kronecker powers of Equation (4.11). It should be noted that, the notations, important identities from matrix calculus that are used in the following sections can be found in Appendix A.

4.2.1.1 Second Order

Using Equation (I.A.91i), for the derivative of $\boldsymbol{x}^{\otimes 2}$ with respect to $\boldsymbol{x}$ we have:

$$\begin{aligned}\frac{\partial \boldsymbol{x}^{\otimes 2}}{\partial \boldsymbol{x}} = \frac{\partial \boldsymbol{x} \otimes \boldsymbol{x}}{\partial \boldsymbol{x}} &= \frac{\partial \boldsymbol{x}}{\partial \boldsymbol{x}} \otimes \boldsymbol{x} + \left(\boldsymbol{I}_K \underset{(K\times K)}{\otimes} \boldsymbol{U}\right)\left(\frac{\partial \boldsymbol{x}}{\partial \boldsymbol{x}} \otimes \boldsymbol{x}\right)\left(\boldsymbol{I}_1 \underset{(1\times 1)}{\otimes} \boldsymbol{U}\right) \\ &= vec\left(\boldsymbol{I}_K\right) \otimes \boldsymbol{x} + \left(\boldsymbol{I}_K \underset{(K\times K)}{\otimes} \boldsymbol{U}\right)\left(vec\left(\boldsymbol{I}_K\right) \otimes \boldsymbol{x}\right) \\ &= \left(\boldsymbol{I}_{K^3} + \boldsymbol{I}_K \underset{(K\times K)}{\otimes} \boldsymbol{U}\right)\left(vec\left(\boldsymbol{I}_K\right) \otimes \boldsymbol{x}\right) \\ &= \left(\boldsymbol{I}_{K^3} + \boldsymbol{I}_K \underset{(K\times K)}{\otimes} \boldsymbol{U}\right)\left(vec\left(\boldsymbol{I}_K \otimes \boldsymbol{x}\right)\right)\end{aligned} \tag{4.13}$$

Introducing the following aliases:

$$\boldsymbol{W3} = \boldsymbol{I}_{K^3} + \boldsymbol{I}_K \underset{(K\times K)}{\otimes} \boldsymbol{U} \tag{4.14a}$$

$$\boldsymbol{VI3}_{K^3\times K} = \underset{(K^2\times K)}{vecI}\left(vec(\boldsymbol{I}_K)\right) \tag{4.14b}$$

and using Equation (I.A.85), Equation (4.13) can be rewritten as:

$$\frac{\partial \boldsymbol{x}^{\otimes 2}}{\partial \boldsymbol{x}} = \boldsymbol{W3VI3x} \tag{4.15}$$

4.2.1.2 Third Order

Employing Equations (I.A.91i) and (4.13), for the derivative of $\boldsymbol{x}^{\otimes 3}$ with respect to $\boldsymbol{x}$ we have:

$$\begin{aligned}\frac{\partial \boldsymbol{x}^{\otimes 3}}{\partial \boldsymbol{x}} = \frac{\partial\left(\boldsymbol{x}\otimes\boldsymbol{x}^{\otimes 2}\right)}{\partial \boldsymbol{x}} &= \frac{\partial \boldsymbol{x}}{\partial \boldsymbol{x}}\otimes\boldsymbol{x}^{\otimes 2} + \left(\boldsymbol{I}_K \otimes \underset{(K\times K^2)}{\boldsymbol{U}}\right)\left(\frac{\partial \boldsymbol{x}^{\otimes 2}}{\partial \boldsymbol{x}}\otimes\boldsymbol{x}\right)\left(\boldsymbol{I}_1 \otimes \underset{(1\times 1)}{\boldsymbol{U}}\right) \\ &= vec\left(\boldsymbol{I}_K\right)\otimes\boldsymbol{x}^{\otimes 2} + \left(\boldsymbol{I}_K \otimes \underset{(K\times K^2)}{\boldsymbol{U}}\right)\left(\left(\boldsymbol{W}\boldsymbol{3}vec\left(\boldsymbol{I}_K\otimes\boldsymbol{x}\right)\right)\otimes\boldsymbol{x}\right) \\ &= \underset{(K^2\times K^2)}{vecI}\left(vec\left(\boldsymbol{I}_K\right)\right)\boldsymbol{x}^{\otimes 2} + \left(\boldsymbol{I}_K \otimes \underset{(K\times K^2)}{\boldsymbol{U}}\right)\left(\left(\boldsymbol{W}\boldsymbol{3}vec\left(\boldsymbol{I}_K\otimes\boldsymbol{x}\right)\right)\otimes\boldsymbol{x}\right)\end{aligned} \tag{4.16}$$

Recalling (I.A.91g) and the structure of $\boldsymbol{I}_K$ that contains only K non-zero entries yields:

$$\begin{aligned}\boldsymbol{W}\boldsymbol{3}\left(vec\left(\boldsymbol{I}_K\otimes\boldsymbol{x}\right)\right) = vec\left(\boldsymbol{W}\boldsymbol{3}\left(vec\left(\boldsymbol{I}_K\otimes\boldsymbol{x}\right)\right)\right) &= \sum_{c=1}^{K^3}\left(\boldsymbol{I}_K\otimes\boldsymbol{x}\right)_{:,c}^{\mathsf{T}}\otimes\boldsymbol{W}\boldsymbol{3}_{:,c} \\ &= \sum_{m=1}^{K}\sum_{j=1}^{K} x_j\boldsymbol{W}\boldsymbol{3}_{:,j+(m-1)(K+1)K}\end{aligned} \tag{4.17}$$

Introducing $m' \triangleq j+(m-1)(K+1)K$ as an alias and substituting Equation (4.17) into (4.33) and considering the fact that x_j is a scalar, we have the following results:

$$\boldsymbol{W}\boldsymbol{3}\left(vec\left(\boldsymbol{I}_K\otimes\boldsymbol{x}\right)\right)\otimes\boldsymbol{x} = \sum_{m=1}^{K}\sum_{j=1}^{K}\left(\boldsymbol{W}\boldsymbol{3}_{:,m'}\right)\otimes\left(x_j\boldsymbol{x}\right) \tag{4.18}$$

On the other hand:

$$\left(x_j\boldsymbol{x}\right) = \underset{(K\times K)}{\boldsymbol{E}\boldsymbol{I}_j}\boldsymbol{x}^{\otimes 2} \tag{4.19}$$

The Kronecker product of Equation (4.19) can be converted to matrix multiplication using Equation (I.A.85):

$$\sum_{m=1}^{K}\sum_{j=1}^{K}\left(\boldsymbol{W}\boldsymbol{3}_{:,m'}\right)\otimes\left(x_j\boldsymbol{x}\right) = \left(\sum_{m=1}^{K}\sum_{j=1}^{K}\underset{(K^3\times K)}{vecI}\left(\boldsymbol{W}\boldsymbol{3}_{:,m'}\right)\underset{(K\times K)}{\boldsymbol{E}\boldsymbol{I}_j}\right)\boldsymbol{x}^{\otimes 2} \tag{4.20}$$

To simplify Equation (4.18) further, first recalling (4.14a) we decompose $\boldsymbol{W3}_{:,m'}$ back to its components again. Both components are permutation matrix types so at each column they have only a single "non-zero" entry, typical of unit vectors.
For the first component, it should be noted that $(\boldsymbol{I}_{K^3})_{:,m'} = \underset{(m')}{\boldsymbol{e}}_{K^3}$. Therefore the summation within $\underset{(\times)}{vecI}()$ operator disappears. Hence:

$$\begin{aligned}\boldsymbol{VI4}_{(K^4\times K^2)} &\triangleq \sum_{m=1}^{K}\sum_{j=1}^{K} \underset{(K^3\times K)}{vecI}\left((\boldsymbol{I}_{K^3})_{:,m'}\right)\underset{(K\times K)}{\boldsymbol{EI}_j} = \sum_{m=1}^{K}\sum_{j=1}^{K}\left(\left(\underset{(K^3)}{\boldsymbol{e}_{m'}}\otimes\boldsymbol{I}_K\right)\left(\underset{(K)}{\boldsymbol{e}^\top_j}\otimes\boldsymbol{I}_K\right)\right)\\ &= \sum_{m=1}^{K}\sum_{j=1}^{K}\left(\left(\underset{(K^3)}{\boldsymbol{e}_{m'}}\underset{(K)}{\boldsymbol{e}^\top_j}\right)\otimes(\boldsymbol{I}_K\boldsymbol{I}_K)\right) = \sum_{m=1}^{K}\sum_{j=1}^{K}\left(\underset{(K^3\times K)}{\boldsymbol{E}_{m'j}}\otimes\boldsymbol{I}_K\right)\end{aligned} \tag{4.21}$$

Therefore $\boldsymbol{VI4}$ has the following structure:

$$\boldsymbol{VI4}_{(K^4\times K^2)} \triangleq \sum_{m=1}^{K}\sum_{j=1}^{K}\left(\underset{(K^3\times K)}{\boldsymbol{E}_{m'j}}\otimes\boldsymbol{I}_K\right) = \begin{array}{c} \\ 1 \\ 2 \\ \vdots \\ K \\ K+1 \\ \vdots \\ K(K+1)+1 \\ K(K+1)+2 \\ \vdots \\ K(K+1)+K \\ \vdots \\ K^3 \end{array}\begin{array}{c} \begin{array}{cccc} 1 & \cdots & & K \end{array} \\ \begin{bmatrix} \boldsymbol{I}_K & \boldsymbol{0}_K & \cdots & \boldsymbol{0}_K \\ \boldsymbol{0}_K & \boldsymbol{I}_K & \cdots & \boldsymbol{0}_K \\ \vdots & \vdots & \ddots & \vdots \\ \boldsymbol{0}_K & \boldsymbol{0}_K & \cdots & \boldsymbol{I}_K \\ \boldsymbol{0}_K & \boldsymbol{0}_K & \cdots & \boldsymbol{0}_K \\ \vdots & \vdots & \ddots & \vdots \\ \boldsymbol{I}_K & \boldsymbol{0}_K & \cdots & \boldsymbol{0}_K \\ \boldsymbol{0}_K & \boldsymbol{I}_K & \cdots & \boldsymbol{0}_K \\ \vdots & \vdots & \ddots & \vdots \\ \boldsymbol{0}_K & \boldsymbol{0}_K & \cdots & \boldsymbol{I}_K \\ \vdots & \vdots & \ddots & \vdots \\ \boldsymbol{0}_K & \boldsymbol{0}_K & \cdots & \boldsymbol{I}_K \end{bmatrix} \end{array} \tag{4.22}$$

In other words, $\boldsymbol{VI4}$ is a block matrix with block dimension $K\times K$ and dimension $K^3\times K$ such that the locations of its non-zero identity blocks are given by:

$$(j+(m-1)(K+1)K, j) \quad j,m\in\{1,2,\cdots,K\} \tag{4.23}$$

Inspecting the second component of $\boldsymbol{W3}$ reveals it has the following structure:

$$\boldsymbol{I}_K \otimes \underset{(K\times K)}{\boldsymbol{U}} = \begin{bmatrix} \underset{(K\times K)}{\boldsymbol{U}} & \boldsymbol{0}_{K^2} & \cdots & \boldsymbol{0}_{K^2} \\ \boldsymbol{0}_{K^2} & \underset{(K\times K)}{\boldsymbol{U}} & \cdots & \boldsymbol{0}_{K^2} \\ \vdots & \ddots & & \boldsymbol{0}_{K^2} \\ \boldsymbol{0}_{K^2} & \boldsymbol{0}_{K^2} & \cdots & \underset{(K\times K)}{\boldsymbol{U}} \end{bmatrix} \tag{4.24}$$

That is a block matrix with block dimension $K^2 \times K^2$ and the outer dimension $K \times K$. The diagonal of this block matrix is comprised of $\underset{(K\times K)}{\boldsymbol{U}}$ elementary permutation matrices. Again, using some mathematical manipulations, considering the location of "1" elements on the right-hand side of Equation (4.24), for the second component we have:

$$\boldsymbol{UI4}_{(K^4\times K^2)} \triangleq \sum_{m=1}^{K}\sum_{j=1}^{K} \underset{(K^3\times K)}{vecI}\left(\left(\boldsymbol{I}_K \otimes \underset{(K\times K)}{\boldsymbol{U}}\right)_{:,m'}\right) \underset{(K\times K)}{\boldsymbol{EI}_j} = \begin{array}{c} \\ 1 \\ 2 \\ \vdots \\ K+1 \\ \vdots \\ 2K+1 \\ \vdots \\ K(K-1)+1 \\ K^2-K \\ \vdots \\ K^2+2 \\ \vdots \\ K^3 \end{array} \begin{array}{c} \begin{array}{ccccc} 1 & 2 & 3 & \cdots & K \end{array} \\ \begin{bmatrix} \boldsymbol{I}_K & \boldsymbol{0}_K & \cdots & & \boldsymbol{0}_K \\ \boldsymbol{0}_K & \boldsymbol{0}_K & \cdots & & \boldsymbol{0}_K \\ \vdots & \vdots & \ddots & & \vdots \\ \boldsymbol{0}_K & \boldsymbol{I}_K & \cdots & & \boldsymbol{0}_K \\ \vdots & \vdots & \ddots & & \vdots \\ \boldsymbol{0}_K & \boldsymbol{0}_K & \boldsymbol{I}_K & \cdots & \boldsymbol{0}_K \\ \vdots & \vdots & \ddots & & \vdots \\ \boldsymbol{0}_K & \boldsymbol{0}_K & \cdots & & \boldsymbol{I}_K \\ \boldsymbol{0}_K & \boldsymbol{0}_K & \cdots & & \boldsymbol{0}_K \\ \vdots & \vdots & \ddots & & \vdots \\ \boldsymbol{I}_K & \boldsymbol{0}_K & \cdots & & \boldsymbol{0}_K \\ \vdots & \vdots & \ddots & & \vdots \\ \boldsymbol{0}_K & \boldsymbol{0}_K & \cdots & & \boldsymbol{I}_K \end{bmatrix} \end{array} \tag{4.25}$$

$\boldsymbol{UI4}$ is therefore a block matrix with block dimension $K \times K$ and outer dimension $K^3 \times K$. The locations of its non-zero identity blocks are given by:

$$\Big((m-1)K^2 + Kj + m - K, j\Big) \quad j, m \in \{1, 2, \cdots, K\} \tag{4.26}$$

Recalling Equation (I.A.85) and the fact that the locations of "1" entries in $vec(\boldsymbol{I}_n)$ are located at $m'' = 1 + (m-1)(n+1) \quad (j = 1 \cdots n)$, for the case of $\boldsymbol{I}_K : m'' = 1 + (m-1)(K+1)$ the

results is:

$$\begin{aligned}\underset{(K^2\times K^2)}{vecI}(vec(\boldsymbol{I}_K)) &= \sum_{m=1}^{K}\left(\underset{(K^2)}{\boldsymbol{e}_{m''}}\otimes\boldsymbol{I}_{K^2}\right)=\sum_{m=1}^{K}\left(\underset{(K^2)}{\boldsymbol{e}_{m''}}\otimes\boldsymbol{I}_K\otimes\boldsymbol{I}_K\right)=\sum_{m=1}^{K}\left(\underset{(K^2)}{\boldsymbol{e}_{m''}}\otimes\left(\sum_{j=1}^{K}\underset{(K)}{\boldsymbol{e}_j}\otimes\underset{(K)}{\boldsymbol{e}^{\intercal}_j}\right)\otimes\boldsymbol{I}_K\right)\\ &= \sum_{m=1}^{K}\sum_{j=1}^{K}\left(\underset{(K^2)}{\boldsymbol{e}_{m''}}\otimes\underset{(K)}{\boldsymbol{e}_j}\right)\otimes\underset{(K)}{\boldsymbol{e}^{\intercal}_j}\otimes\boldsymbol{I}_K\end{aligned} \tag{4.27}$$

On the other hand, using (I.A.83):

$$\underset{(K^2)}{\boldsymbol{e}_{m''}}\otimes\underset{(K)}{\boldsymbol{e}_j}=\underset{(K^2)}{\boldsymbol{e}_{1+(m-1)(K+1)}}\otimes\underset{(K)}{\boldsymbol{e}_j}=\underset{(K^3)}{\boldsymbol{e}_{(1+(m-1)(K+1)-1)K+j}}=\underset{(K^3)}{\boldsymbol{e}_{m'}} \tag{4.28}$$

Therefore:

$$\underset{(K^2\times K^2)}{vecI}(vec(\boldsymbol{I}_K))=\sum_{m=1}^{K}\sum_{j=1}^{K}\left(\underset{(K^3)}{\boldsymbol{e}_{m'}}\otimes\underset{(K)}{\boldsymbol{e}^{\intercal}_j}\right)\otimes\boldsymbol{I}_K=\sum_{m=1}^{K}\sum_{j=1}^{K}\left(\underset{(K^3\times K)}{\boldsymbol{E}_{m'j}}\otimes\boldsymbol{I}_K\right)=\boldsymbol{VI4} \tag{4.29}$$

Defining the following alias:

$$\boldsymbol{W4}=\left(\boldsymbol{I}_K\otimes\underset{(K\times K^2)}{\boldsymbol{U}}\right) \tag{4.30}$$

Subsequently using Equations (4.22),(4.25) and (4.29) yields:

$$\frac{\partial\boldsymbol{x}^{\otimes 3}}{\partial\boldsymbol{x}}\triangleq\boldsymbol{V}_{12}\boldsymbol{x}^{\otimes 2}=(\boldsymbol{VI4}+\boldsymbol{W4}(\boldsymbol{UI4}+\boldsymbol{VI4}))\boldsymbol{x}^{\otimes 2} \tag{4.31}$$

4.2.1.3 Fourth Order

Introducing the following alias:

$$\boldsymbol{W5}=\boldsymbol{I}_{K^5}+\boldsymbol{I}_K\otimes\underset{(K^2\times K^2)}{\boldsymbol{U}} \tag{4.32}$$

and using Equation (I.A.91i), for $\boldsymbol{x}^{\otimes 4}$ we have:

$$\frac{\partial \boldsymbol{x}^{\otimes 4}}{\partial \boldsymbol{x}} = \boldsymbol{W5}\left[(\boldsymbol{W3}\,(vec\,(\boldsymbol{I}_K)\otimes \boldsymbol{x}))\otimes \boldsymbol{x}^{\otimes 2}\right] = \boldsymbol{W5}\left[(\boldsymbol{W3}\,(vec\,(\boldsymbol{I}_K\otimes \boldsymbol{x})))\otimes \boldsymbol{x}^{\otimes 2}\right] \tag{4.33}$$

Taking a similar approach to that presented in Section 4.2.2.2, yields:

$$\begin{aligned}\left[(\boldsymbol{W3}\,(vec\,(\boldsymbol{I}_K)\otimes \boldsymbol{x}))\otimes \boldsymbol{x}^{\otimes 2}\right] = \left[(\boldsymbol{W3}\,(vec\,(\boldsymbol{I}_K\otimes \boldsymbol{x})))\otimes \boldsymbol{x}^{\otimes 2}\right] &= \sum_{m=1}^{K}\sum_{j=1}^{K}(\boldsymbol{W3}_{:,m'})\otimes\left(x_j\boldsymbol{x}^{\otimes 2}\right) \\ &= \left(\sum_{m=1}^{K}\sum_{j=1}^{K}\underset{(K^3\times K^2)}{vecI}(\boldsymbol{W3}_{:,m'})\underset{(K^2\times K)}{\boldsymbol{EI}_j}\right)\boldsymbol{x}^{\otimes 3}\end{aligned} \tag{4.34}$$

Again, decomposing $\boldsymbol{W3}$ back to its components and after some mathematical manipulations and considering the location of "1" entries in each column of $\boldsymbol{I}_{K^3}$ for the first component we have:

$$\boldsymbol{VI5}_{(K^5\times K^3)} \triangleq \sum_{m=1}^{K}\sum_{j=1}^{K}\underset{(K^3\times K^2)}{vecI}\left((\boldsymbol{I}_{K^3})_{:,m'}\right)\underset{(K^2\times K)}{\boldsymbol{EI}_j} = \begin{array}{c} \\ 1 \\ 2 \\ \vdots \\ K \\ K+1 \\ \vdots \\ K(K+1)+1 \\ K(K+1)+2 \\ \vdots \\ K(K+1)+K \\ \vdots \\ K^3 \end{array}\begin{array}{c} \begin{array}{cccc} 1 & & \cdots & K \end{array} \\ \begin{bmatrix} \boldsymbol{I}_{K^2} & \boldsymbol{0}_{K^2} & \cdots & \boldsymbol{0}_{K^2} \\ \boldsymbol{0}_{K^2} & \boldsymbol{I}_{K^2} & \cdots & \boldsymbol{0}_{K^2} \\ \vdots & \vdots & \ddots & \vdots \\ \boldsymbol{0}_{K^2} & \boldsymbol{0}_{K^2} & \cdots & \boldsymbol{I}_{K^2} \\ \boldsymbol{0}_{K^2} & \boldsymbol{0}_{K^2} & \cdots & \boldsymbol{0}_{K^2} \\ \vdots & \vdots & \ddots & \vdots \\ \boldsymbol{I}_{K^2} & \boldsymbol{0}_{K^2} & \cdots & \boldsymbol{0}_{K^2} \\ \boldsymbol{0}_{K^2} & \boldsymbol{I}_{K^2} & \cdots & \boldsymbol{0}_{K^2} \\ \vdots & \vdots & \ddots & \vdots \\ \boldsymbol{0}_{K^2} & \boldsymbol{0}_{K^2} & \cdots & \boldsymbol{I}_{K^2} \\ \vdots & \vdots & \ddots & \vdots \\ \boldsymbol{0}_{K^2} & \boldsymbol{0}_{K^2} & \cdots & \boldsymbol{I}_{K^2} \end{bmatrix} \end{array} \tag{4.35}$$

In other words, $\boldsymbol{VI5}$ has the same structure as $\boldsymbol{VI4}$ with the exception that the former is constructed from block dimension $K^2\times K^2$ instead of $K\times K$.

Similarly, for the second component we have:

$$\boldsymbol{UI5}_{\left(K^5\times K^3\right)} \triangleq \sum_{m=1}^{K}\sum_{j=1}^{K} \underset{(K^3\times K^2)}{vecI}\left(\left(\boldsymbol{I}_K \otimes \underset{(K\times K)}{\boldsymbol{U}}\right)_{:,m'}\right) \underset{(K^2\times K)}{\boldsymbol{EI}_j} = \begin{array}{c} \\ 1 \\ 2 \\ \vdots \\ K+1 \\ \vdots \\ 2K+1 \\ \vdots \\ K(K-1)+1 \\ K^2-K \\ \vdots \\ K^2+2 \\ \vdots \\ K^3 \end{array} \begin{array}{c} \begin{array}{ccccc} 1 & 2 & 3 & \cdots & K \end{array} \\ \begin{bmatrix} \boldsymbol{I}_{K^2} & \boldsymbol{0}_{K^2} & \cdots & & \boldsymbol{0}_{K^2} \\ \boldsymbol{0}_{K^2} & \boldsymbol{0}_{K^2} & \cdots & & \boldsymbol{0}_{K^2} \\ \vdots & \vdots & \ddots & & \vdots \\ \boldsymbol{0}_{K^2} & \boldsymbol{I}_{K^2} & \cdots & & \boldsymbol{0}_{K^2} \\ \vdots & \vdots & \ddots & & \vdots \\ \boldsymbol{0}_{K^2} & \boldsymbol{0}_{K^2} & \boldsymbol{I}_{K^2} & \cdots & \boldsymbol{0}_{K^2} \\ \vdots & \vdots & \ddots & & \vdots \\ \boldsymbol{0}_{K^2} & \boldsymbol{0}_{K^2} & \cdots & & \boldsymbol{I}_{K^2} \\ \boldsymbol{0}_{K^2} & \boldsymbol{0}_{K^2} & \cdots & & \boldsymbol{0}_{K^2} \\ \vdots & \vdots & \ddots & & \vdots \\ \boldsymbol{I}_{K^2} & \boldsymbol{0}_{K^2} & \cdots & & \boldsymbol{0}_{K^2} \\ \vdots & \vdots & \ddots & & \vdots \\ \boldsymbol{0}_{K^2} & \boldsymbol{0}_{K^2} & \cdots & & \boldsymbol{I}_{K^2} \end{bmatrix} \end{array} \tag{4.36}$$

Again ,the only difference between $\boldsymbol{UI5}$ and $\boldsymbol{UI4}$ is that the former is based on block $K^2 \times K^2$ instead of $K \times K$. Therefore:

$$\frac{\partial \boldsymbol{x}^{\otimes 4}}{\partial \boldsymbol{x}} = \boldsymbol{W5}(\boldsymbol{UI5} + \boldsymbol{VI5})\boldsymbol{x}^{\otimes 3} \tag{4.37}$$

4.2.2 System Derivatives

4.2.2.1 Linear-Linear Component

The linear-linear component of energies in the equations of motion has the following shape:

$$\Phi_{11} = \boldsymbol{x}^{\intercal}\boldsymbol{Y_{11}}\boldsymbol{x} \tag{4.38}$$

where the dimensions are: $\boldsymbol{x}_{1\times K}$ and $\boldsymbol{x}_{1\times K}^{\intercal}$ and $\boldsymbol{Y}_{11(K\times K)}$. Using identities of (I.A.91), the derivative of Φ_{11} can be expanded:

$$\begin{aligned}\frac{\partial \Phi_{11}}{\partial \boldsymbol{x}} &= \frac{\partial \boldsymbol{x}^{\intercal}}{\partial \boldsymbol{x}}(\boldsymbol{I}_1 \otimes \boldsymbol{Y_{11}}\boldsymbol{x}) + (\boldsymbol{I}_K \otimes \boldsymbol{x}^{\intercal})\left(\frac{\partial(\boldsymbol{Y_{11}}\boldsymbol{x})}{\partial \boldsymbol{x}}\right) = \boldsymbol{I}_K\boldsymbol{Y_{11}}\boldsymbol{x} + (\boldsymbol{I}_K \otimes \boldsymbol{x}^{\intercal})\,vec\,(\boldsymbol{Y_{11}}) \\ &= \boldsymbol{Y_{11}}\boldsymbol{x} + (\boldsymbol{Y}_{\boldsymbol{11}}^{\intercal} \otimes \boldsymbol{I}_1)\,vec\,(\boldsymbol{x}^{\intercal}) = \boldsymbol{Y_{11}}\boldsymbol{x} + \boldsymbol{Y}_{\boldsymbol{11}}^{\intercal}\boldsymbol{x}\end{aligned} \tag{4.39}$$

It should be noted that if $\boldsymbol{Y_{11}}$ is a symmetric matrix, then $\boldsymbol{Y_{11}} = \boldsymbol{Y}_{\boldsymbol{11}}^{\intercal}$; hence (4.39) becomes:

$$\frac{\partial \Phi_{11}}{\partial \boldsymbol{x}} = 2\boldsymbol{Y_{11}}\boldsymbol{x} \tag{4.40}$$

4.2.2.2 Linear-Nonlinear Component

The nonlinear-linear component has the following form:

$$\Phi_{12} = \boldsymbol{x}^{\intercal}\boldsymbol{Y_{12}}(\boldsymbol{x} \otimes \boldsymbol{x}) \tag{4.41}$$

where the dimensions are: $\boldsymbol{x}_{1\times K}^{\intercal}$, $(\boldsymbol{x} \otimes \boldsymbol{x})_{K^2\times 1}$ and $\boldsymbol{Y_{12}}_{(K\times K^2)}$. For convenience and briefness $\boldsymbol{Y_{12}}$ is denoted $\boldsymbol{Y}$ through this section. At the first step we vectorize Φ_{12} to the following series:

$$\Phi_{12} = \sum_{i=1}^{K^2}\Phi_{12,i} \triangleq \sum_{i=1}^{K^2}\overbrace{\left(\boldsymbol{x}^{\intercal}\boldsymbol{Y}_{:,\boldsymbol{i}}\right)}^{\triangleq f_{1i}}\overbrace{\left(\underset{(K^2)}{\boldsymbol{e}_i^{\intercal}}(\boldsymbol{x} \otimes \boldsymbol{x})\right)}^{\triangleq f_{2i}} \tag{4.42}$$

It should be noted that both f_{1i} and f_{2i} are scalar type, therefore both inner products are commutative or:

$$\left(\boldsymbol{x}^{\intercal}\boldsymbol{Y}_{:,\boldsymbol{i}}\right)\left(\underset{(K^2)}{\boldsymbol{e}_i^{\intercal}}(\boldsymbol{x} \otimes \boldsymbol{x})\right) = \left(\left(\boldsymbol{Y}_{:,\boldsymbol{i}}\right)^{\intercal}\boldsymbol{x}\right)\left((\boldsymbol{x} \otimes \boldsymbol{x})^{\intercal}\underset{(K^2)}{\boldsymbol{e}_i}\right) = \left(\boldsymbol{Y}_{:,\boldsymbol{i}}\right)^{\intercal}\left(\boldsymbol{x}(\boldsymbol{x} \otimes \boldsymbol{x})^{\intercal}\underset{(K^2)}{\boldsymbol{e}_i}\right) \tag{4.43}$$

The second term on the right hand side of Equation (4.43) is a vector with a size of $K^2 \times 1$, therefore employing Equation (I.A.91f) yields:

$$\begin{aligned}\left(\boldsymbol{x}(\boldsymbol{x}\otimes\boldsymbol{x})^{\intercal}\underset{(K^2)}{\boldsymbol{e}_i}\right) &= vec\left(\boldsymbol{x}(\boldsymbol{x}\otimes\boldsymbol{x})^{\intercal}\underset{(K^2)}{\boldsymbol{e}_i}\right) = \left(\underset{(K^2)}{\boldsymbol{e}^{\intercal}_i}\otimes\boldsymbol{I}_K\right)vec\left(\boldsymbol{x}(\boldsymbol{x}\otimes\boldsymbol{x})^{\intercal}\right)\\ &= \left(\underset{(K^2)}{\boldsymbol{e}^{\intercal}_i}\otimes\boldsymbol{I}_K\right)(\boldsymbol{x}\otimes(\boldsymbol{x}\otimes\boldsymbol{x})) = \left(\underset{(K^2)}{\boldsymbol{e}^{\intercal}_i}\otimes\boldsymbol{I}_K\right)\boldsymbol{x}^{\otimes 3}\end{aligned} \tag{4.44}$$

Subsequently:

$$\Phi_{12,i} = \left(\boldsymbol{Y}_{:,\boldsymbol{i}}\right)^{\intercal}\left(\underset{(K^2)}{\boldsymbol{e}^{\intercal}_i}\otimes\boldsymbol{I}_K\right)\boldsymbol{x}^{\otimes 3} = \left[\boldsymbol{Y}^{\intercal}_{\boldsymbol{i},:}\left(\underset{(K^2)}{\boldsymbol{e}^{\intercal}_i}\otimes\boldsymbol{I}_K\right)\right]\boldsymbol{x}^{\otimes 3} \tag{4.45}$$

Recalling Equation (I.A.84), the bracketed term on the left-hand side of Equation (4.45) can be simplified as:

$$\tilde{\boldsymbol{y}}^{\intercal}_{12} = \sum_{i=1}^{K^2}\left[\boldsymbol{Y}^{\intercal}_{\boldsymbol{i},:}\left(\underset{(K^2)}{\boldsymbol{e}^{\intercal}_i}\otimes\boldsymbol{I}_K\right)\right] = \sum_{i=1}^{K^2}\boldsymbol{Y}^{\intercal}_{\boldsymbol{i},:}\underset{(K\times K^2)}{\boldsymbol{E}\boldsymbol{I}_i} = (vec(\boldsymbol{Y}))^{\intercal} \tag{4.46}$$

Therefore:

$$\Phi_{12} = \boldsymbol{x}^{\intercal}\boldsymbol{Y}(\boldsymbol{x}\otimes\boldsymbol{x}) = \tilde{\boldsymbol{y}}^{\intercal}_{12}\boldsymbol{x}^{\otimes 3} \tag{4.47}$$

Using Equations (4.31) and (I.A.91h):

$$\frac{\partial\Phi_{12}}{\partial\boldsymbol{x}} = \frac{\partial\left(\tilde{\boldsymbol{y}}^{\intercal}_{12}\boldsymbol{x}^{\otimes 3}\right)}{\partial\boldsymbol{x}} = \frac{\partial\tilde{\boldsymbol{y}}^{\intercal}_{12}}{\partial\boldsymbol{x}}\left(\boldsymbol{I}_1\otimes\boldsymbol{x}^{\otimes 3}\right) + \left(\boldsymbol{I}_K\otimes\tilde{\boldsymbol{y}}^{\intercal}_{12}\right)\left(\frac{\partial\boldsymbol{x}^{\otimes 3}}{\partial\boldsymbol{x}}\right) = 0 + \left(\boldsymbol{I}_K\otimes\tilde{\boldsymbol{y}}^{\intercal}_{12}\right)(\boldsymbol{V}_{12})\boldsymbol{x}^{\otimes 2} \tag{4.48}$$

Defining the following alias:

$$\tilde{\boldsymbol{Z}}_{12} \triangleq \boldsymbol{I}_K\otimes\tilde{\boldsymbol{y}}^{\intercal}_{12} = \begin{bmatrix} \tilde{\boldsymbol{y}}^{\intercal}_{12} & \boldsymbol{0}_{(1\times K^3)} & \boldsymbol{0}_{(1\times(K^4-2K^3))} \\ \boldsymbol{0}_{(1\times K^3)} & \tilde{\boldsymbol{y}}^{\intercal}_{12} & \boldsymbol{0}_{(1\times(K^4-2K^3))} \\ \vdots & \ddots & \vdots \\ \boldsymbol{0}_{(1\times(K^4-2K^3))} & \boldsymbol{0}_{(1\times K^4)} & \tilde{\boldsymbol{y}}^{\intercal}_{12} \end{bmatrix} \tag{4.49a}$$

The differentiation of Equation (4.48) can be written as:

$$\frac{\partial \Phi_{12}}{\partial \boldsymbol{x}} = \tilde{\boldsymbol{K}}_{12}\boldsymbol{x}^{\otimes 2} \triangleq \left(\tilde{\boldsymbol{Z}}_{12}\boldsymbol{V}_{12}\right)\boldsymbol{x}^{\otimes 2} \tag{4.50}$$

4.2.2.3 Nonlinear-Linear Component

The nonlinear-linear component has the following form:

$$\Phi_{21} = (\boldsymbol{x}\otimes\boldsymbol{x})^{\intercal}\,\boldsymbol{Y}_{\boldsymbol{21}}\boldsymbol{x} \tag{4.51}$$

where the dimensions are: $(\boldsymbol{x}\otimes\boldsymbol{x})^{\intercal}_{1\times K^2}$, $\boldsymbol{x}_{K\times 1}$ and $\boldsymbol{Y}_{\boldsymbol{21}K^2\times K}$. Because this is a scalar and inner products of participating vectors are commutative:

$$\Phi_{21} = (\boldsymbol{x}\otimes\boldsymbol{x})^{\intercal}\,\boldsymbol{Y}_{\boldsymbol{21}}\boldsymbol{x} = (\boldsymbol{Y}_{\boldsymbol{21}}\boldsymbol{x})^{\intercal}\,(\boldsymbol{x}\otimes\boldsymbol{x}) = \boldsymbol{x}^{\intercal}\boldsymbol{Y}_{\boldsymbol{21}}^{\intercal}\,(\boldsymbol{x}\otimes\boldsymbol{x}) \tag{4.52}$$

Equation (4.52) has the same form as Equation (4.41). Therefore, using Equation (4.50), the derivative of Φ_{21} with respect to vector $\boldsymbol{x}$ can be written as:

$$\frac{\partial \Phi_{21}}{\partial \boldsymbol{x}} \triangleq \tilde{\boldsymbol{K}}_{21}\boldsymbol{x}^{\otimes 2} = \left(\tilde{\boldsymbol{Z}}_{21}\boldsymbol{V}_{12}\right)\boldsymbol{x}^{\otimes 2} \tag{4.53}$$

where $\tilde{\boldsymbol{Z}}_{21}$ can be obtained by substituting $\boldsymbol{Y}_{21}^{\intercal}$ in the place of $\boldsymbol{Y}$ in Equations (4.46) and (4.49a).

4.2.2.4 Nonlinear-Nonlinear Component

The fourth term of Φ has the following form:

$$\Phi_{22} = (\boldsymbol{x}\otimes\boldsymbol{x})^{\intercal}\,\boldsymbol{Y}_{\boldsymbol{22}}\,(\boldsymbol{x}\otimes\boldsymbol{x}) \tag{4.54}$$

where the dimensions are: $(\boldsymbol{x}\otimes\boldsymbol{x})^{\intercal}_{1\times K^2}$, $(\boldsymbol{x}\otimes\boldsymbol{x})_{K^2\times 1}$ and $\boldsymbol{Y}_{K^2\times K^2}$. For briefness, through this section $\boldsymbol{Y}_{22}$ is simply shown by $\boldsymbol{Y}$. At the first step we vectorize Φ_{22} to the following series:

$$\Phi_{22}=\sum_{i=1}^{K^2}\Phi_{22,i}\triangleq\sum_{i=1}^{K^2}\overbrace{\left((\boldsymbol{x}\otimes\boldsymbol{x})^{\intercal}\boldsymbol{Y}_{:,\boldsymbol{i}}\right)}^{\triangleq f_{1i}}\overbrace{\left(\underset{(K^2)}{\boldsymbol{e}^{\intercal}}{}_i\,(\boldsymbol{x}\otimes\boldsymbol{x})\right)}^{\triangleq f_{2i}} \tag{4.55}$$

It should be noted that both f_{1i} and f_{2i} are scalar types, therefore both inner products are commutative or:

$$\left((\boldsymbol{x}\otimes\boldsymbol{x})^{\intercal}\boldsymbol{Y}_{:,\boldsymbol{i}}\right)\left(\underset{(K^2)}{\boldsymbol{e}^{\intercal}}{}_i\,(\boldsymbol{x}\otimes\boldsymbol{x})\right)=\left(\left(\boldsymbol{Y}_{:,\boldsymbol{i}}\right)^{\intercal}(\boldsymbol{x}\otimes\boldsymbol{x})\right)\left((\boldsymbol{x}\otimes\boldsymbol{x})^{\intercal}\underset{(K^2)}{\boldsymbol{e}_i}\right)=\left(\boldsymbol{Y}_{:,\boldsymbol{i}}\right)^{\intercal}\left((\boldsymbol{x}\otimes\boldsymbol{x})(\boldsymbol{x}\otimes\boldsymbol{x})^{\intercal}\underset{(K^2)}{\boldsymbol{e}_i}\right) \tag{4.56}$$

The second term on the right-hand side of Equation (4.56) is a vector with a size of $K^2\times 1$; therefore employing Equation (I.A.91f) yields:

$$\begin{aligned}\left((\boldsymbol{x}\otimes\boldsymbol{x})(\boldsymbol{x}\otimes\boldsymbol{x})^{\intercal}\underset{(K^2)}{\boldsymbol{e}_i}\right)&=vec\left((\boldsymbol{x}\otimes\boldsymbol{x})(\boldsymbol{x}\otimes\boldsymbol{x})^{\intercal}\underset{(K^2)}{\boldsymbol{e}_i}\right)=\left(\underset{(K^2)}{\boldsymbol{e}^{\intercal}}{}_i\otimes\boldsymbol{I}_{K^2}\right)vec\left((\boldsymbol{x}\otimes\boldsymbol{x})(\boldsymbol{x}\otimes\boldsymbol{x})^{\intercal}\right)\\&=\left(\underset{(K^2)}{\boldsymbol{e}^{\intercal}}{}_i\otimes\boldsymbol{I}_{K^2}\right)((\boldsymbol{x}\otimes\boldsymbol{x})\otimes(\boldsymbol{x}\otimes\boldsymbol{x}))=\left(\underset{(K^2)}{\boldsymbol{e}^{\intercal}}{}_i\otimes\boldsymbol{I}_{K^2}\right)\boldsymbol{x}^{\otimes 4}\end{aligned} \tag{4.57}$$

Subsequently:

$$\Phi_{22,i}=\left(\boldsymbol{Y}_{:,\boldsymbol{i}}\right)^{\intercal}\left(\underset{(K^2)}{\boldsymbol{e}^{\intercal}}{}_i\otimes\boldsymbol{I}_{K^2}\right)\boldsymbol{x}^{\otimes 4}=\left[\boldsymbol{Y}_{\boldsymbol{i},:}^{\intercal}\left(\underset{(K^2)}{\boldsymbol{e}^{\intercal}}{}_i\otimes\boldsymbol{I}_{K^2}\right)\right]\boldsymbol{x}^{\otimes 4} \tag{4.58}$$

Recalling Equation (I.A.84), the bracketed term on the left hand side of Equation (4.58) can be simplified as:

$$\tilde{\boldsymbol{y}}_{22}^{\intercal}=\sum_{i=1}^{K^2}\left[\boldsymbol{Y}_{\boldsymbol{i},:}^{\intercal}\left(\underset{(K^2)}{\boldsymbol{e}^{\intercal}}{}_i\otimes\boldsymbol{I}_{K^2}\right)\right]=\sum_{i=1}^{K^2}\boldsymbol{Y}_{\boldsymbol{i},:}^{\intercal}\underset{(K^2\times K^2)}{\boldsymbol{E}\boldsymbol{I}_i}=(vec(\boldsymbol{Y}))^{\intercal} \tag{4.59}$$

Subsequently using Equations (4.35), (4.36) and (4.59) yields:

$$\frac{\partial\Phi_{22}}{\partial\boldsymbol{x}}=\sum_{i=1}^{K^2}\frac{\partial\Phi_{22,i}}{\partial\boldsymbol{x}}=0+\sum_{i=1}^{K^2}\left(\left(\boldsymbol{I}_K\otimes\left[\boldsymbol{Y}_{:,\boldsymbol{i}}^{\intercal}\left(\underset{(K^2)}{\boldsymbol{e}^{\intercal}}{}_i\otimes\boldsymbol{I}_{K^2}\right)\right]\right)\right)\frac{\partial\boldsymbol{x}^{\otimes 4}}{\partial\boldsymbol{x}}=\left(\boldsymbol{I}_K\otimes\tilde{\boldsymbol{y}}_{22}^{\intercal}\right)\boldsymbol{W}\boldsymbol{5}(\boldsymbol{V}\boldsymbol{I}\boldsymbol{5}+\boldsymbol{U}\boldsymbol{I}\boldsymbol{5})\boldsymbol{x}^{\otimes 3} \tag{4.60}$$

Defining the following aliases:

$$\tilde{\boldsymbol{Z}}_{22} \triangleq \boldsymbol{I}_K \otimes \tilde{\boldsymbol{y}}_{22}^{\mathsf{T}} = \begin{bmatrix} \tilde{\boldsymbol{y}}_{22}^{\mathsf{T}} & \mathbf{0}_{(1\times K^4)} & \mathbf{0}_{(1\times(K^5-2K^4))} \\ \mathbf{0}_{(1\times K^4)} & \tilde{\boldsymbol{y}}_{22}^{\mathsf{T}} & \mathbf{0}_{(1\times(K^5-2K^4))} \\ \vdots & \ddots & \vdots \\ \mathbf{0}_{(1\times(K^5-2K^4))} & \mathbf{0}_{(1\times K^4)} & \tilde{\boldsymbol{y}}_{22}^{\mathsf{T}} \end{bmatrix} \tag{4.61a}$$

$$\boldsymbol{V}_{22} = \boldsymbol{W5}(\boldsymbol{VI5} + \boldsymbol{UI5}) \tag{4.61b}$$

The differentiation of Equation (4.60) can be written as:

$$\frac{\partial \Phi_{22}}{\partial \boldsymbol{x}} = \tilde{\boldsymbol{K}}_{22}\boldsymbol{x}^{\otimes 3} \triangleq \left(\tilde{\boldsymbol{Z}}_{22}\boldsymbol{V}_{22}\right)\boldsymbol{x}^{\otimes 3} \tag{4.62}$$

4.3 Example of Application: Nonlinear Vibration of a Euler Beam

As an example, in this section the developed formulation is applied to derive the equations of motion of a constant area Euler beam using the generalized coordinates method. The model is then used for simulating the vibration of the beam under certain initial conditions. It should be noted that the objective of this section is to provide a simple example of the developed formulation on a semi-hypothetical problem rather than addressing nonlinear vibration of Euler beams. The beam element used for this analysis has four degrees of freedom (vertical displacement and rotations at each end) and is shown in Figure 4.1. The Hermite shape function for the vertical displacement of this beam is chosen to be[25]:

$$V(\xi) = \left[\mathbf{N}\right]\left\{\mathbf{x}\right\} = \begin{bmatrix} N_1(\xi) & N_2(\xi) & N_3(\xi) & N_4(\xi) \end{bmatrix} \begin{Bmatrix} x_1 \\ x_2 \\ x_3 \\ x_4 \end{Bmatrix} \tag{4.63}$$

where:

$$\begin{aligned} N_1(\xi) &= \frac{1}{4}(2 - 3\xi + \xi^3) \\ N_2(\xi) &= \frac{1}{4}a(1 - \xi - \xi^2 + \xi^3) \\ N_3(\xi) &= \frac{1}{4}(2 + 3\xi - \xi^3) \\ N_4(\xi) &= \frac{1}{4}a(-1 - \xi + \xi^2 + \xi^3) \end{aligned} \tag{4.64}$$

and $\xi = x/a$. The Lagrangian equation of motion based on Hamilton's principle can be expressed as follows:

$$\frac{\mathrm{d}}{\mathrm{dt}}\left[\frac{\partial \mathrm{T}}{\partial \dot{x}_i}\right] - \frac{\partial \mathrm{T}}{\partial x_i} + \frac{\partial \mathrm{U}}{\partial x_i} = \mathrm{q}_i, \quad (i = 1, 2, \cdots, \mathrm{n_{dofs}}) \tag{4.65}$$

where

- $\mathrm{n_{dofs}}$ is the total degrees of freedom of the system after assembling mass and stiffness matrices of elements and applying the constraints
- T is the total kinetic energy of the system
- U is the total elastic strain energy of the system
- q_i is the nodal external force

Equation (4.65) can be rewritten in matrix form as follows:

$$\frac{\mathrm{d}}{\mathrm{dt}}\left[\frac{\partial \mathrm{T}}{\partial \left\{\dot{\mathbf{x}}\right\}}\right] - \frac{\partial \mathrm{T}}{\partial \left\{\mathbf{x}\right\}} + \frac{\partial \mathrm{U}}{\partial \left\{\mathbf{x}\right\}} = \left\{\mathbf{q}\right\} \tag{4.66}$$

4.3.0.1 Kinetic Energy

Neglecting the rotational component, the kinetic energy of an infinitesimal beam section can be obtained from the following equation:

$$\mathrm{dT} = \frac{1}{2}(\dot{V}(\xi)^{\mathsf{T}}\dot{V}(\xi))\mathrm{dm} = \frac{1}{2}\left\{\dot{\mathbf{x}}\right\}^{\mathsf{T}}\left(\left[\mathbf{N}\right]^{\mathsf{T}}\left[\mathbf{N}\right]\mathrm{dm}\right)\left\{\dot{\mathbf{x}}\right\} \tag{4.67}$$

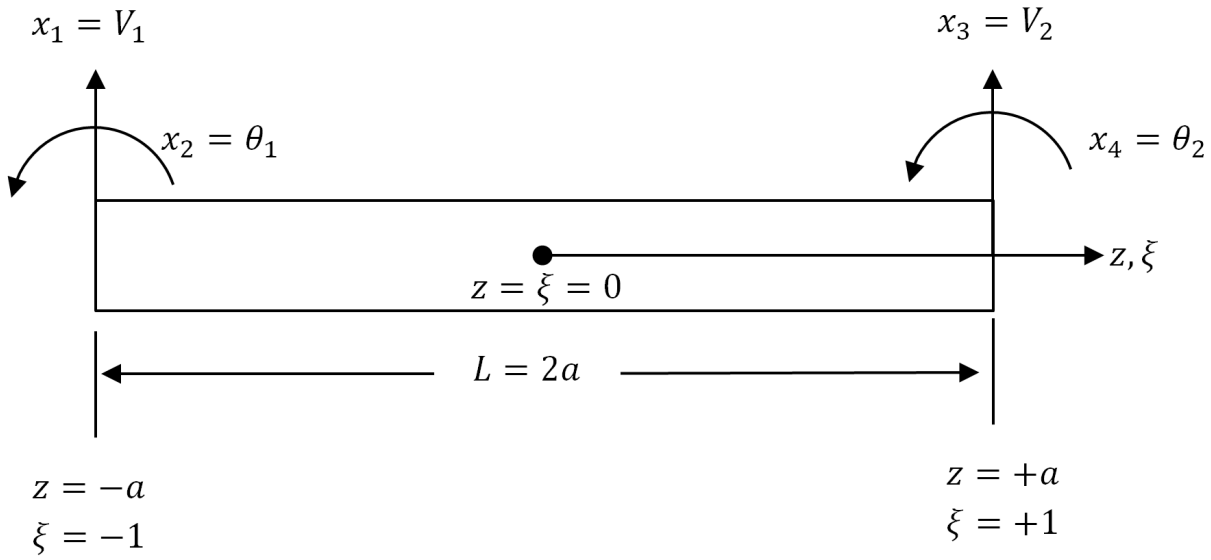

Figure 4.1 Beam Element

where dm = $\rho A_0 dz$ denotes the mass of the section and ρ, A_0 denote the density and cross section area of the beam. The total kinetic energy of the beam element can be obtained by integration over the length of the beam. Using the assumption of constant area of the beam, the mass matrix of the system can be defined as follows:

$$\left[\mathbf{M}\right] = \rho A_0 \int_{-a}^{a} \left[\mathbf{N}\right]^{\mathrm{T}} \left[\mathbf{N}\right] dz \tag{4.68}$$

The total kinetic energy of the beam can be written as:

$$\mathrm{T} = \frac{1}{2} \left\{\dot{\mathbf{x}}\right\}^{\mathrm{T}} \left[\mathbf{M}\right] \left\{\dot{\mathbf{x}}\right\} \tag{4.69}$$

In Equation (4.65) $\frac{\partial \mathrm{T}}{\partial \left\{\mathbf{x}\right\}}$ = 0, because the velocity and displacements are independent. Since the mass matrix is symmetric, using Equation (4.40), for the first derivative in Equation (4.65) yields:

$$\frac{\partial \mathrm{T}}{\partial \left\{\dot{\mathbf{x}}\right\}} = \frac{1}{2} \frac{\partial}{\partial \left\{\dot{\mathbf{x}}\right\}} \left(\left\{\dot{\mathbf{x}}\right\}^{\mathrm{T}} \left[\mathbf{M}\right] \left\{\dot{\mathbf{x}}\right\} \right) = \frac{1}{2} \left(2 \left[\mathbf{M}\right] \left\{\dot{\mathbf{x}}\right\} \right) = \left[\mathbf{M}\right] \left\{\dot{\mathbf{x}}\right\} \tag{4.70}$$

The kinetic energy term of equation (4.65) can therefore be obtained as follows:

$$\frac{\mathrm{d}}{\mathrm{dt}}\left[\frac{\partial \mathrm{T}}{\partial\left\{\dot{\mathbf{x}}\right\}}\right]=\frac{\mathrm{d}}{\mathrm{dt}}\left[\left[\mathbf{M}\right]\left\{\dot{\mathbf{x}}\right\}\right]=\left[\mathbf{M}\right]\left\{\ddot{\mathbf{x}}\right\} \tag{4.71}$$

Equation (4.71) is the well known classic representation of kinetic energy in linear finite element equations of motion.

4.3.0.2 Strain Energy

The strain displacement (kinematics) of this problem is defined as follows:

$$\epsilon_{zz}=-y\left(\frac{\mathrm{d}^2V}{\mathrm{d}z^2}\right)+\frac{1}{2}\left(\left(\frac{\mathrm{d}V}{\mathrm{d}z}\right)^2\right) \tag{4.72}$$

The following aliases are defined: $\left[\mathbf{DN}\right]=\frac{\mathrm{d}}{\mathrm{d}z}\left[\mathbf{N}\right]$, $\left[\mathbf{DN^{\otimes 2}}\right]=\left(\left[\mathbf{DN}\right]\otimes\left[\mathbf{DN}\right]\right)$ and $\left[\mathbf{DDN}\right]=\frac{\mathrm{d}^2}{\mathrm{d}z^2}\left[\mathbf{N}\right]$. Considering the fact that the second term in Equation (4.72) is scalar type, yields:

$$\left(\left(\frac{\mathrm{d}V}{\mathrm{d}z}\right)^2\right)=\left(\left[\mathbf{DN}\right]\left\{\mathbf{x}\right\}\right)\left(\left[\mathbf{DN}\right]\left\{\mathbf{x}\right\}\right)=\left(\left[\mathbf{DN}\right]\otimes\left[\mathbf{DN}\right]\right)\left(\left\{\mathbf{x}\right\}\otimes\left\{\mathbf{x}\right\}\right)=\left[\mathbf{DN^{\otimes 2}}\right]\left\{\mathbf{x}\right\}^{\otimes 2} \tag{4.73}$$

Therefore Equation (4.72) can be rewritten as:

$$\epsilon_{zz}=-y\left[\mathbf{DDN}\right]\left\{\mathbf{x}\right\}+\frac{1}{2}\left[\mathbf{DN^{\otimes 2}}\right]\left\{\mathbf{x}\right\}^{\otimes 2} \tag{4.74}$$

Defining E_0 as the module of elasticity, the stress field associated with this strain field is $\sigma_{zz}=E_0\epsilon_{zz}$. The strain energy of an infinitesimal beam section with a volume equal to $\mathrm{d}V$ can be obtained from:

$$\begin{aligned}\mathrm{dU}=\frac{1}{2}\sigma_{zz}{}^{\intercal}\epsilon_{zz}\mathrm{d}V=\frac{1}{2}\Bigg[&\left\{\mathbf{x}\right\}^{\intercal}\left(y^2E_0\left[\mathbf{DDN}\right]^{\intercal}\left[\mathbf{DDN}\right]\right)\left\{\mathbf{x}\right\}\\&+\left\{\mathbf{x}\right\}^{\intercal}\left(\frac{-E_0}{2}y\left[\mathbf{DDN}\right]^{\intercal}\left[\mathbf{DN^{\otimes 2}}\right]\right)\left\{\mathbf{x}^{\otimes 2}\right\}\\&+\left\{\mathbf{x}^{\otimes 2}\right\}^{\intercal}\left(\frac{-E_0}{2}y\left[\mathbf{DN^{\otimes 2}}\right]^{\intercal}\left[\mathbf{DDN}\right]\right)\left\{\mathbf{x}\right\}\\&+\left\{\mathbf{x}^{\otimes 2}\right\}^{\intercal}\left(\frac{E_0}{4}\left[\mathbf{DN^{\otimes 2}}\right]^{\intercal}\left[\mathbf{DN^{\otimes 2}}\right]\right)\left\{\mathbf{x}^{\otimes 2}\right\}\Bigg]\mathrm{d}V\end{aligned} \tag{4.75}$$

In the first step, assuming S_y and I_y as the first and second moment of area of the beam, the following stiffness matrices can be defined:

$$\begin{aligned}
\left[\mathbf{K_{11}}\right] &= \int_V E_0\left(y^2\left[\mathbf{DDN}\right]^\intercal\left[\mathbf{DDN}\right]\right)\mathrm{d}V = E_0 I_y \int_{-a}^{a}\left[\mathbf{DDN}\right]^\intercal\left[\mathbf{DDN}\right]dz \\
\left[\mathbf{K_{12}}\right] &= \int_V E_0\left(\frac{1}{2}y\left[\mathbf{DDN}\right]^\intercal\left[\mathbf{DN^{\otimes 2}}\right]\right)\mathrm{d}V = \frac{1}{2}E_0 S_y \int_{-a}^{a}\left[\mathbf{DDN}\right]^\intercal\left[\mathbf{DN^{\otimes 2}}\right]dz \\
\left[\mathbf{K_{21}}\right] &= \int_V E_0\left(\frac{1}{2}y\left[\mathbf{DN^{\otimes 2}}\right]^\intercal\left[\mathbf{DDN}\right]\right)\mathrm{d}V = \frac{1}{2}E_0 S_y \int_{-a}^{a}\left[\mathbf{DN^{\otimes 2}}\right]^\intercal\left[\mathbf{DDN}\right]dz \\
\left[\mathbf{K_{22}}\right] &= \int_V E_0\left(\frac{1}{4}\left[\mathbf{DN^{\otimes 2}}\right]^\intercal\left[\mathbf{DN^{\otimes 2}}\right]\right)\mathrm{d}V = \frac{1}{4}E_0 A_0 \int_{-a}^{a}\left[\mathbf{DN^{\otimes 2}}\right]^\intercal\left[\mathbf{DN^{\otimes 2}}\right]dz
\end{aligned} \tag{4.76}$$

It should be recalled that, since polynomials define a ring, careful implementation removes the need to derive any of the differentiations, addition/multiplication operations or integrations by hand and the whole process can be automated. Using these definitions, the strain energy of the beam element can be expressed in the following form:

$$\mathrm{U} = \int_V \mathrm{d}U\mathrm{d}V = \frac{1}{2}\left[\left\{\mathbf{x}\right\}^\intercal\left[\mathbf{K_{11}}\right]\left\{\mathbf{x}\right\} - \left\{\mathbf{x}\right\}^\intercal\left[\mathbf{K_{12}}\right]\left\{\mathbf{x^{\otimes 2}}\right\} - \left\{\mathbf{x^{\otimes 2}}\right\}^\intercal\left[\mathbf{K_{21}}\right]\left\{\mathbf{x}\right\} + \left\{\mathbf{x^{\otimes 2}}\right\}^\intercal\left[\mathbf{K_{22}}\right]\left\{\mathbf{x^{\otimes 2}}\right\}\right] \tag{4.77}$$

4.3.0.3 Equations of Motion and Simulation

Equations (4.77) has the exact same form as (4.10)-(4.11). Therefore, using equations and (4.40), (4.50), (4.53) and (4.62), the strain energy term of Equation (4.66) can be written as:

$$\frac{\partial \mathrm{U}}{\partial\left\{\mathbf{x}\right\}} = \left[\mathbf{K_{11}}\right]\left\{\mathbf{x}\right\} - \frac{1}{2}\left(\left[\tilde{\mathbf{K}}_{\mathbf{12}}\right] + \left[\tilde{\mathbf{K}}_{\mathbf{21}}\right]\right)\left\{\mathbf{x}\right\}^{\otimes 2} + \frac{1}{2}\left[\tilde{\mathbf{K}}_{\mathbf{22}}\right]\left\{\mathbf{x}\right\}^{\otimes 3} \tag{4.78}$$

Finally, by substituting Equations (4.71) and (4.78) into (4.66), the equation of motion of the beam element without the effect of external forces can be expressed as follows:

$$\left[\mathbf{M}\right]\left\{\ddot{\mathbf{x}}\right\} + \left[\mathbf{K_{11}}\right]\left\{\mathbf{x}\right\} - \frac{1}{2}\left(\left[\tilde{\mathbf{K}}_{\mathbf{12}}\right] + \left[\tilde{\mathbf{K}}_{\mathbf{21}}\right]\right)\left\{\mathbf{x}\right\}^{\otimes 2} + \frac{1}{2}\left[\tilde{\mathbf{K}}_{\mathbf{22}}\right]\left\{\mathbf{x}\right\}^{\otimes 3} = 0 \tag{4.79}$$

The global mass and stiffness matrices of all elements can be assembled using classic finite element techniques.

As an example, the developed equations of motion were used to simulate behavior of a cantilever beam ($V = \theta = 0$ at one end) with the following properties: $L = 0.5m$, $E =$

69GPa, $A_0 = 0.006[m^2]$, $Sy = 0.0$, $I_y = 1.8 \times 10^{-6}$ and $\rho = 8700$. The initial condition at $t = 0$ at the free end is assumed to be the result of an impulse: $V = \theta = 0$ and $\dot{V} = 15m/s$. The convergence behavior of the simulation is shown in Figure 4.2 for both linear and nonlinear responses in the middle and at the free end of the beam. As can be seen after increasing the number of elements to more than 20 the solution starts to converge.

4.4 Conclusion

The derivatives of second, third and fourth order Kronecker power of a vector with respect to itself were developed in the form of concise matrix multiplications. These derivatives were used to develop the derivative of fourth order Kronecker power systems with respect to a vector. Application of current formulations to nonlinear dynamics problems was demonstrated by employing them on a nonlinear Euler finite element beam. Some additional notes:

- Describing the nonlinear part of a system in matrix form provides a more efficient way for both simulation and analysis of a nonlinear system. As shown, this method significantly reduces the amount of mathematical effort to derive the equations of motion of fourth order Kronecker product systems such as nonlinear beams and shells.
- The multiplier matrices of $\boldsymbol{W3}$, $\boldsymbol{UI4}$, $\boldsymbol{VI4}$, $\boldsymbol{UI5}$ and $\boldsymbol{VI5}$ depend only on the size of $\boldsymbol{x}$ or K(e.g. degrees of freedom of the system). Therefore, they can be re-used for any other system that has the same principle dimension and different properties.
- These matrices are also highly sparse integer-valued matrices, which makes them an effective tool for numerical implementations.
- Since Kronecker powers of vectors contain repetitive terms (e.g. for a vector of two elements $\boldsymbol{x}^{\otimes 2} = \begin{Bmatrix} x_1^2 & x_1x_2 & x_2x_1 & x_2x_2 \end{Bmatrix}^T$), they can be transformed into more condense forms (e.g. $\begin{Bmatrix} x_1^2 & 2x_1x_2 & x_2x_2 \end{Bmatrix}^T$) to enable further reduction of the memory storage space.

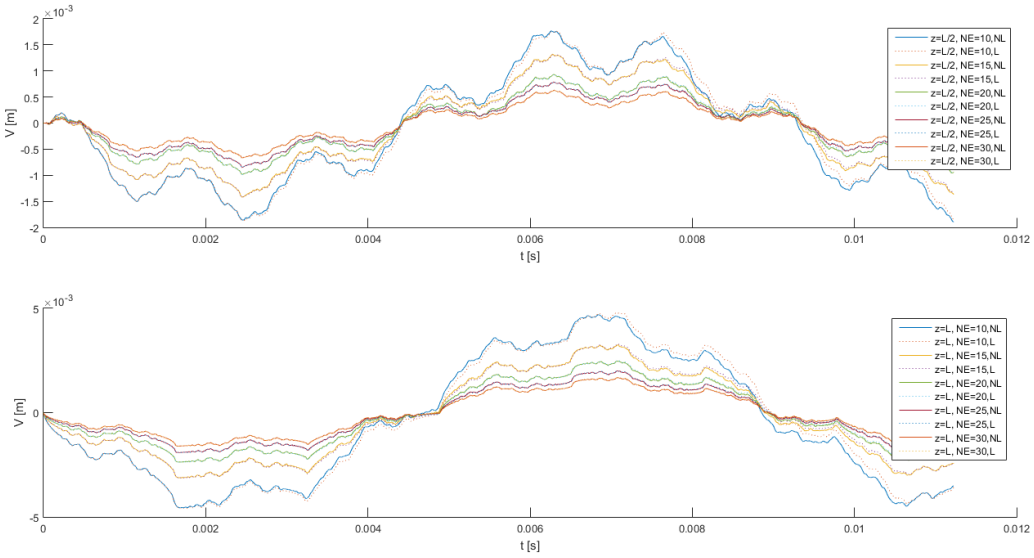

Figure 4.2 Variation of linear (L) and nonlinear (NL) response with time of a cantilever beam using different numbers of finite elements(NE) to an input impulse at time zero: (a) at the middle of the beam; (b) at the free end

References

[1] J. Brewer, "Kronecker products and matrix calculus in system theory," *IEEE Transactions on circuits and systems*, vol. 25, no. 9, pp. 772–781, 1978. [Online]. Available: http://ieeexplore.ieee.org/abstract/document/1084534/

[2] E. Bodewig, *Matrix calculus*. Elsevier, 2014.

[3] H. Neudecker, "Some theorems on matrix differentiation with special reference to Kronecker matrix products," *Journal of the American Statistical Association*, vol. 64, no. 327, pp. 953–963, 1969. [Online]. Available: http://amstat.tandfonline.com/doi/abs/10.1080/01621459.1969.10501027

[4] W. J. Vetter, "Matrix calculus operations and Taylor expansions," *SIAM review*, vol. 15, no. 2, pp. 352–369, 1973. [Online]. Available: http://epubs.siam.org/doi/abs/10.1137/1015034

[5] A. Graham, "Kronecker Products and Matrix Calculus: With Applications." *JOHN*

WILEY & SONS, INC., 605 THIRD AVE., NEW YORK, NY 10158, 1982, 130, 1982.

[6] H. V. Henderson and S. R. Searle, "The vec-permutation matrix, the vec operator and Kronecker products: A review," *Linear and multilinear algebra*, vol. 9, no. 4, pp. 271–288, 1981.

[7] H. Zhang and F. Ding, "On the Kronecker products and their applications," *Journal of Applied Mathematics*, vol. 2013, 2013.

[8] M. Huhtanen, "Real linear Kronecker product operations," *Linear Algebra and its Applications*, vol. 418, no. 1, pp. 347–361, Oct. 2006. [Online]. Available: http://www.sciencedirect.com/science/article/pii/S0024379506001157

[9] Y. Fa-Jun and Z. Hong-Qing, "Constructing New Discrete Integrable Coupling System for Soliton Equation by Kronecker Product," *Communications in Theoretical Physics*, vol. 50, no. 3, p. 561, 2008. [Online]. Available: http://stacks.iop.org/0253-6102/50/i=3/a=04

[10] P. A. Regalia and M. K. Sanjit, "Kronecker products, unitary matrices and signal processing applications," *SIAM review*, vol. 31, no. 4, pp. 586–613, 1989.

[11] M. Amabili, "A comparison of shell theories for large-amplitude vibrations of circular cylindrical shells: Lagrangian approach," *Journal of Sound and Vibration*, vol. 264, no. 5, pp. 1091–1125, 2003. [Online]. Available: http://www.sciencedirect.com/science/article/pii/S0022460X02013858

[12] M. Amabili and F. Pellicano, "Multimode Approach to Nonlinear Supersonic Flutter of Imperfect Circular Cylindrical Shells," *Journal of Applied Mechanics*, vol. 69, no. 2, pp. 117–129, Oct. 2001. [Online]. Available: http://dx.doi.org/10.1115/1.1435366

[13] R. Ramzi and A. Lakis, "Effect of geometric nonlinearities on nonlinear vibrations of closed cylindrical shells," *International Journal of Structural Stability and Dynamics*, vol. 13, no. 4, p. 1250078 (20 pp.), May 2013.

[14] A. Selmane and A. A. Lakis, "Dynamic analysis of anisotropic open cylindrical shells," *Computers & structures*, vol. 62, no. 1, pp. 1–12, 1997. [Online]. Available: http://www.sciencedirect.com/science/article/pii/S0045794996002805

[15] Y. A. Rossikhin and M. V. Shitikova, "Nonlinear dynamic response of a fractionally damped cylindrical shell with a three-to-one internal resonance," *Applied Mathematics and Computation*, vol. 257, pp. 498–525, Apr. 2015. [Online]. Available: http://www.sciencedirect.com/science/article/pii/S0096300315000326

[16] S. Mahmoudkhani, "A Semi-Analytical Method for Calculation of Strongly Nonlinear Normal Modes of Mechanical Systems," *Journal of Computational and Nonlinear Dynamics*, vol. 13, no. 4, pp. 041 005–041 005–12, Feb. 2018. [Online]. Available: http://dx.doi.org/10.1115/1.4039192

[17] M. H. Ghayesh, H. Farokhi, and G. Alici, "Internal Energy Transfer in Dynamical Behavior of Slightly Curved Shear Deformable Microplates," *Journal of Computational and Nonlinear Dynamics*, vol. 11, no. 4, p. 041002, Nov. 2015. [Online]. Available: http://computationalnonlinear.asmedigitalcollection.asme.org/article.aspx?doi=10.1115/1.4031290

[18] M. Amabili, "A new nonlinear higher-order shear deformation theory with thickness variation for large-amplitude vibrations of laminated doubly curved shells," *Journal of Sound and Vibration*, vol. 332, no. 19, pp. 4620–4640, Sep. 2013. [Online]. Available: http://www.sciencedirect.com/science/article/pii/S0022460X13002836

[19] M. Amabili, F. Pellicano, and M. P. Paidoussis, "Nonlinear vibrations of simply supported, circular cylindrical shells, coupled to quiescent fluid," *Journal of Fluids and Structures*, vol. 12, no. 7, pp. 883–918, 1998.

[20] M. Amabili and J. N. Reddy, "A new non-linear higher-order shear deformation theory for large-amplitude vibrations of laminated doubly curved shells," *International Journal of Non-Linear Mechanics*, vol. 45, no. 4, pp. 409–418, May 2010. [Online]. Available: http://www.sciencedirect.com/science/article/pii/S0020746210000028

[21] Y. Kurylov and M. Amabili, "Polynomial versus trigonometric expansions for nonlinear vibrations of circular cylindrical shells with different boundary conditions," *Journal of Sound and Vibration*, vol. 329, no. 9, pp. 1435–1449, Apr. 2010. [Online]. Available: http://www.sciencedirect.com/science/article/pii/

S0022460X09008876

[22] G. Pilgun and M. Amabili, "Non-linear vibrations of shallow circular cylindrical panels with complex geometry. Meshless discretization with the R-functions method," *International Journal of Non-Linear Mechanics*, vol. 47, no. 3, pp. 137–152, 2012.

[23] A. Selmane and A. A. Lakis, "Influence of geometric non-linearities on the free vibrations of orthotropic open cylindrical shells," *International Journal for Numerical Methods in Engineering*, vol. 40, no. 6, pp. 1115–1137, 1997. [Online]. Available: http://onlinelibrary.wiley.com/doi/10.1002/(SICI)1097-0207(19970330)40:6%3C1115::AID-NME105%3E3.0.CO;2-H/abstract

[24] N. Van Khang, "Kronecker product and a new matrix form of Lagrangian equations with multipliers for constrained multibody systems," *Mechanics Research Communications*, vol. 38, no. 4, pp. 294–299, 2011. [Online]. Available: http://www.sciencedirect.com/science/article/pii/S009364131100070X

[25] O. C. Zienkiewicz and R. L. Taylor, *The finite element method for solid and structural mechanics*. Butterworth-heinemann, 2005. [Online]. Available: https://books.google.ca/books?hl=en&lr=&id=VvpU3zssDOwC&oi=fnd&pg=PP1&dq=The+Finite+Element+Method+for+Solid+and+Structural+Mechanics&ots=f2ZafYIF49&sig=0SOX6e_l95pZAb5ozZtMy9E89L4

I.A. Matrix Calculus: Notations, Conventions and Identities

This appendix contains a brief review of matrix calculus including some definitions and identities, that are required for the development of the mathematical relationship presented in the article. Most of the following identities can be found in classic matrix calculus texts and articles including [3], [5] and [4].

To keep the formulations condensed; the notations are similar to what that used by Brewer in [1]. Matrices are shown by upper case bold letters (e.g. $\boldsymbol{A}$) and column vectors are presented with lower case bold letter (e.g $\boldsymbol{x}$). The k^{th} row of a matrix such as $\boldsymbol{A}$ is shown with $\boldsymbol{A}_{k,:}$ and the k^{th} column is shown with $\boldsymbol{A}_{:,k}$. The ik element of $\boldsymbol{A}$ is denoted a_{ik}. The

$n \times n$ unit matrix is denoted $\boldsymbol{I}_n$. The q-dimensional vector which is "1" in the k^{th} and zero elsewhere is called the *unit vector* and is denoted:

$$\underset{(q)}{\boldsymbol{e}}_k \tag{I.A.80}$$

The dimension underscore will be dropped if the dimension can be understood from the context. The *elementary matrix* is defined as:

$$\underset{(p\times q)}{\boldsymbol{E}}_{ik} \triangleq \underset{(p)}{\boldsymbol{e}}_i \underset{(q)}{\boldsymbol{e}}^{\top}{}_k \tag{I.A.81}$$

which has the dimension $(p \times q)$ and has a single "1" element located at ik element and zero elsewhere.

The Kronecker product of $\boldsymbol{A}_{(p\times q)}$ and $\boldsymbol{B}_{(s\times t)}$ denoted by $\boldsymbol{A} \otimes \boldsymbol{B}$ is a $(ps \times qt)$ defined as follows:

$$\boldsymbol{A} \otimes \boldsymbol{B} \triangleq \left[\begin{array}{c|c|c|c} a_{11}\boldsymbol{B} & a_{12}\boldsymbol{B} & \cdots & a_{1q}\boldsymbol{B} \\ \hline a_{21}\boldsymbol{B} & \cdots & & a_{2q}\boldsymbol{B} \\ \hline \vdots & \ddots & & \vdots \\ \hline a_{p1}\boldsymbol{B} & a_{p2}\boldsymbol{B} & \cdots & a_{pq}\boldsymbol{B} \end{array}\right] \tag{I.A.82}$$

It should be noted that:

$$\underset{(p)}{\boldsymbol{e}}_i \otimes \underset{(q)}{\boldsymbol{e}}_k = \underset{(pq)}{\boldsymbol{e}}_{(i-1)q+k} \tag{I.A.83}$$

Another useful definition is the following block-unit matrix that we call the *identity elementary matrix*, that contains an identity matrix at its j^{th} block and zero elsewhere and can be constructed as follows:

$$\underset{(p\times q)}{\boldsymbol{EI}}_j = \underset{(q)}{\boldsymbol{e}}^{\top}{}_j \otimes \boldsymbol{I}_p = \Big[\overbrace{\boldsymbol{0}_{p\times p}}^{1} \quad \overbrace{\boldsymbol{0}_{p\times p}}^{2} \quad \cdots \quad \overbrace{\boldsymbol{I}_p}^{j} \quad \overbrace{\boldsymbol{0}_{p\times p}}^{j+1} \quad \cdots \quad \overbrace{\boldsymbol{0}_{p\times p}}^{q} \Big] \tag{I.A.84}$$

It should be noted that the Kronecker product of two vectors such as $\boldsymbol{a}_{m\times 1}$ and $\boldsymbol{b}_{n\times 1}$ can

be converted to classic matrix multiplication using the following operator:

$$\boldsymbol{a}\otimes\boldsymbol{b}\triangleq\underset{(m\times n)}{vecI}(\boldsymbol{a})\boldsymbol{b}=\left(\sum_{j=1}^{m}a_j\left(\underset{(mj)}{\boldsymbol{e}_j}\otimes\boldsymbol{I}_n\right)\right)\boldsymbol{b}=\begin{bmatrix}a_1\boldsymbol{I}_n\\a_2\boldsymbol{I}_n\\\vdots\\a_m\boldsymbol{I}_n\end{bmatrix}_{mn\times n}\boldsymbol{b} \tag{I.A.85}$$

The vectorization operator generates a vector from a matrix such as $\boldsymbol{A}$ by stacking columns of the matrix on top of each other from left to right.

$$vec(\boldsymbol{A})_{pq\times 1}\triangleq\begin{bmatrix}\boldsymbol{A}_{:,1}\\\hdashline\boldsymbol{A}_{:,2}\\\hdashline\vdots\\\hdashline\boldsymbol{A}_{:,q}\end{bmatrix} \tag{I.A.86}$$

Another important matrix is the *elementary permutation matrix* defined as:

$$\underset{(p\times q)}{\boldsymbol{U}}\triangleq\sum_{i}^{p}\sum_{k}^{q}\underset{(p\times q)}{\boldsymbol{E}}_{ik}\otimes\underset{(q\times p)}{\boldsymbol{E}}_{ki} \tag{I.A.87}$$

A permutation matrix such as $\underset{(p\times q)}{\boldsymbol{U}}$ has only a single "1" entry in each row and column. Given a row number such as r or a column number such as c for an elementary permutation matrix such as $\underset{(p\times q)}{\boldsymbol{U}}$ the corresponding non-zero column or row can be obtained from:

$$c_{"1"}=(1-pq)\left\lceil\frac{r}{q}\right\rceil+p(q+r-1) \tag{I.A.88a}$$

$$r_{"1"}=(1-pq)\left\lceil\frac{c}{p}\right\rceil+q(p+c-1) \tag{I.A.88b}$$

where $\lceil\rceil$ denotes the ceiling function. Following Vetter's convention for the matrix derivative, the derivative of a matrix such as $\boldsymbol{A}_{(p\times q)}$ with respect to a scalar such as b is given as

[4]:

$$\frac{\partial \boldsymbol{A}}{\partial b} = \begin{bmatrix} \frac{\partial a_{11}}{\partial b} & \frac{\partial a_{12}}{\partial b} & \cdots & \frac{\partial a_{1q}}{\partial b} \\ \frac{\partial a_{21}}{\partial b} & & \cdots & \frac{\partial a_{2q}}{\partial b} \\ \vdots & \ddots & & \\ \frac{\partial a_{p1}}{\partial b} & & \cdots & \frac{\partial a_{pq}}{\partial b} \end{bmatrix} \tag{I.A.89}$$

Similarly the Vetter's definition for the derivative of a matrix such as $\boldsymbol{A}_{(p\times q)}$ with respect to another matrix such as $\boldsymbol{B}_{(s\times t)}$ is a partitioned matrix such as $\boldsymbol{C}_{ps\times qt}$ whose $\boldsymbol{C}_{ik}$ partitions is:

$$\boldsymbol{C}_{ik} = \frac{\partial \boldsymbol{A}}{\partial b_{ik}} \tag{I.A.90}$$

Using above definitions, some useful identities can be found in the following equations:

$$\underset{(1\times p)}{\boldsymbol{U}} \underset{(p\times 1)}{\boldsymbol{U}} = \boldsymbol{I}_p \tag{I.A.91a}$$

$$(\boldsymbol{A}\otimes\boldsymbol{B})(\boldsymbol{D}\otimes\boldsymbol{G}) = (\boldsymbol{A}\boldsymbol{D}\otimes\boldsymbol{B}\boldsymbol{G}) \quad \text{(if dimensions allow the operation)} \tag{I.A.91b}$$

$$(\boldsymbol{B}\otimes\boldsymbol{A}) = \underset{(s\times p)}{\boldsymbol{U}}(\boldsymbol{A}\otimes\boldsymbol{B})\underset{(q\times t)}{\boldsymbol{U}} \tag{I.A.91c}$$

$$c(\boldsymbol{A}\otimes\boldsymbol{B}) = (c\boldsymbol{A})\otimes\boldsymbol{B} = \boldsymbol{A}\otimes(c\boldsymbol{B}) \quad (c\in\mathbb{C}) \tag{I.A.91d}$$

$$vec(\boldsymbol{A}^\intercal) = \underset{(p\times q)}{\boldsymbol{U}}\cdot vec(\boldsymbol{A}) \tag{I.A.91e}$$

$$vec(\boldsymbol{A}\boldsymbol{D}) = (\boldsymbol{I}_s\otimes\boldsymbol{A})\,vec(\boldsymbol{D}) = \left(\boldsymbol{D}^\intercal\otimes\boldsymbol{I}_p\right)vec(\boldsymbol{A}) = (\boldsymbol{D}^\intercal\otimes\boldsymbol{A})\,vec\left(\boldsymbol{I}_q\right) \tag{I.A.91f}$$

$$vec(\boldsymbol{AD}) = \sum_{k=1}^{q} (\boldsymbol{D}^{\top})_{:,k} \otimes \boldsymbol{A}_{:,k} \tag{I.A.91g}$$

$$\frac{\partial(\boldsymbol{AF})}{\boldsymbol{B}} = \frac{\partial(\boldsymbol{A})}{\boldsymbol{B}} (\boldsymbol{I}_t \otimes \boldsymbol{F}) + (\boldsymbol{I}_s \otimes \boldsymbol{A}) \frac{\partial(\boldsymbol{F})}{\boldsymbol{B}} \tag{I.A.91h}$$

$$\frac{\partial(\boldsymbol{A} \otimes \boldsymbol{C})}{\boldsymbol{B}} = \frac{\partial(\boldsymbol{A})}{\boldsymbol{B}} \otimes \boldsymbol{C} + \left(\boldsymbol{I}_s \otimes \underset{(p \times r)}{\boldsymbol{U}}\right)\left(\frac{\partial \boldsymbol{C}}{\boldsymbol{B}} \otimes \boldsymbol{A}\right)\left(\boldsymbol{I}_t \otimes \underset{(l \times q)}{\boldsymbol{U}}\right) \tag{I.A.91i}$$

$$\frac{\partial \boldsymbol{y}}{\boldsymbol{y}} = vec\left(\boldsymbol{I}_q\right) \tag{I.A.91j}$$

$$\frac{\partial \boldsymbol{y}^{\top}}{\boldsymbol{y}} = \boldsymbol{I}_q \tag{I.A.91k}$$

Dimensions of matrices and vectors in (I.A.91) are: $\boldsymbol{A}_{p \times q}$, $\boldsymbol{B}_{s \times t}$, $\boldsymbol{C}_{r \times l}$, $\boldsymbol{D}_{q \times s}$, $\boldsymbol{F}_{q \times u}$, $\boldsymbol{G}_{t \times u}$, $\boldsymbol{H}_{p \times q}$ and $\boldsymbol{y}_{q \times 1}$.

CHAPTER 5 ARTICLE 2- NONLINEAR VIBRATION OF TRUNCATED CONICAL SHELLS:DONNELL, SANDERS AND NEMETH THEORIES

Mehrdad Bakhtiari, Aouni A. Lakis, Youcef Kerboua

International Journal of Nonlinear Sciences and Numerical Simulation, 2019(published online ahead of print).

5.1 Abstract

Nonlinear free vibration of truncated conical shells has been investigated for three different shell theories; Donnell, Sanders and Nemeth to investigate the effect of their simplifying assumptions. The displacement field of a finite element model that was obtained from the exact solution of equilibrium equations of Sander's improved first-approximation theory is used to define the nonlinear strain energy of conical shells. Employing generalized coordinates method the equations of motion are derived and subsequently the amplitude equation of nonlinear vibration of conical shells was developed. The amplitude equation is solved for multiple cases of isotropic materials. Linear and nonlinear free vibration results are validated against the existing studies in scientific literature and demonstrate good accordance. The validated model is used to investigate effects of different parameters including circumferential mode number, cone-half angle, length to radius ratio, thickness to radius ratio and boundary conditions for the nonlinear vibration of conical shells.

5.2 Introduction

Conical shells are one of the important structural elements of aerospace vehicles and can be found in different applications ranging from ray-domes up to satellite launch vehicles with large fuel tanks. In comparison to cylindrical shells and flat plates, nonlinear vibration of conical shells has received less attention in scientific literature. One of the earliest studies is the work of Lindholm and Hu [1] which is focused on non-symmetric transverse vibrations of isotropic truncated conical shells using Donnell's type of nonlinear kinematics with a focus on bending and membrane rigidity. Sun and Lu [2] studied the dynamic

response of conical and cylindrical shells under ramp and sinusoidal temperature loads using Donnell's nonlinear shallow shell theory. Bendavid and Mayers [3] developed a nonlinear theory for bending, buckling and vibrations of conical shells based on Sander's nonlinear theory and proposed a variation of the generalized coordinates method to predict the shell's response. Kanaka Raju and Venkateswara Rao [4] studied large -amplitude asymmetric vibrations of shells of revolutions by employing Sander's nonlinear kinematics to obtain finite element stiffness matrix. Their proposed iterative method includes iterating over and refining the stiffness matrix to achieve convergence. Ueda [5] employed an equivalent of Donnell's shallow shell theory to formulate a two degrees of freedom finite element for analyzing the free vibrations of conical shells. He employed the same methodology on cylindrical shells and demonstrated that his results are in good accordance with those of Olson [6]. Liu and Li [7] used Donnell's type of nonlinearities in conjunction with Galerkin's method to study the vibration of shallow conical sandwich shells. They presented the effects of variation of several parameters including boundary conditions and the stiffness of the sandwich core on the nonlinear response of the shell. Xu et al. [8] studied the nonlinear vibration of thick conical shells, using Donnell's shallow shell theory and proposed a solution in form of double Fourier series with time dependent coefficients. Their results show good accordance with exiting data. Fu and Chen [9] took similar solution approach to Xu et al. [8], they presented the effects of various parameters including the relative thickness to radius ratio on the nonlinear frequency. Awrejcewicz et al. [10] and Krysko et al. [11] studied the transition from regular to chaotic vibrations of isotropic spherical and conical shells taking into account Donnell's type of nonlinearities. They studied the effects of various parameters including cone-half angle, the amplitude and frequency of the excitation force and the boundary conditions on the transition to chaotic behavior. Chen and Dai [12][13] employed Donnell's nonlinear theory to study nonlinear vibration and stability of rotary truncated conical shells including the coupling of high and low modal responses and stated that right rotation could have a hardening effect on the shell's stability. Sofiyev [14] studied the nonlinear vibration of truncated conical shells made of functionally graded materials (FGM). They used the Galerkin and harmonic balance methods, and presented their results on the influence of compositional

profiles and shell geometry on the nonlinear dimensionless frequency. In follow up studies Najafov and Sofiyev [15][16] expanded these results to include FGM conical shells surrounded by an elastic medium on a Pasternak-type elastic foundation and truncated cones coated by FGM materials. Sofiyev [17] investigated the large-amplitude vibration of non-homogeneous orthotropic composite truncated conical shells. The Young's modulus and density were assumed to vary exponentially through the thickness of the shell and the effects of various parameters including non-homogeneity, orthotropy and shell geometry on the dynamic response of the shell were presented.

While the the Galerkin method has been the chosen solution method of the majority of prior studies; there are considerable difficulties in using it to handle different boundary conditions. Moreover the case of anisotropic materials has not been formulated in finite element form. The objective of this study is to develop a hybrid finite element model and solution for the nonlinear vibration of anisotropic conical shells. The solution consists of two parts:

- The conical shells finite element displacement functions are derived from exact solution of Sander's improved first order linear shell theory using a method generally similar to [18, 19] and [20].
- Substituting the developed finite element formulation into the nonlinear strain-displacement relationship (kinematics) of Donnell, Sanders and Nemeth nonlinear theories, kinetic and internal strain energies are expressed in terms of nodal displacements. Then, employing the generalized coordinates method, the equations of motion of the nonlinear shell are derived using the Lagrange method. Numerical solution of these equations of motion is used for the dynamic analysis of conical shells.

5.3 Nonlinear Kinematics

Nemeth [21] formulated a shear deformation type of shell theory that can provide Donnell's and Sanders' shell theories as explicit subsets. The kinematics of this theory is developed based on the assumption of small strains and moderate rotations that themselves

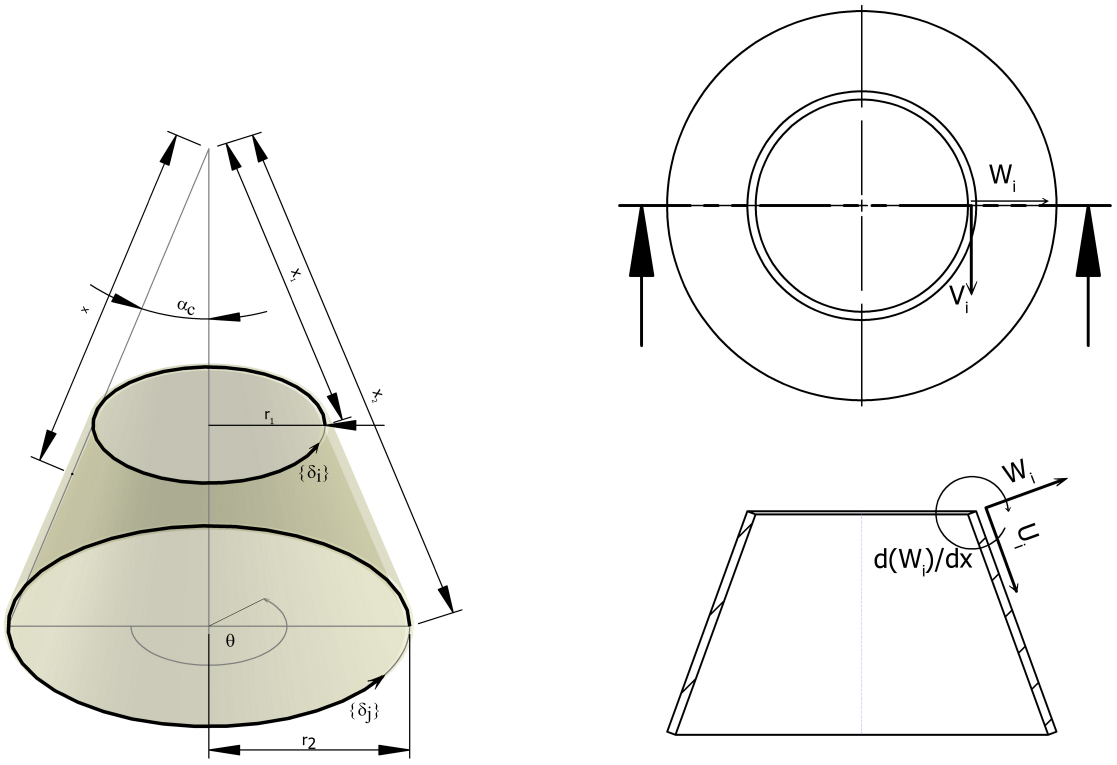

Figure 5.1 Conventions: (5.1a) Geometry and coordinate system; (5.1b) Nodal degrees of freedom

are subsets of the general derivations of none-orthogonal principal coordinates of what he presented in [22]. The geometrical and coordinates system of the truncated cone element of the current study are shown in figure 5.1a. The longitudinal and radial principal-curvature coordinates are denoted by x and θ. The cone half-angle α_c and the slant length of the cone can be obtained from $L = x_2 - x_1$. Assuming the reference surface is located at the middle of the shell thickness and neglecting transverse shear deformation, the three fundamental unknowns in this formulation are two middle-surface tangential displacements $U = u_1(x, \theta)$ and $V = u_2(x, \theta)$ and the normal displacement $W = u_3(x, \theta)$. The tangential and normal displacement fields of a material point $p(x, \theta, \xi_3)$ in a shell expressed

in the orthogonal principal-curvature coordinate systems are given as:

$$\begin{aligned} U_1(x,\theta,\xi_3) &= u_1(x,\theta) + \xi_3[\varphi_1 - \varphi\varphi_2] \\ U_2(x,\theta,\xi_3) &= u_2(x,\theta) + \xi_3[\varphi_2 - \varphi\varphi_1] \\ U_3(x,\theta,\xi_3) &= u_3(x,\theta) - \frac{1}{2}\xi_3\left(\varphi_1^2 + \varphi_2^2\right) \end{aligned} \tag{5.1}$$

where ξ_3 denotes the normal distance from the middle surface. The linear rotation parameters φ_1 , φ_2 and φ are defined as follows:

$$\begin{aligned} \varphi_1(x,\theta) &= -\frac{\partial u_3(x,\theta)}{\partial x} \\ \varphi_2(x,\theta) &= \frac{c_3 u_2(x,\theta)}{x\tan(\alpha_c)} - \frac{1}{x\sin(\alpha_c)}\frac{\partial u_3(x,\theta)}{\partial\theta} \\ \varphi(x,\theta) &= \frac{1}{2}c_3\left(\frac{\partial u_2(x,\theta)}{\partial x} - \frac{1}{x\sin(\alpha_c)}\frac{\partial u_1(x,\theta)}{\partial\theta} + \frac{u_2(x,\theta)}{x}\right) \end{aligned} \tag{5.2}$$

In addition the in-plane linear deformation parameters are defined as:

$$\begin{aligned} e_{11}^{\circ}(x,\theta) &= \frac{\partial u_1(x,\theta)}{\partial x} \\ e_{22}^{\circ}(x,\theta) &= \frac{1}{x\sin(\alpha_c)}\frac{\partial u_2(x,\theta)}{\partial\theta} + \frac{u_1(x,\theta)}{x} + \frac{u_3(x,\theta)}{x\tan(\alpha_c)} \\ 2e_{12}^{\circ}(x,\theta) &= \frac{1}{x\sin(\alpha_c)}\frac{\partial u_1(x,\theta)}{\partial\theta} + \frac{\partial u_2(x,\theta)}{\partial x} - \frac{u_2(x,\theta)}{x} \end{aligned} \tag{5.3}$$

Using the linear rotation and deformation parameters, the strain-displacement relationship on the reference surface of this theory based on the assumption of small strains and moderate rotations are:

$$\left\{\boldsymbol{\epsilon}^{\circ}\right\} = \begin{Bmatrix} \epsilon_{11}^{\circ} \\ \epsilon_{22}^{\circ} \\ \gamma_{12}^{\circ} \end{Bmatrix} = \begin{Bmatrix} e_{11}^{\circ} \\ e_{22}^{\circ} \\ 2e_{12}^{\circ} \end{Bmatrix} + c_{NL}\begin{Bmatrix} \frac{1}{2}\left(\varphi_1^2 + c_2\varphi^2\right) + \frac{1}{2}c_1\left[(e_{11}^{\circ})^2 + e_{12}^{\circ}\left(e_{12}^{\circ} + 2\varphi\right)\right] \\ \frac{1}{2}\left(\varphi_2^2 + c_2\varphi^2\right) + \frac{1}{2}c_1\left[(e_{22}^{\circ})^2 + e_{12}^{\circ}\left(e_{12}^{\circ} - 2\varphi\right)\right] \\ \varphi_1\varphi_2 + c_1\left[e_{11}^{\circ}\left(e_{12}^{\circ} - \varphi\right) + e_{22}^{\circ}\left(e_{12}^{\circ} + \varphi\right)\right] \end{Bmatrix} \tag{5.4a}$$

$$\left\{\boldsymbol{\chi}^{\circ}\right\} = \begin{Bmatrix} \chi_{11}^{\circ} \\ \chi_{22}^{\circ} \\ 2\chi_{12}^{\circ} \end{Bmatrix} = \begin{Bmatrix} \frac{\partial\varphi_1}{\partial x} \\ \frac{1}{x\sin(\alpha_c)}\frac{\partial\varphi_2}{\partial\theta} + \frac{\varphi_1}{x} \\ \frac{1}{x\sin(\alpha_c)}\frac{\partial\varphi_1}{\partial\theta} + \frac{\partial\varphi_2}{\partial x} - \frac{\varphi_2}{x} + \frac{\varphi}{x\tan(\alpha_c)} \end{Bmatrix} \tag{5.4b}$$

In the above formulation:

- Specifying $c_{NL} = 0$ and $c_3 = 1$ simplifies the kinematics to the improved first-approximation linear shell theory of Sanders [23]
- Specifying $c_{NL} = 1, c_1 = c_2 = c_3 = 1$ defines Nemeth's nonlinear theory [21]
- Specifying $c_{NL} = 1, c_1 = 0$ and $c_2 = c_3 = 1$ retrieves Sanders' kinematics [24] [25].
- Specifying $c_{NL} = 1, c_1 = c_2 = 0$ and $c_3 = 1$ retrieves Sanders' kinematics with the nonlinear rotations about the reference-surface normal neglected [24] [25]. This is indicated as "SANDERS-APX" in the results of current study.
- Specifying $c_{NL} = 1, c_1 = c_2 = c_3 = 0$ defines Donnell's strain-displacement relationship [26].

The strains on a point at ξ_3 normal distance from the middle surface can be expressed in the following matrix form:

$$\left\{\boldsymbol{\epsilon}^{\xi_3}\right\} = \left\{\epsilon_{11} \quad \epsilon_{22} \quad \gamma_{12}\right\}^{\mathsf{T}} = \left(1 + \frac{\xi_3}{\mathrm{R}_1}\right)^{-1} \left(1 + \frac{\xi_3}{\mathrm{R}_2}\right)^{-1} \left[\mathbf{S}\right] \left\{\boldsymbol{\Xi}^{\circ}\right\} \tag{5.5}$$

The corresponding strains on the middle surface are defined as:

$$\left\{\boldsymbol{\Xi}^{\circ}\right\} = \left\{\left\{\boldsymbol{\epsilon}^{\circ}\right\} \quad \left\{\boldsymbol{\chi}^{\circ}\right\}\right\}^{\mathsf{T}} \tag{5.6}$$

The definitions of the $\left[\mathbf{S}\right]$ matrices can be found in appendix A of [27].

5.4 Stress-Strain Relationship

When the coordinate system of the elasticity tensor is not aligned with the global coordinate system, the transformed stress and strain fields are given by:

$$\left\{\bar{\boldsymbol{\sigma}}\right\} = \left[\bar{\mathbf{C}}\right] \left\{\bar{\boldsymbol{\epsilon}}\right\} \tag{5.7}$$

where $\bar{\boldsymbol{\sigma}}$ and $\bar{\boldsymbol{\epsilon}}$ are the rotated stress and strain vectors. In the case of a homogenous fully anisotropic material the transformed compliance tensor $\left[\bar{\mathbf{C}}\right]$ of Equation (5.7) can be calculated as follows:

$$\left[\bar{\mathbf{C}}\right] = \left[\mathbf{T}_{\boldsymbol{\sigma}}\right] \left[\mathbf{C}\right] \left[\mathbf{T}_{\boldsymbol{\epsilon}}\right]^{-1} \tag{5.8}$$

The definition of $\left[\mathbf{T}_{\sigma}\right]$ and $\left[\mathbf{T}_{\epsilon}\right]$ are provided in [27]. In the absence of shear deformation, under the plane stress assumption, $\bar{\sigma}_{33} = \bar{\sigma}_{23} = \bar{\sigma}_{13} = 0$. Under these conditions, the stress-strain relationship can be defined as:

$$\left\{\bar{\sigma}_{11} \quad \bar{\sigma}_{22} \quad \bar{\sigma}_{12}\right\}^{\mathsf{T}} = \left[\bar{\mathbf{Q}}\right]_{3\times3}\left\{\bar{\epsilon}_{11} \quad \bar{\epsilon}_{22} \quad 2\bar{\epsilon}_{12}\right\}^{\mathsf{T}} \tag{5.9}$$

The relationships to obtain the plane stress reduced compliance tensor ($\left[\bar{\mathbf{Q}}\right]$) are provided in [27].

5.5 Constitutive Equations

The two dimensional constitutive equations of the shell can be defined as follows:

$$\begin{bmatrix}\{\mathfrak{n}\}\\ \{\mathfrak{m}\}\end{bmatrix} = \left[\mathcal{CC}^{0}\right]\left\{\mathfrak{E}^{\circ}\right\} \triangleq \left[\int_{-\frac{h}{2}}^{+\frac{h}{2}}\left(1+\frac{\xi_3}{R_1}\right)^{-1}\left(1+\frac{\xi_3}{R_2}\right)^{-1}\left[\mathbf{S}\right]^{\mathsf{T}}\left[\bar{\mathbf{Q}}\right]\left[\mathbf{S}\right]d\xi_3\right]\left\{\mathfrak{E}^{\circ}\right\} \tag{5.10}$$

Details of stress resultants of Equation (5.10) and the associated constitutive matrix $\left[\mathcal{CC}^{0}\right]$ can be found in appendix B of [27].

5.6 Linear Solution and Finite Element Formulation

Using the principle of virtual work, three linear equilibrium equations of conical shells based on Sanders' best first approximation [23] and in terms of stress resultants can be obtained [21]. These three equations are presented in 5.10. Substituting work-conjugate stress resultants of (5.10) into the equilibrium Equation (II.A.41) of appendix I.A. results in a system of linear differential equations. These were found to be non-homogeneous in terms of powers of x. Therefore additional assumptions are needed to facilitate obtaining an analytical solution. To this end, it is assumed that the thickness of shell varies linearly along the x coordinates:

$$t = \beta x \tag{5.11}$$

where β denotes the thickness variation proportionality. To simulate constant thickness shells, the value of β is chosen so that the constant thickness occurs in the middle of any

element of the shell.

This variable thickness substitution makes it possible to employ the separation of variables technique using the following form for the solution:

$$u_1 = u_{1,\bar{x}}(\bar{x})(\cos(n_c\theta)) \tag{5.12a}$$

$$u_2 = u_{2,\bar{x}}(\bar{x})(\sin(n_c\theta)) \tag{5.12b}$$

$$u_3 = u_{3,\bar{x}}(\bar{x})(\cos(n_c\theta)) \tag{5.12c}$$

where n_c is the circumferential mode number and $\bar{x} = x/x_m$ is the dimensionless longitudinal coordinates with $x_m = 0.5(x_1 + x_2)$. The longitudinal component of the solution is chosen as:

$$u_{d,\bar{x}} = C_d(\bar{x})^{\frac{(\lambda-1)}{2}} \tag{5.13}$$

where C_d $(d = 1, 2, 3)$ is the arbitrary magnitude of the displacement. Substituting Equation (5.12) in equilibrium equations of (II.A.41) of 5.10 followed by some lengthy mathematical manipulations yields three equations in the following form:

$$\mathfrak{L}_{i,1}\sin(n_c\theta) + \mathfrak{L}_{i,2}\cos(n_c\theta) = 0 \qquad (i = 1, 2, 3) \tag{5.14}$$

where $\mathfrak{L}_{i,j}$ (s) are only functions of $u_{d,\bar{x}}$ and the associated derivatives along x direction, circumferential mode number and shell parameters such as elasticity and geometry. Hence, for any given element with specific dimension and properties, the only variable that appears in $\mathfrak{L}_{i,j}$ is λ. Therefore, it is possible to rewrite the equilibrium equations in the following matrix form:

$$\left[\mathcal{AQ}\right]\left\{\mathbf{A}\right\} = \begin{bmatrix} \mathcal{AQ}_{1,1} & \mathcal{AQ}_{1,2} & \mathcal{AQ}_{1,3} \\ \mathcal{AQ}_{2,1} & \mathcal{AQ}_{2,2} & \mathcal{AQ}_{2,3} \\ \mathcal{AQ}_{3,1} & \mathcal{AQ}_{3,2} & \mathcal{AQ}_{3,3} \end{bmatrix} \begin{Bmatrix} C_1 \\ C_2 \\ C_3 \end{Bmatrix} = 0 \tag{5.15}$$

where elements of $\left[\mathcal{AQ}\right]$ are polynomials in terms of λ and details of their derivation are given in [27]. To satisfy any arbitrary displacement, the determinant of $\left[\mathcal{AQ}\right]$ should be equal to zero and this yields a characteristic polynomial that can be solved to obtain val-

ues of λ.

The number of distinct roots of the characteristic polynomial defines the degrees of freedom of the element. For the case of isotropic materials there are eight distinct roots so the element has eight degrees of freedom. For other types of materials in terms of anisotropy and the shear model up to sixteen degrees of freedom can be observed. Assuming presence of K distinct roots, the final solution of the system is obtained by summation of all these solutions:

$$\mathrm{u_d}(\mathrm{x},\theta) = \left(\sum_{k=1}^{\mathrm{K}} \mathrm{C_{d,k}}\left(\bar{x}^{\frac{(\lambda_k - 1)}{2}}\right)\right)(\sin(n_c\theta)^{\mathrm{se_d}})(\cos(n_c\theta)^{\mathrm{ce_d}}) \tag{5.16}$$

where $\mathrm{se_d}, \mathrm{ce_d} = 0, 1$ for $\mathrm{d} = 1, 3$ and $\mathrm{se_d}, \mathrm{ce_d} = 1, 0$ for , $\mathrm{d} = 2$. At this point, the problem is reduced to defining the unknown arbitrary amplitude of vibrations in terms of degrees of freedom.

The finite element of the current study is bounded by two nodal lines and the degrees of freedom of those nodesδ_i δ_j are shown in figure 5.1a. For the case of isotropic materials four degrees of freedom at each node are chosen as presented for δ_i node in figure 5.1b. Mathematically these degrees of freedom can be written as:

$$\left\{\boldsymbol{\delta_m}\right\} = \begin{Bmatrix} \delta_{m,1} \\ \delta_{m,2} \\ \delta_{m,3} \\ \delta_{m,4} \end{Bmatrix} = \begin{Bmatrix} \mathrm{U_x} \\ \mathrm{V_x} \\ \mathrm{W_x} \\ \frac{\partial \mathrm{W_x}}{\partial \mathrm{x}} \end{Bmatrix} \triangleq \begin{Bmatrix} \mathrm{u}_{1,\bar{x}}(x_m/L) \\ \mathrm{u}_{2,\bar{x}}(x_m/L) \\ \mathrm{u}_{3,\bar{x}}(x_m/L) \\ \partial \mathrm{u}_{3,\bar{x}}(x_m/L)/\partial x \end{Bmatrix} \tag{5.17}$$

where, at $m = i$ and $m = j$, x_m takes values of $x_i = \mathrm{x}_1$ and $x_j = \mathrm{x}_2$ accordingly (figure 5.1a). Using equation (5.15) and recognizing the linear dependency as a result of zero determinant of $\left[\mathcal{AQ}\right]$ matrix, and some mathematical operations that details of them can be found in [27], the unknown amplitudes of vibration (C_1, C_2, C_3) in the displacements of Equation (5.12) can be expressed in terms of each element's degrees of freedom:

$$\left\{\boldsymbol{\delta}\right\}^{e} \triangleq \begin{Bmatrix} \left\{\boldsymbol{\delta_i}\right\} \\ \\ \left\{\boldsymbol{\delta_j}\right\} \end{Bmatrix} = \begin{Bmatrix} \delta_1 \\ \delta_2 \\ \vdots \\ \delta_K \end{Bmatrix} = \begin{bmatrix} a_{1,1} & a_{1,2} & \cdots & a_{1,K} \\ a_{2,1} & a_{2,2} & \cdots & a_{2,K} \\ \vdots & \vdots & \ddots & \vdots \\ a_{K,1} & a_{K,2} & \cdots & a_{K,K} \end{bmatrix} \begin{Bmatrix} C_{1,1} \\ C_{1,2} \\ \vdots \\ C_{1,K} \end{Bmatrix} = \left[\mathbf{A}\right]\left\{\mathbf{C_1}\right\} \tag{5.18}$$

where $\left[\mathbf{A}\right]$ contains only constant real numbers. Subsequently:

$$\left\{\mathbf{C_1}\right\} = \left[\mathbf{A}\right]^{-1}\left\{\boldsymbol{\delta}\right\}^{e} \tag{5.19}$$

Rearranging into a matrix form and substituting (5.19) in Equation (5.12) yields the following displacement matrix:

$$\left\{\mathbf{u}\right\} = \begin{Bmatrix} u_1(x,\theta) \\ u_2(x,\theta) \\ u_3(x,\theta) \end{Bmatrix} = \overbrace{\left[\mathbf{R}(x,\theta)\right]\left[\mathbf{A}\right]^{-1}}^{\left[\mathbf{N}\right]_{3\times K}}\left\{\boldsymbol{\delta}\right\}^{e} = \begin{bmatrix} R_{1,1} & R_{1,2} & \cdots & R_{1,K} \\ R_{2,1} & R_{2,2} & \cdots & R_{2,K} \\ \vdots & \vdots & \ddots & \vdots \\ R_{5,1} & R_{5,2} & \cdots & R_{5,K} \end{bmatrix}\begin{bmatrix} c_{1,1} & c_{1,2} & \cdots & c_{1,K} \\ c_{2,1} & c_{2,2} & \cdots & c_{2,K} \\ \vdots & \vdots & \ddots & \vdots \\ c_{K,1} & c_{5,2} & \cdots & c_{K,K} \end{bmatrix}\begin{Bmatrix} \delta_1 \\ \delta_2 \\ \vdots \\ \delta_K^e \end{Bmatrix} \tag{5.20}$$

where the elements of $\left[\mathbf{R}\right]$ are defined as follows:

$$R_{d,k}(x,\theta) = \left(\frac{x}{x_m}\right)^{\frac{(\lambda_k - 1)}{2}} (\sin(n_c\theta)^{se_d})(\cos(n_c\theta)^{ce_d}) \tag{5.21}$$

Subsequently, the elements of the displacement matrix $\left[\mathbf{N}\right]$ take the following form:

$$N_{d,k}(x,\theta) = \sum_{i=1}^{K} (c_{i,k})\, R_{d,i} \tag{5.22}$$

Assigning the function space defined by Equation (5.21) $\mathbb{S}$ it can be quickly proven[27] that due to associativity, commutativity, existence of zero and one for addition and multiplication operations, this set defines a mathematical ring. Moreover the derivatives of $R_{d,k}(x,\theta)$ with respect to x and θ coordinates belong to the same ring. These properties can be exploited programmatically to derive displacements, strains and stress-strain relationships of equations (5.1)-(5.9) in terms of this type of function.

5.7 Equations of Motion

Shell motion has two components, spatial and temporal. Equation 5.22 defines the spatial component of shell motion. Introducing $\left\{\boldsymbol{\delta}\right\} = \left\{\boldsymbol{\delta}(t)\right\}$ as the temporal (time-dependent) component of shell's motion, it is possible to develop the equations of motion of the shell, using the generalized-coordinates method. Assuming the system consists of N finite elements, each with K degrees of freedom, the Lagrangian equation of motion based on Hamilton's principle can be expressed as follows:

$$\frac{\mathrm{d}}{\mathrm{dt}}\left[\frac{\partial \mathrm{T}}{\partial \dot{\delta}_i}\right] - \frac{\partial \mathrm{T}}{\partial \delta_i} + \frac{\partial \mathrm{V}}{\partial \delta_i} = \mathrm{q}_i, \quad (i = 1, 2, \cdots, \mathrm{D} \triangleq \mathrm{K} \times \mathrm{N}) \tag{5.23}$$

where

- D is the total degrees of freedom of the system after assembling mass and stiffness matrices of elements and applying the constraints
- T is the total kinetic energy of the system
- V is the total elastic strain energy of the system
- q_i is the nodal external force

Equation (5.23) can be rewritten in matrix form as follows:

$$\frac{\mathrm{d}}{\mathrm{dt}}\left[\frac{\partial \mathrm{T}}{\partial \left\{\dot{\boldsymbol{\delta}}\right\}}\right] - \frac{\partial \mathrm{T}}{\partial \left\{\boldsymbol{\delta}\right\}} + \frac{\partial \mathrm{V}}{\partial \left\{\boldsymbol{\delta}\right\}} = \left\{\mathbf{q}\right\} \tag{5.24}$$

5.7.1 Kinetic Energy

The kinetic energy of an element has three components; pure translational ($\mathrm{T_T}$), cross translational-rotational ($\mathrm{T_{TR}}$) and pure rotational $\mathrm{T_R}$. In the absence of shear deformation ($\mathrm{T_{TR}}$) and $\mathrm{T_R}$ are neglected. Therefore the structural mass matrix for a single element can be defined as follows:

$$\left[\mathbf{M_T}\right]^{\mathrm{e}}_{\mathrm{K}\times\mathrm{K}} = \iint_{\Omega} \rho^0 \left(\left[\mathbf{S_T}\right]^{\mathrm{T}} \left[\mathbf{S_T}\right]\right) \mathrm{A}_1 \mathrm{A}_2 \mathrm{d}x\mathrm{d}\theta \tag{5.25}$$

Details of variables of equation 5.25 can be found in [27]). It should be noted that $\left[\mathbf{M_T}\right]^e$ is a symmetric positive definite matrix. The structural mass matrices of all elements can be assembled to obtain the whole system mass matrix using standard finite element assembly procedures. The corresponding assembled matrix is named $\left[\mathbf{M_T}\right]$. Finally by performing some mathematical operations (details are given in [27]), the kinetic energy term of the equations of motion can be obtained from the following equation:

$$\frac{d}{dt}\left[\frac{\partial T}{\partial\left\{\dot{\delta}\right\}}\right]=\left[\mathbf{M_S}\right]\left\{\ddot{\delta}\right\}\triangleq\frac{1}{2}\left(2\left[\mathbf{M_T}\right]\right)\left\{\ddot{\delta}\right\} \tag{5.26}$$

$\left[\mathbf{M_S}\right]$ denotes the assembled structural mass matrix of the whole system.

5.7.2 Internal Strain Energy

The internal strain energy over the shell element surface area (Ω) is defined as:

$$V_e=\frac{1}{2}\iint_\Omega\left(\int_{-h/2}^{h/2}\left\{\sigma^{\xi_3}\right\}^T\left\{\epsilon^{\xi_3}\right\}\left(1+\frac{\xi_3}{R_1}\right)\left(1+\frac{\xi_3}{R_2}\right)d\xi_3\right)d\Omega \tag{5.27}$$

Taking into account Equation (5.5) and (5.9) for variable thickness conical elements, the through-the-thickness integral of Equation (5.27) can be obtained from the following equation:

$$\int_{-h/2}^{h/2}\left\{\sigma^{\xi_3}\right\}^T\left\{\epsilon^{\xi_3}\right\}\left(1+\frac{\xi_3}{R_1}\right)\left(1+\frac{\xi_3}{R_2}\right)d\xi_3=\left\{\mathfrak{E}^\circ\right\}^T\left[\bar{\mathcal{C}}^0\right]\left\{\mathfrak{E}^\circ\right\} \tag{5.28}$$

The constitutive matrix $\left[\bar{\mathcal{C}}^0\right]$ of variable thickness truncated conical elements is given in [27]. The strain vector $\left\{\mathfrak{E}^\circ\right\}$ can be decomposed into its linear and nonlinear components:

$$\left\{\mathfrak{E}^\circ\right\}=\left[\mathbf{S}_{\mathfrak{E}_L^\circ}\right]_{6\times K}\left\{\delta\right\}^e_{K\times1}+\left[\mathbf{S}_{\mathfrak{E}_{NL}^\circ}\right]_{6\times K^2}\left\{\delta^{\otimes2}\right\}^e_{K^2\times1} \tag{5.29}$$

where $\left\{\delta^{\otimes p}\right\}$ is the Kronecker product power *p* of vector $\left\{\delta\right\}$ (e.g.$\left\{\delta^{\otimes2}\right\}=\left\{\delta\right\}\otimes\left\{\delta\right\}$). The rows of $\left[\mathbf{S}_{\mathfrak{E}_L^\circ}\right]$ and $\left[\mathbf{S}_{\mathfrak{E}_{NL}^\circ}\right]$ are provided in appendix I of [27]. The following stiffness matrices for

each element:

$$\left[\mathbf{K_{11}}\right]^e \triangleq \iint_\Omega \left[\mathbf{S_{E_L^\circ}}\right]^T \left[\bar{\mathcal{C}}^0\right] \left[\mathbf{S_{E_L^\circ}}\right] A_1 A_2 dx d\theta \tag{5.30a}$$

$$\left[\mathbf{K_{21}}\right]^e = \left(\left[\mathbf{K_{12}^e}\right]\right)^T \triangleq \iint_\Omega \left[\mathbf{S_{E_{NL}^\circ}}\right]^T \left[\bar{\mathcal{C}}^0\right] \left[\mathbf{S_{E_L^\circ}}\right] A_1 A_2 dx d\theta \tag{5.30b}$$

$$\left[\mathbf{K_{22}}\right]^e \triangleq \iint_\Omega \left[\mathbf{S_{E_{NL}^\circ}}\right]^T \left[\bar{\mathcal{C}}^0\right] \left[\mathbf{S_{E_{NL}^\circ}}\right] A_1 A_2 dx d\theta \tag{5.30c}$$

can be defined. Hence the strain energy of the element can be written as follows:

$$V_e = \frac{1}{2}\left(\left(\left\{\boldsymbol{\delta}\right\}^e\right)^T \left[\mathbf{K_{11}}\right]^e \left\{\boldsymbol{\delta}\right\}^e + \left(\left\{\boldsymbol{\delta}\right\}^e\right)^T \left[\mathbf{K_{12}}\right]^e \left\{\boldsymbol{\delta}^{\otimes 2}\right\}^e + \left(\left\{\boldsymbol{\delta}^{\otimes 2}\right\}^e\right)^T \left[\mathbf{K_{21}}\right]^e \left\{\boldsymbol{\delta}\right\}^e + \left(\left\{\boldsymbol{\delta}^{\otimes 2}\right\}^e\right)^T \left[\mathbf{K_{22}}\right]^e \left\{\boldsymbol{\delta}^{\otimes 2}\right\}^e\right) \tag{5.31}$$

The total strain energy can be obtained from the summation of the strain energies of all elements of the system. Hence, similar to the mass matrices, the structural stiffness matrices of all elements can be assembled to obtain the whole system stiffness matrices. The corresponding assembled stiffness matrices are named $\left[\mathbf{K_{11}}\right]$, $\left[\mathbf{K_{12}}\right]$, $\left[\mathbf{K_{21}}\right]$ and $\left[\mathbf{K_{22}}\right]$. Finally for the whole system, the derivative of the strain energy with respect to the degrees of freedom can be formulated as:

$$\frac{\partial V}{\partial \left\{\boldsymbol{\delta}\right\}} = \left[\mathbf{K_{11}}\right]\left\{\boldsymbol{\delta}\right\} + \left[\tilde{\mathbf{K}}_{\mathbf{12}}\right]\left\{\boldsymbol{\delta}^{\otimes 2}\right\} + \frac{1}{2}\left[\tilde{\mathbf{K}}_{\mathbf{22}}\right]\left\{\boldsymbol{\delta}^{\otimes 3}\right\} \tag{5.32}$$

where $\left[\tilde{\mathbf{K}}_{\mathbf{12}}\right]$ and $\left[\tilde{\mathbf{K}}_{\mathbf{22}}\right]$ are formulated based on $\left[\mathbf{K_{12}}\right]$, $\left[\mathbf{K_{21}}\right]$ and $\left[\mathbf{K_{22}}\right]$ using matrix calculus operations and the details of that are provided in appendix J of [27].

5.7.3 Equations of Motion in Terms of Nodal Displacements

Substituting Equation (5.26) and (5.32) in (5.24) results in the following equation of motion:

$$\left[\mathbf{M_S}\right]_{D\times D}\left\{\ddot{\boldsymbol{\delta}}\right\} + \left[\mathbf{K_{11}}\right]_{D\times D}\left\{\boldsymbol{\delta}\right\} + \left[\tilde{\mathbf{K}}_{\mathbf{12}}\right]_{D\times D^2}\left\{\boldsymbol{\delta}^{\otimes 2}\right\} + \frac{1}{2}\left[\tilde{\mathbf{K}}_{\mathbf{22}}\right]_{D\times D^3}\left\{\boldsymbol{\delta}^{\otimes 3}\right\} - \left\{\mathbf{q}\right\} = 0 \tag{5.33}$$

5.8 Free Vibration

5.8.1 Harmonic Motion and Linear Vibration

Different approaches can be used to obtain nonlinear response of the system from Equation (5.33). One approach is to use the forced vibration response of the system to obtain the backbone curve as the middle curve between the forced vibration response to periodic excitement such as what described in [28]. While this approach simulates the experimental procedure, it requires significant computational time for simulation. Moreover capturing and triggering some phenomena such as response jump in simulations is not a straightforward process. Another common approach that is used in the current study is to develop a nonlinear eigenvalue problem from the equations of motion[29]. Assuming a harmonic solution in the form of $\left\{\boldsymbol{\delta(t)}\right\} = \left\{\boldsymbol{\delta_{max}}\right\}\sin(\omega t)$ with zero external force ($\left\{\mathbf{q}\right\} = 0$), the large amplitude nonlinear free vibration of a truncated conical shell can be expressed in the following form:

$$\left(\left[\mathbf{K_{11}}\right] + \left[\tilde{\mathbf{K}}_{\mathbf{12}}\right]\underset{(\mathrm{D}\times\mathrm{D})}{vecI}\left(\left\{\boldsymbol{\delta_{max}}\right\}\right)\sin(\omega t) + \frac{1}{2}\left[\tilde{\mathbf{K}}_{\mathbf{22}}\right]\underset{(\mathrm{D}^2\times\mathrm{D})}{vecI}\left(\left\{\boldsymbol{\delta}^{\otimes\mathbf{2}}_{\mathbf{max}}\right\}\right)\sin^2(\omega t)\right)\left\{\boldsymbol{\delta_{max}}\right\}\sin(\omega t) - \omega^2\left[\mathbf{M_S}\right]\left\{\boldsymbol{\delta_{max}}\right\}\sin(\omega t) = \left\{\mathbf{R}\right\} \tag{5.34}$$

where $\left\{\mathbf{R}\right\}$ is the residual vector. The definition of operator $\underset{(n\times m)}{vecI}()$ that converts the Kronecker product of two vectors to conventional matrix multiplication can be found in appendix J of [27]. For the linear free vibration case, the nonlinear matrices $\left[\tilde{\mathbf{K}}_{\mathbf{12}}\right]$ and $\left[\tilde{\mathbf{K}}_{\mathbf{22}}\right]$ are dropped and Equation (5.34) is reduced to:

$$\left[\mathbf{K_{11}}\right]\left\{\boldsymbol{\delta}\right\} - \omega_L^2\left[\mathbf{M_S}\right]\left\{\boldsymbol{\delta}\right\} = 0 \tag{5.35}$$

Equation (5.35) can be solved as a classic linear eigenvalue problem to obtain ω_L^2. For better interpretation and analysis, it is convenient to report the dimensionless frequency that is defined as follows:

$$\Omega = \omega R_2\sqrt{\frac{\rho(1-\nu)^2}{E}} \tag{5.36}$$

5.8.2 Nonlinear Free Vibration

Assuming the period of nonlinear vibration to be τ, the maximum displacement $\left\{\boldsymbol{\delta}_{\mathbf{max}}\right\}$ occurs at $t = \tau/4$ where $\omega t = \pi/4$. Under these conditions (5.34) is reduced to:

$$\left(\left[\mathbf{K_{11}}\right] + \left[\tilde{\mathbf{K}}_{\mathbf{12}}\right]_{(\mathrm{D}\times\mathrm{D})} vecI\left(\left\{\boldsymbol{\delta}_{\mathbf{max}}\right\}\right) + \frac{1}{2}\left[\tilde{\mathbf{K}}_{\mathbf{22}}\right]_{(\mathrm{D}^2\times\mathrm{D})} vecI\left(\left\{\boldsymbol{\delta}_{\mathbf{max}}^{\otimes\mathbf{2}}\right\}\right)\right)\left\{\boldsymbol{\delta}_{\mathbf{max}}\right\} - \omega^2\left[\mathbf{M_S}\right]\left\{\boldsymbol{\delta}_{\mathbf{max}}\right\} = \left\{\mathbf{0}\right\} \tag{5.37}$$

It is worthy to mention that some of the earlier studies(e.g. [30] and [31]) have solved Equation (5.37) as an eigenvalue problem and predicted different behavior. Because eigenvalue solution of (5.37) does not satisfy the nonlinear equilibrium equation of (5.33) at all the times in the periodic motion, the nonlinear frequencies calculated by such an approach are not accurate [29][32]. Employing a weighted residual [29] for integration between $t = 0 \rightarrow t = \tau/4$ that represent the amplitude variation between $\left\{\mathbf{0}\right\} \rightarrow \left\{\boldsymbol{\delta}_{\mathbf{max}}\right\}$ yields [32]:

$$\int_0^{\tau/4} \left\{\mathbf{R}\right\} \sin(\omega t) dt = 0 \tag{5.38}$$

Taking into account that $\left\{\boldsymbol{\delta}_{\mathbf{max}}\right\}$ is independent of the time variable and $\int_0^{\tau/4} \sin^2(\omega t) dt = \tau/8$, $\int_0^{\tau/4} \sin^3(\omega t) dt = \tau/3\pi$ and $\int_0^{\tau/4} \sin^4(\omega t) dt = 3\tau/32$, the nonlinear vibration of Equation (5.34) can be transformed into the following eigenvalue problem:

$$\left[\left[\mathbf{K_{11}}\right] + \frac{8}{3\pi}\left[\tilde{\mathbf{K}}_{\mathbf{12}}\right]_{(\mathrm{D}\times\mathrm{D})} vecI\left(\left\{\boldsymbol{\delta}_{\mathbf{max}}\right\}\right) + \frac{3}{8}\left[\tilde{\mathbf{K}}_{\mathbf{22}}\right]_{(\mathrm{D}^2\times\mathrm{D})} vecI\left(\left\{\boldsymbol{\delta}_{\mathbf{max}}^{\otimes\mathbf{2}}\right\}\right)\right]\left\{\boldsymbol{\delta}_{\mathbf{max}}\right\} - \omega^2\left[\mathbf{M_S}\right]\left\{\boldsymbol{\delta}_{\mathbf{max}}\right\} = \left\{\mathbf{0}\right\} \tag{5.39}$$

Equation (5.39) can be solved as an eigenvalue problem using the "vector iteration method" given in [29] and [27].

5.8.3 Convention of Boundary Conditions

Using Tong [33]'s convention, for the case of isotropic materials where a truncated cone has four degrees of freedom at each edge, notations of the nodal boundary conditions are shown in table 5.1. The first and second elements of the boundary conditions in the following sections denote the small and large edge of the truncated cone respectively. For example F-CC4 indicates free at the small edge and clamped at the large edge end as what

Table 5.1 Naming convention for boundary conditions [33]

Name	U	V	W	$\partial W/\partial x$
F	free	free	free	free
SS0	0	free	free	free
SS1	free	free	0	free
SS2	0	free	0	free
SS3	free	0	0	free
SS4	0	0	0	free
CC1	free	free	0	0
CC2	0	free	0	0
CC3	free	0	0	0
CC4	0	0	0	0

described in table 5.1 for "CC4".

5.9 Results and Discussion

5.9.1 Validation: Convergence and Linear Frequencies

An in-house computer program was developed to perform the calculations. To investigate the validity of the model, the first step was a comparison of the convergence and accuracy of the linear frequency of vibration with those of four available experimental cases in the literature. The results are shown in figure 5.2 and table 5.2:

- Case 1: Free-free vibration of conical shells made of cold-rolled steel as reported by Hu et al. [34]. The experimental setup was reported to be: $\alpha_c = 14.2°$, $r_1 = 0.06919m$, $r_2 = 0.1543m$, $h = 2.54\times10^{-4}m$, $E = 203GPa$, $\nu = 0.3$, $\rho = 7988kg/m^3$ [34, 36, 37] and F-F (the data in Fig. 2. in reference [34] was digitized).
- Case 2: Vibration of loosely clamped cold-rolled steel truncated conical shells with the same material properties as Case 1 reported by Lindholm and Hu [1][37]. The other experimental setup parameters were: $\alpha_c = 30.2°$, $r_1 = 0.0889m$, $r_2 = 0.2019m$, $h = 2.54\times10^{-4}m$, and the boundary condition is set to be CC3-CC3 (the data from Fig. 4 in reference [1] was digitized).
- Case 3: Same as Case 2 in terms of material and boundary conditions with the geo-

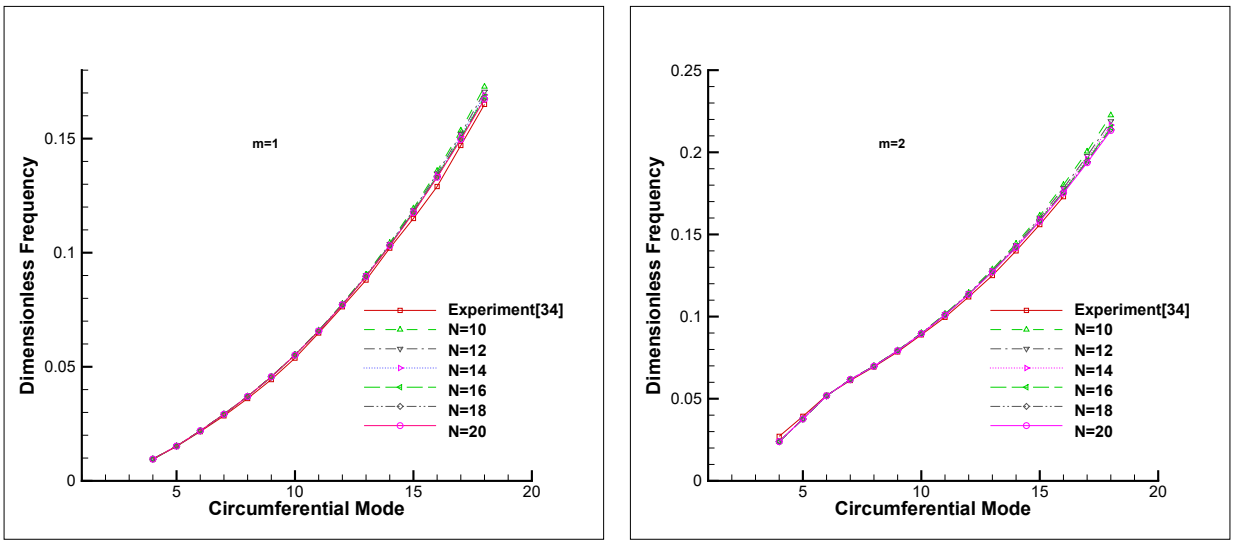

(a) First Mode

(b) Second Mode

Figure 5.2 Validation: Case 1, FEM linear dimensionless natural frequency (Equation (5.36)) compared to the experimental results of Hu et al. [34] for the first (5.2a) and second mode (5.2b) of vibration of a free-free truncated conical shell at different number of finite elements ($N = 10, 12, 14, 16, 18, 20$)

metrical parameters: $\alpha_c = 45.1°$, $r_1 = 0.10115m$, $r_2 = 0.2276m$, $h = 2.54 \times 10^{-4}m$ (the data in Fig. 5 in reference [1] was digitized).

- Case 4: Vibration of clamped-free aluminum truncated conical shells as reported by Adelman [35] where the experimental setup was: $\alpha_c = 60.0°$, $r_1 = 0.0762m$, $r_2 = 0.6097m$, $h = 6.35 \times 10^{-4}m$, $E = 68.948GPa$, $\nu = 0.315$ and $\rho = 2714kg/m^3$ and the boundary conditions were set to CC4-F (the data obtained from table IV in reference [35]).

It should be noted that to maintain accuracy in the current study, the linear part of the kinematics equations has always been modeled using the linear part of Sander's kinematics ($c_3 = 1$ in Equation (5.2)). Figure 5.2 shows the variation of calculated dimensionless frequencies versus the circumferential mode number for different numbers of elements in Case 1 for the first and second modes of vibration. The results show excellent agreement. Considering the results of this case, the number of elements was chosen to be twenty elements for the rest of the linear cases. The correctness of boundary conditions implementation was investigated in cases 2, 3 and 4. The values of the dimensionless

Table 5.2 Comparison of linear natural vibration dimensionless frequency Ω for the first mode (m=1) with the existing experimental studies

nc	Case 2 (30.2°)		Case 3 (45.1°)		Case 4(60°) Ω (rad/s)			
	Present	Ref. [1]	Present	Ref. [1]	Present		Ref. [35]	
2	0.591447	-	.62666	-	.02928	(255.0)	.03017	(262.8)
3	0.358468	-	.47194	-	.01636	(142.5)	.01689	(147.1)
4	0.228965	-	.32698	-	.01053	(91.8)	.01331	(115.9)
5	0.158844	0.157	.18723	-	.01271	(110.7)	.01524	(132.7)
6	0.118549	0.121	.17681	.165	.01940	(169.0)	.01939	(168.9)
7	0.096123	0.097	.14045	.137	.02423	(211.1)	.02422	(211.0)
8	0.086202	0.089	.11828	.120	.02958	(257.7)	.02957	(257.5)
9	0.085335	0.088	.10680	.112	.03548	(309.0)	.03546	(308.9)
10	0.090378	0.091	.10356	.108	-		-	
11	0.098605	0.099	.10632	.110	-		-	
12	0.108286	0.109	.11300	.117	-		-	
13	0.118805	0.117	.12197	.125				

linear natural frequencies are presented in table 5.2 and show good accordance with the experimental results.

5.9.2 Validation: Nonlinear Vibration of Cylindrical Shells

There are a limited number of studies on the nonlinear vibration of conical shells and some lack sufficient data to enable reproduction of the results. Therefore for validation of the nonlinear results of the current study, the case of a cylindrical shell was simulated using a cone with a very small angle. Two cases were studied:

- Case 5: Nonlinear vibration of a cylindrical shell reported by Nowinski [38], Raju and Rao [39] and Selmane and Lakis [40] where the shell parameters were given as: $n_c = 4$, $\alpha_c = 0.01°$, $\mathrm{r}_1 = 0.0254m$ ($\mathrm{r}_2 = 0.025407m$), $\mathrm{L} = 0.0399m$, $h = 2.54E{-}4{\times}10^{-4}m$, $E = 204.08GPa$, $\nu = 0.3$ and $\rho = 7833.5kg/m^3$. The boundary conditions for this case are SS4-SS4. The natural linear vibration frequency obtained in the current study is 8591.32Hz vs 8553.74Hz reported by Raju and Rao [39], this shows good accordance.
- Case 6: Nonlinear vibration of a cylindrical shell reported by Raju and Rao [39] is the same as Case 5 other than the boundary conditions, which were reported to be

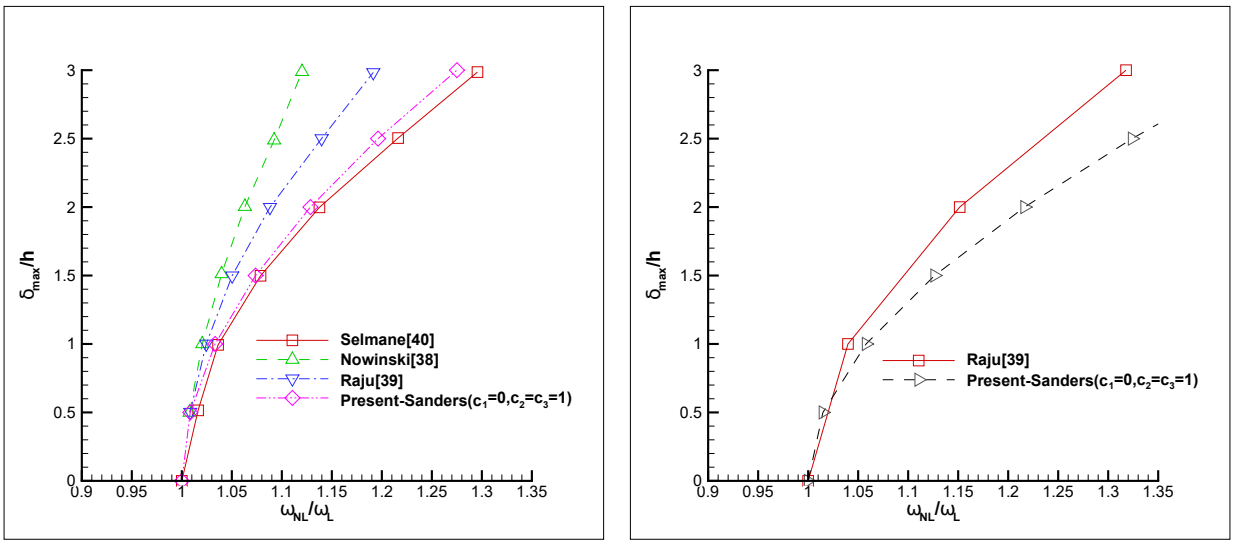

(a) Cylindrical Shell: Case 5

(b) Cylindrical Shell: Case 6

Figure 5.3 Validation: Backbone curve for cylindrical shells: (5.3a) Case 5 reported by Nowinski [38], Raju and Rao [39] and Selmane and Lakis [40]; (5.3b) Case 6 reported by Raju and Rao [39]

SS0-SS0. The natural linear vibration frequency obtained in the current study is 6453.46 Hz vs 6428.07 Hz reported by Raju and Rao [39]; these differ only by 0.5%.

Figure 5.3a shows a comparison of the backbone curve for Case 5. It can be seen the results of current study lie between those reported by Selmane and Lakis [40] and Raju and Rao [39] and show good accordance. Figure 5.3b shows a comparison of the results of the present study and those reported by Raju and Rao [39] for Case 6 and it also shows good agreement. It should be noted that while Nowinski [38] used Donnell's type of nonlinearities in his study, Raju and Rao [39] and Selmane and Lakis [40] employed Sander's theory taking into account the nonlinear rotations around the normal to the surface plane ($c_1 = 0$ and $c_2 = c_3 = 1$). Moreover, Nowinski [38] assumed the mode shapes to have two components, a harmonic and a time variable component. This is intended to satisfy the periodicity of the circumferential displacements that behaves roughly similar to a companion mode and might result in lower nonlinear frequencies. On the other hand, Raju and Rao [39] formulated the finite element solution in terms of a 12-degree polynomial, which is relatively more loose in comparison to the 8 degrees of freedom of this particular

case in the current study. Although the work of Selmane and Lakis [40] is more similar to the current study; the non-diagonal elements of the nonlinear stiffness matrix are neglected. Based on numerical results (not presented here), omitting the non-diagonal elements of the nonlinear stiffness matrix results in higher nonlinear frequencies. An exact match to those reported by Selmane and Lakis [40] could not be obtained with the formulation and tools developed during the current study.

5.9.3 Nonlinear Vibration of Truncated Conical Shells

5.9.3.1 Circumferential Mode Number

Once the developed model was sufficiently validated, the effects of various parameters on the nonlinear frequencies of conical shells were studied. It is worthy to mention that all the results of nonlinear vibration for conical shells were obtained at twenty finite elements. Figure 5.4 shows the variation of nonlinear frequency for different circumferential mode numbers; $n_c = 5-8$ for the loosely clamped truncated cone of Case 3 ($\alpha_c = 45.1°$ and CC3-CC3) both in terms of backbone curve and the nonlinear frequency Hz. The first observation from figure 5.4b is the smaller differences between the predictions of different theories for conical shells in comparison to cylindrical shells. Investigating the mode shapes (not presented here) revealed that this can be partially attributed to the fact that the maximum amplitude of nonlinear vibration of the truncated cone occurs at nodes close to the large edge. For cylindrical shells it occurs close to the middle of the cylinder. Therefore, the effect of the constraint on the amplitude of the vibration is more dominant and it limits the rotational terms in more complex theories. Moreover, as can be seen, increasing the circumferential mode number increases the nonlinearity effects on the relative nonlinear frequency. This can be explained by the appearance of n_c as a multiplier in the differentiations with respect to the second principle coordinates ($\partial/\partial\theta$) in the linear rotation parameters φ_2 and φ of Equation (5.2). Same phenomenon can be observed more clearly in figure 5.4b. While the minimum linear frequency for this case happens at $n_c = 9$, for large amplitude nonlinear vibration; $\delta_{max}/h = 3$, the amplifying effect of the circumferential mode number results in the occurrence of lowest observable nonlinear frequency at $n_c = 7$. Furthermore, the same effect results in multiple cross-overs between the non-

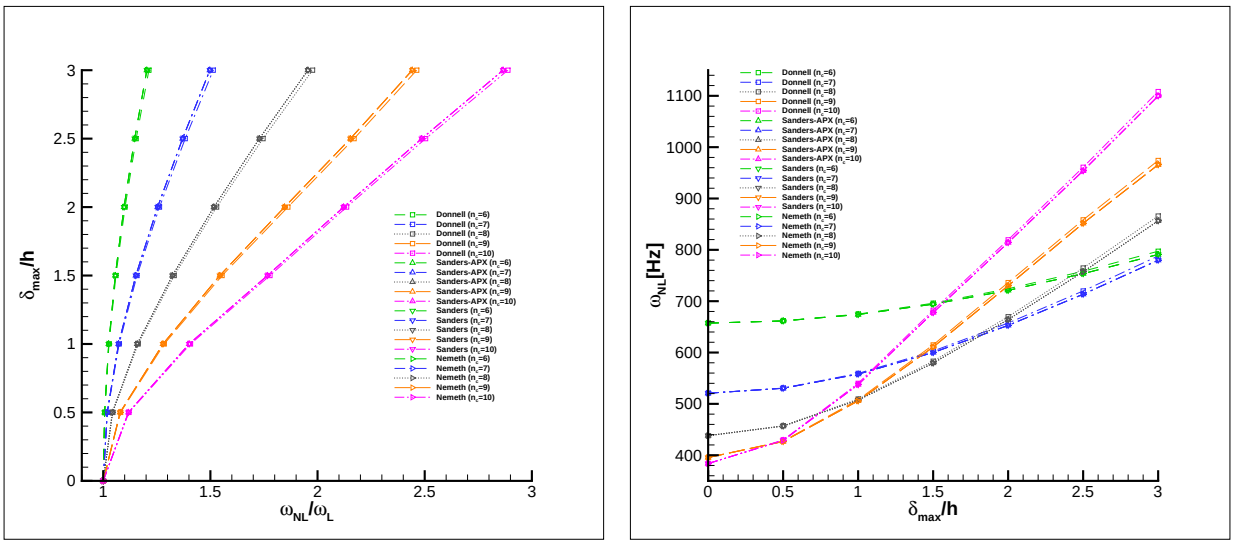

(a) Backbone Curve

(b) Nonlinear Frequency Hz

Figure 5.4 Variation of nonlinear frequency for different circumferential mode numbers($n_c = 6 - 10$) for truncated cone Case 3:(5.4a) backbone curve; (5.4b) nonlinear frequency Hz

linear responses of different circumferential mode numbers. Similar behavior is reported by Sofiyev [17] (figure 6). Therefore to obtain the minimum nonlinear frequency for the amplitude of interest; it is important to perform the nonlinear analysis over a wider range of circumferential mode numbers instead of relying on the lowest linear frequency.

5.9.3.2 Geometry

To investigate the effect of geometrical properties the following cases were studied:

- Case 7: A loosely clamped truncated cone where geometrical properties are $r_1 = 0.10115m$, $L/r_1 = 2$, $h = 2.54 \times 10^{-4}m$. The material properties and the boundary conditions are the same as Case 3 other than the density that is chosen to be $\rho = 7833.5kg/m^3$. The circumferential mode number is selected as $n_c = 7$.
- Case 8: Same as Case 3 with $\alpha_c = 45°$ and $n_c = 7$.
- Case 9: Loosely clamped aluminum truncated cone with the same material properties and dimensions (other than the thickness) as Case 4. The circumferential mode number and the boundary conditions were chosen to be $n_c = 7$ and SS4-SS4 respec-

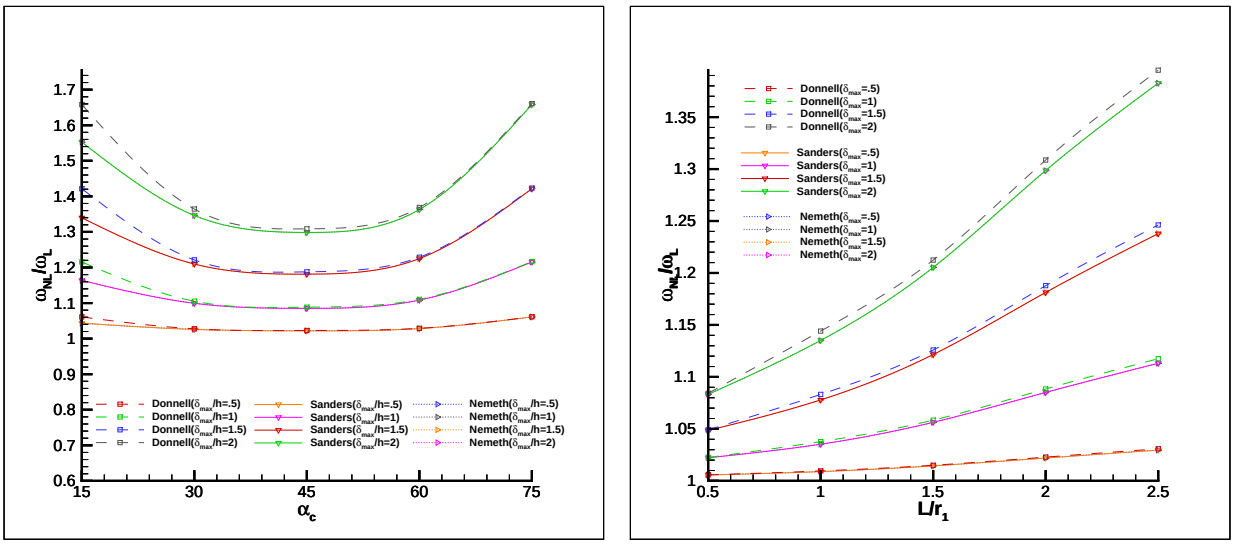

(a) Case 7 (b) Case 8

Figure 5.5 Effects of geometrical parameters: (5.5a) cone half angle; (5.5b) L/r_1 = ratio

tively.

Figure 5.5a shows the effect of cone half angle on the relative nonlinear frequency of the truncated cone shell of Case 7 for three different theories. The cone half angle values are $\alpha_c = 15°$, $30°$, $45°$, $60°$ and $75°$ and the associated first mode natural linear frequencies were calculated as 498.5, 491.1, 438.7, 338.8 and 206.3Hz accordingly. As can be seen the linear frequency decreases as the cone moves from a cylinder towards a flat plate. Same decreasing-flattening trend for the range of $\alpha_c = 15° - 60°$ was presented by Sofiyev [41] (figure 4.a) for the effect of cone half angle at slightly different boundary conditions. The first contributing factor to this behavior is the increase of the lateral area (and subsequently the mass of the cone) for this configuration by about 60% when the angle increases from 15° to 75°.

Notably, the differences between predictions of Donnell's and Sanders' and Nemeth's theories follow the same trend. In case of conical shells in the current formulation $1/R_1 = 1/\rho_{11} = 0$. On the other hand, $1/\sin(\alpha_c)$ and $1/\tan(\alpha_c)$ appear in the denominator of the omitted terms of Donnell's theory (second principle and geodesic radii of curvature). This is another factor that contributes to this behavior. In other words, the tangential displacement ($u_2 = V$) induces stronger nonlinear behavior for cases closer to cylindrical shells

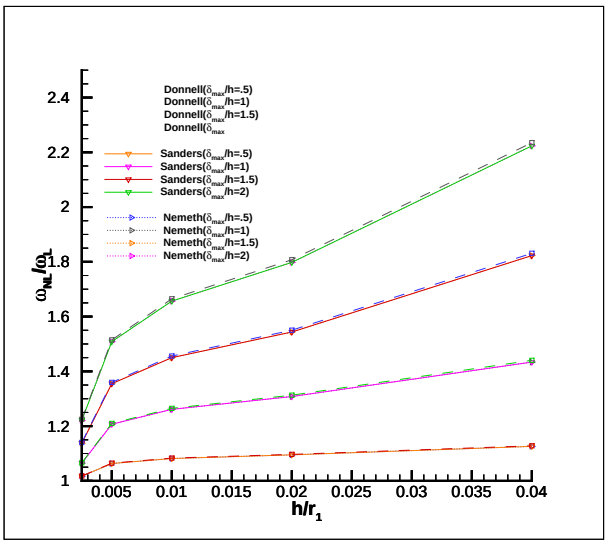

Figure 5.6 Case 9: Variation of relative nonlinear frequency with the "thickness to small radius ratio"

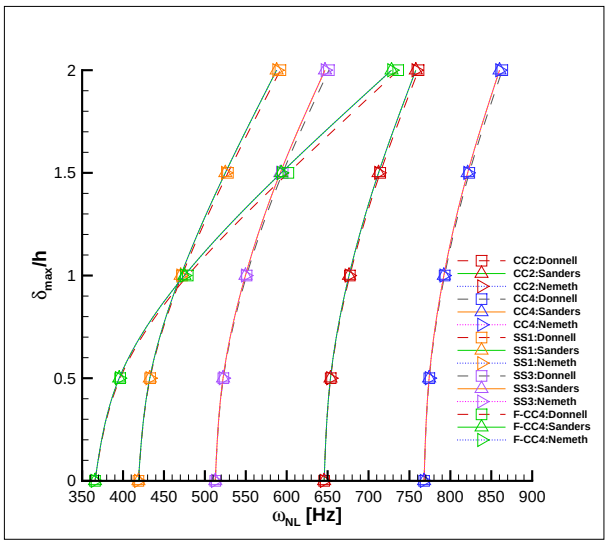

Figure 5.7 Case 3: Absolute nonlinear frequencyHz for different boundary conditions

than those of flat plates. As can be seen the effect of nonlinearity shows its minimum value at 45°.

Figure 5.5b shows the effect of variation of the slant length to small radius ratio for the cone of Case 8. The selected values are L/r_1 = 0.5, 1.0, 1.5, 2.0 and 2.5. The corresponding first mode linear natural frequencies were calculated to be 2636.1, 1428.5, 657.9, 434.5 and 315.1Hz. It can be seen that the relative nonlinear frequency increases with increasing the length of the cone. Longer cones demonstrate stronger nonlinear response at higher amplitudes.

Figure 5.6 shows the variation of the relative nonlinear frequency with the variation of h/r_1 = at r_1/h =400, 200, 100, 50 and 25. The associated linear frequencies were calculated to be 141.5, 147.2, 186.6, 232 and 362.5Hz respectively. Skipping the Case of very thin shells (r_1/h=400), the variation of relative nonlinear frequency with the thickness is seen to follow a linear trend. Recalling figure 5.4a, the variation of relative nonlinear frequency with the absolute amplitude of the vibration follows a semi-second order curve. Figure 5.6 can be explained by the fact that the linear frequencies increase linearly with the thickness and therefore the variation of relative nonlinear frequency with thickness becomes linear as a result of the division of a second order function by a first order one.

Similar behavior was reported by Sofiyev in figure 4 of [14].

5.9.3.3 Boundary Conditions

Though various boundary conditions were applied for the previous cases, the effect of boundary conditions is specifically investigated in this subsection. The cone geometry and material properties were selected to be the same as Case 3 and $n_c = 7$. The selected boundary conditions are: CC2-CC2, CC4-CC4, SS1-SS1,SS3-SS3 and F-CC4. Figure 5.8a presents the backbone curves for boundary conditions CC2, CC4 and F-CC4. The nonlinear responses of simply supported shells are presented in figure 5.8b and demonstrate stronger relative nonlinear response in comparison to clamped shells. As can be seen, constraining more degrees of freedom results in a reduction of the relative nonlinear frequency in both clamped and simply-supported shells. This is more visible by the behavior of F-CC4 shown in figure 5.8a. It should be noted that, as shown in figure 5.7, the more constrained cases demonstrate higher linear frequencies and therefore their reduced nonlinear responses still have higher absolute frequencies. For the case of free-clamped truncated cone, the free end increased the nonlinear response to the extent that it surpassed the more constrained cases.

5.10 Conclusion and Remarks

In the current study the nonlinear vibration of truncated conical shells was formulated for anisotropic materials according to four different shell theories; Donnell, Sanders with nonlinear rotation along the normal to surface neglected, Sanders and Nemeth. The formulation employed finite element exact solution of the linear case in conjunction with the generalized coordinates obtained by Lagrange equations to develop equations of motion of conical shells. The nonlinear amplitude equation of the vibration in the matrix form was solved using a hybrid iterative method to study the effect of various parameters on the nonlinear response of conical shells. Results for the linear frequencies were validated against the existing experimental data in the literature for truncated cones and show good accordance. The nonlinear results were validated against the existing results of cylindrical shells and found to be in good agreement. Effects of various parameters were studied

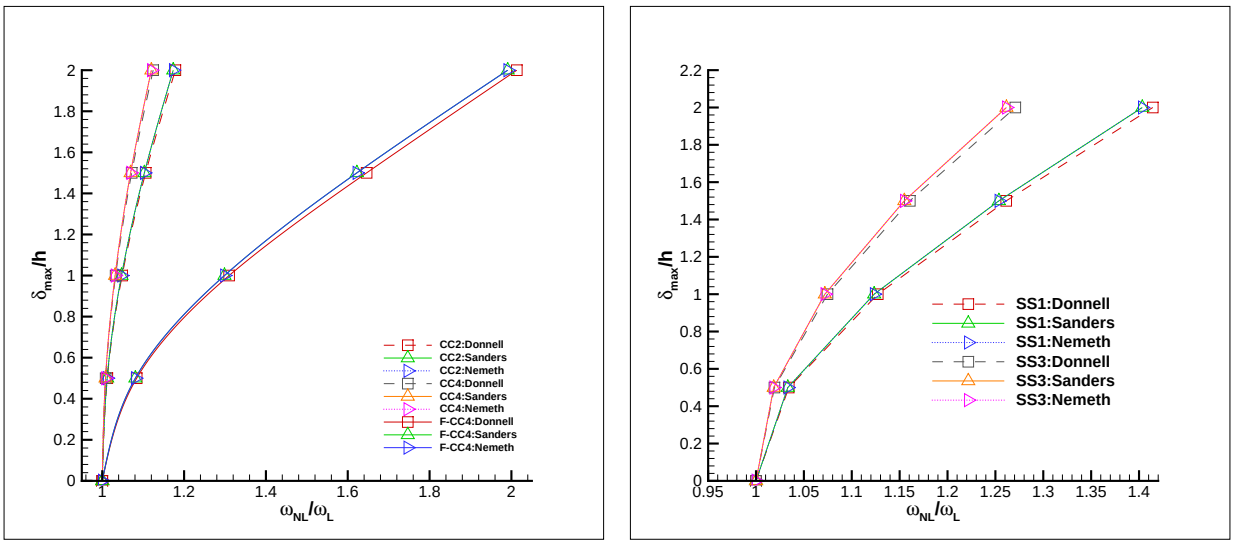

(a) Clamped (b) Simply Supported

Figure 5.8 Effect of boundary conditions on shell of Case 3: (5.8a) clamped; (5.8b) simply supported

and are summarized as follows:

- In all cases Donnell's theory predicted a higher nonlinear relative frequency than the other three theories. Further, in all cases presented in the current study the difference between the predictions of Nemeth's and Sanders' theories was found to be very small, though those of Sander's theory were found to have larger value. Since there is a significant emphasis on shear deformation in the development of Nemeth's theory[21], the above results can be attributed to the relatively thin shells selected for the current study and the corresponding absence of shear deformation. Based on the obtained results and the insignificant differences between Nemeth and Sanders theories, it is more practical to avoid larger amount of computations required by Nemeth theory and use Sanders as a good approximation for this type of problems.
- It was found that higher circumferential numbers result in an amplified nonlinear response.
- The relative nonlinear frequency demonstrated its minimum when the semi-vertex angle of the cone is equal to 45° degree while the difference between Donnell's and other theories is larger at lower semi-vertex angles. It was found that the nonlinear

response increases as the length to small radius ratio increases and this effect is stronger at higher amplitudes of vibration.

- Other than the case of very thin shells, the variation of relative nonlinear frequency with thickness was found to be linear with higher slopes at higher amplitudes of vibration.
- It was found that the shell demonstrates a weaker "relative nonlinear response" (nonlinear to linear frequency ratio) at more rigid constraints, though the absolute value of the nonlinear frequency is higher for more constrained cases.
- Within the range of thicknesses, length to diameter ratios and materials that are investigated in the current work, the differences between predictions of studied theories found to be less than 2 percent.

Refernces

[1] U. S. Lindholm and W. C. Hu, "Non-symmetric transverse vibrations of truncated conical shells," *International Journal of Mechanical Sciences*, vol. 8, no. 9, pp. 561–579, 1966. [Online]. Available: http://www.sciencedirect.com/science/article/pii/0020740366900786

[2] C. L. Sun and S. Y. Lu, "Nonlinear dynamic behavior of heated conical and cylindrical shells," *Nuclear Engineering and Design*, vol. 7, no. 2, pp. 113–122, 1968. [Online]. Available: http://www.sciencedirect.com/science/article/pii/0029549368900538

[3] D. Bendavid and J. Mayers, "A Nonlinear Theory for the Bending, Buckling, and Vibrations of Conical Shells," DTIC Document, Tech. Rep., 1970. [Online]. Available: http://oai.dtic.mil/oai/oai?verb=getRecord&metadataPrefix=html&identifier=AD0873255

[4] K. Kanaka Raju and G. Venkateswara Rao, "Large amplitude asymmetric vibrations of some thin shells of revolution," *Journal of Sound and Vibration*, vol. 44, no. 3, pp. 327–333, Feb. 1976. [Online]. Available: http://www.sciencedirect.com/science/article/pii/0022460X76905058

[5] T. Ueda, "Nonlinear Analysis Of The Supersonic Flutter Of A Truncated Conical Shell Using The Finite Element Method." *Transactions of the Japan Society for Aeronautical and Space Sciences*, vol. 20, no. 50, pp. 225–240, 1978.

[6] M. D. Olson, "Some experimental observations on the nonlinear vibration of cylindrical shells," *AIAA J*, vol. 3, no. 9, pp. 1775–1777, 1965. [Online]. Available: https://arc.aiaa.org/doi/pdfplus/10.2514/3.55196

[7] R.-h. Liu and J. Li, "Non-linear vibration of shallow conical sandwich shells," *International journal of non-linear mechanics*, vol. 30, no. 2, pp. 97–109, 1995. [Online]. Available: http://www.sciencedirect.com/science/article/pii/0020746294000326

[8] C. S. Xu, Z. Q. Xia, and C. Y. Chia, "Non-linear theory and vibration analysis of laminated truncated, thick, conical shells," *International journal of non-linear mechanics*, vol. 31, no. 2, pp. 139–154, 1996. [Online]. Available: http://www.sciencedirect.com/science/article/pii/0020746295000518

[9] Y. M. Fu and C. P. Chen, "Non-linear vibration of elastic truncated conical moderately thick shells in large overall motion," *International Journal of Non-Linear Mechanics*, vol. 36, no. 5, pp. 763–771, Jul. 2001. [Online]. Available: http://www.sciencedirect.com/science/article/pii/S0020746200000421

[10] J. Awrejcewicz, V. A. Krysko, and T. V. Shchekaturova, "Transitions from regular to chaotic vibrations of spherical and conical axially-symmetric shells," *International Journal of Structural Stability and Dynamics*, vol. 05, no. 03, pp. 359–385, Sep. 2005. [Online]. Available: http://www.worldscientific.com/doi/abs/10.1142/S0219455405001623

[11] V. A. Krysko, J. Awrejcewicz, and T. V. Shchekaturova, "Chaotic vibrations of spherical and conical axially symmetric shells," *Archive of Applied Mechanics*, vol. 74, no. 5-6, pp. 338–358, Mar. 2005. [Online]. Available: https://link.springer.com/article/10.1007/s00419-004-0356-3

[12] C. Chen and L. Dai, "Nonlinear vibration and stability of a rotary truncated conical shell with intercoupling of high and low order modals," *Communications in Nonlinear*

Science and Numerical Simulation, vol. 14, no. 1, pp. 254–269, 2009. [Online]. Available: http://www.sciencedirect.com/science/article/pii/S100757040700161X

[13] C. Chen, "Nonlinear Dynamic of a Rotating Truncated Conical Shell," in *Nonlinear Approaches in Engineering Applications*. Springer, New York, NY, 2012, pp. 349–391. [Online]. Available: https://link.springer.com/chapter/10.1007/978-1-4614-1469-8_12

[14] A. H. Sofiyev, "The non-linear vibration of FGM truncated conical shells," *Composite Structures*, vol. 94, no. 7, pp. 2237–2245, 2012. [Online]. Available: http://www.sciencedirect.com/science/article/pii/S0263822312000463

[15] A. M. Najafov and A. H. Sofiyev, "The non-linear dynamics of FGM truncated conical shells surrounded by an elastic medium," *International Journal of Mechanical Sciences*, vol. 66, pp. 33–44, 2013. [Online]. Available: http://www.sciencedirect.com/science/article/pii/S0020740312002251

[16] A. M. Najafov, A. H. Sofiyev, and N. Kuruoglu, "On the solution of nonlinear vibration of truncated conical shells covered by functionally graded coatings," *Acta Mechanica*, vol. 225, no. 2, pp. 563–580, Sep. 2013. [Online]. Available: http://link.springer.com/article/10.1007/s00707-013-0980-5

[17] A. H. Sofiyev, "Large-amplitude vibration of non-homogeneous orthotropic composite truncated conical shell," *Composites Part B: Engineering*, vol. 61, pp. 365–374, 2014. [Online]. Available: http://www.sciencedirect.com/science/article/pii/S135983681300351X

[18] F. Sabri and A. A. Lakis, "Hybrid finite element method applied to supersonic flutter of an empty or partially liquid-filled truncated conical shell," *Journal of Sound and Vibration*, vol. 329, no. 3, pp. 302–316, 2010. [Online]. Available: http://www.sciencedirect.com/science/article/pii/S0022460X09007470

[19] Y. Kerboua, A. A. Lakis, and M. Hmila, "Vibration analysis of truncated conical shells subjected to flowing fluid," *Applied Mathematical Modelling*, vol. 34, no. 3, pp. 791–809, 2010. [Online]. Available: http://www.sciencedirect.com/science/article/

pii/S0307904X09001826

[20] Y. Kerboua and A. A. Lakis, "Numerical model to analyze the aerodynamic behavior of a combined conical–cylindrical shell," *Aerospace Science and Technology*, vol. 58, pp. 601–617, 2016. [Online]. Available: http://www.sciencedirect.com/science/article/pii/S1270963816307064

[21] M. P. Nemeth, "A Leonard-Sanders-Budiansky-Koiter-Type Nonlinear Shell Theory with a Hierarchy of Transverse-Shearing Deformations," Tech. Rep. NASA/TP–2013-218025, Jul. 2013. [Online]. Available: http://ntrs.nasa.gov/search.jsp?R=20140000788

[22] ——, "An Exposition on the Nonlinear Kinematics of Shells, Including Transverse Shearing Deformations," NASA, Tech. Rep. NASA/TM–2013-217964, 2013. [Online]. Available: http://ntrs.nasa.gov/search.jsp?R=20130011025

[23] J. L. Sanders Jr, "An improved first-approximation theory for thin shells," NASA, Tech. Rep. TR R-24, 1959.

[24] J. L. Sanders Jr., "Nonlinear theories for thin shells," DTIC Document, Tech. Rep. AD0253822, 1961. [Online]. Available: http://oai.dtic.mil/oai/oai?verb=getRecord&metadataPrefix=html&identifier=AD0253822

[25] ——, "Nonlinear theories for thin shells," *Quarterly of Applied Mathematics*, pp. 21–36, 1963. [Online]. Available: http://www.jstor.org/stable/43634948

[26] L. H. Donnell, "A new theory for the buckling of thin cylinders under axial compression and bending," *Trans. ASME*, vol. 56, no. 11, pp. 795–806, 1934. [Online]. Available: http://cybra.lodz.pl/Content/6356/AER_56_12.pdf

[27] M. Bakhtiari, A. A. LAKIS, and Y. Kerboua, "Nonlinear vibration of truncated conical shells: Donnell, Sanders and Nemeth theories," Tech. Rep. EPM-RT-2018-01, 2018. [Online]. Available: https://publications.polymtl.ca/3011/1/EPM-RT-2018-01_Bakhtiari.pdf

[28] M. Amabili, *Nonlinear vibrations and stability of shells and plates*. Cambridge University Press, 2008. [Online]. Available: https://books.google.ca/books?hl=en&lr=&id=

0Ymw-pi7-x4C&oi=fnd&pg=PA52&dq=Nonlinear+Vibrations+and+Stability+of+Shells+and+Plates&ots=uZtdkX_GUL&sig=hStbpt8yVKKY4Eeh6L0QEzyT2NY

[29] R. Lewandowski, "Free vibration of structures with cubic non-linearity-remarks on amplitude equation and Rayleigh quotient," *Computer Methods in Applied Mechanics and Engineering*, vol. 192, no. 13, pp. 1681–1709, Mar. 2003. [Online]. Available: http://www.sciencedirect.com/science/article/pii/S0045782503001890

[30] T. Ueda, "Non-linear free vibrations of conical shells," *Journal of Sound and Vibration*, vol. 64, no. 1, pp. 85–95, 1979. [Online]. Available: http://www.sciencedirect.com/science/article/pii/0022460X79905741

[31] M. Shakouri and M. A. Kouchakzadeh, "Analytical solution for vibration of generally laminated conical and cylindrical shells," *International Journal of Mechanical Sciences*, vol. 131-132, no. Supplement C, pp. 414–425, Oct. 2017. [Online]. Available: http://www.sciencedirect.com/science/article/pii/S0020740317311633

[32] M. K. Singha and R. Daripa, "Nonlinear vibration of symmetrically laminated composite skew plates by finite element method," *International Journal of Non-Linear Mechanics*, vol. 42, no. 9, pp. 1144–1152, Nov. 2007. [Online]. Available: http://www.sciencedirect.com/science/article/pii/S0020746207001783

[33] L. Tong, "Free vibration of orthotropic conical shells," *International Journal of Engineering Science*, vol. 31, no. 5, pp. 719–733, 1993.

[34] W. C. Hu, J. F. Gormley, and U. S. Lindholm, "An experimental study and inextensional analysis of vibrations of free-free conical shells," *International Journal of Mechanical Sciences*, vol. 9, no. 3, pp. 123–128, 1967.

[35] H. M. C. Adelman, "A method for computation of vibration modes and frequencies of orthotropic thin shells of revolution having general meridional curvature," Tech. Rep. NASA TN 0-4972, Jan. 1969. [Online]. Available: https://ntrs.nasa.gov/search.jsp?R=19690007137

[36] J. F. H. Gormley, "Flexural vibrations of conical shells with free edges," Tech. Rep. NASA CR-384, Mar. 1966. [Online]. Available: https://ntrs.nasa.gov/search.jsp?R=

19660008884

[37] E. C. Naumann, "On the prediction of the vibratory behavior of free-free truncated conical shells," Tech. Rep. NASA TN D-4772, Sep. 1968. [Online]. Available: https://ntrs.nasa.gov/search.jsp?R=19680023585

[38] J. L. Nowinski, "Nonlinear transverse vibrations of orthotropic cylindrical shells," *AIAA J*, vol. 1, no. 3, pp. 617–620, 1963.

[39] K. K. Raju and G. V. Rao, "Large amplitude asymmetric vibrations of some thin shells of revolution," *Journal of Sound and Vibration*, vol. 44, no. 3, pp. 327–333, 1976.

[40] A. Selmane and A. A. Lakis, "Influence of geometric non-linearities on the free vibrations of orthotropic open cylindrical shells," *International Journal for Numerical Methods in Engineering*, vol. 40, no. 6, pp. 1115–1137, 1997. [Online]. Available: http://onlinelibrary.wiley.com/doi/10.1002/(SICI)1097-0207(19970330)40:6%3C1115::AID-NME105%3E3.0.CO;2-H/abstract

[41] A. H. Sofiyev, "The combined influences of heterogeneity and elastic foundations on the nonlinear vibration of orthotropic truncated conical shells," *Composites Part B: Engineering*, vol. 61, pp. 324–339, May 2014. [Online]. Available: http://www.sciencedirect.com/science/article/pii/S1359836814000572

I.A. Conical Shell Linear Equilibrium Equations in Terms of Stress Resultants

The principle parameters of conical shells can be obtained from the following equation:

$$A_1(x,\theta) = 1, A_2(x,\theta) = x\sin(\alpha_c), \frac{1}{R_1(x,\theta)} = 0, \frac{1}{R_2(x,\theta)} = \frac{1}{x\tan(\alpha_c)}, \frac{1}{\rho_{11}} = 0, \frac{1}{\rho_{22}} = \frac{1}{x} \tag{II.A.40}$$

By introducing the geometrical parameters of conical shells into the general equilibrium equations of Sanders' improved linear theory [23]; one obtains the equilibrium equations of a conical shell as follows.:

$$\frac{\partial n_{11}}{\partial x} + \frac{1}{x\sin(\alpha_c)}\frac{\partial n_{12}}{\partial \theta} + \frac{1}{x}(n_{11} - n_{22}) - \frac{1}{2x^2\sin(\alpha_c)\tan(\alpha_c)}\frac{\partial m_{12}}{\partial \theta} = 0 \tag{II.A.41a}$$

$$\frac{\partial n_{12}}{\partial x}+\frac{1}{x\sin(\alpha_c)}\frac{\partial n_{22}}{\partial \theta}+\frac{2n_{12}}{x}+\frac{3}{2}\frac{1}{x\tan(\alpha_c)}\frac{\partial m_{12}}{\partial x}+\frac{1}{x^2\sin(\alpha_c)\tan(\alpha_c)}\frac{\partial m_{22}}{\partial \theta}+\frac{3}{2}\frac{1}{x^2\tan(\alpha_c)}m_{12}=0 \qquad \text{(II.A.41b)}$$

$$\frac{\partial^2 m_{11}}{\partial x^2}+\frac{2}{x^2\sin(\alpha_c)}\frac{\partial m_{12}}{\partial \theta}+\frac{2}{x\sin(\alpha_c)}\frac{\partial^2 m_{12}}{\partial x\partial \theta}+\frac{2}{x}\frac{\partial m_{11}}{\partial x}-\frac{1}{x}\frac{\partial m_{22}}{\partial x}+\frac{1}{x^2\sin(\alpha_c)^2}\frac{\partial^2 m_{22}}{\partial \theta^2}-\frac{n_{22}}{x\tan(\alpha_c)}=0 \qquad \text{(II.A.41c)}$$

I.B. Nomenclature

A_1, A_2	Surface metrics along x and θ directions
R_1, R_2	Principle radii of curvature along x and θ directions
$\left[\bar{CC}^0\right]$	Symmetric constitutie matrix for conical element
$\left\{\mathfrak{E}^\circ\right\}$	Reference surface total strain vector defined by Equation (5.6)
$e_{11}^\circ, e_{22}^\circ, e_{12}^\circ$	Linear deformation parameters defined by Equation (5.3)
$\left[\mathcal{AQ}\right]$	Characteristic polynomial matrix
$\left[\mathbf{K_{11}}\right], \left[\tilde{\mathbf{K}}_{\mathbf{12}}\right], \left[\tilde{\mathbf{K}}_{\mathbf{22}}\right]$	Assembled first, second and third order structural stiffness matrices
$\left[\mathbf{M_T}\right], \left[\mathbf{M_S}\right]$	Assembled translational and structural mass matrices defined by Equation (5.25) and (5.26)
$\left[\mathbf{N}\right]$	Displacement field matrix of a finite element defined by Equation (5.20)
$U_i (i = 1, 2, 3)$	Displacements along the longitudinal, latheral and normal to surface directions, off the reference surface
$u_i (i = 1, 2, 3)$	Displacements along the longitudinal (U), latheral (V) and normal (W), on the reference surface
c_{NL}, c_1, c_2, c_3	Flag parameters to define different shell theories
L	Truncated cone element length
n_c	Circumferential mode number
α_c	Cone half angle
$\chi_{11}^\circ, \chi_{22}^\circ, \chi_{12}^\circ, \left\{\boldsymbol{\chi}^\circ\right\}$	Linear deformation parameters defined by Equation (5.4b)
δ_m	nodal degrees of freedom associated with $m^{th} node$
$\epsilon_{11}^\circ, \epsilon_{22}^\circ, \left\{\boldsymbol{\epsilon}^\circ\right\}$	Reference surface strains defined by Equation (5.4a)
$\varphi_1, \varphi_2, \varphi$	Linear rotation parameters defined by Equation (5.2)
ρ_{11}, ρ_{22}	Geodesic radii of curvature radii of curvature along x and θ directions
$\left\{\boldsymbol{\delta}\right\}^e$	Vector of element degrees of freedom
$\left\{\boldsymbol{\delta}\right\}$	Vector of whole system degrees of freedom

CHAPTER 6 ARTICLE 3- NONLINEAR SUPERSONIC FLUTTER OF TRUNCATED CONICAL SHELLS

Mehrdad Bakhtiari, Aouni A. Lakis, Youcef Kerboua

Journal of Mechanical Science and Technology 34 (2020): 1375-1388.

Abstract

A numerical model was developed to investigate the flutter instability of truncated conical shells subjected to supersonic flows. The exact solution of Sanders' best first-order approximation was used to develop the finite elements model of the shell. Nonlinear kinematics of Donnell's, Sanders' and Nemeth's theories, in conjunction with the generalized coordinates method, were used to formulate the nonlinear strain energy of the shell. A pressure field was formulated using the piston theory with the correction term for the curvature. Lagrangian equations of motion based on Hamilton's principle were obtained. A variation of the harmonic balance method was used for developing the amplitude equations of the shell, and a numerical method was used for solving these equations. Results of the linear and nonlinear flutter of truncated conical shells were validated against the existing data in the literature. It was observed that geometrical nonlinearities have a softening effect on the stability of the shell in supersonic flows.

6.1 Introduction

The aeroelastic stability of shells and plates interacting with supersonic flow has been the subject of several studies in past decades. While several studies can be found in the literature on the flutter characteristics of cylindrical shells, the number of articles on the supersonic flutter of conical shells is limited. Moreover, even in the existing studies on the flutter of cylindrical shells, very few have employed geometrically nonlinear theories in their analyses. Employing nonlinear shell theories is important since experimental studies have shown that the oscillation amplitude of flutter has the same order of magnitude as the shell thickness [1].

Dixon and Hudson([2],[3] and [4]) studied the flutter, vibration and buckling of truncated orthotropic thin conical shells with generalized elastic edge restraints. They employed the Donnell type of nonlinear kinematics in conjunction with the modified first-order piston theory to model the structure behavior. They argued that for shells subjected to static external pressure loads, divergence governed design conditions for small values of semi-cone angle, flutter for moderate semi-cone angle values and buckling is the dominant phenomena in large semi-cone angles. Miserentino and Dixon [5] expanded those works by performing experimental studies on the vibration and flutter of thin-walled truncated orthotropic conical shells. The experimental results provided the variations of resonant frequency with internal pressure and circumferential wave number at constant Mach number. The results verified the theoretical works of Dixon and Hudson Dixon and Hudson [2] for thin shells with good accuracy. The work of Ueda et al. [6] explored the theoretical and experimental aspects of supersonic flutter in conical shells. In their experiments, they used a truncated cone with a semi vertex angle of 14^{o} to obtain flutter and buckling boundaries of the shell within supersonic flow at Mach number equal to two. They employed the finite elements method for the theoretical analysis and demonstrated good agreement between experimental and theoretical results. They also concluded that FEM is a powerful tool for predicting panel flutter behavior. Bismarck-Nasr and Costa Savio [7] developed a finite element method for supersonic flutter of truncated conical shells using Novozhilov's shell theory. In their work on the shell model, the in-plane inertia was pre-served within kinetic energy formulations while the rotary inertia was neglected. The aerodynamic loads were modeled using the first-order high Mach number piston theory. Based on their results, it was concluded that the curvature effect in modeling the aerodynamic loads has little effect on the stability conditions.

Pidaparti [8] employed a quadrilateral thin shell finite element for analyzing the supersonic flutter of doubly curved composite shells using linear Love-Kirchhoff thin shell theory. Based on the obtained results, it was stated that the fiber angle and orthotropy impose significant effects on flutter boundaries for cylindrical and conical shells and flat plates.

Sabri and Lakis [9] studied the flutter behavior of partially filled truncated conical shells in supersonic flows using a hybrid finite element method, Sanders' linear thin shell theory and first-order piston theory with correction for the effect of curvature. Initial stiffening due to pressurization was also considered in this study. Among the conclusions, it was stated that conical shells are susceptible to coupled-mode flutter. Mahmoudkhani et al. [10] studied the aero-thermoelastic stability of FGM truncated conical shells in supersonic flows using Donnell's theory and the linear piston theory. They employed the eigenvalue analysis to obtain the critical parameters. They showed that larger semi-cone angles reduce shell stability. Davar and Shokrollahi [11] provided an analysis of the supersonic flutter of FGM conical shells with clamped and simply supported boundary conditions using first-order shear deformation and linear shell theory. Their results showed that changing the boundary condition from simply supported to clamped increases all the frequencies but there is no general trend in the critical aerodynamic pressure.

Vasilev [12] presented a new formulation for flutter analysis of isotropic truncated conical shells exposed to supersonic flows using linear shell theory. The author concluded that the linear piston theory significantly overestimates the critical dynamic pressure at low Mach numbers [12]. Yang et al. [13] investigated the supersonic flutter in FGM truncated conical shells employing first-order shear deformation and linear shell theory. It was shown that it is possible to control the periodic and chaotic instabilities by varying the material's compositional profile.

As can be seen, in the earlier works other than the study of Bismarck-Nasr and Costa Savio [7], the few studies limited their kinematic models to Donnell's-type nonlinearities. Moreover, employing Galerkin approach placed additional restraints on the type of boundary conditions that can be used. The focus of the current study is to formulate a hybrid finite element model that can represent the nonlinear behavior of truncated conical shells subjected to supersonic flows using the three different shell theories of Donnell, Sanders and Nemeth. This is performed in the following steps:

- The finite element displacement functions are derived from the exact solution to Sanders' best first-order approximation.
- Using that shape function as the bases of the generalized coordinate method, the

nonlinear internal strain and kinetic energies are formulated in terms of nodal degrees of free-dom.

- In addition, the effects of initial stiffening due to pressurization and axial loads are also expressed in terms of nodal displacements. Then, the Lagrangian equations of motion of the shell are developed based on the Hamilton principle.
- The equations of motion are converted to an amplitude equation by employing a variation of the harmonic balance method.

6.2 Nonlinear Kinematics

Nemeth [14] formulated a shell theory that can provide Donnell's and Sanders' shell theories as parametric subsets [14] and [15]. Figure 6.1a shows the coordinate system and geometrical parameters of the truncated cone element of the this study. The longitudinal and radial principal-curvature coordinates are denoted by x and θ. The cone half-angle is denoted by α_c and the slant length of the cone can be obtained from $L = x_2 - x_1$. The reference surface is assumed at the middle of the shell thickness and neglecting transverse shear deformation, there are three fundamental unknowns in this formulation: two middle-surface tangential displacements $U = u_1(x,\theta)$ and $V = u_2(x,\theta)$ and the normal displacement $W = u_3(x,\theta)$. The displacements of material point of the shell $p(x,\theta,\xi_3)$ in the orthogonal principal-curvature coordinate systems are expressed as[16]:

$$\begin{aligned} U_1(x,\theta,\xi_3) &= u_1(x,\theta) + \xi_3[\varphi_1 - \varphi\varphi_2] \\ U_2(x,\theta,\xi_3) &= u_2(x,\theta) + \xi_3[\varphi_2 - \varphi\varphi_1] \\ U_3(x,\theta,\xi_3) &= u_3(x,\theta) - \frac{1}{2}\xi_3\left(\varphi_1^2 + \varphi_2^2\right) \end{aligned} \tag{6.1}$$

Where ξ_3 is the normal distance from the middle surface. The linear rotation parameters φ_1 , φ_2 and φ are defined as follows:

$$\begin{aligned} \varphi_1(x,\theta) &= -\frac{\partial u_3(x,\theta)}{\partial x} \\ \varphi_2(x,\theta) &= \frac{c_3 u_2(x,\theta)}{x\tan(\alpha_c)} - \frac{1}{x\sin(\alpha_c)}\frac{\partial u_3(x,\theta)}{\partial\theta} \\ \varphi(x,\theta) &= \frac{1}{2}c_3\left(\frac{\partial u_2(x,\theta)}{\partial x} - \frac{1}{x\sin(\alpha_c)}\frac{\partial u_1(x,\theta)}{\partial\theta} + \frac{u_2(x,\theta)}{x}\right) \end{aligned} \tag{6.2}$$

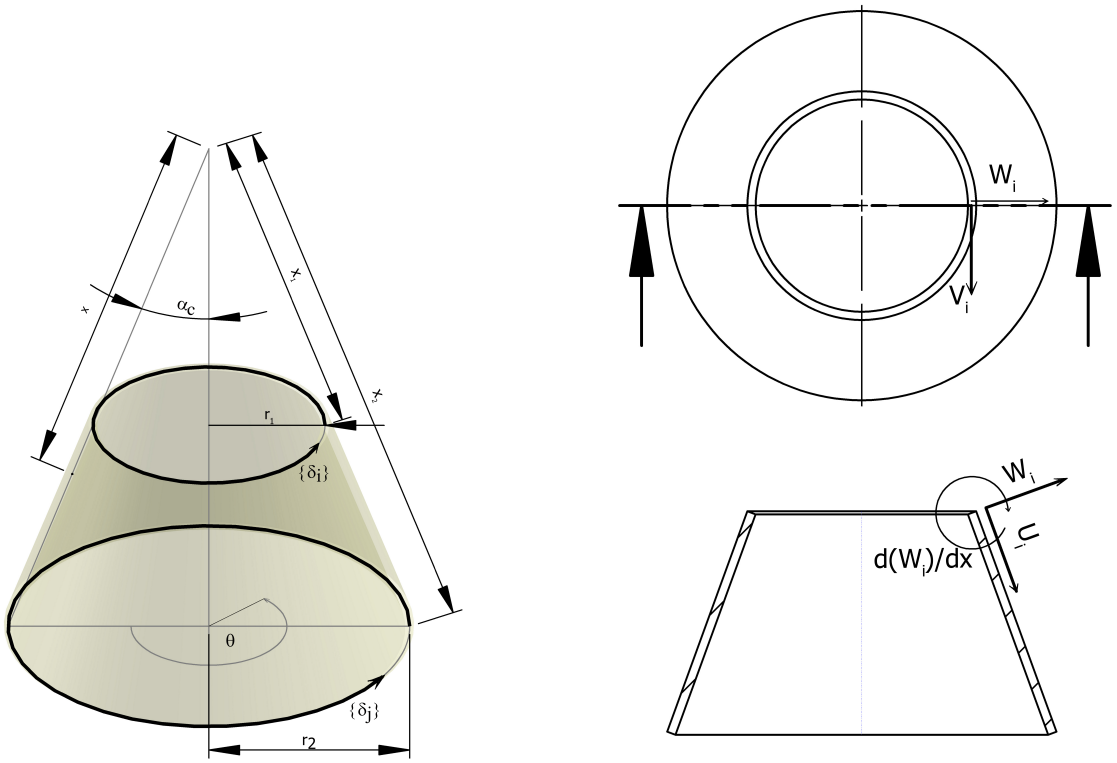

(a) (b)

Figure 6.1 Conventions: (6.1a) Geometry and coordinate system; (6.1b) Nodal degrees of freedom

The in-plane linear deformation parameters are given as:

$$\begin{aligned} e^{\circ}_{11}(x,\theta) &= \frac{\partial u_1(x,\theta)}{\partial x} \\ e^{\circ}_{22}(x,\theta) &= \frac{1}{x\sin(\alpha_c)}\frac{\partial u_2(x,\theta)}{\partial \theta} + \frac{u_1(x,\theta)}{x} + \frac{u_3(x,\theta)}{x\tan(\alpha_c)} \\ 2e^{\circ}_{12}(x,\theta) &= \frac{1}{x\sin(\alpha_c)}\frac{\partial u_1(x,\theta)}{\partial \theta} + \frac{\partial u_2(x,\theta)}{\partial x} - \frac{u_2(x,\theta)}{x} \end{aligned} \tag{6.3}$$

Finally, the relationships of the strain (ϵ) and the linear rotation parameters (χ) relationships with the displacements, on the middle surface are expressed as follows:

$$\left\{\boldsymbol{\epsilon}^{\circ}\right\} = \begin{Bmatrix} \epsilon^{\circ}_{11} \\ \epsilon^{\circ}_{22} \\ \gamma^{\circ}_{12} \end{Bmatrix} = \begin{Bmatrix} e^{\circ}_{11} \\ e^{\circ}_{22} \\ 2e^{\circ}_{12} \end{Bmatrix} + c_{NL} \begin{Bmatrix} \frac{1}{2}\left(\varphi_1^2 + c_2\varphi^2\right) + \frac{1}{2}c_1\left[(e^{\circ}_{11})^2 + e^{\circ}_{12}\left(e^{\circ}_{12} + 2\varphi\right)\right] \\ \frac{1}{2}\left(\varphi_2^2 + c_2\varphi^2\right) + \frac{1}{2}c_1\left[(e^{\circ}_{22})^2 + e^{\circ}_{12}\left(e^{\circ}_{12} - 2\varphi\right)\right] \\ \varphi_1\varphi_2 + c_1\left[e^{\circ}_{11}\left(e^{\circ}_{12} - \varphi\right) + e^{\circ}_{22}\left(e^{\circ}_{12} + \varphi\right)\right] \end{Bmatrix} \tag{6.4a}$$

$$\left\{\chi^{\circ}\right\} = \begin{Bmatrix} \chi^{\circ}_{11} \\ \chi^{\circ}_{22} \\ 2\chi^{\circ}_{12} \end{Bmatrix} = \begin{Bmatrix} \frac{\partial \varphi_1}{\partial x} \\ \frac{1}{x\sin(\alpha_c)}\frac{\partial \varphi_2}{\partial \theta} + \frac{\varphi_1}{x} \\ \frac{1}{x\sin(\alpha_c)}\frac{\partial \varphi_1}{\partial \theta} + \frac{\partial \varphi_2}{\partial x} - \frac{\varphi_2}{x} + \frac{\varphi}{x\tan(\alpha_c)} \end{Bmatrix} \tag{6.4b}$$

In the above formulation:

- Specifying $c_{NL} = 0$ and $c_3 = 1$ simplifies the kinematics to the improved first-approximation linear shell theory of Sanders [17]
- Specifying $c_{NL} = 1, c_1 = c_2 = c_3 = 1$ defines Nemeth's nonlinear theory [14]
- Specifying $c_{NL} = 1, c_1 = 0$ and $c_2 = c_3 = 1$ retrieves Sanders' kinematics [18] [19].
- Specifying $c_{NL} = 1, c_1 = c_2 = 0$ and $c_3 = 1$ retrieves Sanders' kinematics with the nonlinear rotations about the reference-surface normal neglected [18] [19].
- Specifying $c_{NL} = 1, c_1 = c_2 = c_3 = 0$ defines Donnell's strain-displacement relationship [20].

6.3 Constitutive Equations

Using the principle of virtual work, the equilibrium equations of the shell as a function of work-conjugate stress resultants are derived based on Sanders' improved first-order linear theory [17] and given in appendix 6.8. Work-conjugate stress resultants of Equation (III.A.50) are approximated symmetric stress-resultants and can be expressed in terms of fundamental unknowns (u_1, u_2, u_3). Hence, the two dimensional constitutive equations of the shell can be expressed as:

$$\begin{bmatrix} \{\mathfrak{n}\} \\ \{\mathfrak{m}\} \end{bmatrix} = \left[\mathcal{CC}^{\mathbf{0}}\right]\left\{\mathfrak{E}^{\circ}\right\} \triangleq \left[\int_{-\frac{h}{2}}^{+\frac{h}{2}} \left(1 + \frac{\xi_3}{R_1}\right)^{-1} \left(1 + \frac{\xi_3}{R_2}\right)^{-1} \left[\mathbf{S}\right]^{\mathsf{T}} \left[\bar{\mathbf{Q}}\right] \left[\mathbf{S}\right] d\xi_3\right] \left\{\mathfrak{E}^{\circ}\right\} \tag{6.5}$$

Where $\left[\bar{\mathbf{Q}}\right]$ is the conventional plane-stress compliance tensor of the shell's material and:

$$\left\{\mathfrak{E}^{\circ}\right\} = \left\{\left\{\epsilon^{\circ}\right\}^{\mathsf{T}} \quad \left\{\chi^{\circ}\right\}^{\mathsf{T}}\right\}^{\mathsf{T}} \tag{6.6}$$

Details of stress resultants of Equation (6.5) and the associated constitutive matrix $\left[\mathcal{CC}^{\mathbf{0}}\right]$ can be found in appendix B of reference [16].

It should be noted that to produce homogeneous equilibrium equations for conical shells, the shell is approximated with a linearly variable thickness equivalent truncated cone. For such a case $\left[\mathcal{CC}^{\mathbf{0}}\right]$ shows dependency to x and the material and geometrical parameters of the shell. The constitutive matrix with substituted conical principle and geo-desic radii of curvature for linearly variable thickness truncated cones is called $\left[\bar{\mathcal{C}}\bar{\mathcal{C}}^{\mathbf{0}}\right]$ and are given in appendix H of reference [16].

6.4 Linear Solution and Finite Element Formulation

To employ the separation of variables, homogeneous equations are required and therefore it was assumed that the thickness of the shell varies linearly along the x coordinates in a way that the actual constant thickness of the shell occurs in the middle of the element at $x_m = 0.5(x_1 + x_2)$. The displacements on the middle surface are chosen to take the following form:

$$u_1 = u_{1,\bar{x}}(\bar{x})(\cos(n_c\theta)) \tag{6.7a}$$

$$u_2 = u_{2,\bar{x}}(\bar{x})(\sin(n_c\theta)) \tag{6.7b}$$

$$u_3 = u_{3,\bar{x}}(\bar{x})(\cos(n_c\theta)) \tag{6.7c}$$

n_c denotes the circumferential mode number and $\bar{x} = x/x_m$ is the non-dimensional longitudinal coordinates that defined as $x_m = 0.5(x_1 + x_2)$. The longitudinal part of the solution is:

$$u_{d,\bar{x}} = C_d(\bar{x})^{\frac{(\lambda-1)}{2}} \tag{6.8}$$

And C_d $(d = 1,2,3)$ is the arbitrary magnitude of the displacement. Substituting Equation (6.5) into (III.A.50) of 5.10 yields a system of linear differential equations that, by some lengthy mathematical manipulations, produces three equations in the following form:

$$\mathfrak{L}_{i,1}\sin(n_c\theta) + \mathfrak{L}_{i,2}\cos(n_c\theta) = 0 \qquad (i = 1,2,3) \tag{6.9}$$

$\mathfrak{L}_{i,j}$ operators are solely dependent on displacements and their derivatives along x direction on the middle surface, circumferential mode number and shell parameters such as

elasticity and geometry. Therefore, the only variable that shows up in $\mathfrak{L}_{i,j}$ is λ. Hence, the equilibrium Equations (6.8) can be rewritten in the following matrix form:

$$\left[\mathcal{AQ}\right]\left\{\mathbf{A}\right\} = \begin{bmatrix} \mathcal{AQ}_{1,1} & \mathcal{AQ}_{1,2} & \mathcal{AQ}_{1,3} \\ \mathcal{AQ}_{2,1} & \mathcal{AQ}_{2,2} & \mathcal{AQ}_{2,3} \\ \mathcal{AQ}_{3,1} & \mathcal{AQ}_{3,2} & \mathcal{AQ}_{3,3} \end{bmatrix} \begin{Bmatrix} \mathrm{C}_1 \\ \mathrm{C}_2 \\ \mathrm{C}_3 \end{Bmatrix} = 0 \tag{6.10}$$

Elements of $\left[\mathcal{AQ}\right]$ are polynomials in terms of λ and details of them are given in reference [16]. he equilibrium equations should be able to handle any arbitrary magnitude of displacement, therefore the determinant of $\left[\mathcal{AQ}\right]$ should be equal to zero. This produces a characteristic polynomial that can be solved to obtain values of λ.

Solving the characteristic polynomial yields K distinct roots and the final solution of the system is obtained by summation of all these solutions:

$$\mathrm{u_d}(\mathrm{x},\theta) = \left(\sum_{k=1}^{\mathrm{K}} \mathrm{C_{d,k}}\left(\bar{x}^{\frac{(\lambda_k - 1)}{2}}\right)\right)(\sin(n_c\theta)^{\mathrm{se_d}})(\cos(n_c\theta)^{\mathrm{ce_d}}) \tag{6.11}$$

Where $\mathrm{se_d}, \mathrm{ce_d} = 0, 1$ for $\mathrm{d} = 1, 3$ and $\mathrm{se_d}, \mathrm{ce_d} = 1, 0$ for , $\mathrm{d} = 2$.

The finite element of the current study has two nodal lines and the degrees of freedom of those nodes δ_i δ_j are shown in figure 6.1a. For the case of isotropic materials four degrees of freedom at each node are chosen and are shown for δ_i node in figure 6.1b. The mathematical expression of these degrees of freedom for δ_i node is:

$$\left\{\boldsymbol{\delta}_{\mathbf{m}}\right\} = \begin{Bmatrix} \delta_{m,1} \\ \delta_{m,2} \\ \delta_{m,3} \\ \delta_{m,4} \end{Bmatrix} = \begin{Bmatrix} \mathrm{U_x} \\ \mathrm{V_x} \\ \mathrm{W_x} \\ \frac{\partial \mathrm{W_x}}{\partial \mathrm{x}} \end{Bmatrix} \triangleq \begin{Bmatrix} \mathrm{u}_{1,\bar{x}}(x_m/L) \\ \mathrm{u}_{2,\bar{x}}(x_m/L) \\ \mathrm{u}_{3,\bar{x}}(x_m/L) \\ \partial \mathrm{u}_{3,\bar{x}}(x_m/L)/\partial x \end{Bmatrix} \tag{6.12}$$

Where, at $m = i$ and $m = j$, x_m takes values of $x_i = \mathrm{x}_1$ and $x_j = \mathrm{x}_2$ accordingly (figure 6.1a). Employing equation (6.10) and recalling the linear dependency (determinant of $\left[\mathcal{AQ}\right]$ matrix assumed to be zero) and lengthy mathematical manipulations, three unknown amplitudes of vibration (C_1, C_2, C_3) in the displacements of Equation (6.7) can be defined in terms of each element's degrees of freedom:

$$\left\{\boldsymbol{\delta}\right\}^{e} \triangleq \begin{Bmatrix} \\ \left\{\boldsymbol{\delta}_{\mathbf{i}}\right\} \\ \\ \left\{\boldsymbol{\delta}_{\mathbf{j}}\right\} \\ \\ \end{Bmatrix} = \begin{Bmatrix} \delta_1 \\ \delta_2 \\ \vdots \\ \delta_K \end{Bmatrix} = \begin{bmatrix} a_{1,1} & a_{1,2} & \cdots & a_{1,K} \\ a_{2,1} & a_{2,2} & \cdots & a_{2,K} \\ \vdots & \vdots & \ddots & \vdots \\ a_{K,1} & a_{K,2} & \cdots & a_{K,K} \end{bmatrix} \begin{Bmatrix} C_{1,1} \\ C_{1,2} \\ \vdots \\ C_{1,K} \end{Bmatrix} = \left[\mathbf{A}\right]\left\{\mathbf{C_1}\right\} \tag{6.13}$$

Where $\left[\mathbf{A}\right]$ is a constant real matrix. Hence:

$$\left\{\mathbf{C_1}\right\} = \left[\mathbf{A}\right]^{-1}\left\{\boldsymbol{\delta}\right\}^{e} \tag{6.14}$$

Substituting matrix form of (6.14) in Equation (6.7) results the finite element displacement matrix:

$$\left\{\mathbf{u}\right\} = \begin{Bmatrix} u_1(x,\theta) \\ u_2(x,\theta) \\ u_3(x,\theta) \end{Bmatrix} = \overbrace{\left[\mathbf{R}(x,\theta)\right]\left[\mathbf{A}\right]^{-1}}^{\left[\mathbf{N}\right]_{3\times K}}\left\{\boldsymbol{\delta}\right\}^{e} = \begin{bmatrix} R_{1,1} & R_{1,2} & \cdots & R_{1,K} \\ R_{2,1} & R_{2,2} & \cdots & R_{2,K} \\ \vdots & \vdots & \ddots & \vdots \\ R_{5,1} & R_{5,2} & \cdots & R_{5,K} \end{bmatrix}\begin{bmatrix} c_{1,1} & c_{1,2} & \cdots & c_{1,K} \\ c_{2,1} & c_{2,2} & \cdots & c_{2,K} \\ \vdots & \vdots & \ddots & \vdots \\ c_{K,1} & c_{5,2} & \cdots & c_{K,K} \end{bmatrix}\begin{Bmatrix} \delta_1 \\ \delta_2 \\ \vdots \\ \delta_K^e \end{Bmatrix} \tag{6.15}$$

Where the elements of $\left[\mathbf{R}\right]$ follow this equation:

$$R_{d,k}(x,\theta) = \left(\frac{x}{x_m}\right)^{\frac{(\lambda_k - 1)}{2}} (\sin(n_c\theta)^{se_d})(\cos(n_c\theta)^{ce_d}) \tag{6.16}$$

More details on the development of this FEM solution can be found in reference [21].

6.5 Equations of Motion

So far, the spatial component of the shell motion is defined by Equation (6.15). Defining $\left\{\left\{\boldsymbol{\delta}\right\}\right\} = \left\{\boldsymbol{\delta}(t)\right\}$ as the temporal (time-dependent) component of shell's motion, the equations of motion of the shell, can be obtained by the generalized-coordinates method. Assuming the system consists of N finite elements, each with K degrees of freedom, the Lagrangian

equation of motion based on Hamilton's principle can be expressed as follows:

$$\frac{\mathrm{d}}{\mathrm{dt}}\left[\frac{\partial \mathrm{T}}{\partial \dot{\delta}_i}\right]-\frac{\partial \mathrm{T}}{\partial \delta_i}+\frac{\partial \mathrm{V}}{\partial \delta_i}+\frac{\partial \mathrm{V_i}}{\partial \delta_i}=\mathrm{q}_i, \quad (i=1,2,\cdots,\mathrm{D}\triangleq \mathrm{K}\times\mathrm{N}) \tag{6.17}$$

Where

- D is the total degrees of freedom of the system after assem-bling mass and stiffness matrices of elements and applying the constraints.
- T denotes the total kinetic energy of the system.
- V and $\mathrm{V_i}$ accordingly are the internal elastic strain energy and the initial stiffening strain energy due to external axial load and hydrostatic pressure of the system.
- q_i is the nodal external force.

Equation (6.17) can be rewritten in matrix form as follows:

$$\frac{\mathrm{d}}{\mathrm{dt}}\left[\frac{\partial \mathrm{T}}{\partial \left\{\dot{\boldsymbol{\delta}}\right\}}\right]-\frac{\partial \mathrm{T}}{\partial \left\{\boldsymbol{\delta}\right\}}+\frac{\partial \mathrm{V}}{\partial \left\{\boldsymbol{\delta}\right\}}+\frac{\partial \mathrm{V_i}}{\partial \left\{\boldsymbol{\delta}\right\}}=\left\{\mathbf{q}\right\} \tag{6.18}$$

6.5.1 Kinetic Energy

Neglecting rotational and cross translational-rotational com-ponents of the kinetic energy due to absence of shear deformation in the theory of the current study and keeping the pure translational ($\mathrm{T_T}$) part of the kinetic energy, the structural mass matrix for a single element can be defined as follows:

$$\left[\mathbf{M_T}\right]^{\mathrm{e}}_{\mathrm{K}\times\mathrm{K}}=\iint_{\Omega}\rho^0\left(\left[\mathbf{S_T}\right]^{\mathrm{T}}\left[\mathbf{S_T}\right]\right)\mathrm{A}_1\mathrm{A}_2\mathrm{d}x\mathrm{d}\theta \tag{6.19}$$

Details of variables of Equation (6.19) can be found in reference [16]. The structural mass matrices of all elements can be assembled to obtain the whole system mass matrix using standard finite element assembly procedures. The corresponding assembled matrix is named $\left[\mathbf{M_T}\right]$. Finally by performing some mathematical operations, the kinetic energy

component of the equations of motion can be obtained from the following equation:

$$\frac{d}{dt}\left[\frac{\partial T}{\partial\left\{\dot{\delta}\right\}}\right]=\left[M_S\right]\left\{\ddot{\delta}\right\}\triangleq\frac{1}{2}\left(2\left[M_T\right]\right)\left\{\ddot{\delta}\right\} \tag{6.20}$$

$\left[M_S\right]$ denotes the assembled structural mass matrix of the whole system.

6.5.2 Internal Strain Energy

The internal strain energy over the shell element surface area (Ω) is defined as:

$$V_e=\frac{1}{2}\iint_\Omega\left(\int_{-h/2}^{h/2}\left\{\sigma^{\xi_3}\right\}^T\left\{\epsilon^{\xi_3}\right\}\left(1+\frac{\xi_3}{R_1}\right)\left(1+\frac{\xi_3}{R_2}\right)d\xi_3\right)d\Omega \tag{6.21}$$

The through-the-thickness integral of Equation (6.21) can be obtained as follows:

$$\int_{-h/2}^{h/2}\left\{\sigma^{\xi_3}\right\}^T\left\{\epsilon^{\xi_3}\right\}\left(1+\frac{\xi_3}{R_1}\right)\left(1+\frac{\xi_3}{R_2}\right)d\xi_3=\left\{\mathfrak{E}^\circ\right\}^T\left[\bar{\mathcal{C}}^0\right]\left\{\mathfrak{E}^\circ\right\} \tag{6.22}$$

The strain vector $\left\{\mathfrak{E}^\circ\right\}$ has two linear and nonlinear components:

$$\left\{\mathfrak{E}^\circ\right\}=\left[S_{\mathfrak{E}_L^\circ}\right]_{6\times K}\left\{\delta\right\}^e_{K\times1}+\left[S_{\mathfrak{E}_{NL}^\circ}\right]_{6\times K^2}\left\{\delta^{\otimes2}\right\}^e_{K^2\times1} \tag{6.23}$$

where $\left\{\delta^{\otimes p}\right\}$ is the Kronecker product power *p* of vector $\left\{\delta\right\}$ (e.g.$\left\{\delta^{\otimes2}\right\}=\left\{\delta\right\}\otimes\left\{\delta\right\}$). The rows of $\left[S_{\mathfrak{E}_L^\circ}\right]$ and $\left[S_{\mathfrak{E}_{NL}^\circ}\right]$ are provided in Appendix I of reference [16]. The following stiffness matrices for each element can be defined:

$$\left[K_{11}\right]^e\triangleq\iint_\Omega\left[S_{\mathfrak{E}_L^\circ}\right]^T\left[\bar{\mathcal{C}}^0\right]\left[S_{\mathfrak{E}_L^\circ}\right]A_1A_2dxd\theta \tag{6.24a}$$

$$\left[K_{21}\right]^e=\left(\left[K_{12}^e\right]\right)^T\triangleq\iint_\Omega\left[S_{\mathfrak{E}_{NL}^\circ}\right]^T\left[\bar{\mathcal{C}}^0\right]\left[S_{\mathfrak{E}_L^\circ}\right]A_1A_2dxd\theta \tag{6.24b}$$

$$\left[K_{22}\right]^e\triangleq\iint_\Omega\left[S_{\mathfrak{E}_{NL}^\circ}\right]^T\left[\bar{\mathcal{C}}^0\right]\left[S_{\mathfrak{E}_{NL}^\circ}\right]A_1A_2dxd\theta \tag{6.24c}$$

can be defined. Hence the strain energy of the element can be written in the following form:

$$V_e = \frac{1}{2}\left(\left(\left\{\boldsymbol{\delta}\right\}^e\right)^T\left[\mathbf{K_{11}}\right]^e\left\{\boldsymbol{\delta}\right\}^e + \left(\left\{\boldsymbol{\delta}\right\}^e\right)^T\left[\mathbf{K_{12}}\right]^e\left\{\boldsymbol{\delta}^{\otimes 2}\right\}^e + \left(\left\{\boldsymbol{\delta}^{\otimes 2}\right\}^e\right)^T\left[\mathbf{K_{21}}\right]^e\left\{\boldsymbol{\delta}\right\}^e + \left(\left\{\boldsymbol{\delta}^{\otimes 2}\right\}^e\right)^T\left[\mathbf{K_{22}}\right]^e\left\{\boldsymbol{\delta}^{\otimes 2}\right\}^e\right) \quad (6.25)$$

The total strain energy is equal to the sum of the strain energies of all elements. Therefore, using standard finite element assembly procedures, the structural stiffness matrices of all elements can be assembled into the the whole system stiffness matrices. The corresponding assembled stiffness matrices are named $\left[\mathbf{K_{11}}\right]$, $\left[\mathbf{K_{12}}\right]$, $\left[\mathbf{K_{21}}\right]$ and $\left[\mathbf{K_{22}}\right]$. But substituting Equation (6.25) into (6.18) requires proper mathematical formulation for the derivative of Kronecker powers of vectors using matrix calculus. The necessary mathematical formulations is developed by the authors and can be found in Bakhtiari et al. [22] or Appendix J of reference [16]. Subsequently, the derivative of the strain energy with respect to the degrees of freedom can be expressed as:

$$\frac{\partial V}{\partial\left\{\boldsymbol{\delta}\right\}} = \left[\mathbf{K_{11}}\right]\left\{\boldsymbol{\delta}\right\} + \left[\tilde{\mathbf{K}}_{\mathbf{12}}\right]\left\{\boldsymbol{\delta}^{\otimes 2}\right\} + \frac{1}{2}\left[\tilde{\mathbf{K}}_{\mathbf{22}}\right]\left\{\boldsymbol{\delta}^{\otimes 3}\right\} \quad (6.26)$$

Where matrices $\left[\tilde{\mathbf{K}}_{\mathbf{12}}\right]$ and $\left[\tilde{\mathbf{K}}_{\mathbf{22}}\right]$ are formulated based on $\left[\mathbf{K_{12}}\right]$, $\left[\mathbf{K_{21}}\right]$ and $\left[\mathbf{K_{22}}\right]$ using matrix calculus operations that the details of them are provided in [22].

6.5.3 Aerodynamic Pressure Field

The improved linear piston theory that takes into account the effect of curvature, suggests the following relationship for the aerodynamic pressure field over the shell [23] and [24]:

$$P_{Aero,L} = -C_{A,1}\left[C_{A,2}\dot{u}_3 + \frac{\partial u_3}{\partial x} - C_{A,3}\frac{u_3}{x\tan(\alpha_c)}\right] \quad (6.27)$$

Where:

$$C_{A,1} = \frac{\gamma_a P_l M_l^2}{\left(M_l^2-1\right)^{(1/2)}}, \quad C_{A,2} = \frac{1}{M_l a_l}\left(\frac{M_l^2-2}{M_l^2-1}\right), \quad C_{A,3} = \frac{1}{2\left(M_l^2-1\right)^{(1/2)}} \quad (6.28)$$

And γ_a, P, M and a accordingly denotes to the adiabatic index, static pressure, Mach number and speed of sound. The subscript l denote to the local stream condition after the

conical shock at the tip of the cone that can be obtained from the free stream condition (denoted by ∞ symbol) using Taylor-Maccoll analysis or pre-calculated look-up tables. To express the aerodynamics pressure field in terms of nodal displacements, first recalling Equation (6.15) the displacement along the third curvilinear coordinates is:

$$u_3 = \left[\mathbf{N_W}\right]\left\{\boldsymbol{\delta_e}\right\} = \begin{bmatrix}0 & 0 & 1\end{bmatrix}\left[\mathbf{N}\right]\left\{\boldsymbol{\delta_e}\right\} \tag{6.29}$$

Substituting Equation (6.29) in Equation (6.27), yields:

$$\left\{\mathbf{p_{AERO}}\right\} = -C_{A,1}C_{A,2}\left[\mathbf{N_W}\right]\left\{\dot{\boldsymbol{\delta}}_\mathbf{e}\right\} - \left(C_{A,1}\frac{\partial}{\partial x}\left[\mathbf{N_W}\right] - \frac{C_{A,1}C_{A,3}}{x\tan(\alpha_c)}\left[\mathbf{N_W}\right]\right)\left\{\boldsymbol{\delta}_\mathbf{e}\right\} \tag{6.30}$$

The general nodal force vector as a result of this pressure field is defined as:

$$\left\{\mathbf{q_{AERO}}\right\}^e = \iint_\Omega \left[\mathbf{N}\right]^\intercal \left\{\mathbf{p_{AERO}}\right\} \mathrm{A}_1\mathrm{A}_2\mathrm{d}x\mathrm{d}\theta \tag{6.31}$$

Hence, substituting Equation (6.29) into Equation (6.31) yields aerodynamics stiffness and damping matrices as follows:

$$\left[\mathbf{K_{AERO}}\right]^e = -C_{A,1}C_{A,2}\iint_\Omega \left[\mathbf{N}\right]^\intercal \left[\mathbf{N_W}\right] \mathrm{A}_1\mathrm{A}_2\mathrm{d}x\mathrm{d}\theta + C_{A,1}C_{A,3}\iint_\Omega \left[\mathbf{N}\right]^\intercal \frac{1}{x\tan(\alpha_c)}\left[\mathbf{N_W}\right] \mathrm{A}_1\mathrm{A}_2\mathrm{d}x\mathrm{d}\theta \tag{6.32a}$$

$$\left[\mathbf{C_{AERO}}\right]^e = -C_{A,1}\iint_\Omega \left[\mathbf{N}\right]^\intercal \frac{\partial}{\partial x}\left[\mathbf{N_W}\right] \mathrm{A}_1\mathrm{A}_2\mathrm{d}x\mathrm{d}\theta \tag{6.32b}$$

The whole structure aerodynamics and stiffness matrices $\left[\mathbf{K_{AERO}}\right]$ and $\left[\mathbf{C_{AERO}}\right]$ can be constructed using classic finite element assembly procedures.

6.5.4 Initial Stiffening Due to Axial Load and Hydrostatic Pressure

The stress resultants due to the combination of the axial load F_A and hydrostatic pressure pm can be formulated as follows[25]:

$$\mathfrak{n}_{\theta A} = -x\tan(\alpha_c)p_m \tag{6.33a}$$

$$\mathfrak{n}_{xA} = -\frac{x\tan(\alpha_c)}{2}p_m - \frac{F_A}{\pi\sin(2\alpha_c)} \tag{6.33b}$$

An element's strain potential energy as a result of these stress resultants is equal to[9]:

$$V_i^e = \iint_\Omega \left[\text{n}_{\theta A} \varphi_1^2 + \text{n}_{xA} \varphi_2^2 (\text{n}_{\theta A} + \text{n}_{xA}) \varphi_1^2 \right] A_1 A_2 \text{dx} \text{d}\theta \tag{6.34a}$$

Defining $\left[\mathbf{N_U}\right] = \begin{bmatrix} 1 & 0 & 0 \end{bmatrix}\left[\mathbf{N}\right]$ and $\left[\mathbf{N_V}\right] = \begin{bmatrix} 0 & 1 & 0 \end{bmatrix}\left[\mathbf{N}\right]$ and taking the same approach as Equations (6.29) and(6.30), the linear rotation parameters of Equation (6.2) can be expressed in terms of nodal displacements:

$$\begin{aligned} \left[\mathbf{N_{\varphi_1}}\right] &= -\frac{\partial}{\partial \text{x}}\left[\mathbf{N_W}\right] \\ \left[\mathbf{N_{\varphi_2}}\right] &= \frac{1}{\text{x}\tan(\alpha_c)}\left[\mathbf{N_V}\right] - \frac{1}{\text{x}\sin(\alpha_c)}\frac{\partial}{\partial \theta}\left[\mathbf{N_W}\right] \\ \left[\mathbf{N_\varphi}\right] &= \frac{1}{2}\left(\frac{\partial}{\partial \text{x}}\left[\mathbf{N_V}\right] - \frac{1}{\text{x}\sin(\alpha_c)}\frac{\partial}{\partial \theta}\left[\mathbf{N_U}\right] + \frac{1}{\text{x}}\left[\mathbf{N_V}\right]\right) \end{aligned} \tag{6.35a}$$

Therefore, the initial stiffness matrices due to hydrostatic pressure and axial load are obtained as follows:

$$\left[\mathbf{K_{i,pm}}\right]^e = p_m \iint_\Omega \left(-x\tan(\alpha_c)\left[\mathbf{N_{\varphi_1}}\right]^\text{T}\left[\mathbf{N_{\varphi_1}}\right] + \frac{x\tan(\alpha_c)}{2}\left[\mathbf{N_{\varphi_2}}\right]^\text{T}\left[\mathbf{N_{\varphi_2}}\right] - x\tan(\alpha_c)\left[\mathbf{N_\varphi}\right]^\text{T}\left[\mathbf{N_\varphi}\right]\right) A_1 A_2 \text{dx} \text{d}\theta \tag{6.36a}$$

$$\left[\mathbf{K_{i,FA}}\right]^e = F_A \iint_\Omega \left(\frac{1}{\pi\sin(2\alpha_c)}\left[\mathbf{N_{\varphi_2}}\right]^\text{T}\left[\mathbf{N_{\varphi_2}}\right] + \frac{1}{\pi\sin(2\alpha_c)}\left[\mathbf{N_\varphi}\right]^\text{T}\left[\mathbf{N_\varphi}\right]\right) A_1 A_2 \text{dx} \text{d}\theta \tag{6.36b}$$

Using general finite elements assembly procedures, the whole structure initial stiffening matrices $\left[\mathbf{K_{i,pm}}\right]$ and $\left[\mathbf{K_{i,FA}}\right]$ can be constructed. Therefore, employing the same approach described for the internal strain energy, the initial stiffness component of the equations of motions is:

$$\frac{\partial \text{V}_\text{i}}{\partial\left\{\boldsymbol{\delta}\right\}} = \left[\mathbf{K_{i,pm}}\right]\left\{\boldsymbol{\delta}\right\} + \left[\mathbf{K_{i,FA}}\right]\left\{\boldsymbol{\delta}\right\} \tag{6.37}$$

6.5.5 Equations of Motion in Terms of Nodal Displacements

Substituting Equations (6.20), (6.26), (6.33) and (6.37) in Equation (6.18) results in the following equation of motion:

$$\left[\mathbf{M_S}\right]\left\{\ddot{\boldsymbol{\delta}}\right\} + \left[\mathbf{C_{AERO}}\right]\left\{\dot{\boldsymbol{\delta}}\right\} + \left[\mathbf{K_{tot}}\right]\left\{\boldsymbol{\delta}\right\} + \left[\tilde{\mathbf{K}}_{\mathbf{12}}\right]\left\{\boldsymbol{\delta}^{\otimes 2}\right\} + \frac{1}{2}\left[\tilde{\mathbf{K}}_{\mathbf{22}}\right]\left\{\boldsymbol{\delta}^{\otimes 3}\right\} = \left\{\mathbf{q}\right\} \tag{6.38}$$

Where:

$$\left[\mathbf{K_{11,tot}}\right] = \left[\mathbf{K_{11}}\right] + \left[\mathbf{K_{AERO}}\right] + \left[\mathbf{K_{i,pm}}\right] + \left[\mathbf{K_{i,FA}}\right] \tag{6.39}$$

6.6 Dynamic Stability in Supersonic Flow

6.6.1 Harmonic Motion

In case of free motion when there is no excitation force, the left hand side of Equation (6.38) should be equal to zero or a negligible residual such as $R(t)$:

$$R(t) = \left[\mathbf{M_S}\right]\left\{\ddot{\boldsymbol{\delta}}\right\} + \left[\mathbf{C_{AERO}}\right]\left\{\dot{\boldsymbol{\delta}}\right\} + \left[\mathbf{K_{11,tot}}\right]\left\{\boldsymbol{\delta}\right\} + \left[\tilde{\mathbf{K}}_{12}\right]\left\{\boldsymbol{\delta}^{\otimes 2}\right\} + \frac{1}{2}\left[\tilde{\mathbf{K}}_{22}\right]\left\{\boldsymbol{\delta}^{\otimes 3}\right\} \tag{6.40}$$

A variation of harmonic balance method proposed by Lewandowski [26] is used to obtain the nonlinear response of the system. The temporal component of the response is assumed to have the following periodical structure:

$$\left\{\boldsymbol{\delta}\right\} = \left\{\boldsymbol{\delta}_\mathbf{c}\right\}\cos(\omega t) + \left\{\boldsymbol{\delta}_\mathbf{s}\right\}\sin(\omega t) \tag{6.41}$$

In order to the obtain the amplitude equation, the in-time Galerkin method is applied to the residual [27]:

$$2/T \int_0^{T/4} R(t)\cos(\omega t)dt = 0 \tag{6.42a}$$

$$2/T \int_0^{T/4} R(t)\sin(\omega t)dt = 0 \tag{6.42b}$$

Defining the $\left\{\boldsymbol{\delta}_\mathbf{cs}\right\} = \left\{\left\{\boldsymbol{\delta}_\mathbf{c}\right\} \quad \left\{\boldsymbol{\delta}_\mathbf{s}\right\}\right\}^\mathsf{T}$, substituting Equation (6.41) into Equation (6.40), re-arranging in the matrix form and some lengthy mathematical operations yield the ampli-

tude equation as follows:

$$
\begin{aligned}
-\omega^2 &\begin{bmatrix} \frac{1}{4}\mathbf{M_S} & \frac{1}{2\pi}\mathbf{M_S} \\ \frac{1}{2\pi}\mathbf{M_S} & \frac{1}{4}\mathbf{M_S} \end{bmatrix} \left\{\boldsymbol{\delta_{cs}}\right\} + \omega \begin{bmatrix} \frac{-1}{2\pi}\mathbf{C_{AERO}} & \frac{1}{4}\mathbf{C_{AERO}} \\ \frac{-1}{4}\mathbf{C_{AERO}} & \frac{1}{2\pi}\mathbf{C_{AERO}} \end{bmatrix} \left\{\boldsymbol{\delta_{cs}}\right\} + \begin{bmatrix} \frac{-1}{4}\mathbf{K_{11,tot}} & \frac{1}{2\pi}\mathbf{K_{11,tot}} \\ \frac{-1}{2\pi}\mathbf{K_{11,tot}} & \frac{1}{4}\mathbf{K_{11,tot}} \end{bmatrix} \left\{\boldsymbol{\delta_{cs}}\right\} \\
&+ \begin{bmatrix} \frac{2}{3\pi}\tilde{\mathbf{K}}_{\mathbf{12}} & \frac{1}{3\pi}\tilde{\mathbf{K}}_{\mathbf{12}} & \frac{1}{3\pi}\tilde{\mathbf{K}}_{\mathbf{12}} & \frac{1}{3\pi}\tilde{\mathbf{K}}_{\mathbf{12}} \\ \frac{1}{3\pi}\tilde{\mathbf{K}}_{\mathbf{12}} & \frac{1}{3\pi}\tilde{\mathbf{K}}_{\mathbf{12}} & \frac{1}{3\pi}\tilde{\mathbf{K}}_{\mathbf{12}} & \frac{2}{3\pi}\tilde{\mathbf{K}}_{\mathbf{12}} \end{bmatrix} \left\{\boldsymbol{\delta_{cs}}\right\}^{\otimes 2} \\
&+ \begin{bmatrix} \frac{3}{16}\tilde{\mathbf{K}}_{\mathbf{22}} & \frac{1}{4\pi}\tilde{\mathbf{K}}_{\mathbf{22}} & \frac{1}{4\pi}\tilde{\mathbf{K}}_{\mathbf{22}} & \frac{1}{16}\tilde{\mathbf{K}}_{\mathbf{22}} & \frac{1}{4\pi}\tilde{\mathbf{K}}_{\mathbf{22}} & \frac{1}{16}\tilde{\mathbf{K}}_{\mathbf{22}} & \frac{1}{16}\tilde{\mathbf{K}}_{\mathbf{22}} & \frac{1}{4\pi}\tilde{\mathbf{K}}_{\mathbf{22}} \\ \frac{1}{4\pi}\tilde{\mathbf{K}}_{\mathbf{22}} & \frac{1}{16}\tilde{\mathbf{K}}_{\mathbf{22}} & \frac{1}{16}\tilde{\mathbf{K}}_{\mathbf{22}} & \frac{1}{4\pi}\tilde{\mathbf{K}}_{\mathbf{22}} & \frac{1}{16}\tilde{\mathbf{K}}_{\mathbf{22}} & \frac{1}{4\pi}\tilde{\mathbf{K}}_{\mathbf{22}} & \frac{1}{4\pi}\tilde{\mathbf{K}}_{\mathbf{22}} & \frac{3}{16}\tilde{\mathbf{K}}_{\mathbf{22}} \end{bmatrix} \left\{\boldsymbol{\delta_{cs}}\right\}^{\otimes 3} = 0
\end{aligned}
\tag{6.43}
$$

Where T is the period of the response.

6.6.2 Linear Solution

Equation (6.43) can be rewritten in the following compressed form where only the short names for matrices substituted their expanded form:

$$
-\omega^2 \left[\mathbf{MM_S}\right]\left\{\boldsymbol{\delta_{cs}}\right\} + \omega \left[\mathbf{CC_{AERO}}\right]\left\{\boldsymbol{\delta_{cs}}\right\} + \left[\mathbf{KK_{11,tot}}\right]\left\{\boldsymbol{\delta_{cs}}\right\} + \left[\mathbf{K\tilde{K}_{12}}\right]\left\{\boldsymbol{\delta_{cs}}\right\}^{\otimes 2} + \left[\mathbf{K\tilde{K}_{22}}\right]\left\{\boldsymbol{\delta_{cs}}\right\}^{\otimes 3} = 0 \tag{6.44}
$$

In case of linear dynamic response, all the nonlinear terms that include Kronecker product are assumed to be zero. By factorizing $\left\{\boldsymbol{\delta_{cs}}\right\}$ and dropping the trivial solution of $\left\{\boldsymbol{\delta_{cs}}\right\} = 0$ equation, (6.44) takes the following form:

$$
-\omega^2 \left[\mathbf{MM_S}\right] + \omega \left[\mathbf{CC_{AERO}}\right] + \left[\mathbf{KK_{11,tot}}\right] = 0 \tag{6.45}
$$

This is a classic generalized eigenvalue problem whose exact solution can be obtained using generalized Schur decomposition. In the current study, the LAPACK numerical library [28] used to solve the linear generalized eigenvalue problem and to obtain the frequencies. Linear flutter in conical and cylindrical shells is a Hopf bifurcation and occurs as a result of merging two adjacent modes; see references [9] and [29]. The flutter onset can be detected by appearance of negative imaginary parts in the frequencies that are obtained from the solution of the generalized eigenvalue problem. While the real parts denote

the frequency, the imaginary part represents damping. Hence, negative damping leads to instability. In the current study, an algorithm using the secant method is developed to accurately identify the linear critical pressure where the flutter onset occurs. In short, using two initial guesses for dynamic pressure where one resides in the stable region and the other is placed in the unstable region, a new pressure in between is iteratively calculated using a secant root-finding algorithm that yields a frequency with a very small negative imaginary part. This is a good replacement for the common trial and error that was employed in some of the earlier studies (Sabri et al. [30] and Kerboua and Lakis [31]).

6.6.3 Nonlinear Solution

For solving the nonlinear amplitude equations a variation of the algorithm described by Lewandowski [26] was employed. The algorithm contains two major steps. The first step utilizes trust region optimization [32] to obtain solution of generalized coordinates vector ($\left\{\boldsymbol{\delta_{cs}}\right\}$) for a given constant harmonic frequency (ω). The next step utilizes the calculated vector to calculate the nonlinear components and then correct the harmonic frequency by treating it as a linear problem.The results of the linear solution or the previous amplitude step are used as the initial guess.

Let us define the following cost function:

$$\begin{aligned} F(\omega,\left\{\boldsymbol{\delta_{cs}}\right\}) = &-\omega^2\left[\mathbf{MM_S}\right]\left\{\boldsymbol{\delta_{cs}}\right\} + \omega\left[\mathbf{CC_{AERO}}\right]\left\{\boldsymbol{\delta_{cs}}\right\} \\ &+\left(\left[\mathbf{KK_{11,tot}}\right] + \left[\tilde{\mathbf{KK}}_{\mathbf{12}}\right] \underset{(\times)}{vecI}\left(\left\{\boldsymbol{\delta_{cs}}\right\}\right) + \left[\tilde{\mathbf{KK}}_{\mathbf{22}}\right] \underset{(\times)}{vecI}\left(\left\{\boldsymbol{\delta_{cs}}\right\}^{\otimes 2}\right)\right)\left\{\boldsymbol{\delta_{cs}}\right\} \end{aligned} \tag{6.46}$$

Obviously, the solution for a desired amplitude such as A should yield $F(\omega,\left\{\boldsymbol{\delta_{cs}}\right\}) = 0$. But the solution also should be constrained in a way that the maximum value of the elements within $\left\{\boldsymbol{\delta_{cs}}\right\}$ that are associated with displacement in normal to surface directions (W) be equal to A. Let us call such vector $\left\{\boldsymbol{\delta_{cs}}\right\}_A$.

The outline of the algorithm can be described as follows:

1. In the first step of the algorithm, using a guess for ω such as ω^* (the initial guess can be obtained from the linear frequencies) and keeping that constant, Equation (6.46)

is solved to obtain a $\left\{\boldsymbol{\delta}_{\mathbf{cs}}\right\}^{*}$ vector that minimizes $F(\omega, \left\{\boldsymbol{\delta}_{\mathbf{cs}}\right\})$.

2. $\left\{\boldsymbol{\delta}_{\mathbf{cs}}\right\}^{*}$ vector is rescaled to $\left\{\boldsymbol{\delta}_{\mathbf{cs}}\right\}_{A}^{*}$ so it satisfies the amplitude constraint.

3. This scaled vector is substituted as a constant vector within the rearranged version of Equation (6.44) that has the following form:

$$\left(-\omega^{2}\left[\mathbf{MM_S}\right]+\omega\left[\mathbf{CC_{AERO}}\right] + \left(\left[\mathbf{KK_{11,tot}}\right]+\left[\tilde{\mathbf{KK}}_{\mathbf{12}}\right]\underset{(\times)}{vecI}\left(\left\{\boldsymbol{\delta}_{\mathbf{cs}}\right\}_{A}^{*}\right)+\left[\tilde{\mathbf{KK}}_{\mathbf{22}}\right]\underset{(\times)}{vecI}\left(\left\{\boldsymbol{\delta}_{\mathbf{cs}}\right\}_{A}^{*\otimes 2}\right)\right)\right)\left\{\boldsymbol{\delta}_{\mathbf{cs}}\right\}=0 \tag{6.47}$$

Mathematical definition of operator $\underset{(\times)}{vecI}(a)$ is given in [22] but in short this operator converts the Kronecker product of two vectors into a matrix multiplication. It should be noted that since $\left\{\boldsymbol{\delta}_{\mathbf{cs}}\right\}^{*}$ is assumed constant, Equation (6.47) now has the same structure as the linear generalized eigenvalue problem of Equation (6.45). Solving that linear problem provides an update for ω^{*}.

4. The convergence is checked by calculating $F(\omega^{*}, \left\{\boldsymbol{\delta}_{\mathbf{cs}}\right\}_{A}^{*})$vector to see if the average of its absolute is below a small threshold. Otherwise, the new ω^{*} in addition to $\left\{\boldsymbol{\delta}_{\mathbf{cs}}\right\}_{A}^{*}$ are fed back as the initial guesses into the first step and the iteration continues until the convergence is achieved.

It should be noted that to ensure and improve the convergence, the implementation of the algorithm employs additional features such as concepts similar to under relaxation factor, the gradual incrementing of the amplitude and reusing the solution of the previous amplitude as the initial guess for the next larger amplitude step. The high level flowchart of the algorithm is shown in Figure 6.2 .

6.6.4 Convention of Boundary Conditions

Tong's [33] convention is used to identify the boundary conditions for a truncated cone

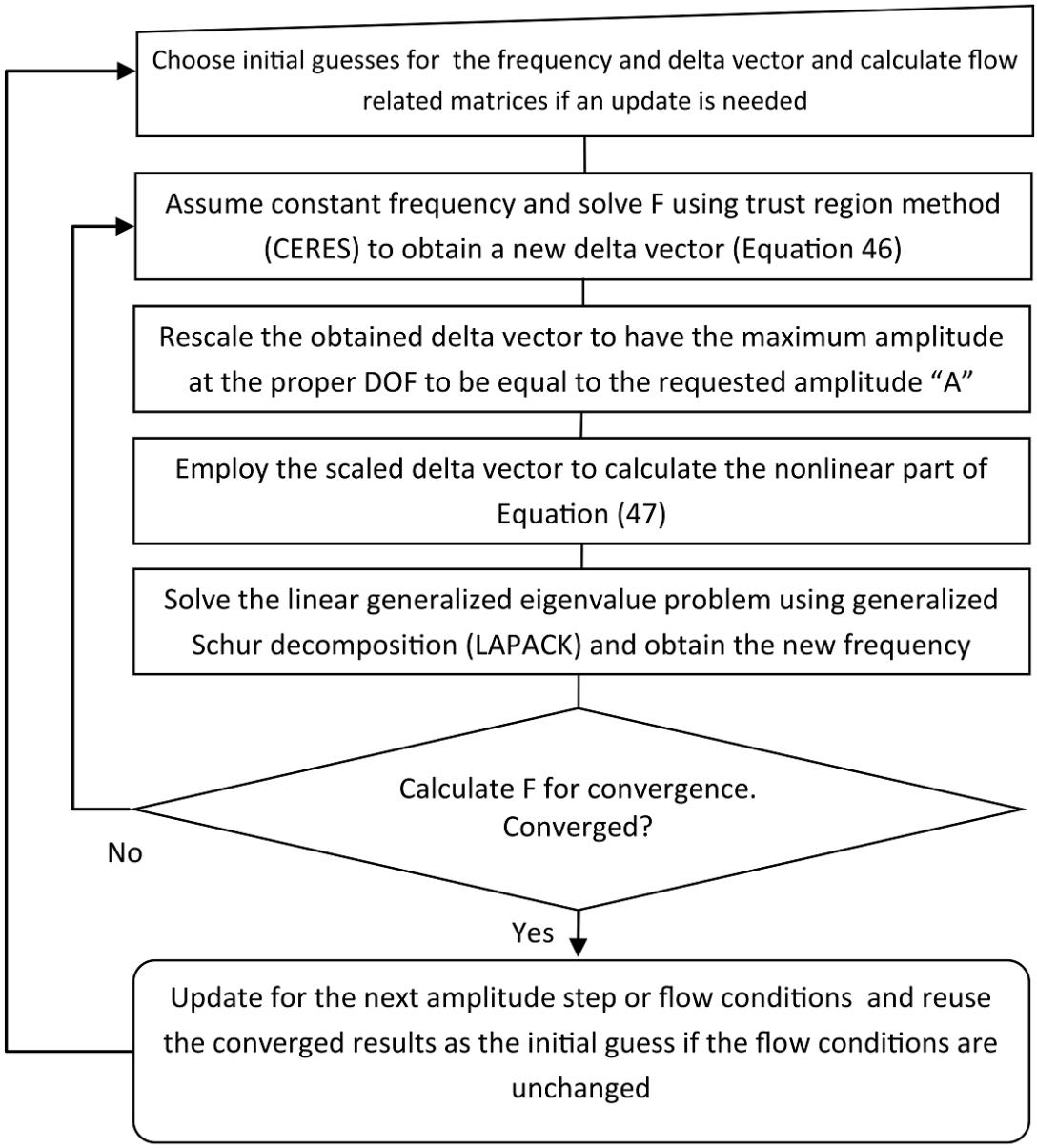

Figure 6.2 Overview of the nonlinear harmonic frequency solver algorithm

that has four degrees of freedom at each end:

- "F": all degrees of freedom are free (U, V, W, $\partial W/\partial x$)
- "CC4": all degrees of freedom are clamped ($U = V = W = \partial W/\partial x = 0$,)
- "SS0": simply supported where $U = 0$ and the rest are free
- "SS4": simply supported where $U = V = W = 0$ and $\partial W/\partial x$ is free
- "SS5": where $V = 0$ and the rest are free

For example, F-SS0 indicates free boundary condition at the small end and simply supported according to what is described above at the larger end.

6.7 Results and Discussion

6.7.1 Small Amplitude Vibration and Flutter

It is important to validate the linear dynamic behavior of the shell to ensure the correctness of the model and also to provide a baseline for nonlinear analysis. Hence, for the first case of the current study's calculations, the small amplitude flutter of thin conical shells for the linearized version of Equation (6.39) (all the nonlinear terms are dropped) was investigated by different authors [2, 7, 9, 10, 31, 34] on a truncated conical shell with the following properties: $t = 1.295mm(0.051in)$, $R_1 = 191.72mm(7.548in)$, $L = 1558.7mm(61.365in)$, $\alpha_c = 5°$, $E = 44.82GPa(6.5 \times 10^6 lbfin^{-2})$, $\nu = 0.29$, $\rho = 8902kgm^-3(8.33 \times 10^{-4} lbfsin^{-4})$, $M_\infty = 3$, $a_\infty = 213m/s(8400ins^{-1})$, $\gamma_a = 1.4$, $P_l/P_\infty = 1.03$ and $M_l = 2.89$. M_l and P_l denote to the local Mach number and pressure after the conical shock on conditions have been calculated using [35]. Moreover, the calculated flutter onset static pressure should be re-adjusted by this pressure ratio to obtain the free stream static pressure. The boundary conditions for this case is set to SS4-SS4. The flutter critical parameter is defined as follows:

$$\Lambda_{cr} = \frac{12(1-\nu^2)\gamma P_\infty R_1^3}{Et^3 (M^2-1)^{(1/2)}} \tag{6.48a}$$

The results including the critical circumferential mode number (n_{cr}) are shown in Table 6.1 and show good agreement with existing studies reported in literature. Based on the provided numbers, it seems that a few of earlier works (e.g. [9] and [31]) overlooked the important effect of the formation of conical shock at the tip of the cone and subsequently the reduced local Mach number and increased local static pressure. This led to the slight differences between those values and what is reported here that practically employed the same FEM method. It seems that Shulman [34] used insufficient number of terms in employing the Galerkin implementations. Moreover, the current study employed the correction terms for considering the effect of curvature in its linear piston theory while Dixon and Hudson [2] and Bismarck-Nasr and Costa Savio [7] ignored that effect.

The validity of real and imaginary components of the frequency of the current study were compared favorably with the work of Kerboua and Lakis [31]. The dimensions and physical properties of the shell are the same as the case presented for Table 6.1, $M_l = 3$ and SS4-SS4 The local Mach number and the boundary conditions were chosen to be $M_l = 3$ and SS4-SS4 were chosen as the local Mach number and the boundary conditions, respectively. The results are shown in figure 6.3 and demonstrate good accordance. The small differences can be attributed to the Newton-Raphson iterative method that was employed for calculating the flutter onset in that study, while in the current study, the exact solution using generalized Schur decomposition is employed.

In the third case, for the breathing vibration of conical shells, experimental results provided by Miserentino and Dixon [5] were selected for validation. The truncated conical shell has the following properties $t = 0.047cm$, $R_1 = 3.05cm$, $R_2 = 38.1cm$, $\alpha_c = 15°$, $E = 200GPa$, $\nu = 0.28$, $\rho = 7640kgm^{-3}$ and the boundary conditions are reported to be SS5-SS5. The shell was pressurized with air. Results for four different internal pressures are shown in Figure 6.4 and demonstrate good agreement. It should be noted that due to the configuration of the installed shell in this experiment, the internal pressure produced an axial load that was taken into account by multiplying the pressure on the sum of the shell's area at both ends. The slight difference could be attributed to the shell boundary conditions in the experiments that as described by Miserentino and Dixon [5] had some deviations from the assumed free degrees of freedom.

Table 6.1 Validation: Small amplitude flutter critical parameter

Reference	Method	Λ_{cr}	n_{cr}
Shulman [34]			6
	Galerkin, 4 terms	669	
Dixon and Hudson [2]			
	Galerkin, 4 terms	492	5
	Galerkin, 8 terms	588	5
	Galerkin, 12 terms	590	5
Bismarck-Nasr and Costa Savio [7]			6
	FEM	702	6
Sabri and Lakis [9]			
	Hybrid FEM	598	6
Pidaparti and Yang [36]			
		576	5
Mahmoudkhani et al. [10]			
		570	5
Present (Linear)			
		554	5
Present (Linear)			
		420	6

The flutter critical pressures and first mode frequencies at different values of internal pressure, for the shell described in the second case are shown in Figure 6.5. As can be seen, the flutter critical pressure increases with the internal pressure due to its stiffening effect and this is supported by what was reported by Sabri and Lakis [9] and Kerboua and Lakis [31].

6.7.2 Large Amplitude Flutter

Due to lack of enough data to reproduce the few cases of nonlinear flutter of conical shells, one case of cylindrical shell that was studied by Fung and Olson [37] is simulated with a truncated cone with a very small semi-cone angle ($\alpha_c = 0.01°$) and was employed for validation of large amplitude flutter. The properties are: $t = 1.016mm(0.004in)$, $R_1 = 203.2mm(8.00in)$, $L = 391.16(15.40in)$, $\alpha_c = 0.01°$, $E = 110.3GPa(16 \times 10^6 lbfin^{-2})$, $\nu = 0.35$, $\rho = 8902kgm^-3(8.33 \times 10^{-4} lbfs^2 in^{-4})$, $M_\infty = 3$, $a_\infty = 213m/s(8400ins^{-1})$, $\gamma = 1.4$,

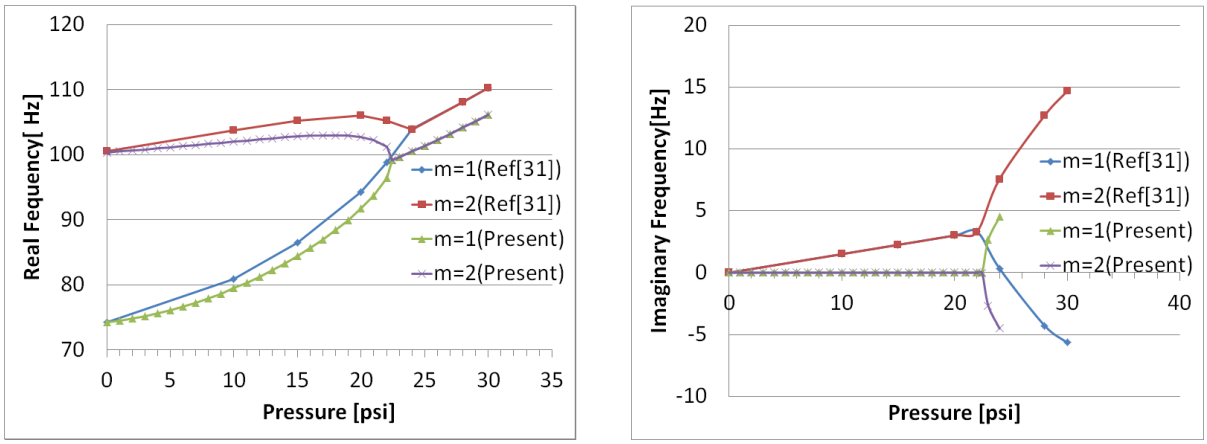

(a) (b)

Figure 6.3 Comparison of (6.3a) the real and (6.3b) the imaginary parts of the first and second mode of vibration with those reported by Kerboua and Lakis [31]

$n_c = 23$ and $p_m = 3447Pa(0.5psi)$. The results of large amplitude flutter static pressure to the linear flutter for different nondimensional amplitudes of vibrations are shown in Figure 6.6 and demonstrate good accordance.

Nonlinear flutter of a pressurized truncated cone with physical boundary conditions and geometrical properties similar to the second case was studied using Sanders' nonlinear thin shell theory for modeling the kinematics of the shell. The internal pressure was set to $p_m = 9.0kPa$ and the associated axial load was also considered for calculations. This is the case of a pressurized truncated conical shell that was described in the second case and was the subject of experimental study by Miserentino and Dixon [5]. The flutter critical pressure in that experiment was reported to be $p_L = 332.2kPa$ at $n_c = 9$. In the current study, the linear critical pressure was calculated as $P_{cr} = 389.305kPa$.

Investigating the first ten modes of nonlinear response that are not presented here, revealed that nonlinear flutter onset and instability within the amplitude range of the current study (1.2-1.5 times of the shell thickness) occurs in the first four modes of oscillation. Hence, the presented results here are focused on those four modes. The convention in literature is to provide the stability curves in terms of static pressure. On the other hand the common practice in the few existing experiments was to keep the static pressure constant and induce the flutter by reducing the internal pressure, mostly because the gradual change in the static pressure of the supersonic wind tunnel is not practical.

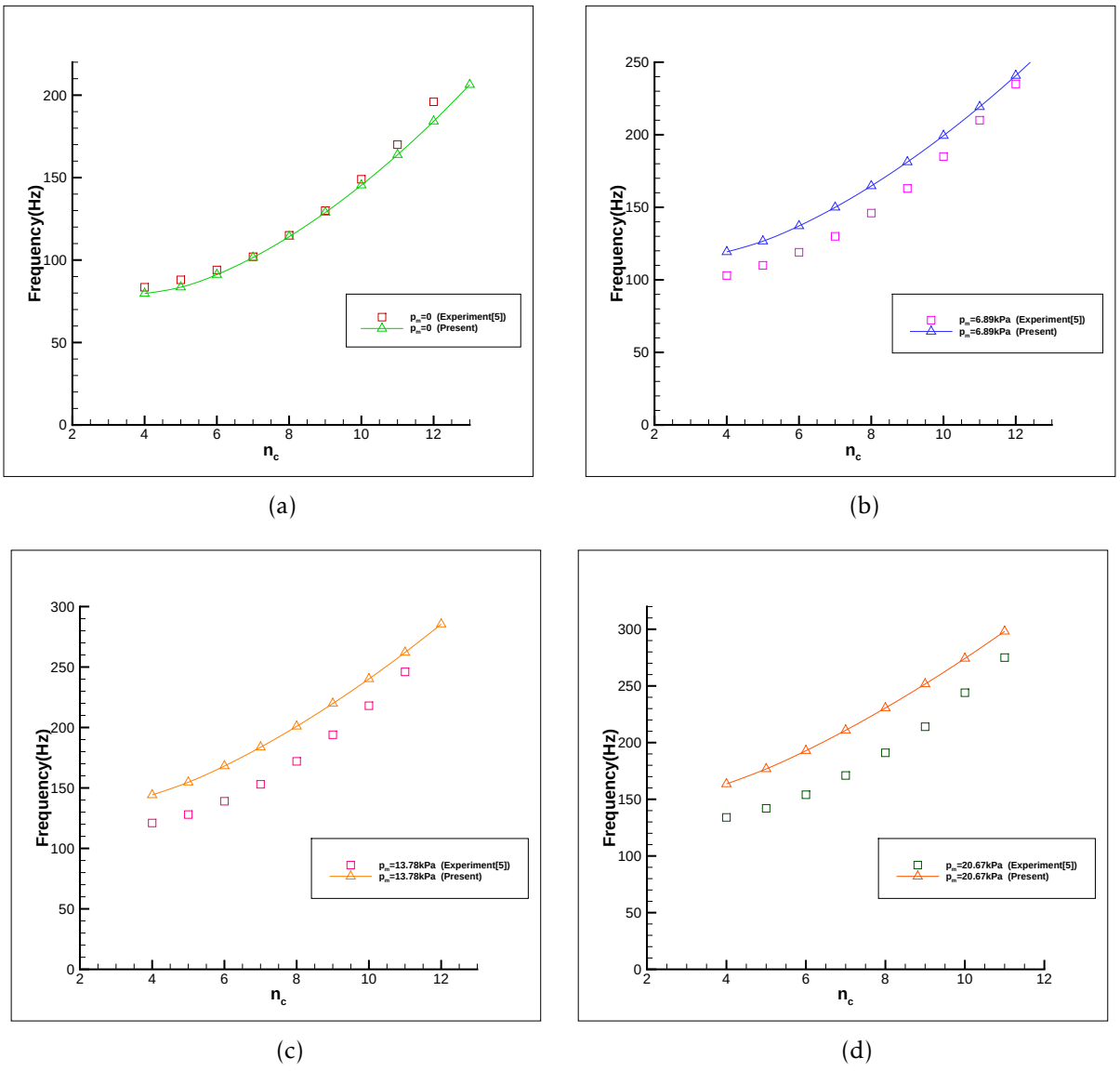

Figure 6.4 Comparison of vibration frequencies of simply supported truncated conical shell at different internal pressures against those presented by Miserentino and Dixon [5]

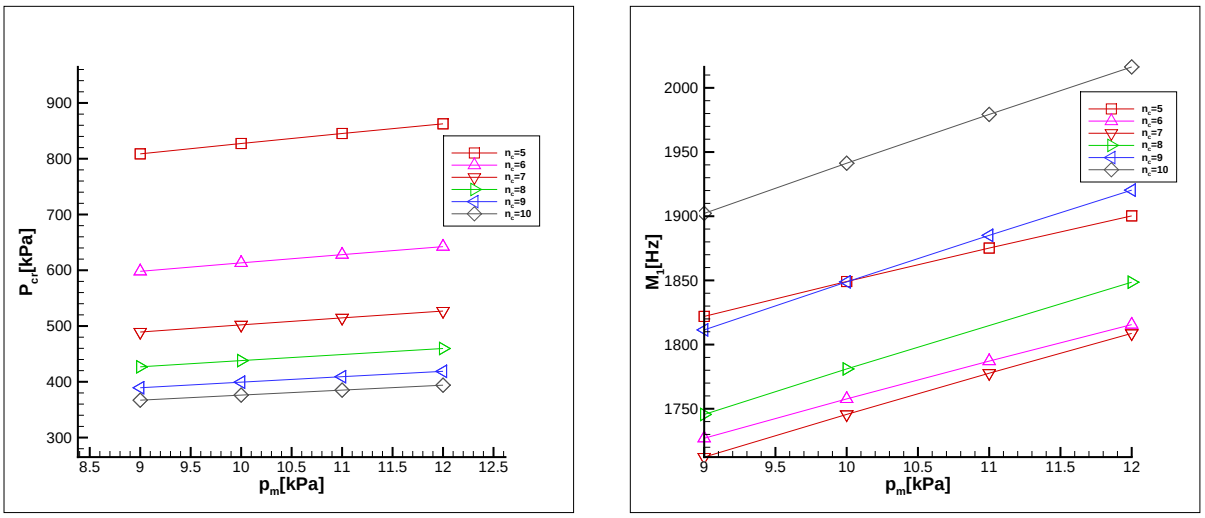

(a) (b)

Figure 6.5 Pressurized shell flutter onset (6.5a) critical static pressure (6.5b) first mode frequency for different circumferential mode numbers

Hence, we focused the results around the flutter onset for varying amplitude of vibration. Figure 6.7 shows the variation of dimensionless flutter frequency versus the amplitude of flutter vibration for all three different theories for the first and the second longitudinal modes of this case. As can be seen, all theories predicted a softening behavior for the effect of geometrical nonlinearities. Moreover, in both modes, Donnell's theory predicted stronger softening effect but the prediction of Sanders and Nemeth theories at lower amplitudes are relatively close. Since the contribution of additional terms in Nemeth theory compared to Sanders' is more effective in thicker shells and in the presence of shear deformation, producing close results for this particular thin shell is expected. Notably, all three theories predicted unstable branches of vibration for both modes that are different from toggling between stability and instability for the linear solution. This is a result of Neimark-Sacker bifurcations of the periodic orbit.

Figure 6.8 shows the variation of non-dimensional flutter amplitude versus non-dimensional flutter frequency for the third and the fourth longitudinal modes of Sanders' theory. This has been calculated at a very small post-flutter critical pressure $P_{cr} = 390.0kPa$ to achieve numerical convergence.

The alternating stable-unstable behavior between modes that results in a shift in the sta-

bility to the higher modes is consistent with the general behavior described for the nonlinear flutter in cylindrical shells [29]. The next Neimark-Sacker bifurcation results in establishing the stability in lower modes while destabilizes the higher modes. Moreover, as can be seen in all of the results, the deviations from the linear frequency are not significant and that is in line with what is reported in the experimental work of Miserentino and Dixon [5]. It should be noted due to the presence of $\sin(\omega t)$ in Equation (6.41), one additional mode emerges between each two linear modes. In other words, in terms of frequency, the first two modes on nonlinear vibration have close values to the first linear mode and similarly, the third and fourth nonlinear frequencies have values that emerged from the second linear mode of vibration.

6.8 Conclusion

A nonlinear hybrid finite element model was developed for truncated conical shells, based on the exact solution of Sander's linear shell theory. Using the generalized coordinates method and the displacement function of the FEM model, the internal strain energy of the shell for three different types of geometrical nonlinearities (Donnell, Sanders and Nemeth) was defined in terms of nodal displacements. Linear piston theory with correction term for the effect of curvature employed for modeling the pressure field and transformed in terms of nodal displacements. The effect of initial stiffening due to internal pressure and axial loads was also formulated in terms of nodal displacements. Equations of motion of the shell were developed using Lagrangian approach. Then employing a variation of harmonic balance method, the amplitude equations of the shell were obtained. The linear flutter problem was solved using the exact solution of generalized Schur decomposition of the system and an iterative method was developed for the nonlinear solution. Results of vibration of pressurized truncated conical shells were compared with those existing in the literature, and these showed good agreement.

Linear and large amplitude flutter characteristics were also compared with the existing experimental data for conical and cylindrical shells accordingly, and these demonstrated good accordance. The large amplitude flutter responses of truncated conical shells were obtained and these showed softening behavior. In addition, it was observed that, as

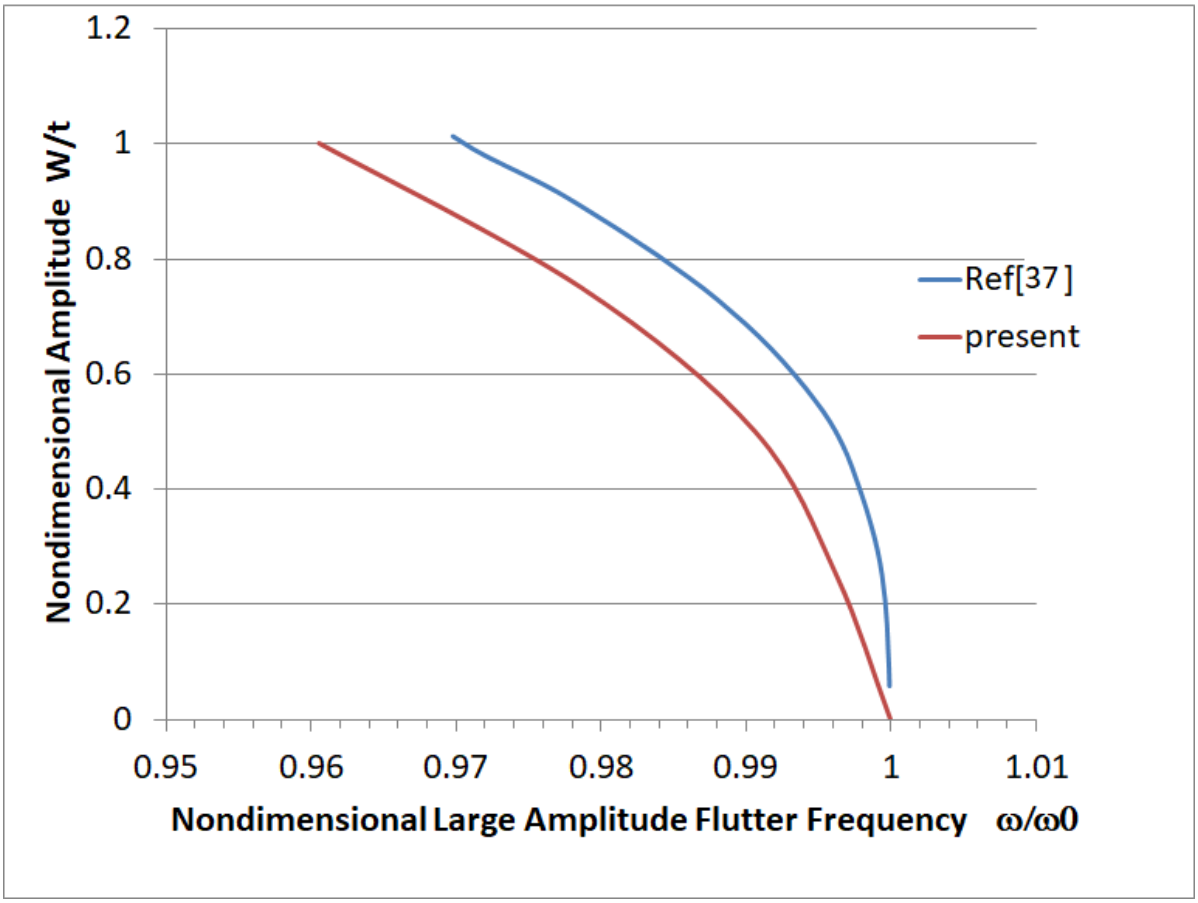

Figure 6.6 Comparison of the large amplitude dimensionless flutter frequency of a cylindrical shell with Reference[37]

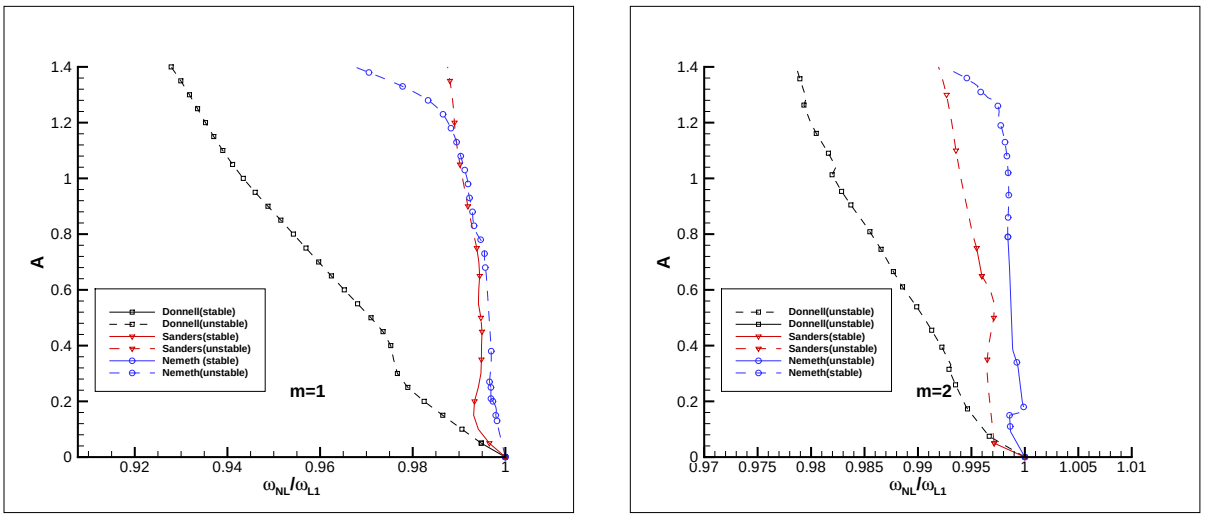

(a) (b)

Figure 6.7 Nondimensional flutter amplitude versus nondimensional flutter frequency; $\omega_{m,NL}/\omega_{1,L}$; (__)stable branches, - - unstable branches; for the first and second longitudinal modes, comparison of Donnell, Sanders and Nemeth theories ($n_c = 9$, $\omega_{1,L} = 1811Hz$, $P_{cr} = 389.305kPa$)

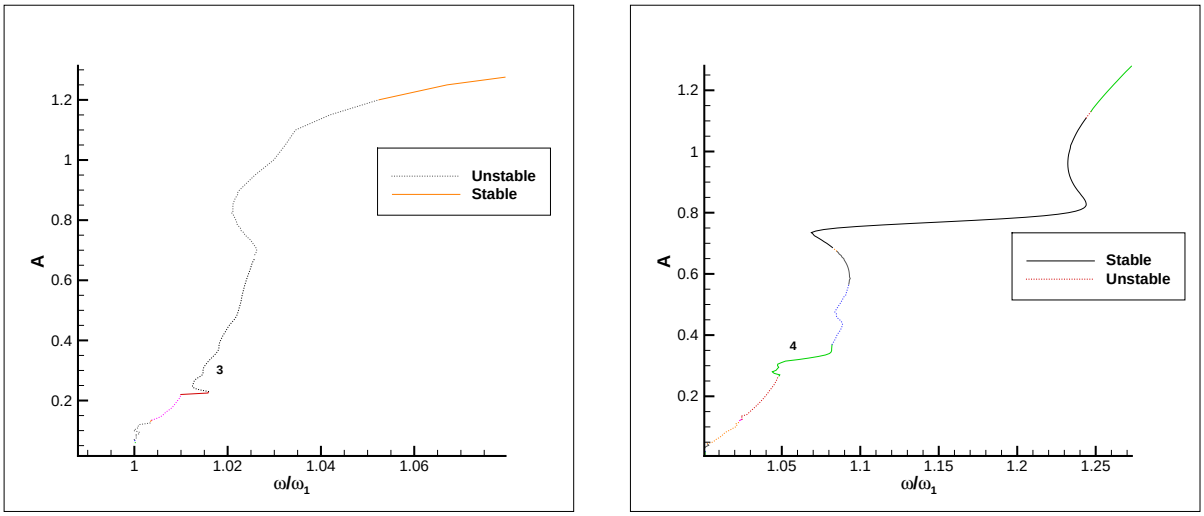

(a) (b)

Figure 6.8 Nondimensional flutter amplitude versus nondimensional flutter frequency; $\omega_{m,NL}/\omega_{1,L}$; (__)stable branches, - - unstable branches; for the third and fourth longitudinal modes predicted by Sanders theory($n_c = 9, \omega_{1,L} = 1811Hz, P_{cr} = 389.305kPa$)

the amplitude of the vibration increased, the instability shifted to higher modes due to Neimark-Sacker bifurcation.

References

[1] M. Amabili and F. Pellicano, "Nonlinear Supersonic Flutter of Circular Cylindrical Shells," *AIAA Journal*, vol. 39, no. 4, pp. 564–573, 2001. [Online]. Available: http://dx.doi.org/10.2514/2.1365

[2] S. C. Dixon and M. L. Hudson, "Flutter, vibration, and buckling of truncated orthotropic conical shells with generalized elastic edge restraint," Tech. Rep. NASA-TN-D-5759, L-6663, Jul. 1970. [Online]. Available: http://ntrs.nasa.gov/search.jsp?R=19700024015

[3] ——, "Flutter, vibration, and buckling of truncated orthotropic conical shells with generalized elastic edge restraint, supplement," Tech. Rep. NASA-TN-D-5759-SUPPL, Jul. 1970. [Online]. Available: http://ntrs.nasa.gov/search.jsp?R=19700024016

[4] ——, "Supersonic asymmetric flutter and divergence of truncated conical shells with ring supported edges," Tech. Rep. NASA-TN-D-6223, L-7527, May 1971. [Online]. Available: http://ntrs.nasa.gov/search.jsp?R=19710016314

[5] R. Miserentino and S. C. Dixon, "Vibration and flutter tests of a pressurized thin-walled truncated conical shell," Tech. Rep. NASA-TN-D-6106, L-7345, 1971. [Online]. Available: http://ntrs.nasa.gov/archive/nasa/casi.ntrs.nasa.gov/19710007880.pdf

[6] T. Ueda, S. Kobayashi, and M. Kihira, "Supersonic Flutter of Truncated Conical Shells." *Transactions of the Japan Society for Aeronautical and Space Sciences*, vol. 20, no. 47, pp. 13–30, 1977.

[7] M. N. Bismarck-Nasr and H. R. Costa Savio, "Finite-element solution of the supersonic flutter of conical shells," *AIAA Journal*, vol. 17, no. 10, pp. 1148–1150,

1979. [Online]. Available: http://arc.aiaa.org/doi/pdf/10.2514/3.61291

[8] R. Pidaparti, "Flutter analysis of cantilevered curved composite panels," *Proceedings of the 7th International Conference on Composite Structures, August 1, 1993 - August 1, 1993*, vol. 25, no. 1-4, pp. 89–93, 1993.

[9] F. Sabri and A. A. Lakis, "Hybrid finite element method applied to supersonic flutter of an empty or partially liquid-filled truncated conical shell," *Journal of Sound and Vibration*, vol. 329, no. 3, pp. 302–316, 2010. [Online]. Available: http://www.sciencedirect.com/science/article/pii/S0022460X09007470

[10] S. Mahmoudkhani, H. Haddadpour, and H. Navazi, "Supersonic flutter prediction of functionally graded conical shells," *Composite Structures*, vol. 92, no. 2, pp. 377–386, 2010.

[11] A. Davar and H. Shokrollahi, "Flutter of functionally graded open conical shell panels subjected to supersonic air flow," *Proceedings of the Institution of Mechanical Engineers, Part G: Journal of Aerospace Engineering*, pp. 1036–1052, 2012. [Online]. Available: http://pig.sagepub.com/content/early/2012/06/06/0954410012448340.abstract

[12] A. Vasilev, "Flutter of conical shells under external flow of a supersonic gas," *Moscow University Mechanics Bulletin*, vol. 70, no. 2, pp. 23–27, 2015.

[13] S. W. Yang, Y. X. Hao, W. Zhang, and S. B. Li, "Nonlinear Dynamic Behavior of Functionally Graded Truncated Conical Shell Under Complex Loads," *International Journal of Bifurcation and Chaos*, vol. 25, no. 2, p. 1550025(33 pp.), Feb. 2015, wOS:000350485800011.

[14] M. P. Nemeth, "A Leonard-Sanders-Budiansky-Koiter-Type Nonlinear Shell Theory with a Hierarchy of Transverse-Shearing Deformations," Tech. Rep. NASA/TP–2013-218025, Jul. 2013. [Online]. Available: http://ntrs.nasa.gov/search.jsp?R=20140000788

[15] ——, "An Exposition on the Nonlinear Kinematics of Shells, Including Transverse Shearing Deformations," NASA, Tech. Rep. NASA/TM–2013-217964, 2013.

[Online]. Available: http://ntrs.nasa.gov/search.jsp?R=20130011025

[16] M. Bakhtiari, A. A. LAKIS, and Y. Kerboua, "Nonlinear vibration of truncated conical shells: Donnell, Sanders and Nemeth theories," Tech. Rep. EPM-RT-2018-01, 2018. [Online]. Available: https://publications.polymtl.ca/3011/1/EPM-RT-2018-01_Bakhtiari.pdf

[17] J. L. Sanders Jr, "An improved first-approximation theory for thin shells," NASA, Tech. Rep. TR R-24, 1959.

[18] J. L. Sanders Jr., "Nonlinear theories for thin shells," DTIC Document, Tech. Rep. AD0253822, 1961. [Online]. Available: http://oai.dtic.mil/oai/oai?verb=getRecord&metadataPrefix=html&identifier=AD0253822

[19] ——, "Nonlinear theories for thin shells," *Quarterly of Applied Mathematics*, pp. 21–36, 1963. [Online]. Available: http://www.jstor.org/stable/43634948

[20] L. H. Donnell, "A new theory for the buckling of thin cylinders under axial compression and bending," *Trans. ASME*, vol. 56, no. 11, pp. 795–806, 1934. [Online]. Available: http://cybra.lodz.pl/Content/6356/AER_56_12.pdf

[21] M. Bakhtiari, A. A. Lakis, and Y. Kerboua, "Nonlinear Vibration of Truncated Conical Shells: Donnell, Sanders and Nemeth Theories," *International Journal of Nonlinear Sciences and Numerical Simulation*, vol. 0, no. 0, 2019. [Online]. Available: https://www.degruyter.com/view/j/ijnsns.ahead-of-print/ijnsns-2018-0377/ijnsns-2018-0377.xml?lang=de

[22] ——, "Derivatives of fourth order Kronecker power systems with applications in nonlinear elasticity," *Applied Mathematics and Computation*, vol. 362, p. 124501, 2019.

[23] M. Amabili, *Nonlinear vibrations and stability of shells and plates*. Cambridge University Press, 2008. [Online]. Available: https://books.google.ca/books?hl=en&lr=&id=0Ymw-pi7-x4C&oi=fnd&pg=PA52&dq=Nonlinear+Vibrations+and+Stability+of+Shells+and+Plates&ots=uZtdkX_GUL&sig=hStbpt8yVKKY4Eeh6L0QEzyT2NY

[24] H. Krumhaar, "The Accuracy of Applying Linear Piston Theory to Cylindrical

Shells," Tech. Rep. AD0408387, Mar. 1963.

[25] S. G. P. Castro, C. Mittelstedt, F. A. C. Monteiro, M. A. Arbelo, R. Degenhardt, and G. Ziegmann, "A semi-analytical approach for linear and non-linear analysis of unstiffened laminated composite cylinders and cones under axial, torsion and pressure loads," *Thin-Walled Structures*, vol. 90, pp. 61–73, May 2015. [Online]. Available: http://www.sciencedirect.com/science/article/pii/S0263823115000051

[26] R. Lewandowski, "Free vibration of structures with cubic non-linearity-remarks on amplitude equation and Rayleigh quotient," *Computer Methods in Applied Mechanics and Engineering*, vol. 192, no. 13, pp. 1681–1709, Mar. 2003. [Online]. Available: http://www.sciencedirect.com/science/article/pii/S0045782503001890

[27] ——, "Non-linear steady state vibrations of beams excited by vortex shedding," *Journal of sound and vibration*, vol. 252, no. 4, pp. 675–696, 2002.

[28] E. Anderson, Z. Bai, C. Bischof, L. S. Blackford, J. Demmel, J. Dongarra, J. Du Croz, A. Greenbaum, S. Hammarling, and A. McKenney, *LAPACK Users' guide*. SIAM, 1999.

[29] M. Amabili and F. Pellicano, "Multimode Approach to Nonlinear Supersonic Flutter of Imperfect Circular Cylindrical Shells," *Journal of Applied Mechanics*, vol. 69, no. 2, pp. 117–129, Oct. 2001. [Online]. Available: http://dx.doi.org/10.1115/1.1435366

[30] F. Sabri, A. Lakis, and M. Toorani, "Hybrid finite element method in supersonic flutter analysis of circular cylindrical shells," in *31st International Conference on Boundary Elements and Other Mesh Reduction Methods*, *BEM/MRM 31*, ser. WIT Transactions on Modelling and Simulation, vol. 49. WITPress, 2009, pp. 233–244.

[31] Y. Kerboua and A. A. Lakis, "Numerical model to analyze the aerodynamic behavior of a combined conical–cylindrical shell," *Aerospace Science and Technology*, vol. 58, pp. 601–617, 2016. [Online]. Available: http://www.sciencedirect.com/science/article/pii/S1270963816307064

[32] S. Agarwal, K. Mierle, and Others, "Ceres Solver, http://ceres-solver.org, access date," Dec. 2018. [Online]. Available: http://ceres-solver.org

[33] L. Tong, "Free vibration of orthotropic conical shells," *International Journal of Engineering Science*, vol. 31, no. 5, pp. 719–733, 1993.

[34] Y. Shulman, *Vibration and flutter of cylindrical and conical shells*. Air Force Office of Scientific Research, Air Research and Development Command, United States Air Force, 1959.

[35] A. R. Staff, "Equations, tables, and charts for compressible flow," NASA Ames Aeronautical Laboratory, Moffett Field, California, Tech. Rep. 1135, 1953. [Online]. Available: https://www.nasa.gov/sites/default/files/734673main_Equations-Tables-Charts-CompressibleFlow-Report-1135.pdf

[36] R. Pidaparti and H. T. Yang, "Supersonic flutter analysis of composite plates and shells," *AIAA journal*, vol. 31, no. 6, pp. 1109–1117, 1993.

[37] Y. C. Fung and M. D. Olson, "Comparing theory and experiment for the supersonic flutter of circular cylindrical shells." *AIAA Journal*, vol. 5, no. 10, pp. 1849–1856, 1967. [Online]. Available: https://doi.org/10.2514/3.4315

I.A. Conical Shell Linear Equilibrium Equations in Terms of Stress Resultants

The principle parameters of conical shells can be obtained from the following equation:

$$A_1(x,\theta) = 1, A_2(x,\theta) = x\sin(\alpha_c), \frac{1}{R_1(x,\theta)} = 0, \frac{1}{R_2(x,\theta)} = \frac{1}{x\tan(\alpha_c)}, \frac{1}{\rho_{11}} = 0, \frac{1}{\rho_{22}} = \frac{1}{x} \tag{III.A.49}$$

By introducing the geometrical parameters of conical shells into the general equilibrium equations of Sanders' improved linear theory [17]; one obtains the equilibrium equations of a conical shell as follows.:

$$\frac{\partial n_{11}}{\partial x} + \frac{1}{x\sin(\alpha_c)}\frac{\partial n_{12}}{\partial \theta} + \frac{1}{x}(n_{11} - n_{22}) - \frac{1}{2x^2\sin(\alpha_c)\tan(\alpha_c)}\frac{\partial m_{12}}{\partial \theta} = 0 \tag{III.A.50a}$$

$$\frac{\partial n_{12}}{\partial x} + \frac{1}{x\sin(\alpha_c)}\frac{\partial n_{22}}{\partial \theta} + \frac{2n_{12}}{x} + \frac{3}{2}\frac{1}{x\tan(\alpha_c)}\frac{\partial m_{12}}{\partial x} + \frac{1}{x^2\sin(\alpha_c)\tan(\alpha_c)}\frac{\partial m_{22}}{\partial \theta} + \frac{3}{2}\frac{1}{x^2\tan(\alpha_c)}m_{12} = 0 \tag{III.A.50b}$$

$$\frac{\partial^2 m_{11}}{\partial x^2} + \frac{2}{x^2\sin(\alpha_c)}\frac{\partial m_{12}}{\partial \theta} + \frac{2}{x\sin(\alpha_c)}\frac{\partial^2 m_{12}}{\partial x \partial \theta} + \frac{2}{x}\frac{\partial m_{11}}{\partial x} - \frac{1}{x}\frac{\partial m_{22}}{\partial x} + \frac{1}{x^2\sin(\alpha_c)^2}\frac{\partial^2 m_{22}}{\partial \theta^2} - \frac{n_{22}}{x\tan(\alpha_c)} = 0 \tag{III.A.50c}$$

III.B. Nomenclature

$\left[\mathcal{AQ}\right]$	Characteristic polynomial matrix
c_{NL}, c_1, c_2, c_3	Flag parameters to define different shell theories
$\left[\bar{\mathcal{C}}^0\right]$	Symmetric constitutive matrix for conical element
$e_{11}^\circ, e_{22}^\circ, e_{12}^\circ$	Linear deformation parameters defined by Equation (6.3)
$\left[\mathbf{K_{11}}\right], \left[\tilde{\mathbf{K}}_{\mathbf{12}}\right], \left[\tilde{\mathbf{K}}_{\mathbf{22}}\right]$	Assembled first, second and third order structural stiffness matrices
L	Truncated cone element length
M, M_l	Flow Mach number and Local flow Mach number(after the oblique shock)
$\left[\mathbf{M_T}\right]$, $\left[\mathbf{M_S}\right]$	Assembled translational and structural mass matrices defined by Equation (6.19) and (6.20)
n_c	Circumferential mode number
$\left[\mathbf{N}\right]$	Displacement field matrix of a finite element defined by Equation (6.15)
p_∞	Flow static pressure
$\mathrm{U}_i (i = 1, 2, 3)$	Displacements along the longitudinal, lateral and normal to surface directions, off the reference surface
$\mathrm{u}_i (i = 1, 2, 3)$	Displacements along the longitudinal (U), lateral (V) and normal (W), on the reference surface
α_c	Cone half angle
$\chi_{11}^\circ, \chi_{22}^\circ, \chi_{12}^\circ, \left\{\boldsymbol{\chi}^\circ\right\}$	Linear deformation parameters defined by Equation (6.4b)
δ_m	nodal degrees of freedom associated with $m^{th} node$
$\epsilon_{11}^\circ, \epsilon_{22}^\circ, \left\{\boldsymbol{\epsilon}^\circ\right\}$	Reference surface strains defined by Equation (6.4a)
$\varphi_1, \varphi_2, \varphi$	Linear rotation parameters defined by Equation (6.2)
ρ_{11}, ρ_{22}	Geodesic radii of curvature radii of curvature along x and θ directions
$\left\{\boldsymbol{\delta}\right\}^{\mathrm{e}}$	Vector of element degrees of freedom
$\left\{\boldsymbol{\delta}\right\}$	Vector of whole system degrees of freedom

CHAPTER 7 GENERAL DISCUSSION

The common approach in developing equations of motion for third-order geometrically nonlinear systems usually employ the expanded form of the strain energy. The final equations take the form of large nested summations with many terms. This approach is not effective and susceptible to errors. Moreover, this expanded form of equations of motion is difficult to code into computer programs. Hence, the mathematically concise way to develop and express equations of motion for shells is to employ matrix multiplication and the Kronecker product. In the current thesis, a new mathematical framework to express equations of motion for third-order nonlinear elastic systems such as shells was developed. This required a novel methodical approach to obtain the general derivatives of Kronecker powers of vectors. The applications of this framework have potentials in other fields such as signal processing and dynamic modeling.

The current thesis investigated the geometrically nonlinear vibrations and supersonic flutter of truncated conical shells under the initial stiffening effects of internal pressurization and axial loads. The three different theories employed were those of Donnell, Sanders and Nemeth. This provided the ability to study the differences between the predictions of those theories. The hybrid finite element tool developed in this study provided accurate predictions for the small amplitude vibration of truncated conical shells in low to moderate circumferential mode numbers when a reasonably fine mesh was used. This was confirmed by validation of linear vibration frequencies against three different experimental data sets available in literature that had different properties and boundary conditions. In addition, it was observed that the natural frequency of vibration increased as a result of internal pressurization. The axisymmetric nonlinear vibrational response of conical shells was found to be from hardening types. Among the three chosen theories, Donnell's theory predicted stronger nonlinear response while the difference between the results of Nemeth's and Sanders' theories were found to be insignificant. This important finding revealed that the thinness assumptions in Sanders' theory could provide accurate results with significantly less modeling and numerical efforts for the classes of shells that were

studied in this work. For the studied cases, it was found that the weakest nonlinear response occurred when the cone half-angle was equal to 45°, while the nonlinear effects got stronger when the cone half-angle moved away from that value. Effects of other parameters such as boundary conditions and thickness-to-small-radius ratio were also investigated. One notable observation in the studied cases was that, under certain conditions, looser constraints led to stronger nonlinear response to the extent that its value surpassed more constrained cases for larger amplitudes of vibration.

The linear supersonic flutter of truncated conical shells was found to be of the Hopf bifurcation type. The linear flutter onset occurred as a result of the coalescence of the two eigen-frequencies corresponding to the first and second mode of vibration. The flutter dynamic pressure onset of pressurized truncated conical shells was found to be higher than the empty ones, and the tensile axial load resulted in a similar behavior.

The nonlinear flutter onset demonstrated a rather more complicated behavior. While at low amplitudes of vibrations, the instability occurred at the first and second mode of vibration; as the amplitude of vibration increased, the instability shifted to higher modes. In other words, when the amplitude of the vibration increased, the lower mode became stable while the adjacent higher mode started demonstrating unstable behavior that could be identified in the imaginary part of the supersonic vibration frequency. This alternating stable–unstable behavior between modes that resulted in the shifting of the instability to the higher modes was consistent with the general behavior described for the nonlinear flutter in cylindrical shells. It should be noted that the actual Mach number on the surface of the cone should be adjusted using oblique shock relationships. This might explain the differences between numerical and experimental results reported in some of the earlier studies.

CHAPTER 8 CONCLUSION

8.1 Summary of Works

In the current study, the following tasks have been achieved:

- The linear and nonlinear vibration and supersonic flutter of truncated conical shell are investigated in this thesis. To perform this, first the general mathematical solution to the problem derivatives of the Kronecker powers of a vector was provided and its application in third-order geometrically nonlinear elasticity was presented. This paved the way for a mathematically concise solution for nonlinear equations of motion for thin shells. The developed solution presented a new ability in the applications of matrix calculus that goes beyond the mechanics of materials and elasticity science. This can be used in other fields such as nonlinear dynamics, electrical and communications engineering, stochastic simulations and, possibly, a host of others.
- A linear hybrid finite element solution based on best first approximation of Sanders' theory was developed for truncated conical shells that could support a wide range of boundary conditions.
- The nonlinear kinematics of three different shell theories from Donnell, Sanders and Nemeth were used to formulate nonlinear equations of motion for truncated conical shells.
- The initial stiffening effect induced by internal pressure and axial loads were modeled.
- Linear piston theory was used to introduce the supersonic pressure field as a nodal force in the model.
- Two variants of the harmonic response method based on Galerkin's method in time domain were used to obtain the nonlinear vibration and supersonic flutter response of truncated conical shells.

The developed model and the numerical tool allows for predictions under various boundary conditions in the presence of internal pressures and axial loads by taking into account

the following:

- Linear vibration of truncated conical shells.
- Linear supersonic flutter of truncated conical shells.
- Large amplitude nonlinear vibration of truncated conical shells.
- Large amplitude nonlinear supersonic flutter and divergence of truncated conical shells.

One notable contribution of the current study is the ability to provide comparative results for truncated conical shells using different nonlinear shell theories. The developed tool can be efficiently used in conceptual and preliminary designs of aerospace vehicles. Due to the magnitude of complexities between those theories both in terms of development effort and computational costs, this tool can provide the necessary information required in choosing the nonlinear shell theory for detailed design.

8.2 Future Research

Future works should focus on improving different aspects of the current study on two fronts. The first one is improvements on the physical and mathematical model that can include:

- Nonlinear aerodynamics: The current study employed the linear part of the Taylor expansion for the supersonic pressure field predicted by piston theory. Precisely quantifying the effect of omitted higher order terms could improve the accuracy of the results or demonstrate the bounds of parameters where linear aerodynamics can provide satisfactory results.
- Employing shear deformation theory to investigate these phenomena for moderately thick shells and the effect of thinness assumptions on the predictions of the existing model.
- Using the existing tool to investigate the behavior of advanced materials including FGM and orthotropic layered composites.

The second area of improvement is related to the numerical solution of the developed nonlinear model. A comparative study between the results of the modified harmonic response method in the current study with other existing approaches including numerical continuation and excited vibration could improve the understanding about the limitations of each method. It should be noted that, despite its wide applications, the nonlinear eigenvalue problem that appears in the family of harmonic response methods has not yet found a robust general solution.

CHAPTER 9 SELECTED APPENDICES FROM THE TECHNICAL REPORT EPM-RT-2018-01

.1 Appendix IV.A Through-the-thickness Strain Deformation Matrix

Defining the following aliases:

$$z_1 = \left(1 + \frac{\xi_3}{R_1}\right) \tag{IV.A.1a}$$

$$z_2 = \left(1 + \frac{\xi_3}{R_2}\right) \tag{IV.A.1b}$$

$$Z = \frac{1}{2}\left(\frac{\xi_3}{R_2} - \frac{\xi_3}{R_1}\right) \tag{IV.A.1c}$$

Through-the-thickness strain deformation matrix is defined as follows:

$$\left[\mathbf{S}\right] = \begin{bmatrix} \left[\mathbf{S_0}\right]_{3\times3} & \left[\mathbf{S_1}\right]_{3\times3} & \left[\mathbf{S_2}\right]_{3\times2} & \left[\mathbf{S_3}\right]_{3\times2} & \left[\mathbf{S_4}\right]_{3\times2} \\ \left[\mathbf{0}\right]_{2\times3} & \left[\mathbf{0}\right]_{2\times3} & \left[\mathbf{0}\right]_{2\times2} & \left[\mathbf{0}\right]_{2\times2} & \left[\mathbf{S_5}\right]_{2\times2} \end{bmatrix} \tag{IV.A.2}$$

The block matrices of equation (IV.A.2) can be obtained from the following equations [1] :

$$\left[\mathbf{S_0}\right] = \begin{bmatrix} z_2 & 0 & 0 \\ 0 & z_1 & 0 \\ 0 & 0 & \frac{1}{2}\left[z_1 + z_2 + Z\right] \end{bmatrix} \tag{IV.A.3a}$$

$$\left[\mathbf{S_1}\right] = \begin{bmatrix} z_2 & 0 & 0 \\ 0 & z_1 & 0 \\ 0 & 0 & \frac{1}{2}\left[z_1 + z_2\right] \end{bmatrix} \tag{IV.A.3b}$$

$$\left[\mathbf{S_2}\right] = z_2 \begin{bmatrix} \mathrm{F}_1(\xi_3) & 0 \\ 0 & 0 \\ 0 & \mathrm{F}_2(\xi_3) \end{bmatrix} \tag{IV.A.3c}$$

$$\left[\mathbf{S_3}\right] = z_1 \begin{bmatrix} 0 & 0 \\ 0 & \mathrm{F}_2(\xi_3) \\ \mathrm{F}_1(\xi_3) & 0 \end{bmatrix} \tag{IV.A.3d}$$

$$\left[\mathbf{S_4}\right] = \begin{bmatrix} 0 & -\frac{z_2}{\rho_{11}}\mathrm{F}_2(\xi_3) \\ \frac{z_1}{\rho_{22}}\mathrm{F}_1(\xi_3) & 0 \\ \frac{z_2}{\rho_{11}}\mathrm{F}_1(\xi_3) & -\frac{z_1}{\rho_{22}}\mathrm{F}_2(\xi_3) \end{bmatrix} \tag{IV.A.3e}$$

$$\left[\mathbf{S_5}\right] = \begin{bmatrix} z_2\left[z_1\mathrm{F'}_1(\xi_3) - \frac{\mathrm{F}_1(\xi_3)}{\mathrm{R}_1}\right] & 0 \\ 0 & z_1\left[z_2\mathrm{F'}_2(\xi_3) - \frac{\mathrm{F}_2(\xi_3)}{\mathrm{R}_2}\right] \end{bmatrix} \tag{IV.A.3f}$$

.2 Appendix IV.B Work Conjugate Stress-Resultants

The work-conjugate stress resultants are given as [1]:

$$\{\mathfrak{n}\} = \begin{bmatrix} \mathfrak{n}_{11} \\ \mathfrak{n}_{22} \\ \mathfrak{n}_{12} \end{bmatrix} \triangleq \int_{-\mathrm{h}/2}^{\mathrm{h}/2} \left[\mathbf{S_0}\right]^{\mathsf{T}} \begin{Bmatrix} \bar{\sigma}_{11} \\ \bar{\sigma}_{22} \\ \bar{\sigma}_{12} \end{Bmatrix} \mathrm{d}\xi_3 \tag{IV.B.1a}$$

$$\{\mathfrak{m}\} = \begin{bmatrix} \mathfrak{m}_{11} \\ \mathfrak{m}_{22} \\ \mathfrak{m}_{12} \end{bmatrix} \triangleq \int_{-h/2}^{h/2} \left[\mathbf{S_1}\right]^{\intercal} \begin{Bmatrix} \bar{\sigma}_{11} \\ \bar{\sigma}_{22} \\ \bar{\sigma}_{12} \end{Bmatrix} d\xi_3 \tag{IV.B.1b}$$

$$\{\mathfrak{f}_1\} = \begin{bmatrix} \mathfrak{f}_{11} \\ \mathfrak{f}_{12} \end{bmatrix} \triangleq \int_{-h/2}^{h/2} \left[\mathbf{S_2}\right]^{\intercal} \begin{Bmatrix} \bar{\sigma}_{11} \\ \bar{\sigma}_{22} \\ \bar{\sigma}_{12} \end{Bmatrix} d\xi_3 \tag{IV.B.1c}$$

$$\{\mathfrak{f}_2\} = \begin{bmatrix} \mathfrak{f}_{21} \\ \mathfrak{f}_{22} \end{bmatrix} \triangleq \int_{-h/2}^{h/2} \left[\mathbf{S_3}\right]^{\intercal} \begin{Bmatrix} \bar{\sigma}_{11} \\ \bar{\sigma}_{22} \\ \bar{\sigma}_{12} \end{Bmatrix} d\xi_3 \tag{IV.B.1d}$$

$$\{\mathfrak{q}\} = \begin{bmatrix} \mathfrak{q}_{13} \\ \mathfrak{q}_{23} \end{bmatrix} \triangleq \int_{-h/2}^{h/2} \left[\mathbf{S_4}\right]^{\intercal} \begin{Bmatrix} \bar{\sigma}_{11} \\ \bar{\sigma}_{22} \\ \bar{\sigma}_{12} \end{Bmatrix} d\xi_3 + \int_{-h/2}^{h/2} \left[\mathbf{S_5}\right]^{\intercal} \begin{Bmatrix} \bar{\sigma}_{13} \\ \bar{\sigma}_{23} \end{Bmatrix} d\xi_3 \tag{IV.B.1e}$$

.3 Appendix IV.C Elements of Symmetric Constitutive Matrix

$$\mathcal{CC}_{1,1} = +A_{11}^0 + \tau_0\left(-\frac{1}{R_1}A_{11}^1 + \frac{1}{R_2}A_{11}^1\right) + \tau\left(+\frac{1}{(R_1^2)}A_{11}^2 - \frac{1}{R_1R_2}A_{11}^2\right) \tag{IV.C.1}$$

$$\mathcal{CC}_{1,2} = +A_{12}^0 \tag{IV.C.2}$$

$$\begin{aligned}\mathcal{CC}_{1,3} = +A_{16}^0 + \tau_0\left(-0.5\frac{1}{R_1}A_{16}^1 + 0.5\frac{1}{R_2}A_{16}^1\right) + \tau\left(+0.75\frac{1}{(R_1^2)}A_{16}^2 - \frac{1}{R_1R_2}A_{16}^2\right. \\ \left. + 0.25\frac{1}{(R_2^2)}A_{16}^2\right)\end{aligned} \tag{IV.C.3}$$

$$\mathcal{CC}_{1,4} = +A_{11}^1 + \tau_0\left(-\frac{1}{R_1}A_{11}^2 + \frac{1}{R_2}A_{11}^2\right) + \tau\left(+\frac{1}{(R_1^2)}A_{11}^3 - \frac{1}{R_1R_2}A_{11}^3\right) \tag{IV.C.4}$$

$$\mathcal{CC}_{1,5} = +\,A^{1}_{12} \tag{IV.C.5}$$

$$\mathcal{CC}_{1,6} = +\,A^{1}_{16} + \tau_0\left(-0.5\frac{1}{R_1}A^{2}_{16} + 0.5\frac{1}{R_2}A^{2}_{16}\right) + \tau\left(+0.5\frac{1}{(R^{2}_{1})}A^{3}_{16} - 0.5\frac{1}{R_1R_2}A^{3}_{16}\right) \tag{IV.C.6}$$

$$\mathcal{CC}_{1,7} = +\,R^{10}_{11} + \tau_0\left(-\frac{1}{R_1}R^{11}_{11} + \frac{1}{R_2}R^{11}_{11}\right) + \tau\left(+\frac{1}{(R^{2}_{1})}R^{12}_{11} - \frac{1}{R_1R_2}R^{12}_{11}\right) \tag{IV.C.7}$$

$$\mathcal{CC}_{1,8} = +\,R^{20}_{16} + \tau_0\left(-\frac{1}{R_1}R^{21}_{16} + \frac{1}{R_2}R^{21}_{16}\right) + \tau\left(+\frac{1}{(R^{2}_{1})}R^{22}_{16} - \frac{1}{R_1R_2}R^{22}_{16}\right) \tag{IV.C.8}$$

$$\mathcal{CC}_{1,9} = +\,R^{10}_{16} \tag{IV.C.9}$$

$$\mathcal{CC}_{1,10} = +\,R^{20}_{12} \tag{IV.C.10}$$

$$\begin{aligned}\mathcal{CC}_{1,11} = {} & +\,W^{10}_{15} + \tau_0\left(-\frac{1}{R_1}R^{10}_{15} + \frac{1}{\rho_{11}}R^{10}_{16} + \frac{1}{\rho_{22}}R^{10}_{12} + \frac{1}{(R^{2}_{1})}R^{11}_{15}\right.\\ & - \frac{1}{R_1R_2}R^{11}_{15} - \frac{1}{R_1\rho_{11}}R^{11}_{16} + \frac{1}{R_2\rho_{11}}R^{11}_{16} + \frac{1}{R_2}W^{11}_{15}\Big) + \tau\Big(-\frac{1}{(R^{3}_{1})}R^{12}_{15}\\ & \left. + \frac{1}{(R^{2}_{1})R_2}R^{12}_{15} + \frac{1}{(R^{2}_{1})\rho_{11}}R^{12}_{16} - \frac{1}{R_1R_2\rho_{11}}R^{12}_{16}\right)\end{aligned} \tag{IV.C.11}$$

$$\begin{aligned}\mathcal{CC}_{1,12} = {} & +\,W^{20}_{14} + \tau_0\left(-\frac{1}{R_2}R^{20}_{14} - \frac{1}{\rho_{11}}R^{20}_{11} - \frac{1}{\rho_{22}}R^{20}_{16} + \frac{1}{R_1\rho_{11}}R^{21}_{11}\right.\\ & \left. - \frac{1}{R_2\rho_{11}}R^{21}_{11} + \frac{1}{R_2}W^{21}_{14}\right) + \tau\left(-\frac{1}{(R^{2}_{1})\rho_{11}}R^{22}_{11} + \frac{1}{R_1R_2\rho_{11}}R^{22}_{11}\right)\end{aligned} \tag{IV.C.12}$$

$$\mathcal{CC}_{2,2} = +\,A^{0}_{22} + \tau_0\left(+\frac{1}{R_1}A^{1}_{22} - \frac{1}{R_2}A^{1}_{22}\right) + \tau\left(-\frac{1}{R_1R_2}A^{2}_{22} + \frac{1}{(R^{2}_{2})}A^{2}_{22}\right) \tag{IV.C.13}$$

$$\begin{aligned}\mathcal{CC}_{2,3} = {} & +\,A^{0}_{26} + \tau_0\left(+0.5\frac{1}{R_1}A^{1}_{26} - 0.5\frac{1}{R_2}A^{1}_{26}\right) + \tau\left(+0.25\frac{1}{(R^{2}_{1})}A^{2}_{26} - \frac{1}{R_1R_2}A^{2}_{26}\right.\\ & \left. + 0.75\frac{1}{(R^{2}_{2})}A^{2}_{26}\right)\end{aligned} \tag{IV.C.14}$$

$$\mathcal{CC}_{2,4} = +\,A^{1}_{12} \tag{IV.C.15}$$

$$\mathcal{CC}_{2,5} = +\,A^{1}_{22} + \tau_0\left(+\frac{1}{R_1}A^{2}_{22} - \frac{1}{R_2}A^{2}_{22}\right) + \tau\left(-\frac{1}{R_1R_2}A^{3}_{22} + \frac{1}{(R^{2}_{2})}A^{3}_{22}\right) \tag{IV.C.16}$$

$$\mathcal{CC}_{2,6} = +\,A^{1}_{26} + \tau_0\left(+0.5\frac{1}{R_1}A^{2}_{26} - 0.5\frac{1}{R_2}A^{2}_{26}\right) + \tau\left(-0.5\frac{1}{R_1R_2}A^{3}_{26} + 0.5\frac{1}{(R^{2}_{2})}A^{3}_{26}\right) \tag{IV.C.17}$$

$$\mathcal{CC}_{2,7} = +\,R^{10}_{12} \tag{IV.C.18}$$

$$\mathcal{CC}_{2,8} = + R_{26}^{20} \tag{IV.C.19}$$

$$\mathcal{CC}_{2,9} = + R_{26}^{10} + \tau_0\left(+\frac{1}{R_1}R_{26}^{11} - \frac{1}{R_2}R_{26}^{11}\right) + \tau\left(-\frac{1}{R_1R_2}R_{26}^{12} + \frac{1}{(R_2^2)}R_{26}^{12}\right) \tag{IV.C.20}$$

$$\mathcal{CC}_{2,10} = + R_{22}^{20} + \tau_0\left(+\frac{1}{R_1}R_{22}^{21} - \frac{1}{R_2}R_{22}^{21}\right) + \tau\left(-\frac{1}{R_1R_2}R_{22}^{22} + \frac{1}{(R_2^2)}R_{22}^{22}\right) \tag{IV.C.21}$$

$$\begin{aligned}\mathcal{CC}_{2,11} = {} & + W_{25}^{10} + \tau_0\left(-\frac{1}{R_1}R_{25}^{10} + \frac{1}{\rho_{11}}R_{26}^{10} + \frac{1}{\rho_{22}}R_{22}^{10} + \frac{1}{R_1\rho_{22}}R_{22}^{11}\right. \\ & \left. - \frac{1}{R_2\rho_{22}}R_{22}^{11} + \frac{1}{R_1}W_{25}^{11}\right) + \tau\left(-\frac{1}{R_1R_2\rho_{22}}R_{22}^{12} + \frac{1}{(R_2^2)\rho_{22}}R_{22}^{12}\right)\end{aligned} \tag{IV.C.22}$$

$$\begin{aligned}\mathcal{CC}_{2,12} = {} & + W_{24}^{20} + \tau_0\left(-\frac{1}{R_2}R_{24}^{20} - \frac{1}{\rho_{11}}R_{12}^{20} - \frac{1}{\rho_{22}}R_{26}^{20} - \frac{1}{R_1R_2}R_{24}^{21}\right. \\ & - \frac{1}{R_1\rho_{22}}R_{26}^{21} + \frac{1}{(R_2^2)}R_{24}^{21} + \frac{1}{R_2\rho_{22}}R_{26}^{21} + \frac{1}{R_1}W_{24}^{21}\Big) + \tau\Big(+\frac{1}{R_1(R_2^2)}R_{24}^{22} \\ & \left. + \frac{1}{R_1R_2\rho_{22}}R_{26}^{22} - \frac{1}{(R_2^3)}R_{24}^{22} - \frac{1}{(R_2^2)\rho_{22}}R_{26}^{22}\right)\end{aligned} \tag{IV.C.23}$$

$$\mathcal{CC}_{3,3} = + A_{66}^{0} + 0.75\frac{1}{(R_1^2)}A_{66}^{2} - 1.5\frac{1}{R_1R_2}A_{66}^{2} + 0.75\frac{1}{(R_2^2)}A_{66}^{2} \tag{IV.C.24}$$

$$\begin{aligned}\mathcal{CC}_{3,4} = {} & + A_{16}^{1} + \tau_0\left(-0.5\frac{1}{R_1}A_{16}^{2} + 0.5\frac{1}{R_2}A_{16}^{2}\right) + \tau\left(+0.75\frac{1}{(R_1^2)}A_{16}^{3} - \frac{1}{R_1R_2}A_{16}^{3}\right. \\ & \left. + 0.25\frac{1}{(R_2^2)}A_{16}^{3}\right)\end{aligned} \tag{IV.C.25}$$

$$\begin{aligned}\mathcal{CC}_{3,5} = {} & + A_{26}^{1} + \tau_0\left(+0.5\frac{1}{R_1}A_{26}^{2} - 0.5\frac{1}{R_2}A_{26}^{2}\right) + \tau\left(+0.25\frac{1}{(R_1^2)}A_{26}^{3} - \frac{1}{R_1R_2}A_{26}^{3}\right. \\ & \left. + 0.75\frac{1}{(R_2^2)}A_{26}^{3}\right)\end{aligned} \tag{IV.C.26}$$

$$\mathcal{CC}_{3,6} = + A_{66}^{1} + 0.5\frac{1}{(R_1^2)}A_{66}^{3} - \frac{1}{R_1R_2}A_{66}^{3} + 0.5\frac{1}{(R_2^2)}A_{66}^{3} \tag{IV.C.27}$$

$$\begin{aligned}\mathcal{CC}_{3,7} = {} & + R_{16}^{10} + \tau_0\left(-0.5\frac{1}{R_1}R_{16}^{11} + 0.5\frac{1}{R_2}R_{16}^{11}\right) + \tau\left(+0.75\frac{1}{(R_1^2)}R_{16}^{12} - \frac{1}{R_1R_2}R_{16}^{12}\right. \\ & \left. + 0.25\frac{1}{(R_2^2)}R_{16}^{12}\right)\end{aligned} \tag{IV.C.28}$$

$$\begin{aligned}\mathcal{CC}_{3,8} = {} & + R_{66}^{20} + \tau_0\left(-0.5\frac{1}{R_1}R_{66}^{21} + 0.5\frac{1}{R_2}R_{66}^{21}\right) + \tau\left(+0.75\frac{1}{(R_1^2)}R_{66}^{22} - \frac{1}{R_1R_2}R_{66}^{22}\right. \\ & \left. + 0.25\frac{1}{(R_2^2)}R_{66}^{22}\right)\end{aligned} \tag{IV.C.29}$$

$$\mathcal{CC}_{3,9} = +\mathrm{R}_{66}^{10} + \tau_0\left(+0.5\frac{1}{\mathrm{R}_1}\mathrm{R}_{66}^{11} - 0.5\frac{1}{\mathrm{R}_2}\mathrm{R}_{66}^{11}\right) + \tau\left(+0.25\frac{1}{(\mathrm{R}_1^2)}\mathrm{R}_{66}^{12} - \frac{1}{\mathrm{R}_1\mathrm{R}_2}\mathrm{R}_{66}^{12} + 0.75\frac{1}{(\mathrm{R}_2^2)}\mathrm{R}_{66}^{12}\right) \tag{IV.C.30}$$

$$\mathcal{CC}_{3,10} = +\mathrm{R}_{26}^{20} + \tau_0\left(+0.5\frac{1}{\mathrm{R}_1}\mathrm{R}_{26}^{21} - 0.5\frac{1}{\mathrm{R}_2}\mathrm{R}_{26}^{21}\right) + \tau\left(+0.25\frac{1}{(\mathrm{R}_1^2)}\mathrm{R}_{26}^{22} - \frac{1}{\mathrm{R}_1\mathrm{R}_2}\mathrm{R}_{26}^{22} + 0.75\frac{1}{(\mathrm{R}_2^2)}\mathrm{R}_{26}^{22}\right) \tag{IV.C.31}$$

$$\begin{aligned}\mathcal{CC}_{3,11} = {} & +\mathrm{W}_{56}^{10} + \tau_0\left(-\frac{1}{\mathrm{R}_1}\mathrm{R}_{56}^{10} + \frac{1}{\rho_{11}}\mathrm{R}_{66}^{10} + \frac{1}{\rho_{22}}\mathrm{R}_{26}^{10} + 0.5\frac{1}{(\mathrm{R}_1^2)}\mathrm{R}_{56}^{11}\right. \\ & - 0.5\frac{1}{\mathrm{R}_1\mathrm{R}_2}\mathrm{R}_{56}^{11} - 0.5\frac{1}{\mathrm{R}_1\rho_{11}}\mathrm{R}_{66}^{11} + 0.5\frac{1}{\mathrm{R}_1\rho_{22}}\mathrm{R}_{26}^{11} + 0.5\frac{1}{\mathrm{R}_2\rho_{11}}\mathrm{R}_{66}^{11} - 0.5\frac{1}{\mathrm{R}_2\rho_{22}}\mathrm{R}_{26}^{11} \\ & \left. + 0.5\frac{1}{\mathrm{R}_1}\mathrm{W}_{56}^{11} + 0.5\frac{1}{\mathrm{R}_2}\mathrm{W}_{56}^{11}\right) + \tau\left(-0.75\frac{1}{(\mathrm{R}_1^3)}\mathrm{R}_{56}^{12} + \frac{1}{(\mathrm{R}_1^2)\mathrm{R}_2}\mathrm{R}_{56}^{12} + 0.75\frac{1}{(\mathrm{R}_1^2)\rho_{11}}\mathrm{R}_{66}^{12}\right. \\ & + 0.25\frac{1}{(\mathrm{R}_1^2)\rho_{22}}\mathrm{R}_{26}^{12} - 0.25\frac{1}{\mathrm{R}_1(\mathrm{R}_2^2)}\mathrm{R}_{56}^{12} - \frac{1}{\mathrm{R}_1\mathrm{R}_2\rho_{11}}\mathrm{R}_{66}^{12} - \frac{1}{\mathrm{R}_1\mathrm{R}_2\rho_{22}}\mathrm{R}_{26}^{12} \\ & \left. + 0.25\frac{1}{(\mathrm{R}_2^2)\rho_{11}}\mathrm{R}_{66}^{12} + 0.75\frac{1}{(\mathrm{R}_2^2)\rho_{22}}\mathrm{R}_{26}^{12} + 0.25\frac{1}{(\mathrm{R}_1^2)}\mathrm{W}_{56}^{12} - 0.5\frac{1}{\mathrm{R}_1\mathrm{R}_2}\mathrm{W}_{56}^{12} + 0.25\frac{1}{(\mathrm{R}_2^2)}\mathrm{W}_{56}^{12}\right)\end{aligned} \tag{IV.C.32}$$

$$\begin{aligned}\mathcal{CC}_{3,12} = {} & +\mathrm{W}_{46}^{20} + \tau_0\left(-\frac{1}{\mathrm{R}_2}\mathrm{R}_{46}^{20} - \frac{1}{\rho_{11}}\mathrm{R}_{16}^{20} - \frac{1}{\rho_{22}}\mathrm{R}_{66}^{20} - 0.5\frac{1}{\mathrm{R}_1\mathrm{R}_2}\mathrm{R}_{46}^{21}\right. \\ & + 0.5\frac{1}{\mathrm{R}_1\rho_{11}}\mathrm{R}_{16}^{21} - 0.5\frac{1}{\mathrm{R}_1\rho_{22}}\mathrm{R}_{66}^{21} + 0.5\frac{1}{(\mathrm{R}_2^2)}\mathrm{R}_{46}^{21} - 0.5\frac{1}{\mathrm{R}_2\rho_{11}}\mathrm{R}_{16}^{21} + 0.5\frac{1}{\mathrm{R}_2\rho_{22}}\mathrm{R}_{66}^{21} \\ & \left. + 0.5\frac{1}{\mathrm{R}_1}\mathrm{W}_{46}^{21} + 0.5\frac{1}{\mathrm{R}_2}\mathrm{W}_{46}^{21}\right) + \tau\left(-0.25\frac{1}{(\mathrm{R}_1^2)\mathrm{R}_2}\mathrm{R}_{46}^{22} - 0.75\frac{1}{(\mathrm{R}_1^2)\rho_{11}}\mathrm{R}_{16}^{22} - 0.25\frac{1}{(\mathrm{R}_1^2)\rho_{22}}\mathrm{R}_{66}^{22}\right. \\ & + \frac{1}{\mathrm{R}_1(\mathrm{R}_2^2)}\mathrm{R}_{46}^{22} + \frac{1}{\mathrm{R}_1\mathrm{R}_2\rho_{11}}\mathrm{R}_{16}^{22} + \frac{1}{\mathrm{R}_1\mathrm{R}_2\rho_{22}}\mathrm{R}_{66}^{22} - 0.75\frac{1}{(\mathrm{R}_2^3)}\mathrm{R}_{46}^{22} \\ & \left. - 0.25\frac{1}{(\mathrm{R}_2^2)\rho_{11}}\mathrm{R}_{16}^{22} - 0.75\frac{1}{(\mathrm{R}_2^2)\rho_{22}}\mathrm{R}_{66}^{22} + 0.25\frac{1}{(\mathrm{R}_1^2)}\mathrm{W}_{46}^{22} - 0.5\frac{1}{\mathrm{R}_1\mathrm{R}_2}\mathrm{W}_{46}^{22} + 0.25\frac{1}{(\mathrm{R}_2^2)}\mathrm{W}_{46}^{22}\right)\end{aligned} \tag{IV.C.33}$$

$$\mathcal{CC}_{4,4} = +\mathrm{A}_{11}^{2} + \tau_0\left(-\frac{1}{\mathrm{R}_1}\mathrm{A}_{11}^{3} + \frac{1}{\mathrm{R}_2}\mathrm{A}_{11}^{3}\right) + \tau\left(+\frac{1}{(\mathrm{R}_1^2)}\mathrm{A}_{11}^{4} - \frac{1}{\mathrm{R}_1\mathrm{R}_2}\mathrm{A}_{11}^{4}\right) \tag{IV.C.34}$$

$$\mathcal{CC}_{4,5} = +\mathrm{A}_{12}^{2} \tag{IV.C.35}$$

$$\mathcal{CC}_{4,6} = +\mathrm{A}_{16}^{2} + \tau_0\left(-0.5\frac{1}{\mathrm{R}_1}\mathrm{A}_{16}^{3} + 0.5\frac{1}{\mathrm{R}_2}\mathrm{A}_{16}^{3}\right) + \tau\left(+0.5\frac{1}{(\mathrm{R}_1^2)}\mathrm{A}_{16}^{4} - 0.5\frac{1}{\mathrm{R}_1\mathrm{R}_2}\mathrm{A}_{16}^{4}\right) \tag{IV.C.36}$$

$$\mathcal{CC}_{4,7} = +\mathrm{R}_{11}^{11} + \tau_0\left(-\frac{1}{\mathrm{R}_1}\mathrm{R}_{11}^{12} + \frac{1}{\mathrm{R}_2}\mathrm{R}_{11}^{12}\right) + \tau\left(+\frac{1}{(\mathrm{R}_1^2)}\mathrm{R}_{11}^{13} - \frac{1}{\mathrm{R}_1\mathrm{R}_2}\mathrm{R}_{11}^{13}\right) \tag{IV.C.37}$$

$$\mathcal{CC}_{4,8} = +\mathrm{R}_{16}^{21} + \tau_0\left(-\frac{1}{\mathrm{R}_1}\mathrm{R}_{16}^{22} + \frac{1}{\mathrm{R}_2}\mathrm{R}_{16}^{22}\right) + \tau\left(+\frac{1}{(\mathrm{R}_1^2)}\mathrm{R}_{16}^{23} - \frac{1}{\mathrm{R}_1\mathrm{R}_2}\mathrm{R}_{16}^{23}\right) \tag{IV.C.38}$$

$$\mathcal{CC}_{4,9} = +\mathrm{R}_{16}^{11} \tag{IV.C.39}$$

$$\mathcal{CC}_{4,10} = +\mathrm{R}_{12}^{21} \tag{IV.C.40}$$

$$\begin{aligned}\mathcal{CC}_{4,11} = {} & +\mathrm{W}_{15}^{11} + \tau_0\left(-\frac{1}{\mathrm{R}_1}\mathrm{R}_{15}^{11} + \frac{1}{\rho_{11}}\mathrm{R}_{16}^{11} + \frac{1}{\rho_{22}}\mathrm{R}_{12}^{11} + \frac{1}{(\mathrm{R}_1^2)}\mathrm{R}_{15}^{12}\right. \\ & \left. - \frac{1}{\mathrm{R}_1\mathrm{R}_2}\mathrm{R}_{15}^{12} - \frac{1}{\mathrm{R}_1\rho_{11}}\mathrm{R}_{16}^{12} + \frac{1}{\mathrm{R}_2\rho_{11}}\mathrm{R}_{16}^{12} + \frac{1}{\mathrm{R}_2}\mathrm{W}_{15}^{12}\right) + \tau\left(-\frac{1}{(\mathrm{R}_1^3)}\mathrm{R}_{15}^{13}\right. \\ & \left. + \frac{1}{(\mathrm{R}_1^2)\mathrm{R}_2}\mathrm{R}_{15}^{13} + \frac{1}{(\mathrm{R}_1^2)\rho_{11}}\mathrm{R}_{16}^{13} - \frac{1}{\mathrm{R}_1\mathrm{R}_2\rho_{11}}\mathrm{R}_{16}^{13}\right)\end{aligned} \tag{IV.C.41}$$

$$\begin{aligned}\mathcal{CC}_{4,12} = {} & +\mathrm{W}_{14}^{21} + \tau_0\left(-\frac{1}{\mathrm{R}_2}\mathrm{R}_{14}^{21} - \frac{1}{\rho_{11}}\mathrm{R}_{11}^{21} - \frac{1}{\rho_{22}}\mathrm{R}_{16}^{21} + \frac{1}{\mathrm{R}_1\rho_{11}}\mathrm{R}_{11}^{22}\right. \\ & \left. - \frac{1}{\mathrm{R}_2\rho_{11}}\mathrm{R}_{11}^{22} + \frac{1}{\mathrm{R}_2}\mathrm{W}_{14}^{22}\right) + \tau\left(-\frac{1}{(\mathrm{R}_1^2)\rho_{11}}\mathrm{R}_{11}^{23} + \frac{1}{\mathrm{R}_1\mathrm{R}_2\rho_{11}}\mathrm{R}_{11}^{23}\right)\end{aligned} \tag{IV.C.42}$$

$$\mathcal{CC}_{5,5} = +\mathrm{A}_{22}^{2} + \tau_0\left(+\frac{1}{\mathrm{R}_1}\mathrm{A}_{22}^{3} - \frac{1}{\mathrm{R}_2}\mathrm{A}_{22}^{3}\right) + \tau\left(-\frac{1}{\mathrm{R}_1\mathrm{R}_2}\mathrm{A}_{22}^{4} + \frac{1}{(\mathrm{R}_2^2)}\mathrm{A}_{22}^{4}\right) \tag{IV.C.43}$$

$$\mathcal{CC}_{5,6} = +\mathrm{A}_{26}^{2} + \tau_0\left(+0.5\frac{1}{\mathrm{R}_1}\mathrm{A}_{26}^{3} - 0.5\frac{1}{\mathrm{R}_2}\mathrm{A}_{26}^{3}\right) + \tau\left(-0.5\frac{1}{\mathrm{R}_1\mathrm{R}_2}\mathrm{A}_{26}^{4} + 0.5\frac{1}{(\mathrm{R}_2^2)}\mathrm{A}_{26}^{4}\right) \tag{IV.C.44}$$

$$\mathcal{CC}_{5,7} = +\mathrm{R}_{12}^{11} \tag{IV.C.45}$$

$$\mathcal{CC}_{5,8} = +\mathrm{R}_{26}^{21} \tag{IV.C.46}$$

$$\mathcal{CC}_{5,9} = +\mathrm{R}_{26}^{11} + \tau_0\left(+\frac{1}{\mathrm{R}_1}\mathrm{R}_{26}^{12} - \frac{1}{\mathrm{R}_2}\mathrm{R}_{26}^{12}\right) + \tau\left(-\frac{1}{\mathrm{R}_1\mathrm{R}_2}\mathrm{R}_{26}^{13} + \frac{1}{(\mathrm{R}_2^2)}\mathrm{R}_{26}^{13}\right) \tag{IV.C.47}$$

$$\mathcal{CC}_{5,10} = +\mathrm{R}_{22}^{21} + \tau_0\left(+\frac{1}{\mathrm{R}_1}\mathrm{R}_{22}^{22} - \frac{1}{\mathrm{R}_2}\mathrm{R}_{22}^{22}\right) + \tau\left(-\frac{1}{\mathrm{R}_1\mathrm{R}_2}\mathrm{R}_{22}^{23} + \frac{1}{(\mathrm{R}_2^2)}\mathrm{R}_{22}^{23}\right) \tag{IV.C.48}$$

$$\begin{aligned}\mathcal{CC}_{5,11} = {} & +\mathrm{W}_{25}^{11} + \tau_0\left(-\frac{1}{\mathrm{R}_1}\mathrm{R}_{25}^{11} + \frac{1}{\rho_{11}}\mathrm{R}_{26}^{11} + \frac{1}{\rho_{22}}\mathrm{R}_{22}^{11} + \frac{1}{\mathrm{R}_1\rho_{22}}\mathrm{R}_{22}^{12}\right. \\ & \left. - \frac{1}{\mathrm{R}_2\rho_{22}}\mathrm{R}_{22}^{12} + \frac{1}{\mathrm{R}_1}\mathrm{W}_{25}^{12}\right) + \tau\left(-\frac{1}{\mathrm{R}_1\mathrm{R}_2\rho_{22}}\mathrm{R}_{22}^{13} + \frac{1}{(\mathrm{R}_2^2)\rho_{22}}\mathrm{R}_{22}^{13}\right)\end{aligned} \tag{IV.C.49}$$

$$\mathcal{CC}_{5,12} = +W_{24}^{21} + \tau_0\left(-\frac{1}{R_2}R_{24}^{21} - \frac{1}{\rho_{11}}R_{12}^{21} - \frac{1}{\rho_{22}}R_{26}^{21} - \frac{1}{R_1R_2}R_{24}^{22} - \frac{1}{R_1\rho_{22}}R_{26}^{22} + \frac{1}{(R_2^2)}R_{24}^{22} + \frac{1}{R_2\rho_{22}}R_{26}^{22} + \frac{1}{R_1}W_{24}^{22}\right) + \tau\left(+\frac{1}{R_1(R_2^2)}R_{24}^{23} + \frac{1}{R_1R_2\rho_{22}}R_{26}^{23} - \frac{1}{(R_2^3)}R_{24}^{23} - \frac{1}{(R_2^2)\rho_{22}}R_{26}^{23}\right) \quad \text{(IV.C.50)}$$

$$\mathcal{CC}_{6,6} = +A_{66}^{2} + 0.25\frac{1}{(R_1^2)}A_{66}^{4} - 0.5\frac{1}{R_1R_2}A_{66}^{4} + 0.25\frac{1}{(R_2^2)}A_{66}^{4} \quad \text{(IV.C.51)}$$

$$\mathcal{CC}_{6,7} = +R_{16}^{11} + \tau_0\left(-0.5\frac{1}{R_1}R_{16}^{12} + 0.5\frac{1}{R_2}R_{16}^{12}\right) + \tau\left(+0.5\frac{1}{(R_1^2)}R_{16}^{13} - 0.5\frac{1}{R_1R_2}R_{16}^{13}\right) \quad \text{(IV.C.52)}$$

$$\mathcal{CC}_{6,8} = +R_{66}^{21} + \tau_0\left(-0.5\frac{1}{R_1}R_{66}^{22} + 0.5\frac{1}{R_2}R_{66}^{22}\right) + \tau\left(+0.5\frac{1}{(R_1^2)}R_{66}^{23} - 0.5\frac{1}{R_1R_2}R_{66}^{23}\right) \quad \text{(IV.C.53)}$$

$$\mathcal{CC}_{6,9} = +R_{66}^{11} + \tau_0\left(+0.5\frac{1}{R_1}R_{66}^{12} - 0.5\frac{1}{R_2}R_{66}^{12}\right) + \tau\left(-0.5\frac{1}{R_1R_2}R_{66}^{13} + 0.5\frac{1}{(R_2^2)}R_{66}^{13}\right) \quad \text{(IV.C.54)}$$

$$\mathcal{CC}_{6,10} = +R_{26}^{21} + \tau_0\left(+0.5\frac{1}{R_1}R_{26}^{22} - 0.5\frac{1}{R_2}R_{26}^{22}\right) + \tau\left(-0.5\frac{1}{R_1R_2}R_{26}^{23} + 0.5\frac{1}{(R_2^2)}R_{26}^{23}\right) \quad \text{(IV.C.55)}$$

$$\mathcal{CC}_{6,11} = +W_{56}^{11} + \tau_0\left(-\frac{1}{R_1}R_{56}^{11} + \frac{1}{\rho_{11}}R_{66}^{11} + \frac{1}{\rho_{22}}R_{26}^{11} + 0.5\frac{1}{(R_1^2)}R_{56}^{12} - 0.5\frac{1}{R_1R_2}R_{56}^{12} - 0.5\frac{1}{R_1\rho_{11}}R_{66}^{12} + 0.5\frac{1}{R_1\rho_{22}}R_{26}^{12} + 0.5\frac{1}{R_2\rho_{11}}R_{66}^{12} - 0.5\frac{1}{R_2\rho_{22}}R_{26}^{12} + 0.5\frac{1}{R_1}W_{56}^{12} + 0.5\frac{1}{R_2}W_{56}^{12}\right) + \tau\left(-0.5\frac{1}{(R_1^3)}R_{56}^{13} + 0.5\frac{1}{(R_1^2)R_2}R_{56}^{13} + 0.5\frac{1}{(R_1^2)\rho_{11}}R_{66}^{13} - 0.5\frac{1}{R_1R_2\rho_{11}}R_{66}^{13} - 0.5\frac{1}{R_1R_2\rho_{22}}R_{26}^{13} + 0.5\frac{1}{(R_2^2)\rho_{22}}R_{26}^{13}\right) \quad \text{(IV.C.56)}$$

$$\mathcal{CC}_{6,12} = +W_{46}^{21} + \tau_0\left(-\frac{1}{R_2}R_{46}^{21} - \frac{1}{\rho_{11}}R_{16}^{21} - \frac{1}{\rho_{22}}R_{66}^{21} - 0.5\frac{1}{R_1R_2}R_{46}^{22} + 0.5\frac{1}{R_1\rho_{11}}R_{16}^{22} - 0.5\frac{1}{R_1\rho_{22}}R_{66}^{22} + 0.5\frac{1}{(R_2^2)}R_{46}^{22} - 0.5\frac{1}{R_2\rho_{11}}R_{16}^{22} + 0.5\frac{1}{R_2\rho_{22}}R_{66}^{22} + 0.5\frac{1}{R_1}W_{46}^{22} + 0.5\frac{1}{R_2}W_{46}^{22}\right) + \tau\left(-0.5\frac{1}{(R_1^2)\rho_{11}}R_{16}^{23} + 0.5\frac{1}{R_1(R_2^2)}R_{46}^{23} + 0.5\frac{1}{R_1R_2\rho_{11}}R_{16}^{23} + 0.5\frac{1}{R_1R_2\rho_{22}}R_{66}^{23} - 0.5\frac{1}{(R_2^3)}R_{46}^{23} - 0.5\frac{1}{(R_2^2)\rho_{22}}R_{66}^{23}\right) \quad \text{(IV.C.57)}$$

$$\mathcal{CC}_{7,7} = +Q_{11}^{110} + \tau_0\left(-\frac{1}{R_1}Q_{11}^{111} + \frac{1}{R_2}Q_{11}^{111}\right) + \tau\left(+\frac{1}{(R_1^2)}Q_{11}^{112} - \frac{1}{R_1R_2}Q_{11}^{112}\right) \quad \text{(IV.C.58)}$$

$$\mathcal{CC}_{7,8} = +\,Q_{16}^{120} + \tau_0\left(-\frac{1}{R_1}Q_{16}^{121} + \frac{1}{R_2}Q_{16}^{121}\right) + \tau\left(+\frac{1}{(R_1^2)}Q_{16}^{122} - \frac{1}{R_1R_2}Q_{16}^{122}\right) \tag{IV.C.59}$$

$$\mathcal{CC}_{7,9} = +\,Q_{16}^{110} \tag{IV.C.60}$$

$$\mathcal{CC}_{7,10} = +\,Q_{12}^{120} \tag{IV.C.61}$$

$$\begin{aligned}\mathcal{CC}_{7,11} = {} & +\,Y_{15}^{110} + \tau_0\left(-\frac{1}{R_1}Q_{15}^{110} + \frac{1}{\rho_{11}}Q_{16}^{110} + \frac{1}{\rho_{22}}Q_{12}^{110} + \frac{1}{(R_1^2)}Q_{15}^{111}\right. \\ & \left. - \frac{1}{R_1R_2}Q_{15}^{111} - \frac{1}{R_1\rho_{11}}Q_{16}^{111} + \frac{1}{R_2\rho_{11}}Q_{16}^{111} + \frac{1}{R_2}Y_{15}^{111}\right) + \tau\left(-\frac{1}{(R_1^3)}Q_{15}^{112}\right. \\ & \left. + \frac{1}{(R_1^2)R_2}Q_{15}^{112} + \frac{1}{(R_1^2)\rho_{11}}Q_{16}^{112} - \frac{1}{R_1R_2\rho_{11}}Q_{16}^{112}\right)\end{aligned} \tag{IV.C.62}$$

$$\begin{aligned}\mathcal{CC}_{7,12} = {} & +\,Y_{14}^{210} + \tau_0\left(-\frac{1}{R_2}Q_{14}^{120} - \frac{1}{\rho_{11}}Q_{11}^{120} - \frac{1}{\rho_{22}}Q_{16}^{120} + \frac{1}{R_1\rho_{11}}Q_{11}^{121}\right. \\ & \left. - \frac{1}{R_2\rho_{11}}Q_{11}^{121} + \frac{1}{R_2}Y_{14}^{211}\right) + \tau\left(-\frac{1}{(R_1^2)\rho_{11}}Q_{11}^{122} + \frac{1}{R_1R_2\rho_{11}}Q_{11}^{122}\right)\end{aligned} \tag{IV.C.63}$$

$$\mathcal{CC}_{8,8} = +\,Q_{66}^{220} + \tau_0\left(-\frac{1}{R_1}Q_{66}^{221} + \frac{1}{R_2}Q_{66}^{221}\right) + \tau\left(+\frac{1}{(R_1^2)}Q_{66}^{222} - \frac{1}{R_1R_2}Q_{66}^{222}\right) \tag{IV.C.64}$$

$$\mathcal{CC}_{8,9} = +\,Q_{66}^{120} \tag{IV.C.65}$$

$$\mathcal{CC}_{8,10} = +\,Q_{26}^{220} \tag{IV.C.66}$$

$$\begin{aligned}\mathcal{CC}_{8,11} = {} & +\,Y_{56}^{120} + \tau_0\left(-\frac{1}{R_1}Q_{56}^{120} + \frac{1}{\rho_{11}}Q_{66}^{120} + \frac{1}{\rho_{22}}Q_{26}^{120} + \frac{1}{(R_1^2)}Q_{56}^{121}\right. \\ & \left. - \frac{1}{R_1R_2}Q_{56}^{121} - \frac{1}{R_1\rho_{11}}Q_{66}^{121} + \frac{1}{R_2\rho_{11}}Q_{66}^{121} + \frac{1}{R_2}Y_{56}^{121}\right) + \tau\left(-\frac{1}{(R_1^3)}Q_{56}^{122}\right. \\ & \left. + \frac{1}{(R_1^2)R_2}Q_{56}^{122} + \frac{1}{(R_1^2)\rho_{11}}Q_{66}^{122} - \frac{1}{R_1R_2\rho_{11}}Q_{66}^{122}\right)\end{aligned} \tag{IV.C.67}$$

$$\begin{aligned}\mathcal{CC}_{8,12} = {} & +\,Y_{46}^{220} + \tau_0\left(-\frac{1}{R_2}Q_{46}^{220} - \frac{1}{\rho_{11}}Q_{16}^{220} - \frac{1}{\rho_{22}}Q_{66}^{220} + \frac{1}{R_1\rho_{11}}Q_{16}^{221}\right. \\ & \left. - \frac{1}{R_2\rho_{11}}Q_{16}^{221} + \frac{1}{R_2}Y_{46}^{221}\right) + \tau\left(-\frac{1}{(R_1^2)\rho_{11}}Q_{16}^{222} + \frac{1}{R_1R_2\rho_{11}}Q_{16}^{222}\right)\end{aligned} \tag{IV.C.68}$$

$$\mathcal{CC}_{9,9} = +\,Q_{66}^{110} + \tau_0\left(+\frac{1}{R_1}Q_{66}^{111} - \frac{1}{R_2}Q_{66}^{111}\right) + \tau\left(-\frac{1}{R_1R_2}Q_{66}^{112} + \frac{1}{(R_2^2)}Q_{66}^{112}\right) \tag{IV.C.69}$$

$$\mathcal{CC}_{9,10} = +\,Q_{26}^{120} + \tau_0\left(+\frac{1}{R_1}Q_{26}^{121} - \frac{1}{R_2}Q_{26}^{121}\right) + \tau\left(-\frac{1}{R_1R_2}Q_{26}^{122} + \frac{1}{(R_2^2)}Q_{26}^{122}\right) \tag{IV.C.70}$$

$$\mathcal{CC}_{9,11} = +\,Y_{56}^{110} + \tau_0\Big(-\frac{1}{R_1}Q_{56}^{110} + \frac{1}{\rho_{11}}Q_{66}^{110} + \frac{1}{\rho_{22}}Q_{26}^{110} + \frac{1}{R_1\rho_{22}}Q_{26}^{111} - \frac{1}{R_2\rho_{22}}Q_{26}^{111} + \frac{1}{R_1}Y_{56}^{111}\Big) + \tau\Big(-\frac{1}{R_1R_2\rho_{22}}Q_{26}^{112} + \frac{1}{(R_2^2)\rho_{22}}Q_{26}^{112}\Big) \tag{IV.C.71}$$

$$\mathcal{CC}_{9,12} = +\,Y_{46}^{210} + \tau_0\Big(-\frac{1}{R_2}Q_{46}^{120} - \frac{1}{\rho_{11}}Q_{16}^{120} - \frac{1}{\rho_{22}}Q_{66}^{120} - \frac{1}{R_1R_2}Q_{46}^{121} - \frac{1}{R_1\rho_{22}}Q_{66}^{121} + \frac{1}{(R_2^2)}Q_{46}^{121} + \frac{1}{R_2\rho_{22}}Q_{66}^{121} + \frac{1}{R_1}Y_{46}^{211}\Big) + \tau\Big(+\frac{1}{R_1(R_2^2)}Q_{46}^{122} + \frac{1}{R_1R_2\rho_{22}}Q_{66}^{122} - \frac{1}{(R_2^3)}Q_{46}^{122} - \frac{1}{(R_2^2)\rho_{22}}Q_{66}^{122}\Big) \tag{IV.C.72}$$

$$\mathcal{CC}_{10,10} = +\,Q_{22}^{220} + \tau_0\Big(+\frac{1}{R_1}Q_{22}^{221} - \frac{1}{R_2}Q_{22}^{221}\Big) + \tau\Big(-\frac{1}{R_1R_2}Q_{22}^{222} + \frac{1}{(R_2^2)}Q_{22}^{222}\Big) \tag{IV.C.73}$$

$$\mathcal{CC}_{10,11} = +\,Y_{25}^{120} + \tau_0\Big(-\frac{1}{R_1}Q_{25}^{120} + \frac{1}{\rho_{11}}Q_{26}^{120} + \frac{1}{\rho_{22}}Q_{22}^{120} + \frac{1}{R_1\rho_{22}}Q_{22}^{121} - \frac{1}{R_2\rho_{22}}Q_{22}^{121} + \frac{1}{R_1}Y_{25}^{121}\Big) + \tau\Big(-\frac{1}{R_1R_2\rho_{22}}Q_{22}^{122} + \frac{1}{(R_2^2)\rho_{22}}Q_{22}^{122}\Big) \tag{IV.C.74}$$

$$\mathcal{CC}_{10,12} = +\,Y_{24}^{220} + \tau_0\Big(-\frac{1}{R_2}Q_{24}^{220} - \frac{1}{\rho_{11}}Q_{12}^{220} - \frac{1}{\rho_{22}}Q_{26}^{220} - \frac{1}{R_1R_2}Q_{24}^{221} - \frac{1}{R_1\rho_{22}}Q_{26}^{221} + \frac{1}{(R_2^2)}Q_{24}^{221} + \frac{1}{R_2\rho_{22}}Q_{26}^{221} + \frac{1}{R_1}Y_{24}^{221}\Big) + \tau\Big(+\frac{1}{R_1(R_2^2)}Q_{24}^{222} + \frac{1}{R_1R_2\rho_{22}}Q_{26}^{222} - \frac{1}{(R_2^3)}Q_{24}^{222} - \frac{1}{(R_2^2)\rho_{22}}Q_{26}^{222}\Big) \tag{IV.C.75}$$

$$\begin{aligned}\mathcal{CC}_{11,11} = {} & +\,Z_{55}^{110} + \tau_0\Big(+\frac{1}{(R_1^2)}Q_{55}^{110} - 2\frac{1}{R_1\rho_{11}}Q_{56}^{110} - 2\frac{1}{R_1\rho_{22}}Q_{25}^{110} + \frac{1}{(\rho_{11}^2)}Q_{66}^{110} \\ & + 2\frac{1}{\rho_{11}\rho_{22}}Q_{26}^{110} + \frac{1}{(\rho_{22}^2)}Q_{22}^{110} - 2\frac{1}{R_1}Y_{55}^{110} + 2\frac{1}{\rho_{11}}Y_{56}^{110} + 2\frac{1}{\rho_{22}}Y_{25}^{110} - \frac{1}{(R_1^3)}Q_{55}^{111} \\ & + \frac{1}{(R_1^2)R_2}Q_{55}^{111} + 2\frac{1}{(R_1^2)\rho_{11}}Q_{56}^{111} - 2\frac{1}{R_1R_2\rho_{11}}Q_{56}^{111} - \frac{1}{R_1(\rho_{11}^2)}Q_{66}^{111} \\ & + \frac{1}{R_1(\rho_{22}^2)}Q_{22}^{111} + \frac{1}{R_2(\rho_{11}^2)}Q_{66}^{111} - \frac{1}{R_2(\rho_{22}^2)}Q_{22}^{111} - 2\frac{1}{R_1R_2}Y_{55}^{111} + 2\frac{1}{R_1\rho_{22}}Y_{25}^{111} \\ & + 2\frac{1}{R_2\rho_{11}}Y_{56}^{111} + \frac{1}{R_1}Z_{55}^{111} + \frac{1}{R_2}Z_{55}^{111}\Big) + \tau\Big(+\frac{1}{(R_1^4)}Q_{55}^{112} - \frac{1}{(R_1^3)R_2}Q_{55}^{112} \\ & - 2\frac{1}{(R_1^3)\rho_{11}}Q_{56}^{112} + 2\frac{1}{(R_1^2)R_2\rho_{11}}Q_{56}^{112} + \frac{1}{(R_1^2)(\rho_{11}^2)}Q_{66}^{112} - \frac{1}{R_1R_2(\rho_{11}^2)}Q_{66}^{112} \\ & - \frac{1}{R_1R_2(\rho_{22}^2)}Q_{22}^{112} + \frac{1}{(R_2^2)(\rho_{22}^2)}Q_{22}^{112} + \frac{1}{R_1R_2}Z_{55}^{112}\Big)\end{aligned} \tag{IV.C.76}$$

$$\begin{aligned}\mathcal{CC}_{11,12} = &+ Z_{45}^{120} + \tau_0\Big(+\frac{1}{R_1R_2}Q_{45}^{120} + \frac{1}{R_1\rho_{11}}Q_{15}^{120} + \frac{1}{R_1\rho_{22}}Q_{56}^{120}\\
&- \frac{1}{R_2\rho_{11}}Q_{46}^{120} - \frac{1}{R_2\rho_{22}}Q_{24}^{120} - \frac{1}{(\rho_{11}^2)}Q_{16}^{120} - \frac{1}{\rho_{11}\rho_{22}}Q_{12}^{120} - \frac{1}{\rho_{11}\rho_{22}}Q_{66}^{120}\\
&- \frac{1}{(\rho_{22}^2)}Q_{26}^{120} - \frac{1}{R_1}Y_{45}^{210} + \frac{1}{\rho_{11}}Y_{46}^{210} + \frac{1}{\rho_{22}}Y_{24}^{210} - \frac{1}{R_2}Y_{45}^{120} - \frac{1}{\rho_{11}}Y_{15}^{120}\\
&- \frac{1}{\rho_{22}}Y_{56}^{120} - \frac{1}{(R_1^2)\rho_{11}}Q_{15}^{121} + \frac{1}{R_1R_2\rho_{11}}Q_{15}^{121} - \frac{1}{R_1R_2\rho_{22}}Q_{24}^{121}\\
&+ \frac{1}{R_1(\rho_{11}^2)}Q_{16}^{121} - \frac{1}{R_1(\rho_{22}^2)}Q_{26}^{121} + \frac{1}{(R_2^2)\rho_{22}}Q_{24}^{121} - \frac{1}{R_2(\rho_{11}^2)}Q_{16}^{121} + \frac{1}{R_2(\rho_{22}^2)}Q_{26}^{121}\\
&- \frac{1}{R_1R_2}Y_{45}^{211} + \frac{1}{R_1\rho_{22}}Y_{24}^{211} + \frac{1}{R_2\rho_{11}}Y_{46}^{211} - \frac{1}{R_1R_2}Y_{45}^{121} - \frac{1}{R_1\rho_{22}}Y_{56}^{121}\\
&- \frac{1}{R_2\rho_{11}}Y_{15}^{121} + \frac{1}{R_1}Z_{45}^{121} + \frac{1}{R_2}Z_{45}^{121}\Big) + \tau\Big(+\frac{1}{(R_1^3)\rho_{11}}Q_{15}^{122} - \frac{1}{(R_1^2)R_2\rho_{11}}Q_{15}^{122}\\
&- \frac{1}{(R_1^2)(\rho_{11}^2)}Q_{16}^{122} + \frac{1}{R_1(R_2^2)\rho_{22}}Q_{24}^{122} + \frac{1}{R_1R_2(\rho_{11}^2)}Q_{16}^{122} + \frac{1}{R_1R_2(\rho_{22}^2)}Q_{26}^{122}\\
&- \frac{1}{(R_2^3)\rho_{22}}Q_{24}^{122} - \frac{1}{(R_2^2)(\rho_{22}^2)}Q_{26}^{122} + \frac{1}{R_1R_2}Z_{45}^{122}\Big)\end{aligned} \tag{IV.C.77}$$

$$\begin{aligned}\mathcal{CC}_{12,12} = &+ Z_{44}^{220} + \tau_0\Big(+\frac{1}{(R_2^2)}Q_{44}^{220} + 2\frac{1}{R_2\rho_{11}}Q_{14}^{220} + 2\frac{1}{R_2\rho_{22}}Q_{46}^{220} + \frac{1}{(\rho_{11}^2)}Q_{11}^{220}\\
&+ 2\frac{1}{\rho_{11}\rho_{22}}Q_{16}^{220} + \frac{1}{(\rho_{22}^2)}Q_{66}^{220} - 2\frac{1}{R_2}Y_{44}^{220} - 2\frac{1}{\rho_{11}}Y_{14}^{220} - 2\frac{1}{\rho_{22}}Y_{46}^{220} + \frac{1}{R_1(R_2^2)}Q_{44}^{221}\\
&+ 2\frac{1}{R_1R_2\rho_{22}}Q_{46}^{221} - \frac{1}{R_1(\rho_{11}^2)}Q_{11}^{221} + \frac{1}{R_1(\rho_{22}^2)}Q_{66}^{221} - \frac{1}{(R_2^3)}Q_{44}^{221} - 2\frac{1}{(R_2^2)\rho_{22}}Q_{46}^{221}\\
&+ \frac{1}{R_2(\rho_{11}^2)}Q_{11}^{221} - \frac{1}{R_2(\rho_{22}^2)}Q_{66}^{221} - 2\frac{1}{R_1R_2}Y_{44}^{221} - 2\frac{1}{R_1\rho_{22}}Y_{46}^{221} - 2\frac{1}{R_2\rho_{11}}Y_{14}^{221}\\
&+ \frac{1}{R_1}Z_{44}^{221} + \frac{1}{R_2}Z_{44}^{221}\Big) + \tau\Big(+\frac{1}{(R_1^2)(\rho_{11}^2)}Q_{11}^{222} - \frac{1}{R_1(R_2^3)}Q_{44}^{222}\\
&- 2\frac{1}{R_1(R_2^2)\rho_{22}}Q_{46}^{222} - \frac{1}{R_1R_2(\rho_{11}^2)}Q_{11}^{222} - \frac{1}{R_1R_2(\rho_{22}^2)}Q_{66}^{222} + \frac{1}{(R_2^4)}Q_{44}^{222}\\
&+ 2\frac{1}{(R_2^3)\rho_{22}}Q_{46}^{222} + \frac{1}{(R_2^2)(\rho_{22}^2)}Q_{66}^{222} + \frac{1}{R_1R_2}Z_{44}^{222}\Big)\end{aligned} \tag{IV.C.78}$$

.4 Appendix IV.D Through-the-thickness Elasticity Coefficient Integrals

.4.1 Compliance Tensor

The through-the-thickness integrals of the compliance tensor are defined as follows ($F' = dF/d\xi_3$):

$$A^k_{pq} = \int_{-\frac{h}{2}}^{+\frac{h}{2}} \bar{Q}_{pq} (\xi_3)^k \, d\xi_3 \tag{IV.D.1a}$$

$$R^{jk}_{pq} = \int_{-\frac{h}{2}}^{+\frac{h}{2}} \bar{Q}_{pq} (\xi_3)^k F_j d\xi_3 \tag{IV.D.1b}$$

$$Q^{ijk}_{pq} = \int_{-\frac{h}{2}}^{+\frac{h}{2}} \bar{Q}_{pq} (\xi_3)^k F_i F_j d\xi_3 \tag{IV.D.1c}$$

$$W^{jk}_{pq} = \int_{-\frac{h}{2}}^{+\frac{h}{2}} \bar{Q}_{pq} (\xi_3)^k F'_j d\xi_3 \tag{IV.D.1d}$$

$$Y^{ijk}_{pq} = \int_{-\frac{h}{2}}^{+\frac{h}{2}} \bar{Q}_{pq} (\xi_3)^k F'_i F_j d\xi_3 \tag{IV.D.1e}$$

$$Z^{ijk}_{pq} = \int_{-\frac{h}{2}}^{+\frac{h}{2}} \bar{Q}_{pq} (\xi_3)^k F'_i F'_j d\xi_3 \tag{IV.D.1f}$$

If shell consists of N_{LYRS} layers, each with a constant thickness such as t_l, that each one presents constant properties through the thickness of the shell element ($\bar{Q}_{pq,l} = cte$), integrals of equation (IV.D.1) can be replaced with summations. The A^k_{pq} for zero and first order shear deformation model is the same. For zero order shear deformation (when $F_i = F_j = 0$), $R^{jk}_{pq} = Q^{ijk}_{pq} = W^{jk}_{pq} = Y^{ijk}_{pq} = Z^{ijk}_{pq} = 0$. For first order shear deformation model (when $F_i = F_j = \xi_3$), the through-the-thickness integrals can be obtained from the following summations:

$$A^k_{pq} = \sum_{l=1}^{N_{LYRS}} \left(I^{A,k}() - I^{A,k}() \right) \bar{Q}_{pq,l}; \quad I^{A,k}(\xi_3) = \frac{\xi_3^{k+1}}{k+1} \tag{IV.D.2a}$$

$$R^{jk}_{pq} = \sum_{l=1}^{N_{LYRS}} \left(I^{R,k}() - I^{R,k}() \right) \bar{Q}_{pq,l}; \quad I^{R,k}(\xi_3) = \frac{\xi_3^{k+2}}{k+2} \tag{IV.D.2b}$$

$$Q_{pq}^{ijk} = \sum_{l=1}^{N_{LYRS}} \left(I^{Q,k}() - I^{Q,k}()\right)\bar{Q}_{pq,l}; \quad I^{Q,k}(\xi_3) = \frac{\xi_3^{k+3}}{k+3} \tag{IV.D.2c}$$

$$W_{pq}^{k} = \sum_{l=1}^{N_{LYRS}} \left(I^{W,k}() - I^{W,k}()\right)\bar{Q}_{pq,l}; \quad I^{Q,k}(\xi_3) = \frac{\xi_3^{k+1}}{k+1} \tag{IV.D.2d}$$

$$Y_{pq}^{k} = \sum_{l=1}^{N_{LYRS}} \left(I^{Y,k}() - I^{Y,k}()\right)\bar{Q}_{pq,l}; \quad I^{Y,k}(\xi_3) = \frac{\xi_3^{k+2}}{k+2} \tag{IV.D.2e}$$

$$Z_{pq}^{k} = \sum_{l=1}^{N_{LYRS}} \left(I^{Z,k}() - I^{Z,k}()\right)\bar{Q}_{pq,l}; \quad I^{Z,k}(\xi_3) = \frac{\xi_3^{k+1}}{k+1} \tag{IV.D.2f}$$

where:

$$= + \sum_{m=1}^{l} (t_m) \tag{IV.D.3a}$$

$$= -\frac{1}{2} \sum_{m=1}^{N_{LYRS}} (t_m) \tag{IV.D.3b}$$

When a constant thickness lamina is replaced with its equivalent linearly-variable thickness layer that presents the same thickness at a location such as x =, the coordinates-free through-the-thickness coefficients can be obtained from the following equation:

$$\begin{aligned} \bar{A}_{pq}^{k} &= ^{-(k+1)} A_{pq}^{k}; \quad \bar{R}_{pq}^{k} = ^{-(k+2)} R_{pq}^{k}; \quad \bar{Q}_{pq}^{k} = ^{-(k+3)} Q_{pq}^{k}; \\ \bar{W}_{pq}^{k} &= ^{-(k+1)} W_{pq}^{k}; \quad \bar{Y}_{pq}^{k} = ^{-(k+2)} Y_{pq}^{k}; \quad \bar{Z}_{pq}^{k} = ^{-(k+1)} Z_{pq}^{k}; \end{aligned} \tag{IV.D.4}$$

.4.2 Density

Assuming the volumetric density of the shell through the thickness is defined as $\rho(\xi_3)$ function, the areal densities are defined as follows:

$$\rho^{k} = \int_{-\frac{h}{2}}^{+\frac{h}{2}} [\rho(\xi_3)](\xi_3)^{k} \left(1 + \frac{\xi_3}{R_1}\right)\left(1 + \frac{\xi_3}{R_2}\right) d\xi_3 \quad (k = 0, 1, 2) \tag{IV.D.5}$$

Similar to the previous section, if the shell consists of N_{LYRS} layers, each with a constant thickness such as t_l, that each one presents a constant density through the thickness of the shell element ($\rho_l = cte$), above integrals converts to the following summations:

$$\rho^k = \rho_0^k + \tau_0 \rho_{\tau_0}^k + \tau_0 \tau \rho_\tau^k \tag{IV.D.6}$$

where:

$$\rho_0^k = \sum_{l=1}^{N_{LYRS}} \left(I^{A,k}() - I^{A,k}() \right) \rho_l \tag{IV.D.7a}$$

$$\rho_{\tau_0}^k = \left(\frac{1}{R_1} + \frac{1}{R_2} \right) \sum_{l=1}^{N_{LYRS}} \left(I^{A,k+1}() - I^{A,k+1}() \right) \rho_l \tag{IV.D.7b}$$

$$\rho_\tau^k = \left(\frac{1}{R_1 R_2} \right) \sum_{l=1}^{N_{LYRS}} \left(I^{A,k+2}() - I^{A,k+2}() \right) \rho_l \tag{IV.D.7c}$$

The definition of is as same as what has been given in equation (IV.D.3), the definition of $I^{A,k}(\xi_3)$ is same as (IV.D.2a) and $\tau_0, \tau \in \{0, 1\}$ are flag parameters to neglect or to consider the effects of principle radii of curvature at zero, one and third order.

When a constant thickness lamina is replaced with its equivalent linearly-variable thickness layer that presents the same thickness at a location such as x =, the areal densities demonstrate dependency to x coordinates and can be obtained from the following equation:

$$\rho^k = \left({}^{-(k+1)} \right) \left[\rho_{c,0}^k \right] \left(x^{k+1} \right) + \tau_0 \left({}^{-(k+2)} \right) \left[\rho_{c,\tau_0}^k \right] \left(x^{k+2} \right) + \tau_0 \tau \left({}^{-(k+3)} \right) \left[\rho_{c,\tau}^k \right] \left(x^{k+3} \right) \tag{IV.D.8}$$

where ρ_c^k is the calculated areal density for the original constant thickness shell using equation (IV.D.6).

.5 Properties of The Solution Basis Function

The following operators and differentiations has the closed-form result over the functions space defined by $\mathbb{S}$:

$$\forall r \in \mathbb{R}: \quad r = H(0, 0.5r, 0, 0) \in \mathbb{S} \tag{IV.E.1a}$$

$$\forall r \in \mathbb{R}, \quad \forall H \in \mathbb{S}: \quad r * H = H(\beta, r * c, se, ce) \in \mathbb{S} \tag{IV.E.1b}$$

$$\forall H_1, H_2 \in \mathbb{S}: \quad H(\beta_1, c_1, se_1, ce_1) + H(\beta_2, c_2, se_2, ce_2) \in \mathbb{S} \tag{IV.E.1c}$$

$$\begin{aligned} &\forall H_1, H_2 \in \mathbb{S}: \quad H(\beta_1, c_1, se_1, ce_1) * H(\beta_2, c_2, se_2, ce_2) = \\ &H(\beta_1\beta_2, c_1c_2, se_1 + se_2, ce_1 + ce_2) + H(\beta_1{\beta_2}^*, c_1{c_2}^*, se_1 + se_2, ce_1 + ce_2) \in \mathbb{S} \end{aligned} \tag{IV.E.1d}$$

$$\forall H \in \mathbb{S}(\beta \neq 0): \quad \frac{\partial}{\partial \mathrm{x}} H(\beta, c, se, ce) = H(\beta - 1, c * \beta/L, se, ce) \in \mathbb{S} \tag{IV.E.1e}$$

$$\begin{aligned} &\forall H \in \mathbb{S}(se \neq 0, \quad ce \neq 0): \quad \frac{\partial}{\partial \theta} H(\beta, c, se, ce) = \\ &H(\beta, n_c * c, se - 1, ce + 1) + H(\beta, -n_c * c, se + 1, ce - 1) \in \mathbb{S} \end{aligned} \tag{IV.E.1f}$$

Moreover, the "One" and "Zero" constants for multiplication and addition over this function space are $H(0, 1.0, 0, 0)$ and $H(0, 0, 0, 0)$ accordingly. It is also worth mentioning that multiplication of a complex number to a basis function of this type is not a member of this space ($\exists \quad z \in \mathbb{C} \Rightarrow z * H \notin \mathbb{S}$). Using the definition of "One" it is possible to define any real constant (such as elements of $\left[\mathcal{C}\bar{\mathcal{C}}^{\mathbf{0}}\right]$ matrix) as a member of $\mathbb{S}$ function space. The metrics, principle and geodesic radii of the curvature of conical shells can also be defined

in form of the basis function:

$$\begin{aligned}
&H_{\mathrm{A}_1} \triangleq \mathrm{A}_1(\mathrm{x},\theta) = H(0,0.5,0,0), \quad H_{\mathrm{A}_2} \triangleq \mathrm{A}_2(\mathrm{x},\theta) = H(1,0.5L\sin(\alpha_c),0,0),\\
&H_{1/\mathrm{A}_1} \triangleq \tfrac{1}{\mathrm{A}_1(\mathrm{x},\theta)} = H(0,0.5,0,0), \quad H_{1/\mathrm{A}_2} \triangleq \tfrac{1}{\mathrm{A}_2(\mathrm{x},\theta)} = H(-1,0.5/(L\sin(\alpha_c)),0,0),\\
&H_{1/\mathrm{R}_1} \triangleq \tfrac{1}{\mathrm{R}_1(\mathrm{x},\theta)} = H(0,0,0,0), \quad H_{1/\mathrm{R}_2} \triangleq \tfrac{1}{\mathrm{R}_2(\mathrm{x},\theta)} = H(-1,0.5/(L\tan(\alpha_c)),0,0),\\
&H_{1/\rho_{11}} \triangleq \tfrac{1}{\rho_{11}} = H(0,0,0,0), \quad H_{1/\rho_{22}} \triangleq \tfrac{1}{\rho_{22}} = H(-1,0.5/L,0,0)
\end{aligned} \tag{IV.E.2}$$

Moreover by assuming:

$$\beta_R = \Re\mathfrak{e}(\beta) \qquad \beta_I = \Im\mathfrak{m}(\beta) \quad c_R = \Re\mathfrak{e}(c) \qquad c_I = \Im\mathfrak{m}(c) \qquad y = \ln\left(\tfrac{\mathrm{x}}{L}\right) \tag{IV.E.3}$$

Evaluation at a point results:

$$H(\beta,c,se,ce)\Big|_{\mathrm{x},\theta} = 2.0\left(\frac{\mathrm{x}}{L}\right)^{\beta_R}\left[c_R\cos(\beta_I y) - c_I\sin(\beta_I y)\right](\sin(nc\theta))^{se}(\cos(nc\theta))^{ce} \quad (\in \mathbb{R}) \tag{IV.E.4}$$

Finite integral over x is given by:

$$\int H(\beta,c,0,0) = H(\beta+1,cL/(\beta+1),0,0)\Big| - H(\beta+1,cL/(\beta+1),0,0)\Big| \quad (\in \mathbb{R}) \tag{IV.E.5}$$

The surface element of a truncated conical surface is defined as:

$$d\Omega = \mathrm{A}_1\mathrm{A}_2 d\mathrm{x} d\theta = 1 \times \sin(\alpha_c)\mathrm{x} d\mathrm{x} d\theta = H(1,0.5L\sin(\alpha_c)) d\mathrm{x} d\theta \tag{IV.E.6}$$

The integration over a truncated conical shell elements defined over a domain such as $\Omega = (..,0..2\pi)$, can be obtained from:

$$\begin{aligned}
\iint_\Omega H(\beta,c,se,ce)d\Omega = &\left(H(\beta+2,0.5*cL^2\sin(\alpha_c)/(\beta+2),0,0)\Big|\right)\\
&\times\left(\int_0^{2\pi}\sin(n_c\theta)^{se}\cos(n_c\theta)^{ce}\right)d\theta
\end{aligned} \tag{IV.E.7}$$

Due to small set of possible values for *se* and *ce*, the second term of the right hand side of equation (IV.E.7) can be calculated using a small look up table. For the most occurring cases of $(se=0,ce=2)$ and $(se=2,ce=0)$ that term is given by:

.6 Appendix IV.E Constitutive Matrix for Variable Thickness Conical Shells

The upper-right elements of $\left[\bar{\mathcal{C}}\bar{\mathcal{C}}^{\mathbf{0}}\right]$ symmetric matrix multiplied by the associated x exponent on the left hand side, can be obtained as follows:

$$x^{-1}\bar{\mathcal{C}}_{1,1} = +\bar{A}_{11}^{0} + \tau_0\left[+\bar{A}_{11}^{1}\frac{1}{tn}\right] \tag{IV.F.1}$$

$$x^{-1}\bar{\mathcal{C}}_{1,2} = +\bar{A}_{12}^{0} \tag{IV.F.2}$$

$$x^{-1}\bar{\mathcal{C}}_{1,3} = +\bar{A}_{16}^{0} + \tau_0\left[+0.5\bar{A}_{16}^{1}\frac{1}{tn}\right] + \tau\left[+0.25\bar{A}_{16}^{2}\frac{1}{(tn^2)}\right] \tag{IV.F.3}$$

$$x^{-2}\bar{\mathcal{C}}_{1,4} = +\bar{A}_{11}^{1} + \tau_0\left[+\bar{A}_{11}^{2}\frac{1}{tn}\right] \tag{IV.F.4}$$

$$x^{-2}\bar{\mathcal{C}}_{1,5} = +\bar{A}_{12}^{1} \tag{IV.F.5}$$

$$x^{-2}\bar{\mathcal{C}}_{1,6} = +\bar{A}_{16}^{1} + \tau_0\left[+0.5\bar{A}_{16}^{2}\frac{1}{tn}\right] \tag{IV.F.6}$$

$$x^{-2}\bar{\mathcal{C}}_{1,7} = +\bar{R}_{11}^{10} + \tau_0\left[+\bar{R}_{11}^{11}\frac{1}{tn}\right] \tag{IV.F.7}$$

$$\mathrm{x}^{-2}\mathcal{C}\bar{\mathcal{C}}_{1,8} = +\bar{\mathrm{R}}_{16}^{20} + \tau_0\left[+\bar{\mathrm{R}}_{16}^{21}\frac{1}{tn}\right] \tag{IV.F.8}$$

$$\mathrm{x}^{-2}\mathcal{C}\bar{\mathcal{C}}_{1,9} = +\bar{\mathrm{R}}_{16}^{10} \tag{IV.F.9}$$

$$\mathrm{x}^{-2}\mathcal{C}\bar{\mathcal{C}}_{1,10} = +\bar{\mathrm{R}}_{12}^{20} \tag{IV.F.10}$$

$$\mathrm{x}^{-1}\mathcal{C}\bar{\mathcal{C}}_{1,11} = +\bar{\mathrm{W}}_{15}^{10} + \tau_0\left[+\bar{\mathrm{R}}_{12}^{10} + \bar{\mathrm{W}}_{15}^{11}\frac{1}{tn}\right] \tag{IV.F.11}$$

$$\mathrm{x}^{-1}\mathcal{C}\bar{\mathcal{C}}_{1,12} = +\bar{\mathrm{W}}_{14}^{20} + \tau_0\left[-\bar{\mathrm{R}}_{14}^{20}\frac{1}{tn} - \bar{\mathrm{R}}_{16}^{20} + \bar{\mathrm{W}}_{14}^{21}\frac{1}{tn}\right] \tag{IV.F.12}$$

$$\mathrm{x}^{-1}\mathcal{C}\bar{\mathcal{C}}_{2,2} = +\bar{\mathrm{A}}_{22}^{0} + \tau_0\left[-\bar{\mathrm{A}}_{22}^{1}\frac{1}{tn}\right] + \tau\left[+\bar{\mathrm{A}}_{22}^{2}\frac{1}{(tn^2)}\right] \tag{IV.F.13}$$

$$\mathrm{x}^{-1}\mathcal{C}\bar{\mathcal{C}}_{2,3} = +\bar{\mathrm{A}}_{26}^{0} + \tau_0\left[-0.5\bar{\mathrm{A}}_{26}^{1}\frac{1}{tn}\right] + \tau\left[+0.75\bar{\mathrm{A}}_{26}^{2}\frac{1}{(tn^2)}\right] \tag{IV.F.14}$$

$$\mathrm{x}^{-2}\mathcal{C}\bar{\mathcal{C}}_{2,4} = +\bar{\mathrm{A}}_{12}^{1} \tag{IV.F.15}$$

$$x^{-2}\mathcal{C}\bar{\mathcal{C}}_{2,5} = +\bar{A}^{1}_{22} + \tau_0\left[-\bar{A}^{2}_{22}\frac{1}{tn}\right] + \tau\left[+\bar{A}^{3}_{22}\frac{1}{(tn^2)}\right] \tag{IV.F.16}$$

$$x^{-2}\mathcal{C}\bar{\mathcal{C}}_{2,6} = +\bar{A}^{1}_{26} + \tau_0\left[-0.5\bar{A}^{2}_{26}\frac{1}{tn}\right] + \tau\left[+0.5\bar{A}^{3}_{26}\frac{1}{(tn^2)}\right] \tag{IV.F.17}$$

$$x^{-2}\mathcal{C}\bar{\mathcal{C}}_{2,7} = +\bar{R}^{10}_{12} \tag{IV.F.18}$$

$$x^{-2}\mathcal{C}\bar{\mathcal{C}}_{2,8} = +\bar{R}^{20}_{26} \tag{IV.F.19}$$

$$x^{-2}\mathcal{C}\bar{\mathcal{C}}_{2,9} = +\bar{R}^{10}_{26} + \tau_0\left[-\bar{R}^{11}_{26}\frac{1}{tn}\right] + \tau\left[+\bar{R}^{12}_{26}\frac{1}{(tn^2)}\right] \tag{IV.F.20}$$

$$x^{-2}\mathcal{C}\bar{\mathcal{C}}_{2,10} = +\bar{R}^{20}_{22} + \tau_0\left[-\bar{R}^{21}_{22}\frac{1}{tn}\right] + \tau\left[+\bar{R}^{22}_{22}\frac{1}{(tn^2)}\right] \tag{IV.F.21}$$

$$x^{-1}\mathcal{C}\bar{\mathcal{C}}_{2,11} = +\bar{W}^{10}_{25} + \tau_0\left[+\bar{R}^{10}_{22} - \bar{R}^{11}_{22}\frac{1}{tn}\right] + \tau\left[+\bar{R}^{12}_{22}\frac{1}{(tn^2)}\right] \tag{IV.F.22}$$

$$\begin{aligned} x^{-1}\mathcal{C}\bar{\mathcal{C}}_{2,12} = +\bar{W}^{20}_{24} + \tau_0\Bigg[-\bar{R}^{20}_{24}\frac{1}{tn} - \bar{R}^{20}_{26} + \bar{R}^{21}_{24}\frac{1}{(tn^2)} + \bar{R}^{21}_{26}\frac{1}{tn}\Bigg] + \tau\Bigg[\\ -\bar{R}^{22}_{24}\frac{1}{(tn^3)} - \bar{R}^{22}_{26}\frac{1}{(tn^2)}\Bigg] \end{aligned} \tag{IV.F.23}$$

$$\mathrm{x}^{-1}\bar{\mathcal{C}}_{3,3} = +\bar{\mathrm{A}}^{0}_{66} + 0.75\bar{\mathrm{A}}^{2}_{66}\frac{1}{(tn^2)} \tag{IV.F.24}$$

$$\mathrm{x}^{-2}\bar{\mathcal{C}}_{3,4} = +\bar{\mathrm{A}}^{1}_{16} + \tau_0\left[+0.5\bar{\mathrm{A}}^{2}_{16}\frac{1}{tn}\right] + \tau\left[+0.25\bar{\mathrm{A}}^{3}_{16}\frac{1}{(tn^2)}\right] \tag{IV.F.25}$$

$$\mathrm{x}^{-2}\bar{\mathcal{C}}_{3,5} = +\bar{\mathrm{A}}^{1}_{26} + \tau_0\left[-0.5\bar{\mathrm{A}}^{2}_{26}\frac{1}{tn}\right] + \tau\left[+0.75\bar{\mathrm{A}}^{3}_{26}\frac{1}{(tn^2)}\right] \tag{IV.F.26}$$

$$\mathrm{x}^{-2}\bar{\mathcal{C}}_{3,6} = +\bar{\mathrm{A}}^{1}_{66} + 0.5\bar{\mathrm{A}}^{3}_{66}\frac{1}{(tn^2)} \tag{IV.F.27}$$

$$\mathrm{x}^{-2}\bar{\mathcal{C}}_{3,7} = +\bar{\mathrm{R}}^{10}_{16} + \tau_0\left[+0.5\bar{\mathrm{R}}^{11}_{16}\frac{1}{tn}\right] + \tau\left[+0.25\bar{\mathrm{R}}^{12}_{16}\frac{1}{(tn^2)}\right] \tag{IV.F.28}$$

$$\mathrm{x}^{-2}\bar{\mathcal{C}}_{3,8} = +\bar{\mathrm{R}}^{20}_{66} + \tau_0\left[+0.5\bar{\mathrm{R}}^{21}_{66}\frac{1}{tn}\right] + \tau\left[+0.25\bar{\mathrm{R}}^{22}_{66}\frac{1}{(tn^2)}\right] \tag{IV.F.29}$$

$$\mathrm{x}^{-2}\bar{\mathcal{C}}_{3,9} = +\bar{\mathrm{R}}^{10}_{66} + \tau_0\left[-0.5\bar{\mathrm{R}}^{11}_{66}\frac{1}{tn}\right] + \tau\left[+0.75\bar{\mathrm{R}}^{12}_{66}\frac{1}{(tn^2)}\right] \tag{IV.F.30}$$

$$\mathrm{x}^{-2}\bar{\mathcal{C}}_{3,10} = +\bar{\mathrm{R}}^{20}_{26} + \tau_0\left[-0.5\bar{\mathrm{R}}^{21}_{26}\frac{1}{tn}\right] + \tau\left[+0.75\bar{\mathrm{R}}^{22}_{26}\frac{1}{(tn^2)}\right] \tag{IV.F.31}$$

$$\mathrm{x}^{-1}\mathcal{C}\bar{\mathcal{C}}_{3,11} = +\bar{\mathrm{W}}_{56}^{10} + \tau_0\left[+\bar{\mathrm{R}}_{26}^{10} - 0.5\bar{\mathrm{R}}_{26}^{11}\frac{1}{tn} + 0.5\bar{\mathrm{W}}_{56}^{11}\frac{1}{tn}\right] + \tau\left[+0.75\bar{\mathrm{R}}_{26}^{12}\frac{1}{(tn^2)} + 0.25\bar{\mathrm{W}}_{56}^{12}\frac{1}{(tn^2)}\right] \tag{IV.F.32}$$

$$\mathrm{x}^{-1}\mathcal{C}\bar{\mathcal{C}}_{3,12} = +\bar{\mathrm{W}}_{46}^{20} + \tau_0\left[-\bar{\mathrm{R}}_{46}^{20}\frac{1}{tn} - \bar{\mathrm{R}}_{66}^{20} + 0.5\bar{\mathrm{R}}_{46}^{21}\frac{1}{(tn^2)} + 0.5\bar{\mathrm{R}}_{66}^{21}\frac{1}{tn} + 0.5\bar{\mathrm{W}}_{46}^{21}\frac{1}{tn}\right] + \tau\left[-0.75\bar{\mathrm{R}}_{46}^{22}\frac{1}{(tn^3)} - 0.75\bar{\mathrm{R}}_{66}^{22}\frac{1}{(tn^2)} + 0.25\bar{\mathrm{W}}_{46}^{22}\frac{1}{(tn^2)}\right] \tag{IV.F.33}$$

$$\mathrm{x}^{-3}\mathcal{C}\bar{\mathcal{C}}_{4,4} = +\bar{\mathrm{A}}_{11}^{2} + \tau_0\left[+\bar{\mathrm{A}}_{11}^{3}\frac{1}{tn}\right] \tag{IV.F.34}$$

$$\mathrm{x}^{-3}\mathcal{C}\bar{\mathcal{C}}_{4,5} = +\bar{\mathrm{A}}_{12}^{2} \tag{IV.F.35}$$

$$\mathrm{x}^{-3}\mathcal{C}\bar{\mathcal{C}}_{4,6} = +\bar{\mathrm{A}}_{16}^{2} + \tau_0\left[+0.5\bar{\mathrm{A}}_{16}^{3}\frac{1}{tn}\right] \tag{IV.F.36}$$

$$\mathrm{x}^{-3}\mathcal{C}\bar{\mathcal{C}}_{4,7} = +\bar{\mathrm{R}}_{11}^{11} + \tau_0\left[+\bar{\mathrm{R}}_{11}^{12}\frac{1}{tn}\right] \tag{IV.F.37}$$

$$\mathrm{x}^{-3}\mathcal{C}\bar{\mathcal{C}}_{4,8} = +\bar{\mathrm{R}}_{16}^{21} + \tau_0\left[+\bar{\mathrm{R}}_{16}^{22}\frac{1}{tn}\right] \tag{IV.F.38}$$

$$\mathrm{x}^{-3}\mathcal{C}\bar{\mathcal{C}}_{4,9} = +\bar{\mathrm{R}}_{16}^{11} \tag{IV.F.39}$$

$$x^{-3}\mathcal{C}\bar{\mathcal{C}}_{4,10} = +\bar{R}_{12}^{21} \tag{IV.F.40}$$

$$x^{-2}\mathcal{C}\bar{\mathcal{C}}_{4,11} = +\bar{W}_{15}^{11} + \tau_0\left[+\bar{R}_{12}^{11} + \bar{W}_{15}^{12}\frac{1}{tn}\right] \tag{IV.F.41}$$

$$x^{-2}\mathcal{C}\bar{\mathcal{C}}_{4,12} = +\bar{W}_{14}^{21} + \tau_0\left[-\bar{R}_{14}^{21}\frac{1}{tn} - \bar{R}_{16}^{21} + \bar{W}_{14}^{22}\frac{1}{tn}\right] \tag{IV.F.42}$$

$$x^{-3}\mathcal{C}\bar{\mathcal{C}}_{5,5} = +\bar{A}_{22}^{2} + \tau_0\left[-\bar{A}_{22}^{3}\frac{1}{tn}\right] + \tau\left[+\bar{A}_{22}^{4}\frac{1}{(tn^2)}\right] \tag{IV.F.43}$$

$$x^{-3}\mathcal{C}\bar{\mathcal{C}}_{5,6} = +\bar{A}_{26}^{2} + \tau_0\left[-0.5\bar{A}_{26}^{3}\frac{1}{tn}\right] + \tau\left[+0.5\bar{A}_{26}^{4}\frac{1}{(tn^2)}\right] \tag{IV.F.44}$$

$$x^{-3}\mathcal{C}\bar{\mathcal{C}}_{5,7} = +\bar{R}_{12}^{11} \tag{IV.F.45}$$

$$x^{-3}\mathcal{C}\bar{\mathcal{C}}_{5,8} = +\bar{R}_{26}^{21} \tag{IV.F.46}$$

$$x^{-3}\mathcal{C}\bar{\mathcal{C}}_{5,9} = +\bar{R}_{26}^{11} + \tau_0\left[-\bar{R}_{26}^{12}\frac{1}{tn}\right] + \tau\left[+\bar{R}_{26}^{13}\frac{1}{(tn^2)}\right] \tag{IV.F.47}$$

$$x^{-3}\mathcal{C}\bar{\mathcal{C}}_{5,10} = +\bar{R}_{22}^{21} + \tau_0\left[-\bar{R}_{22}^{22}\frac{1}{tn}\right] + \tau\left[+\bar{R}_{22}^{23}\frac{1}{(tn^2)}\right] \tag{IV.F.48}$$

$$x^{-2}\mathcal{C}\bar{\mathcal{C}}_{5,11} = +\bar{W}_{25}^{11} + \tau_0\left[+\bar{R}_{22}^{11} - \bar{R}_{22}^{12}\frac{1}{tn}\right] + \tau\left[+\bar{R}_{22}^{13}\frac{1}{(tn^2)}\right] \tag{IV.F.49}$$

$$\begin{aligned} x^{-2}\mathcal{C}\bar{\mathcal{C}}_{5,12} = &+\bar{W}_{24}^{21} + \tau_0\left[-\bar{R}_{24}^{21}\frac{1}{tn} - \bar{R}_{26}^{21} + \bar{R}_{24}^{22}\frac{1}{(tn^2)} + \bar{R}_{26}^{22}\frac{1}{tn}\right] + \tau\Big[\\ &- \bar{R}_{24}^{23}\frac{1}{(tn^3)} - \bar{R}_{26}^{23}\frac{1}{(tn^2)}\Big] \end{aligned} \tag{IV.F.50}$$

$$x^{-3}\mathcal{C}\bar{\mathcal{C}}_{6,6} = +\bar{A}_{66}^{2} + 0.25\bar{A}_{66}^{4}\frac{1}{(tn^2)} \tag{IV.F.51}$$

$$x^{-3}\mathcal{C}\bar{\mathcal{C}}_{6,7} = +\bar{R}_{16}^{11} + \tau_0\left[+0.5\bar{R}_{16}^{12}\frac{1}{tn}\right] \tag{IV.F.52}$$

$$x^{-3}\mathcal{C}\bar{\mathcal{C}}_{6,8} = +\bar{R}_{66}^{21} + \tau_0\left[+0.5\bar{R}_{66}^{22}\frac{1}{tn}\right] \tag{IV.F.53}$$

$$x^{-3}\mathcal{C}\bar{\mathcal{C}}_{6,9} = +\bar{R}_{66}^{11} + \tau_0\left[-0.5\bar{R}_{66}^{12}\frac{1}{tn}\right] + \tau\left[+0.5\bar{R}_{66}^{13}\frac{1}{(tn^2)}\right] \tag{IV.F.54}$$

$$x^{-3}\mathcal{C}\bar{\mathcal{C}}_{6,10} = +\bar{R}_{26}^{21} + \tau_0\left[-0.5\bar{R}_{26}^{22}\frac{1}{tn}\right] + \tau\left[+0.5\bar{R}_{26}^{23}\frac{1}{(tn^2)}\right] \tag{IV.F.55}$$

$$x^{-2}\bar{\mathcal{C}}_{6,11} = +\bar{W}_{56}^{11} + \tau_0\left[+\bar{R}_{26}^{11} - 0.5\bar{R}_{26}^{12}\frac{1}{tn} + 0.5\bar{W}_{56}^{12}\frac{1}{tn}\right] + \tau\left[+0.5\bar{R}_{26}^{13}\frac{1}{(tn^2)}\right] \tag{IV.F.56}$$

$$\begin{aligned} x^{-2}\bar{\mathcal{C}}_{6,12} = +\bar{W}_{46}^{21} + \tau_0\Big[&-\bar{R}_{46}^{21}\frac{1}{tn} - \bar{R}_{66}^{21} + 0.5\bar{R}_{46}^{22}\frac{1}{(tn^2)} + 0.5\bar{R}_{66}^{22}\frac{1}{tn} \\ &+ 0.5\bar{W}_{46}^{22}\frac{1}{tn}\Big] + \tau\left[-0.5\bar{R}_{46}^{23}\frac{1}{(tn^3)} - 0.5\bar{R}_{66}^{23}\frac{1}{(tn^2)}\right] \end{aligned} \tag{IV.F.57}$$

$$x^{-3}\bar{\mathcal{C}}_{7,7} = +\bar{Q}_{11}^{110} + \tau_0\left[+\bar{Q}_{11}^{111}\frac{1}{tn}\right] \tag{IV.F.58}$$

$$x^{-3}\bar{\mathcal{C}}_{7,8} = +\bar{Q}_{16}^{120} + \tau_0\left[+\bar{Q}_{16}^{121}\frac{1}{tn}\right] \tag{IV.F.59}$$

$$x^{-3}\bar{\mathcal{C}}_{7,9} = +\bar{Q}_{16}^{110} \tag{IV.F.60}$$

$$x^{-3}\bar{\mathcal{C}}_{7,10} = +\bar{Q}_{12}^{120} \tag{IV.F.61}$$

$$x^{-2}\bar{\mathcal{C}}_{7,11} = +\bar{Y}_{15}^{110} + \tau_0\left[+\bar{Q}_{12}^{110} + \bar{Y}_{15}^{111}\frac{1}{tn}\right] \tag{IV.F.62}$$

$$x^{-2}\bar{\mathcal{C}}_{7,12} = +\bar{Y}_{14}^{210} + \tau_0\left[-\bar{Q}_{14}^{120}\frac{1}{tn} - \bar{Q}_{16}^{120} + \bar{Y}_{14}^{211}\frac{1}{tn}\right] \tag{IV.F.63}$$

$$\mathrm{x}^{-3}\mathcal{C}\bar{\mathcal{C}}_{8,8} = +\bar{\mathrm{Q}}_{66}^{220} + \tau_0\left[+\bar{\mathrm{Q}}_{66}^{221}\frac{1}{tn}\right] \tag{IV.F.64}$$

$$\mathrm{x}^{-3}\mathcal{C}\bar{\mathcal{C}}_{8,9} = +\bar{\mathrm{Q}}_{66}^{120} \tag{IV.F.65}$$

$$\mathrm{x}^{-3}\mathcal{C}\bar{\mathcal{C}}_{8,10} = +\bar{\mathrm{Q}}_{26}^{220} \tag{IV.F.66}$$

$$\mathrm{x}^{-2}\mathcal{C}\bar{\mathcal{C}}_{8,11} = +\bar{\mathrm{Y}}_{56}^{120} + \tau_0\left[+\bar{\mathrm{Q}}_{26}^{120} + \bar{\mathrm{Y}}_{56}^{121}\frac{1}{tn}\right] \tag{IV.F.67}$$

$$\mathrm{x}^{-2}\mathcal{C}\bar{\mathcal{C}}_{8,12} = +\bar{\mathrm{Y}}_{46}^{220} + \tau_0\left[-\bar{\mathrm{Q}}_{46}^{220}\frac{1}{tn} - \bar{\mathrm{Q}}_{66}^{220} + \bar{\mathrm{Y}}_{46}^{221}\frac{1}{tn}\right] \tag{IV.F.68}$$

$$\mathrm{x}^{-3}\mathcal{C}\bar{\mathcal{C}}_{9,9} = +\bar{\mathrm{Q}}_{66}^{110} + \tau_0\left[-\bar{\mathrm{Q}}_{66}^{111}\frac{1}{tn}\right] + \tau\left[+\bar{\mathrm{Q}}_{66}^{112}\frac{1}{(tn^2)}\right] \tag{IV.F.69}$$

$$\mathrm{x}^{-3}\mathcal{C}\bar{\mathcal{C}}_{9,10} = +\bar{\mathrm{Q}}_{26}^{120} + \tau_0\left[-\bar{\mathrm{Q}}_{26}^{121}\frac{1}{tn}\right] + \tau\left[+\bar{\mathrm{Q}}_{26}^{122}\frac{1}{(tn^2)}\right] \tag{IV.F.70}$$

$$\mathrm{x}^{-2}\mathcal{C}\bar{\mathcal{C}}_{9,11} = +\bar{\mathrm{Y}}_{56}^{110} + \tau_0\left[+\bar{\mathrm{Q}}_{26}^{110} - \bar{\mathrm{Q}}_{26}^{111}\frac{1}{tn}\right] + \tau\left[+\bar{\mathrm{Q}}_{26}^{112}\frac{1}{(tn^2)}\right] \tag{IV.F.71}$$

$$\mathrm{x}^{-2}\mathcal{C}\bar{\mathcal{C}}_{9,12} = +\bar{\mathrm{Y}}_{46}^{210} + \tau_0\left[-\bar{\mathrm{Q}}_{46}^{120}\frac{1}{tn} - \bar{\mathrm{Q}}_{66}^{120} + \bar{\mathrm{Q}}_{46}^{121}\frac{1}{(tn^2)} + \bar{\mathrm{Q}}_{66}^{121}\frac{1}{tn}\right] + \tau\left[- \bar{\mathrm{Q}}_{46}^{122}\frac{1}{(tn^3)} - \bar{\mathrm{Q}}_{66}^{122}\frac{1}{(tn^2)}\right] \tag{IV.F.72}$$

$$\mathrm{x}^{-3}\mathcal{C}\bar{\mathcal{C}}_{10,10} = +\bar{\mathrm{Q}}_{22}^{220} + \tau_0\left[-\bar{\mathrm{Q}}_{22}^{221}\frac{1}{tn}\right] + \tau\left[+\bar{\mathrm{Q}}_{22}^{222}\frac{1}{(tn^2)}\right] \tag{IV.F.73}$$

$$\mathrm{x}^{-2}\mathcal{C}\bar{\mathcal{C}}_{10,11} = +\bar{\mathrm{Y}}_{25}^{120} + \tau_0\left[+\bar{\mathrm{Q}}_{22}^{120} - \bar{\mathrm{Q}}_{22}^{121}\frac{1}{tn}\right] + \tau\left[+\bar{\mathrm{Q}}_{22}^{122}\frac{1}{(tn^2)}\right] \tag{IV.F.74}$$

$$\mathrm{x}^{-2}\mathcal{C}\bar{\mathcal{C}}_{10,12} = +\bar{\mathrm{Y}}_{24}^{220} + \tau_0\left[-\bar{\mathrm{Q}}_{24}^{220}\frac{1}{tn} - \bar{\mathrm{Q}}_{26}^{220} + \bar{\mathrm{Q}}_{24}^{221}\frac{1}{(tn^2)} + \bar{\mathrm{Q}}_{26}^{221}\frac{1}{tn}\right] + \tau\left[- \bar{\mathrm{Q}}_{24}^{222}\frac{1}{(tn^3)} - \bar{\mathrm{Q}}_{26}^{222}\frac{1}{(tn^2)}\right] \tag{IV.F.75}$$

$$\mathrm{x}^{-1}\mathcal{C}\bar{\mathcal{C}}_{11,11} = +\bar{\mathrm{Z}}_{55}^{110} + \tau_0\left[+\bar{\mathrm{Q}}_{22}^{110} - \bar{\mathrm{Q}}_{22}^{111}\frac{1}{tn} + 2\bar{\mathrm{Y}}_{25}^{110} + \bar{\mathrm{Z}}_{55}^{111}\frac{1}{tn}\right] + \tau\left[+ \bar{\mathrm{Q}}_{22}^{112}\frac{1}{(tn^2)}\right] \tag{IV.F.76}$$

$$\mathrm{x}^{-1}\mathcal{C}\bar{\mathcal{C}}_{11,12} = +\bar{\mathrm{Z}}_{45}^{120} + \tau_0\left[-\bar{\mathrm{Q}}_{24}^{120}\frac{1}{tn} - \bar{\mathrm{Q}}_{26}^{120} + \bar{\mathrm{Q}}_{24}^{121}\frac{1}{(tn^2)} + \bar{\mathrm{Q}}_{26}^{121}\frac{1}{tn} - \bar{\mathrm{Y}}_{45}^{120}\frac{1}{tn} - \bar{\mathrm{Y}}_{56}^{120} + \bar{\mathrm{Y}}_{24}^{210} + \bar{\mathrm{Z}}_{45}^{121}\frac{1}{tn}\right] + \tau\left[-\bar{\mathrm{Q}}_{24}^{122}\frac{1}{(tn^3)} - \bar{\mathrm{Q}}_{26}^{122}\frac{1}{(tn^2)}\right] \tag{IV.F.77}$$

$$\begin{aligned}\mathrm{x}^{-1}\mathcal{C}\bar{\mathcal{C}}_{12,12} = &+\bar{\mathrm{Z}}_{44}^{220}+\tau_0\Big[+\bar{\mathrm{Q}}_{44}^{220}\frac{1}{(tn^2)}+2\bar{\mathrm{Q}}_{46}^{220}\frac{1}{tn}+\bar{\mathrm{Q}}_{66}^{220}-\bar{\mathrm{Q}}_{44}^{221}\frac{1}{(tn^3)}\\ &-2\bar{\mathrm{Q}}_{46}^{221}\frac{1}{(tn^2)}-\bar{\mathrm{Q}}_{66}^{221}\frac{1}{tn}-2\bar{\mathrm{Y}}_{44}^{220}\frac{1}{tn}-2\bar{\mathrm{Y}}_{46}^{220}+\bar{\mathrm{Z}}_{44}^{221}\frac{1}{tn}\Big]+\tau\Big[+\bar{\mathrm{Q}}_{44}^{222}\frac{1}{(tn^4)}\\ &+2\bar{\mathrm{Q}}_{46}^{222}\frac{1}{(tn^3)}+\bar{\mathrm{Q}}_{66}^{222}\frac{1}{(tn^2)}\Big]\end{aligned} \tag{IV.F.78}$$

.7 Appendix IV.H Total Strain Vector Components in $\mathbb{S}$ Function Space

The rows of linear component of $\left\{\mathfrak{E}^{\circ}\right\}$ can be formulated as follows:

$$\left[\mathrm{S}_{\mathfrak{E}_{\mathrm{L}}^{\circ}}\right]_{1,1:\mathrm{K}}=\left\{\mathrm{S}_{\mathfrak{e}_{11}^{\circ}}\right\} \tag{IV.G.1a}$$

$$\left[\mathrm{S}_{\mathfrak{E}_{\mathrm{L}}^{\circ}}\right]_{2,1:\mathrm{K}}=\left\{\mathrm{S}_{\mathfrak{e}_{22}^{\circ}}\right\} \tag{IV.G.1b}$$

$$\left[\mathrm{S}_{\mathfrak{E}_{\mathrm{L}}^{\circ}}\right]_{3,1:\mathrm{K}}=2\left\{\mathrm{S}_{\mathfrak{e}_{12}^{\circ}}\right\} \tag{IV.G.1c}$$

$$\left[\mathrm{S}_{\mathfrak{E}_{\mathrm{L}}^{\circ}}\right]_{4,1:\mathrm{K}}=\left\{\mathrm{S}_{\chi_{11}^{\circ}}\right\} \tag{IV.G.1d}$$

$$\left[\mathrm{S}_{\mathfrak{E}_{\mathrm{L}}^{\circ}}\right]_{5,1:\mathrm{K}}=\left\{\mathrm{S}_{\chi_{22}^{\circ}}\right\} \tag{IV.G.1e}$$

$$\left[\mathrm{S}_{\mathfrak{E}_{\mathrm{L}}^{\circ}}\right]_{6,1:\mathrm{K}}=2\left\{\mathrm{S}_{\chi_{12}^{\circ}}\right\} \tag{IV.G.1f}$$

$$\left[\mathrm{S}_{\mathfrak{E}_{\mathrm{L}}^{\circ}}\right]_{7:8,1:\mathrm{K}}=\left\{\mathrm{S}_{\gamma}^{\mathrm{x}}\right\} \tag{IV.G.1g}$$

$$\left[\mathbf{S}_{\mathfrak{E}_L^\circ}\right]_{9:10,1:K} = \left\{\mathbf{S}_{\boldsymbol{\gamma}}^{\boldsymbol{\theta}}\right\} \tag{IV.G.1h}$$

$$\left[\mathbf{S}_{\mathfrak{E}_L^\circ}\right]_{11:12,1:K} = \left\{\mathbf{S}_{\boldsymbol{\gamma}}\right\} \tag{IV.G.1i}$$

The rows of nonlinear component of $\left\{\mathfrak{E}^\circ\right\}$ can be formulated as follows:

$$\left[\mathbf{S}_{\mathfrak{E}_L^\circ}\right]_{1,1:K^2} = \frac{1}{2}\left(\left\{\mathbf{S}_{\boldsymbol{\phi_1}\otimes\boldsymbol{\phi_1}}\right\} + c_2\left\{\mathbf{S}_{\boldsymbol{\phi}\otimes\boldsymbol{\phi}}\right\}\right) + \frac{1}{2}c_1\left(\left\{\mathbf{S}_{\mathbf{e}_{i1}^\circ\otimes\mathbf{e}_{i1}^\circ}\right\} + \left\{\mathbf{S}_{\mathbf{e}_{i2}^\circ\otimes\mathbf{e}_{i2}^\circ}\right\} + 2\left\{\mathbf{S}_{\mathbf{e}_{i2}^\circ\otimes\boldsymbol{\phi}}\right\}\right) \tag{IV.G.2a}$$

$$\left[\mathbf{S}_{\mathfrak{E}_L^\circ}\right]_{2,1:K^2} = \frac{1}{2}\left(\left\{\mathbf{S}_{\boldsymbol{\phi_2}\otimes\boldsymbol{\phi_2}}\right\} + c_2\left\{\mathbf{S}_{\boldsymbol{\phi}\otimes\boldsymbol{\phi}}\right\}\right) + \frac{1}{2}c_1\left(\left\{\mathbf{S}_{\mathbf{e}_{22}^\circ\otimes\mathbf{e}_{22}^\circ}\right\} + \left\{\mathbf{S}_{\mathbf{e}_{i2}^\circ\otimes\mathbf{e}_{i2}^\circ}\right\} + 2\left\{\mathbf{S}_{\mathbf{e}_{i2}^\circ\otimes\boldsymbol{\phi}}\right\}\right) \tag{IV.G.2b}$$

$$\left[\mathbf{S}_{\mathfrak{E}_L^\circ}\right]_{3,1:K^2} = \left\{\mathbf{S}_{\boldsymbol{\phi_1}\otimes\boldsymbol{\phi_2}}\right\} + c_1\left(\left\{\mathbf{S}_{\mathbf{e}_{i1}^\circ\otimes\mathbf{e}_{i2}^\circ}\right\} - \left\{\mathbf{S}_{\mathbf{e}_{i1}^\circ\otimes\boldsymbol{\phi}}\right\} + \left\{\mathbf{S}_{\mathbf{e}_{22}^\circ\otimes\mathbf{e}_{i2}^\circ}\right\} + \left\{\mathbf{S}_{\mathbf{e}_{22}^\circ\otimes\boldsymbol{\phi}}\right\}\right) \tag{IV.G.2c}$$

$$\left[\mathbf{S}_{\mathfrak{E}_L^\circ}\right]_{4:12,1:K^2} = \left[\mathbf{H}(0,0,0,0)\right]_{9\times K^2} \tag{IV.G.2d}$$

References

[1] M. P. Nemeth, "A Leonard-Sanders-Budiansky-Koiter-Type Nonlinear Shell Theory with a Hierarchy of Transverse-Shearing Deformations," Tech. Rep. NASA/TP–2013-218025, Jul. 2013. [Online]. Available: http://ntrs.nasa.gov/search.jsp?R=20140000788